PhD Thesis – Tesis Doctoral

Study of the role of neuropilin-1 in the development, prognosis and cellular response to lenvatinib in human hepatocellular carcinoma

Estudio del papel de la neuropilina-1 en el desarrollo, pronóstico y la respuesta celular a lenvatinib en el carcinoma hepatocelular humano

Paula Fernández Palanca

Doctoral Program in Biomedicine and Health Sciences
Programa de Doctorado en Biomedicina y Ciencias de la Salud

Tutor: Prof. Dr. José Luis Mauriz Gutiérrez

Supervisors - Directores
Prof. Dr. Javier González Gallego and
Prof. Dr. José Luis Mauriz Gutiérrez

Institute of Biomedicine (IBIOMED), University of León
Instituto de Biomedicina (IBIOMED), Universidad de León

León, 2023

The results presented in this PhD Thesis have been published in the following scientific articles:

1. **Neuropilin-1 as a potential biomarker of prognosis and invasive-related parameters in liver and colorectal cancer: A systematic review and meta-analysis of human studies.**
   Fernández-Palanca P, Payo-Serafín T, Fondevila F, Méndez-Blanco C, San-Miguel B, Romero MR, Tuñón MJ, Marin JJG, González-Gallego J, Mauriz JL.
   Cancers (Basel). 2022;14:3455.
   JCR Impact Factor: 6.575
   Rank in Oncology: 60/245 (Q1)

2. **Hepatocellular carcinoma cells loss lenvatinib efficacy *in vitro* through autophagy and hypoxia response-derived neuropilin-1 degradation.**
   Fernández-Palanca P, Payo-Serafín T, San-Miguel B., Méndez-Blanco C, Tuñón MJ, González-Gallego J, Mauriz JL.
   Acta Pharmacol Sin. 2022. https://doi.org/10.1038/s41401-022-01021-2.
   JCR Impact Factor: 7.165
   Rank in Pharmacology & Pharmacy: 28/279 (Q1)
   Rank in Chemistry, Multidisciplinary: 44/179 (Q1)

3. **Neuropilins as potential biomarkers in hepatocellular carcinoma: A systematic review of basic and clinical implications.**
   Fernández-Palanca P, Payo-Serafín T, Méndez-Blanco C, San-Miguel B, Tuñón MJ, González-Gallego J, Mauriz JL.
   Clin Mol Hepatol. 2023. https://doi.org/10.3350/cmh.2022.0425
   JCR Impact Factor: 8.337
   Rank in Gastroenterology & Hepatology: 19/93 (Q1)

In addition, the scientific articles detailed below have been also published during the predoctoral period:

1. **Anti-tumoral activity of single and combined regorafenib treatments in preclinical models of liver and gastrointestinal cancers.**
   Fondevila F, Méndez-Blanco C, Fernández-Palanca P, González-Gallego J, Mauriz JL.
   Exp Mol Med. 2019;51:109.
   JCR Impact Factor: 5.418
   Rank in Biochemistry & Molecular Biology: 46/297 (Q1)
   Rank in Medicine, Research & Experimental: 21/139 (Q1)

2. **Antitumor effects of quercetin in hepatocarcinoma in vitro and in vivo models: A systematic review.**
   Fernández-Palanca P, Fondevila F, Méndez-Blanco C, Tuñón MJ, González-Gallego J, Mauriz JL.
   Nutrients. 2019;11:2875.
   JCR Impact Factor: 4.546
   Rank in Nutrition & Dietetics: 17/89 (Q1)

3. **Stabilization of hypoxia-inducible factors and BNIP3 promoter methylation contribute to acquired sorafenib resistance in human hepatocarcinoma cells.**
   Méndez-Blanco C, Fondevila F, Fernández-Palanca P, García-Palomo A, van Pelt J, Verslype C, González-Gallego J, Mauriz JL.
   Cancers (Basel). 2019;11:1984.
   JCR Impact Factor: 6.126
   Rank in Oncology: 37/244 (Q1)

4. **Melatonin modulates mitophagy, innate immunity and circadian clocks in a model of viral-induced fulminant hepatic failure.**
   Crespo I, Fernández-Palanca P, San-Miguel B, Álvarez M, González-Gallego J, Tuñón MJ.
   J Cell Mol Med. 2020;24:7625-7636.
   JCR Impact Factor: 5.310
   Rank in Medicine, Research & Experimental: 44/140 (Q2)
   Rank in Cell Biology: 73/195 (Q2)

5. **Melatonin as an antitumor agent against liver cancer: An updated systematic review.**

   Fernández-Palanca P, Méndez-Blanco C, Fondevila F, Tuñón MJ, Reiter RJ, Mauriz JL, González-Gallego J.

   Antioxidants. 2021;10:103.

   JCR Impact Factor: 7.675

   Rank in Biochemistry & Molecular Biology: 50/296 (Q1)

   Rank in Chemistry, Medicinal: 4/63 (Q1)

   Rank in Food Science & Technology: 12/143 (Q1)

6. **Prognostic and clinicopathological significance of hypoxia-inducible factors 1α and 2α in hepatocellular carcinoma: A systematic review with meta-analysis.**

   Méndez-Blanco C, Fernández-Palanca P, Fondevila F, González-Gallego J, Mauriz JL.

   Ther Adv Med Oncol. 2021;13:1-28.

   JCR Impact Factor: 5.485

   Rank in Oncology: 80/245 (Q2)

7. **Association of FOXO3 expression with tumor pathogenesis, prognosis and clinicopathological features in hepatocellular carcinoma: a systematic review with meta-analysis.**

   Fondevila F, Fernández-Palanca P, Méndez-Blanco C, Payo-Serafín T, Lozano E, Marin JJG, González-Gallego J, Mauriz JL.

   Cancers (Basel). 2021;13:5349.

   JCR Impact Factor: 6.575

   Rank in Oncology: 60/245 (Q1)

8. **Autophagy-related chemoprotection against sorafenib in human hepatocarcinoma: Role of FOXO3 upregulation and modulation by regorafenib**

   Fondevila F, Méndez-Blanco C, Fernández-Palanca P, Payo-Serafín T, van Pelt J, Verslype C, González-Gallego J, Mauriz JL.

   Int J Mol Sci. 2021;22:11770.

   JCR Impact Factor: 6.208

   Rank in Biochemistry & Molecular Biology: 69/296 (Q1)

   Rank in Chemistry, Multidisciplinary: 50/179 (Q2)

9. **Beneficial effects of melatonin on liver fibrosis: A systematic review of current biological evidence**

   San-Miguel B, Fernández-Palanca P, Mauriz JL, González-Gallego J, Tuñón MJ.

   J Cell Physiol. 2022;1:18.

   JCR Impact Factor: 6.513

   Rank in Physiology: 10/81 (Q1)

   Rank in Cell Biology: 62/194 (Q2)

10. **Spatial modeling reveals nuclear phosphorylation and subcellular shuttling of YAP upon drug-induced liver injury**

    Wehling L, Keegan L, Fernández-Palanca P, Hassan R, Ghallab A, Schmitt J, Tang Y, Le Marois M, Roessler S, Schirmacher P, Kummer U, Hengstler JG, Sahle S, Breuhahn K.

    eLife. 2022;11:e78540.

    JCR Impact Factor: 8.713

    Rank in Biology: 8/94 (Q1)

Part of the results obtained during the predoctoral period and those exposed in this PhD Thesis have been presented in the following national and international congresses:

1. **XLIV Congreso Anual de la Asociación Española para el Estudio del Hígado (AEEH).** Madrid (España), 20-22/02/2019.
   La estabilización de los factores inducibles por hipoxia contribuye al desarrollo de resistencia a sorafenib en células de hepatocarcinoma humano. Fondevila F, Méndez-Blanco C, Fernández-Palanca P, García-Palomo A, González-Gallego J, Mauriz JL. Gastroenterol Hepatol. 2019;42(S1):42.

2. **13th Annual Biotechnology Congress (BAC) – Congress of the Spanish Federation of Biotechnologists (FEBiotec)**. Madrid (España). 10-12/07/2019.
   Study of acquired resistance to sorafenib in an *in vitro* HCC model: effect of regorafenib on AKT/mTOR and ERK signaling. Martín-Álvarez C, Fernández-Palanca P, Fondevila F, Méndez-Blanco C, García-Palomo A, González-Gallego J, Mauriz JL.

3. **XLV Congreso Anual de la Asociación Española para el Estudio del Hígado (AEEH).** Madrid (España), 12-14/02/2020.
   La hipermetilación del promotor de BNIP3 contribuye a la adquisición de resistencia a sorafenib en hepatocarcinoma humano. Fernández-Palanca P, Fondevila F, Méndez-Blanco C, González-Gallego J, Mauriz JL. Gastroenterol Hepatol. 2020;43(S1):47.

4. **27th Congress of the European Association for Cancer Research (EACR).** Virtual Congress – Innovative Cancer Science: Better Outcomes Through Research. 09-12/06/2021.
   Identification of prognostic value of HIF-2α and a potential role in sorafenib resistance development in hepatocarcinoma. Fernández-Palanca P, Méndez-Blanco C, Fondevila F, González-Gallego J, Mauriz JL.

5. **XLVI Congreso Anual de la Asociación Española para el Estudio del Hígado (AEEH)**. Madrid (España), 14-16/06/2021.
   Identificación del potencial valor pronóstico del factor inducible por hipoxia 2α en pacientes con hepatocarcinoma. Fernández-Palanca P, Méndez-Blanco C, Fondevila F, González-Gallego J, Mauriz JL. Gastroenterol Hepatol. 2021;44(S2):42.

6. **XLVI Congreso Anual de la Asociación Española para el Estudio del Hígado (AEEH).** Madrid (España), 14-16/06/2021.

   FOXO3 en cáncer hepático primario: Nuevo biomarcador con potencial diagnóstico y pronóstico. Fondevila F, Méndez-Blanco C, Fernández-Palanca P, Payo-Serafín T, González-Gallego J, Mauriz JL. Gastroenterol Hepatol. 2021;44(S2):42.

7. **The International Liver Congress™ (ILC) by the European Association for the Study of the Liver (EASL)**. Virtual Congress. 23-26/06/2021.

   Role of hypoxia-inducible factors 1α and 2α in prognosis and sorafenib chemoresistance in hepatocarcinoma. Méndez-Blanco C, Fondevila F, Fernández-Palanca P, van Pelt J, Verslype C, González-Gallego J, Mauriz JL. J Hepatol. 2021;75(2):S294-S803.

8. **The International Liver Congress™ (ILC) by the European Association for the Study of the Liver (EASL)**. Virtual Congress. 23-26/06/2021.

   Resistance to sorafenib in hepatocarcinoma: role of BCL2 interacting protein 3 promoter hypermethylation. Fernández-Palanca P, Méndez-Blanco C, Fondevila F, van Pelt J, Verslype C, González-Gallego J, Mauriz JL. J Hepatol. 2021;75(2):S294-S803.

9. **14th Annual Biotechnology Congress (BAC) – Congress of the Spanish Federation of Biotechnologists (FEBiotec)**. Zaragoza (España). 08-09/07/2021.

   Diagnostic and prognostic value of FOXO3 in patients with primary liver cancer. Fondevila F, Fernández-Palanca P, Méndez-Blanco C, Payo-Serafín T, González-Gallego J, Mauriz JL.

10. **The Liver Meeting 2021 by the American Association for the Study of Liver Diseases (AASLD).** Anaheim, California (EEUU), 12-15/11/2021.

    FOXO3 as a new biomarker for human hepatocarcinoma: role of diagnosis, prognosis and autophagy-mediated sorafenib resistance acquisition. Fondevila F, Fernández-Palanca P, Méndez-Blanco C, Payo-Serafín T, Jorquera F, González-Gallego J, Mauriz JL. Hepatol. 2021;74(S1):300.

11. **The Liver Meeting 2021 by the American Association for the Study of Liver Diseases (AASLD).** Anaheim, California (EEUU), 12-15/11/2021.

HIF-1α on prognosis, recurrence and acquisition of resistance to sorafenib in hepatocarcinoma. Méndez-Blanco C, Fondevila F, Fernández-Palanca P, Jorquera F, González-Gallego J, Mauriz JL. Hepatol. 2021;74(S1):300.

12. **The Liver Meeting 2021 by the American Association for the Study of Liver Diseases (AASLD).** Anaheim, California (EEUU), 12-15/11/2021.
    HIF-2α as a novel prognostic biomarker and therapeutic target associated to sorafenib resistance in hepatocarcinoma. Fernández-Palanca P, Méndez-Blanco C, Fondevila F, Jorquera F, González-Gallego J, Mauriz JL. Hepatol. 2021;74(S1):301.

13. **XLVII Congreso Anual de la Asociación Española para el Estudio del Hígado (AEEH)**. Madrid (España), 25-27/05/2022.
    Eficacia antitumoral del lenvatinib en el hepatocarcinoma humano: papel de la degradación de NRP1 mediada por autofagia. Fernández-Palanca P, Payo-Serafín T, Fondevila F, Méndez-Blanco C, González-Gallego J, Mauriz JL. Gastroenterol Hepatol. 2022;45(SC2):39.

14. **The International Liver Congress™ (ILC) by the European Association for the Study of the Liver (EASL)**. Londres (Reino Unido), 22-26/06/2022.
    Role of autophagy-mediated neuropilin-1 degradation on lenvatinib efficacy in human hepatocarcinoma. Fernández-Palanca P, Payo-Serafín T, Fondevila F, Méndez-Blanco C, González-Gallego J, Mauriz JL. J Hepatol. 2022;77(S1):S639.

15. **XL Congreso de la Sociedad Española de Ciencias Fisiológicas (SECF).** Badajoz (España), 19-22/09/2022.
    Role of the hypoxia-derived response and autophagy interplay in the loss of lenvatinib sensitivity: Neuropilin-1 as a potential therapeutic target in human hepatocellular carcinoma. Fernández-Palanca P, Payo-Serafín T, San-Miguel B, Tuñón MJ, González-Gallego J, Mauriz JL. J Physiol Biochem. 2022;P2-28.

16. **XL Congreso de la Sociedad Española de Ciencias Fisiológicas (SECF).** Badajoz (España), 19-22/09/2022.
    Identification of neuropilin-1 as a novel biomarker on prognosis and invasive-related features in colorectal and liver cancer patients. Fernández-Palanca P, Payo-Serafín T, Fondevila F, Méndez-Blanco C, San-Miguel B, Romero MR, Tuñón MJ, Marin JJG, González-Gallego J, Mauriz JL. J Physiol Biochem. 2022;P2-27.

17. **XL Congreso de la Sociedad Española de Ciencias Fisiológicas (SECF).** Badajoz (España), 19-22/09/2022.

    Hypoxia-inducible factor 1α-dependent response to hypoxia through apoptosis and autophagy modulation promotes cell survival in hepatocellular carcinoma. Payo-Serafín T, Fernández-Palanca P, Méndez-Blanco C, Fondevila F, San-Miguel B, García-Palomo A, de Ortiz Urbina JJ, González-Gallego J, Tuñón MJ, Mauriz JL. J Physiol Biochem. 2022,P2-30.

Funding

During the realization of this PhD Thesis, Paula Fernández Palanca has been awarded with a FPU predoctoral grant of the Spanish program for professional training of university lecturers, included in the program "*Formación del Profesorado Universitario*" (FPU) from the *Ministerio de Educación, Cultura y Deporte*, enclosed in the *Programa Estatal de Promoción del Talento y su Empleabilidad* (*Plan Estatal de Investigación Científica y Técnica y de Innovación 2013-2016).* This grant has been identified by the reference FPU17/01995, funded by MCIN/AEI/10.13039/501100011033.

Likewise, Paula Fernández Palanca was awarded with a mobility grant for FPU beneficiaries to perform short stays and temporary transfers in national or international research centers ("*Ayudas complementarias de movilidad del Subprograma de Formación del Profesorado Universitario (FPU)*", *convocatoria 2020*) from the Ministry of Universities with the reference EST19/00340. The short stay was performed for three months (01/05/2021-31/07/2021) in the research group of Prof. Dr. Kai Breuhahn at the Institute of Pathology from the University Hospital Heidelberg (Heidelberg, Germany).

Moreover, this PhD Thesis has been developed within a research group supported by the following projects or grants:

- "*Estudio del efecto de inhibidores de tirosín quinasas en la modulación de la supervivencia y muerte celular en diferentes tipos de cáncer"*. Z367. *Fundación de Investigación Sanitaria en León (España)*. 29/01/2018-29/01/2019
- "*Estudio de la modulación de la autofagia y la apoptosis en hepatocarcinoma tras la administración de inhibidores tirosín quinasa"*. Z390. *Universidad de León (España)*. 19/11/2019-18/11/2020
- "*Generación de un modelo knockout de los factores inducibles por hipoxia para la mejora de la sensibilidad a inhibidores tirosina-quinasa en el tratamiento del hepatocarcinoma".* Z413. *Ministerio de Ciencia e Innovación (España)*. 01/09/2021-31/08/2024

The present PhD Thesis has been performed at the Institute of Biomedicine (IBIOMED) of the University of León (Spain), under the supervision of Prof. Dr. Javier González Gallego and Prof. Dr. José Luis Mauriz Gutiérrez, members of the Area of Physiology, of the Department of Biomedical Sciences and IBIOMED at this University.

“Doing what you love is never a waste of time.”

Anonymous

“The easy path won’t lead you to the best views.”

Anonymous

A todos los que me han acompañado durante esta etapa,

en especial a mi padre y mis hermanas.

Agradecimientos

Con esta memoria termina mi etapa predoctoral y, con ello, empieza un nuevo camino en mi carrera investigadora que no habría llegado sin todas esas personas que me habéis ayudado y habéis hecho que esto sea posible.

En primer lugar, quiero agradecer a mis directores de tesis, José y Javier, por haberme permitido realizar esta Tesis Doctoral en su grupo, por todo el apoyo y por la confianza que he recibido durante estos años. Esta oportunidad me ha permitido aprender y crecer profesionalmente, así como introducirme en el mundo de la ciencia acompañada de dos grandes investigadores. Sin duda, no habría podido encontrar mejor grupo en el que comenzar mi carrera investigadora y docente.

A todos mis compañeros del Área de Fisiología del Departamento de Ciencias Biomédicas. Gracias por todos los momentos, la ayuda y lo que he aprendido durante esta etapa, sobre todo durante las prácticas. Habéis hecho que mi paso por el Área haya sido enriquecedor tanto a nivel académico como profesional.

Por supuesto, a todos mis compañeros de laboratorio del IBIOMED, todos los que habéis pasado por él y hemos compartido charlas. Porque sois muchos los que estabais cuando empecé y también los que continuáis, que habéis hecho de mi paso por el laboratorio una etapa inolvidable, llena de buenos recuerdos y mucho aprendizaje. Sin duda habéis contribuido a mi crecimiento personal y profesional. En especial agradecer a Brisa por todas las charlas constructivas, a María, Sara, Marta y Esther, mis compañeras de despacho, a Bea y María Jesús por su confianza y apoyo, y sobre todo a Rebeca, por ayudarme siempre en todo lo que podía.

Especial mención merecen mis compañeras Carolina y Flavia, qué deciros que no sepáis. Gracias por haberme enseñado todo lo que sabéis y por todos los momentos, sobre todo buenos, que hemos compartido y vivido estos años. Mi paso por el IBIOMED no habría sido lo mismo sin vosotras. Y a Tania como no, porque, aunque acaba de empezar, lo ha hecho con muchas ganas y me ha contagiado la motivación durante esta última etapa del doctorado, quizás la más dura. Junto con Jenny, muchas gracias por querer formar parte de este grupo.

To every member of the Institute of Pathology of the University Hospital Heidelberg, especially the AG Breuhahn members, thanks for making my short stay in Heidelberg an

enriching time and making me feel like a lab member. Specially, thanks to Prof. Dr. Kai Breuhahn for letting me be a part of his group, guiding me and teaching me during that short stay more things that I would have expected. Thanks to Lilija for sharing with me her knowledge and scientific criteria, for being a hearted person, a valuable scientist and making me feel like home. I also want to thank my labmates Yingyue, Nada, Asli, Raisa and Yalda, for sharing those good moments with me and making my stay at Heidelberg enjoyable, letting me to carry a part of this small city with me.

Por último, quería agradecer a mi familia y amigos, porque sin ellos no habría podido completar esta etapa. En especial a mi padre y a mis hermanas, Ana y María, siempre habéis estado ahí y me habéis apoyado en todo, y en honor a mi madre por ser mi inspiración. A mis cuñados, Adrián y Sergio, y a José Luis, por los buenos momentos que me habéis hecho pasar. Una mención especial a Noelia por todos los buenos momentos que hemos pasado, las anécdotas y las críticas siempre constructivas, una hermana más para mí. A mis amigas *biotec* Leticia, Alba, Laura, Miriam y Lucía, por ayudarme a desahogarme y compartir tan buenos recuerdos juntas. También a mis amigos del pueblo Pablo, Lore, Dácil y Noemí, por las escapadas y comidas de desconexión por nuestra tierra.

Todos me habéis acompañado durante esta etapa y sé que estaréis en las siguientes, ha sido un placer haber compartido esto con vosotros.

PhD Thesis

Study of the role of neuropilin-1 in the development, prognosis and cellular response to lenvatinib in human hepatocellular carcinoma

Paula Fernández Palanca

Supervisors: Prof. Dr. Javier González Gallego and
Prof. Dr. José Luis Mauriz Gutiérrez

Department of Biomedical Sciences
Institute of Biomedicine (IBIOMED), University of León

León, 2023

Contents

List of figures

List of tables

List of abbreviations

3-MA	3-methyladenine
ABCB1	ATP binding cassette transporter B1
ADAMTSL5	A disintegrin-like and metalloprotease domain containing thrombospondin type 1 motif-like protein 5
ADRB2	Beta-2-adrenergic receptor
AFB1	Aflatoxin B1
AFP	Alpha fetoprotein
AKT	RAC-alpha serine/threonine-protein kinase
AMPK	AMP-activated protein kinase
APS	Ammonium persulfate
ARID1A	AT-rich interaction domain 1A
ARID2	AT-rich interaction domain 2
ARNT	Aryl hydrocarbon receptor nuclear translocator
ATG	Autophagy-related genes
ATG14L	ATG14-like protein
AURKA	Aurora kinase A
Baf	Bafilomycin A1
BCLC	Barcelona Clinic Liver Cancer
BCRP	Breast cancer resistance protein
BMP1	Complement binding factors C1r/C1s, Uegf, bone morphogenetic protein 1
BSA	Bovine serum albumin
BSC	Best supportive care
CAF	Cancer-associated fibroblast
CBP	CREB-binding protein
CDKN2	Cyclin dependent kinase inhibitor 2A
CHX	Cycloheximide
CI	Confidence interval
circMED27	Circular RNA mediator complex subunit 27
circRNA	Circular RNA
CMA	Chaperone-mediated autophagy
CQ	Chloroquine
CREB	cAMP response element-binding protein
CSC	Cancer stem cell
CT	Computed tomography
CTCF	Corrected total cell fluorescence

CTNNB1	Catenin beta-1
CUB	Cubilin homology
DCR	Disease control rate
DEN	Diethylnitrosamine
DMSO	Dimethyl sulfoxide
DUSP9	Dual specificity phosphatase 9
E2F2	Transcription factor E2F2
EASL	European Association for the Study of the Liver
ECM	Extracellular matrix
ECOG	Eastern Cooperative Oncology Group
EGFR	Epidermal growth factor receptor
EMT	Epithelial-to-mesenchymal transition
ERK	Extracellular signal-regulated kinase
ETS-1	Protein C-ets-1
FBS	Fetal bovine serum
FBXO9	F-box only protein 9
FDA	Food and Drug Administration
FGFR	Fibroblast growth factor receptor
FIH	Factor inhibiting HIF-α
FIP200	FAK family kinase-interacting protein of 200 kDa
FoxM1	Forkhead box protein M1
FOXO3	Forkhead box protein O3
FV/VIII	FV/VIII domains
GDC	Genomic Data Commons
GEO	Gene Expression Omnibus
GEPIA	Gene Expression Profiling Interactive Analysis
GLUT	Glucose transporter
GPX2	Glutathione peroxidase 2
GTEx	Genotype-Tissue Expression
HBsAg	Hepatitis B Surface Antigen
HBV	Hepatitis B virus
HCC	Hepatocellular carcinoma
HCV	Hepatitis C virus
HDV	Hepatitis D virus
HGF	Hepatocyte growth factor
HIFs	Hypoxia-inducible factors
HIF-1α	Hypoxia-inducible factor 1α

HPA	Human Protein Atlas
HR	Hazard ratio
HRE	Hypoxia-responsive element
HRP	Horseradish peroxidase
HSCs	Hepatic stellate cells
HSP90	Heat shock protein 90
IC_{50}	Half maximal inhibitory concentration
iCCA	Intrahepatic cholangiocarcinoma
IBIOMED	Institute of Biomedicine
IFN	Interferon
IGF1R	Insulin-like growth factor 1 receptor
IHC	Immunohistochemistry
IL	Interleukin
IL6R	Interleukin 6 receptor
INSR	Insulin receptor
IRF2	Interferon regulatory factor 2
ITGB8	Integrin beta-8
IV	Inverse variance
JAK1	Janus kinase 1
KEAP1	Kelch-like ECH-associated protein 1
KIT	Mast/stem cell growth factor receptor
KLRB1	Killer cell lectin-like receptor B1
LAPTM5	Lysosomal-associated transmembrane protein 5
LC3	Microtubule-associated protein light chain 3
lncRNA	Long non-coding RNA
LT	Liver transplant
MAFLD	Metabolic dysfunction-associated fatty liver disease
MAM	Meprin-like protease/A5 antigen/receptor tyrosine phosphatase μ and κ
MAPK	MAP kinase
MDR1	Multidrug resistance protein 1
MDSCs	Myeloid-derived suppressor cells
MEK	Mitogen-activated protein kinase kinase
MET	Hepatocyte growth factor receptor
METTL1	tRNA (guanine-N(7)-)-methyltransferase
METTL3	N6-methyladenosine
miRNA	MicroRNA

MMPs	Matrix metalloproteinases
MRI	Magnetic resonance imaging
MTD	Maximum tolerable dose
mTOR	Mammalian target of rapamycin
MTT	3-(4,5-dimethylthiazol-2-yl)-2,5-diphenyl-tetrazolium bromide
MWA	Microwave ablation
NASH	Non-alcoholic steatohepatitis
NAFLD	Non-alcoholic fatty liver disease
NF1	Neurofibromin
NF-κB	Nuclear factor-κB
NOS	Newcastle-Ottawa scale
NQO1	NAD(P)H dehydrogenase [quinone] 1
Nrf2	Nuclear factor erythroid 2-related factor 2
NRPs	Neuropilins
NSCLC	Non-small cell lung cancer
OCT1	Organic cation transporter 1
OR	Odds ratio
ORR	Objective response rate
OS	Overall survival
p62/SQSTM1	Sequestosome-1
P/S	Penicillin/Streptomycin
PBS	Phosphate buffered saline
PBS-T	0.05% PBS-Tween 20
pDCs	Plasmacytoid dendritic cells
PDGFR	Platelet-derived growth factor receptor
PDZ	PSF-95/Dlg/ZO-1
PE	Phosphatidylethanolamine
Pearson-CC	Pearson-coefficient correlation
PFS	Progression-free survival
PHDs	Prolyl-4-hydroxilases
PI3K	Phosphatidylinositol 3-kinase
PI3P	Phosphatidylinositol-3-phosphate
PIVKA-II	Vitamin K deficiency or antagonist-II
PPT1	Palmitoyl-protein thioesterase 1
PRISMA	Preferred Reporting Items for Systematic Reviews and Meta-Analyses
PS	Performance status

PVDF	Polyvinylidene difluoride
qRT-PCR	quantitative real-time reverse transcription polymerase chain reaction
REML	Restricted Maximum Likelihood
RET	Proto-oncogene tyrosine-protein kinase receptor
RFA	Radiofrequency ablation
RFS	Recurrence-free survival
ROS	Reactive oxygen species
RT	Room temperature
RTKs	Tyrosine kinase receptors
SCAP	SREBP cleavage-activating protein
SD	Standard deviation
SDS	Sodium dodecyl sulfate
SDS-PAGE	SDS-polyacrylamide gel electrophoresis
SEA	Serine-glutamic acid-alanine
SEMA3	Class 3 semaphorins
SHARP	Sorafenib Hepatocellular Carcinoma Assessment Randomized Protocol
SIP1	SMAD-interacting protein 1
SNAI1	Snail homolog 1
sNRP1	Soluble form of NRP1
sNRP2	Soluble form of NRP2
SREBP2	Sterol regulatory element-binding protein 2
STAT	Signal transducer and activator of transcription
STOML2	Stomatin-like protein 2, mitochondrial
SVR	Sustained virologic response
TACE	Transarterial chemoembolization
TAMs	Tumor-associated macrophages
TARE	Tumor radioembolization
TCGA	The Cancer Genome Atlas
TEC	Tumor-associated endothelial cell
TEMED	Tetramethylethylenediamine
TERT	Telomerase reverse transcriptase
TGF-βR	Transforming growth factor-β receptor
TIMPs	Inhibitors of MMPs
TKI	Tyrosine kinase inhibitor
TNF-α	Tumor necrosis factor α

TNM	Tumor-node-metastasis
TTP	Time to progression
TTR	Time to recurrence
TXNRD1	Thioredoxin reductase 1
UCSC	University of California Santa Cruz
ULK1	ATG1/unc-51-like autophagy activating kinase 1
USP2-AS1	Ubiquitin specific peptidase 2 antisense RNA 1
VEGFR	Vascular endothelial growth factor receptor
VPS15	Phosphoinositide 3-kinase regulatory subunit 4
VPS34	Phosphatidylinositol 3-kinase catalytic subunit type 3
WIPI	WD repeat domain phosphoinositide interacting protein
WOS	Web Of Science
YAP	Yes-associated protein
YRDC	Threonylcarbamoyl-AMP synthase

1 Abstract

Hepatocellular carcinoma (HCC), the main type of primary liver cancer, constitutes the sixth most common and third most deadly cancer worldwide, respectively. Due to the late diagnosis and the molecular heterogeneity of this tumor, the clinical onset of HCC patients remains complex, with a high rate of therapeutic failure and recurrence. Although novel findings have been accomplished in recent years, the precise mechanisms underlying the processes of tumor development, progression and drug responsiveness remain unclear. In this line, autophagy, responsible for the maintenance of cell homeostasis, acts as a double-edged process in cancer, displaying a key function in the progression and cellular response to targeted drugs. Furthermore, increasing evidence highlights the crucial role of the hypoxic microenvironment in the chemoresistance development in solid tumors, and mainly in HCC, where the hypoxia-inducible factor 1α (HIF-1α) acts as the main mediator of the cellular response to hypoxia.

The interplay between these mechanisms is closely associated to the therapeutic use of tyrosine kinase inhibitors (TKIs), such as lenvatinib, that primarily act by disrupting tumor angiogenesis through inhibition of tyrosine kinase receptors (RTKs) activity. The transmembrane glycoprotein neuropilin-1 (NRP1) has exhibited an interesting function in the modulation of tumor-associated signaling pathways and processes by interacting with key RTKs, such as vascular endothelial growth factor receptor (VEGFR) or platelet-derived growth factor receptors (PDGFR) among others, and their corresponding ligands. Despite the interesting role that NRP1 seems to have in cancer cell survival and drug efficacy, fewer studies have evaluated the potential value of NRP1 as a tumor biomarker or therapeutic target in HCC.

For this reason, we aimed at assessing the clinical significance of the receptor NRP1 in the prognosis, diagnosis and other tumor-associated features in HCC patients, as well as to determine the role of NRP1 in the underlying mechanisms of lenvatinib efficacy with potential implication in the loss of cellular sensitivity to lenvatinib.

To accomplish these purposes, we conducted a systematic review with meta-analysis including all the articles that evaluate the clinical correlation of NRP1 overexpression with tumor prognosis, development and/or other clinicopathological features in patients diagnosed with HCC. On the other hand, we confirmed these results using datasets of human HCC samples from publicly available databases, and we also assessed the potential role of NRP1 in the lenvatinib efficacy employing three HCC cell lines, HepG2, Hep3B and Huh-7 as the *in vitro* model for the experimental study.

Initially, a total of 1305 patients from seven articles were included in the quantitative analysis, where approximately 53.81% of patients exhibited NRP1 overexpression. After meta-analysis, increased levels of NRP1 showed to be significantly correlated with poor prognosis, represented by shorter overall survival (OS), as well as with tumor pathogenesis by observing higher NRP1 expression in tumor tissue samples from 692 HCC patients. In addition, a significant association was found between NRP1 overexpression and patient's age, younger than 50 years old, and increased risk of venous invasion, highlighting the potential of NRP1 as a tumor biomarker in HCC.

Meanwhile, results from the experimental study showed higher NRP1 levels in HCC samples from public databases compared to normal liver tissue, and a strong correlation with advanced tumor stages and nodal metastasis status. When analyzed in an *in vitro* model of HCC, NRP1 was overexpressed in the Hep3B and Huh-7 cell lines in comparison to the HepG2 HCC line, also showing a higher susceptibility to lenvatinib the Hep3B and Huh-7 cells. Analysis of cell proliferation and migration revealed that NRP1 downregulation derived from lenvatinib treatment was involved in the antitumor effects of this drug. To deeply evaluate the potential role of NRP1 in the underlying mechanisms of the lenvatinib effectiveness, we further analyzed the modulation exerted by lenvatinib in NRP1 expression. The double-edged process of autophagy was revealed as the main mechanism responsible for the lenvatinib-derived downregulation of NRP1 in the Hep3B and Huh-7 cell lines, where autophagy blockade restrained the lenvatinib efficacy, being prevented by specific NRP1 targeting. Furthermore, after hypoxia induction, protein levels of NRP1 were significantly diminished through a hypoxia-related autophagy increase. Interestingly, NRP1 expression was also modulated by HIF-1α, showing lower levels of NRP1 after HIF-1α silencing. Even though autophagy blockade increased cell survival even after hypoxia induction and lenvatinib treatment, gene silencing of HIF-1α achieved to prevent this loss of lenvatinib effectiveness and the recovery of protein NRP1 expression in Hep3B and Huh-7 cell lines.

Altogether, results from this study suggest that NRP1 might constitute a valuable biomarker for prognosis, diagnosis and risk of invasion in patients with HCC, together with the potential role that NRP1 seems to play in the underlying mechanisms of the lenvatinib efficacy in HCC cells, where both the double-edged autophagy and the HIF-1α-related hypoxia response are involved. Therefore, NRP1 could be a novel tumor biomarker and therapeutic target for improving the clinical landscape of advanced HCC.

2 Introduction

Liver cancer is a highly common and deadly disease worldwide, where hepatocellular carcinoma (HCC) represents 75%-85% cases. HCC is characterized by a complex molecular heterogeneity associated to the broad diversity of etiologic agents that accounts for hepatocarcinogenesis. Furthermore, most HCC cases are diagnosed in advanced stages, due to the absence of symptoms at initial stages and the cirrhotic background. Although patients with early HCC can be subjected to curative treatments, such as hepatic resection or liver transplant, most of them are late diagnosed and, in consequence, not eligible for curative but for palliative therapies. Systemic therapy remains the only available option against advanced HCC, where current therapies, represented by tyrosine kinase inhibitors (TKIs) and monoclonal antibodies, have ameliorated the therapeutic landscape. Unfortunately, survival is increased only for up to two years, which highlights the necessity of further investigations to improve the patient's outcomes in these stages.

TKIs constitute the backbone of the systematic treatment of this type of cancer, where sorafenib remained the only molecular targeted drug available for the treatment of advanced HCC for over a decade. Only lenvatinib proved to be as effective as sorafenib in the first-line treatment, leading to its approval in 2018 and establishing a key starting point in the therapeutic landscape of HCC. Nonetheless, as previously observed with sorafenib, tumor cells are able to develop an adaptive response that abolish drug effectiveness and trigger resistance acquisition. Although several studies have focused on the identification of the cellular and molecular processes involved in the loss of drug sensitivity, the exact mechanisms are still unknown.

Neuropilin-1 (NRP1) is a transmembrane glycoprotein from the neuropilins (NRPs) family located in the cell membrane of different cell types, such as hepatocytes. NRP1 acts as a coreceptor of key proteins involved in signaling pathways that drives survival and progression of cancer cells, including several growth factors and their corresponding receptors. For this reason, recent investigations have evaluated the likely role of NRP1 in the different steps of hepatocarcinogenesis, HCC progression, as well as drug responsiveness. Even though angiogenesis and migration ability of tumor cells seem to be the main processes directly modulated by NRP1 in HCC, recent findings have revealed a broader number of processes modulated by this protein, highlighting the potential of NRP1 in the research field of HCC.

Multiple cellular processes interact and participate in the tumor development and progression. Among them, autophagy has exhibited a double-edged role by acting either as a tumor suppressor or promoter mechanism depending on the HCC stage. Autophagy is a self-degradative process that, under physiological conditions, maintains cellular homeostasis by removing damaged proteins and organelles. However, under pathological conditions, autophagy is differentially modulated as part of the cellular response to stress signals, promoting or disrupting tumor progression in HCC. Moreover, drug responsiveness is also influenced by autophagy, which has shown to endorse loss of drug efficacy in HCC cells. Nevertheless, the precise role played by autophagy in HCC is still uncertain.

Tumor microenvironment is essential for tumor progression. Solid tumors, such as HCC, are characterized by a hypoxic microenvironment caused by the excessive cell proliferation and oxygen demand compared to the oxygen supply. Under hypoxia conditions, the hypoxia-inducible factors (HIFs) mediate the cellular response, in which HIF-1α represents the main transcription factor involved in tumor hypoxia. Induction of a HIF-1α-related hypoxia response has been strongly associated to an increased cell survival, proliferation, angiogenesis, invasion and migration abilities, among others, that promote tumor aggressiveness. Additionally, this transcription factor has exhibited to prompt an adaptive cell response after sustained treatment with molecular targeted drugs, e.g. sorafenib, which conduct to the development of drug resistance and, therefore, therapeutic failure.

Overall, human HCC remains a global challenge, where multiple processes are involved in the development, progression and drug resistance acquisition. Despite novel findings, further studies need to be conducted to clarify the precise mechanisms underlying HCC, in order to identify useful biomarkers and potential targets that improve the clinical landscape of patients with advanced HCC.

3 Literature review

3.1 HEPATOCELLULAR CARCINOMA

Primary liver cancer constitutes an important health problem due to the high incidence and mortality rates, which are also expected to increase in the future[1]. This cancer type is characterized by a complex molecular heterogeneity[2] and is constituted by different malignant tumors[3]. The major primary liver tumor is hepatocellular carcinoma (HCC), which accounts for 75%-85% of cases, followed by intrahepatic cholangiocarcinoma (iCCA), 10%-15% of cases, and other less common malignancies, such as hepatoblastoma, angiosarcoma or hepatocellular adenoma[1,3,4].

3.1.1 Epidemiology

Among all tumor types, liver cancer remains a leading cause of cancer-related death, standing as the sixth most common and the third most deadly cancer worldwide, after lung and colorectal tumors[1,5] (**Figure 1A**).

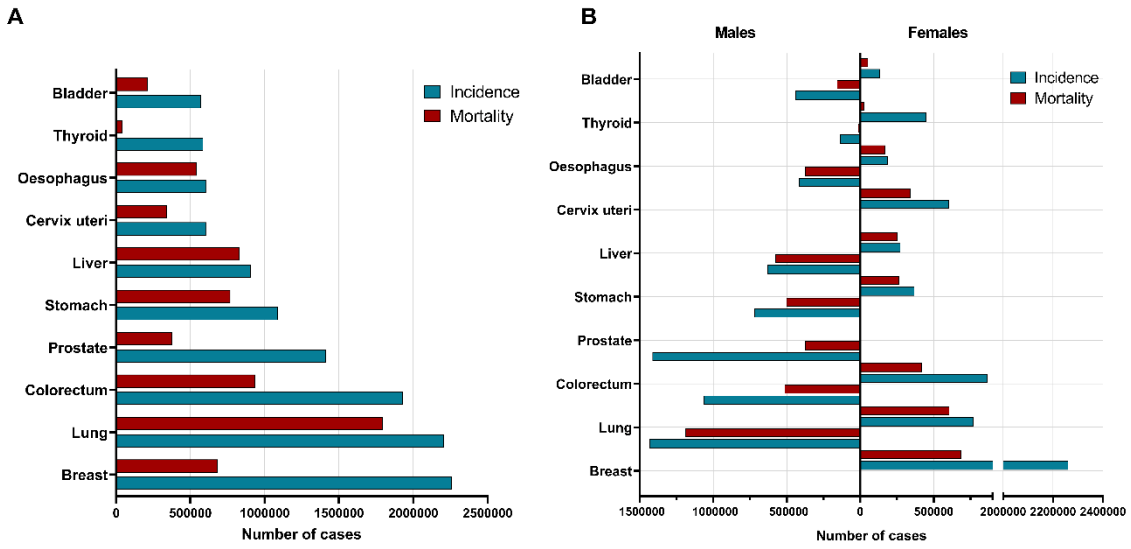

Figure 1. Estimated number of cases and deaths for the top 10 most common cancers in 2020 for (**A**) both sexes, (**B**) men and women, with data from GLOBOCAN 2020. Available online and modified from [6].

In terms of incidence, more than 900,000 cases were diagnosed in 2020, with a 2.3-fold higher rate in men, placing liver cancer as the fifth and the seventh most commonly diagnosed tumor in men and women, respectively[1,4] (**Figure 1B**). Marked differences are also observed in the mortality rates by sex, being the second and the sixth cause of cancer-related death in men and women, respectively; liver cancer accounted for

approximately 830,000 deaths in 2020, which highlights the elevated mortality rate of this tumor type[1] (**Figure 1B**).

The worldwide incidence is highly heterogeneous because of the diverse prevalence of the risk factors[2,5]. Approximately 80-85% of liver cancer cases occur in low or middle-resource countries, mainly in sub-Saharan Africa and Eastern Asia, where chronic hepatitis B infection and aflatoxin B1 (AFB1) stand as the main risk factors[2,7]. In other countries, such as Japan, Italy and Egypt, hepatitis C virus (HCV) infection is the predominant cause of liver cancer development, while in Mongolia co-infections of hepatitis B virus (HBV) and HCV mainly contribute to the high burden[1,2]. Although these countries are high-risk areas of liver cancer, the incidence and mortality rates have decreased in the last years due to the vaccination campaigns against HBV and a lower exposure to AFB1[1]. On the other hand, low-risk countries, which include those across Europe, Northern America, Australia, and South America, have experienced an increase in the incidence and mortality possibly caused by a higher prevalence of obesity and diabetes among population, as well as alcohol consumption[1,5,7].

3.1.2 Etiology

Pathogenesis of HCC is complex and involves multiple molecular alterations, being mostly developed in the setting of chronic liver disease[4,5]. Viral infections by HBV and HCV are the main risk factors, accounting for 80% of HCC cases[7], followed by alcohol, diabetes, obesity-related non-alcoholic steatohepatitis (NASH) and non-alcoholic fatty liver disease (NAFLD), among other[5,8] (**Figure 2**).

Viral infections

Chronic hepatitis caused by HBV and HCV is a crucial risk factor for HCC, in which HBV infection is associated to 50-60% of HCC cases[4,8]. However, prevalence of both HBV and HCV shows differences based on the geographic localization[4].

HBV is a double-stranded DNA virus able to integrate into the host genome[4,8] strongly associated to HCC development in regions of Africa and East Asia[5,7]. Most cases of HBV-derived HCC are detected by measuring Hepatitis B Surface Antigen (HBsAg), which is used for definition of chronic infection when HBsAg persists for more than six months[4]. In addition, although cirrhosis is present in 80%-90% of HCC cases, HBV is able to promote HCC even in the absence of cirrhosis, increasing the risk of HCC[4,7,8]

(**Figure 2**). For this reason, HBV immunization should be further implemented in more regions, since HBV vaccination is estimated to markedly reduce HCC incidence particularly in Asia and sub-Saharan Africa[5,8].

Additionally, risk derived from HBV infection could be potentiated by a hepatitis D virus (HDV)/HBV co-infection[8]. HDV is an RNA virus able to replicate only in presence of HBV surface antigens, which has been related to increase severity of liver disease progression. Several studies suggest that there is a higher HCC risk by co-infection of HBV/HDV than HBV infection alone[8].

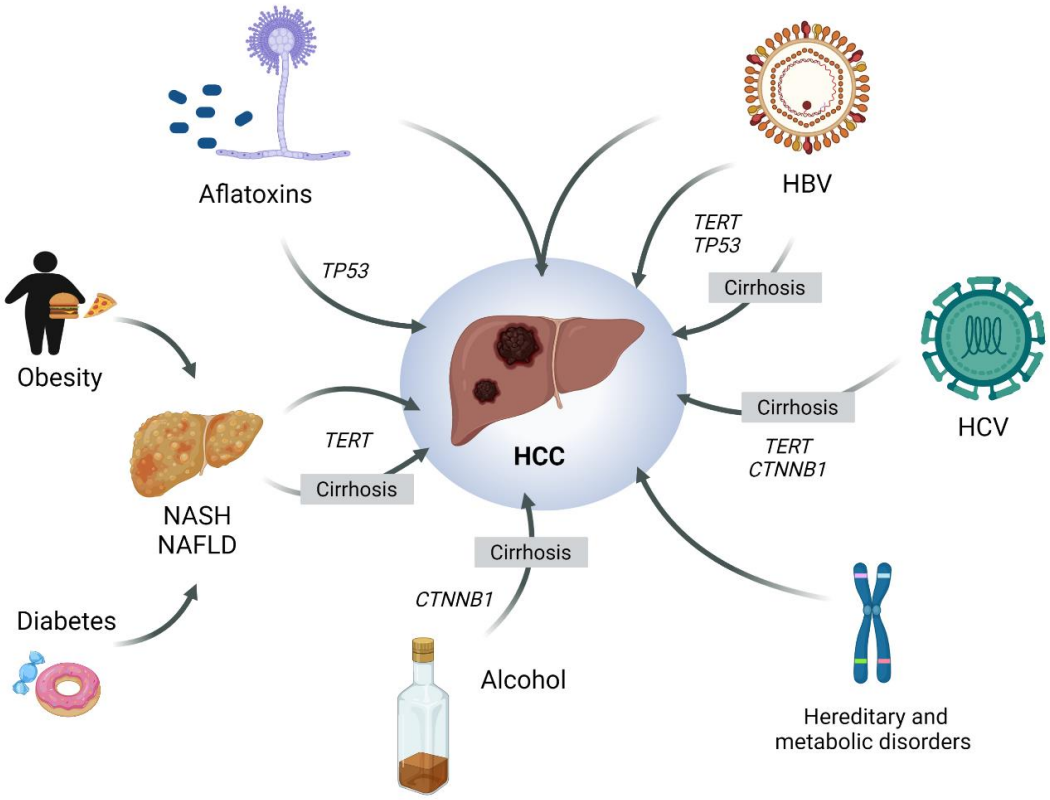

Figure 2. Main etiologic agents of HCC. Representation of the main risk factors for HCC development with the major genetic alterations associated to each one and the probability of a cirrhosis-mediated induction of HCC. CTNNB1, catenin beta-1; TERT, telomerase reverse transcriptase. Created with BioRender.com.

On the other hand, HCV is a single-stranded RNA virus that encodes structural and nonstructural viral proteins, and, unlike HBV, this virus does not integrate into the host genome[4,8]. HCV infection remains the most common cause of HCC development in Europe, North America and Japan[7,8] (**Figure 2**) and, although there are not vaccine available, antiviral therapies are able to decrease HCC incidence[5]. Risk of HCC caused

by HCV infection is mainly associated to the presence of cirrhosis as well as a sustained virologic response (SVR), being recommended a close surveillance of patients[5,8].

NASH and NAFLD-derived HCC

Among population of developed countries, prevalence of diabetes and obesity is very high and predicted to increase, which places NASH and NAFLD as major risk factors of HCC in these regions[5,7]. Despite the incidence of viral-induced cirrhosis is higher than NASH-derived cirrhosis, growing evidence prove that both NASH and NAFLD strongly contribute to HCC development[5,8] (**Figure 2**). Moreover, NASH is considered a precursor step of HCC in patients diagnosed with diabetes or obesity and is one of the main causes of cirrhosis[8]. Whereas NAFLD shows a lower risk of HCC than NASH, the increasing number of individuals diagnosed with NAFLD places it as one of the main risk factors, with a 2.6-fold increased risk of HCC in NAFLD patients[5,7].

These metabolic disorders are closely associated to the high levels of sedentary behavior in recent years, which has aroused for a new term of metabolic dysfunction-associated fatty liver disease (MAFLD) to replace the previous term NAFLD[9]. This liver disease is originated by a systemic metabolic dysfunction and has a complex and heterogeneous pathophysiology mainly modulating liver metabolism[9]. Together with NASH, MAFLD represents a key risk factor of HCC in developed countries[5,9].

Alcohol

Chronic alcohol consumption also represents a risk factor of HCC development, which is proportional to the alcohol intake[4]. In particular, alcoholic cirrhosis is the second most common risk factor in countries of Europe and USA[7]. Excessive alcohol consumption leads to a chronic liver damage characterized by a steatotic liver, which is followed by cirrhosis and HCC, and, along with NASH, alcohol abuse accounts for most cirrhosis-derived HCC cases[4,8] (**Figure 2**).

Several studies have also described that alcohol intake increases the risk of HCC from other etiologies, such as HBV-derived hepatitis, since some of these etiologic agents share pathophysiological features during hepatocarcinogenesis[8].

Aflatoxins

Aflatoxins are toxic compounds with strong hepatocarcinogenic properties produced by different fungal species, mainly by *Aspergillus flavus*[4,7]. These mycotoxins are usually found as contaminants of staple cereals and oilseeds in areas of Africa and Asia[5,7] and, although there have been described more than 20 different aflatoxins, AFB1 is distinguished as the most hepatocarcinogenic toxin[4] (**Figure 2**). Derived effects from aflatoxin exposure in the liver are strongly associated to mutations on the codon 249 of *TP53* gene as the main driver of hepatocarcinogenesis in patients from regions with a high aflatoxin-associated risk of HCC[5,7].

Dietary intake of AFB1 is a relevant co-factor for HCC development due to the high increment of HCC risk that AFB1 has in HBV-infected patients[4,5]. Both etiologic agents are able to increase up to 70% the risk of developing HCC[4]. The strong interaction observed between them is due to the ability of HBV for inducing the AFB1 metabolization through cytochrome P450, generating the mutagenic metabolite AFB1-8,9-epoxide, which in turn induces DNA damage in the hepatocytes[4,7].

Other factors

There are several factors that also contribute to HCC development, not as independent factors but strongly increasing the HCC risk[4,8].

Different sociodemographic characteristics are directly associated to a higher risk of HCC, including age, sex and ethnicity, among others[8]. Particularly, individuals older than 70 years have an increased probability of developing this liver tumor, existing also a male predominance in HCC cases and Hispanic people[8]. Daily habits such as smoking, and diet have also been described as risk factors for HCC, although the precise role is still unclear[8].

In addition to environmental agents, genetic factors are markedly related to an increased risk of HCC development[4]. Among them, there are different genetic conditions that are predisposing, but interaction with another etiologic agent is crucial for developing HCC[4]. This group of agents is constituted by a broad variety of chronic liver diseases, from hereditary to metabolic pathologies, which includes alpha 1-antitrypsin deficiency, autoimmune hepatitis, hereditary hemochromatosis, porphyria, tyrosinemia type 1 and glycogen storage diseases[4,7] (**Figure 2**).

Interestingly, aside from risk agents, protective factors that reduce the risk of developing HCC have also been identified[7,8]. Coffee, aspirin, metformin or statins have proved to protect from HCC development in several observational studies, being coffee consumption recommended by the European Association for the Study of the Liver (EASL) clinical guidelines for HCC[7].

The broad diversity of etiologic agents that may be involved in the development of this liver cancer is also associated to the complex heterogeneity found in the hepatocarcinogenic process described below.

3.1.3 Hepatocarcinogenesis

Hepatocarcinogenesis is a complex multistep process that represents the molecular heterogeneity of HCC and usually takes place in the context of liver cirrhosis[7,10,11]. Different genetic, molecular and cellular alterations are involved in the development of HCC, with an interesting role of the microenvironment[3,8,12].

Molecular drivers

Recent advances using high throughput analysis have yielded relevant progresses in the genomic field of HCC, identifying cancer driver genes with oncogenic or tumor suppressor roles[8,12]. Both genetic and epigenetic alteration mechanisms are responsible for the malignant transformation of dysplastic liver nodules[13]. Most genetic alterations observed during HCC development are telomerase reverse transcriptase (*TERT*) promoter mutations leading to telomerase activation, chromosome translocations, viral insertions or gene amplifications, which have been identified in approximately 80% of HCC cases[8].

Specific mutations in the *TERT* promoter or in genes such as catenin beta-1 (*CTNNB1*) (encoding β-catenin), and *TP53* (a key regulator of cell cycle), are the most common genetic alterations observed in carcinogenesis[7]. Telomere shortening is a very frequent event during hepatocarcinogenesis and is accentuated in chronic liver injury[12]. Somatic mutations in *TERT* promoter are observed in 44%-65% of HCC patients, although *TERT* promoter amplifications, translocations and viral insertions have also been identified in 20% of cases[7,12,13]. Less common genetic alterations are also present during HCC development, in which 11%-37% of patients presents mutations in *CTNNB1* and *AXIN1* genes, triggering the activation of the Wnt/β-catenin pathway[11,12]. Likewise, *TP53* pathway mutations are identified in 18%-50% of HCC patients, being considered a

driver mutation, where the codified protein p53 acts as a tumor suppressor and its loss prompts HCC progression[3,12]. Even though these represents the main genetic alterations that occur during hepatocarcinogenesis, several investigations have also identified numerous gene mutations with a key role, such as AT-rich interaction domain 1A (*ARID1A),* AT-rich interaction domain 2 (*ARID2),* cyclin dependent kinase inhibitor 2A (*CDKN2A),* Janus kinase 1 (*JAK1),* interleukin 6 receptor (*IL6R),* Kelch-like ECH-associated protein 1 (*KEAP1)* genes, among others[11,12].

Epigenetic has become an interesting field, due to its relevance in several human pathologies, mainly in different cancers including HCC[12]. DNA hypermethylation, including abnormal promoter methylation, histone modifications via methylation or acetylation, or chromosome remodeling are very frequent events in the complex process of hepatocarcinogenesis[3,12].

Specific HCC etiologies are correlated with some of these molecular alterations[7]. The most common molecular drivers, *TERT* promoter and *TP53* mutations, are widely observed in HBV-derived HCC cases, whereas mutations in the *CTNNB1* gene are associated with an alcohol-derived etiology[7,8,11] (**Figure 2**). Likewise, NASH or NAFLD-associated HCC development have been related to alterations in interleukin (IL)-6-JAK-signal transducer and activator of transcription (STAT) signaling pathways without *CTNNB1* or *TP53* mutations[7,14], and AFB1 exposure leads to a specific *TP53* mutation hotspot in HCC patients[10,11] (**Figure 2**).

Cellular origin

The cellular origin of HCC is still uncertain considering the high heterogeneity found in this liver tumor, in which cell plasticity has emerged as a key concept[8,11]. Although initial studies focused on the role of stem cells as the cellular source of HCC, increasing evidence accounts for mature hepatocytes as the main source[8]. Mature hepatocytes are long-lived cells with proliferative potential and plasticity, that could transform and express progenitor cell markers[8,11]. Interestingly, two different hypotheses have been established as possible ways of mature hepatocytes to generate liver tumor cells, by directly transforming into cancer cells which experience sequential genetic and molecular alterations, or by dedifferentiating into precursor cells that could lately transform into HCC cells[13].

Role of the microenvironment

The development of HCC is a multistep process in which the molecular and cellular components play a key role[10,11]. Hepatic injury and inflammation accounts for the majority of HCC cases, more than 90%, and are derived from the viral infection with HBV or HCV, AFB1 exposure, excessive alcohol consumption, and NAFLD or NASH[3,11]. Chronic damage in the liver leads to the recruitment of macrophages, lymphocytes, hepatic stellate cells (HSCs), that interact with hepatocytes[10,11]. Although the exact mechanisms responsible for inducing the first steps of HCC carcinogenesis are still unclear, there are some key mediators that have been described, which include the nuclear factor-κB (NF-κB) and JAK/STAT pathways[3,10].

A chronic injured and inflammatory microenvironment promotes the activation of HSCs, responsible for secreting cytokines, such as IL-6 and tumor necrosis factor α (TNF-α), producing extracellular matrix (ECM) components, increasing tissue stiffness and promoting immunosuppression[3,10,11]. An excessive production of ECM components, mainly collagen, together with cytokines, growth factors, prostaglandins and pro-angiogenic factors endorse the establishment of a pro-tumorigenic stroma[3,10]. Not only HSCs, but also other cell populations including hepatic fibroblasts, macrophages and endothelial cells modulate the response to the chronic liver damage, contributing to the loss of hepatic architecture, and hepatic fibrosis development[11,12]. The interplay between all the genetic, molecular and cellular components leads to the survival of damaged hepatocytes that avoid cell death and immune-mediated suppression, leading to cirrhosis[3,8] (**Figure 3**).

The pathway to carcinogenesis is complex and the etiology has a key role, being described different molecular and cellular patterns in the development of NAFLD-derived HCC from other etiologies[14,15]. Insulin resistance, hyperinsulinemia or an increased angiogenesis are some of the main mechanisms involved in the process of HCC pathophysiology from a liver steatosis[14,15]. However, this process shares some characteristics with viral or alcohol-induced HCC, since cell populations of the immune system also participate and several cytokines, IL-6, TNF-α, leptin, resistin, are released and promote carcinogenesis[14] (**Figure 3**).

Regardless of etiology, cirrhosis precedes HCC in 80%-90% of cases[3,12]. Initially, an established cirrhotic state of the liver is constituted by nodules of abnormal and immature hepatocytes that compose pre-malignant lesions known as dysplastic foci (<1 cm) and dysplastic nodules (≥1 cm)[11,12] (**Figure 3**). Hepatocytes from these pre-neoplastic lesions accumulate more genetic and epigenetic mutations, progressing to early-stage HCC and, in turn, to advanced HCC[3,11] (**Figure 3**). A minority of HCC cases develop in absence of cirrhosis, approximately 20% of cases, in which chronic HBV infection or NAFLD seem to act as a pro-tumorigenic background that leads to HCC development[11].

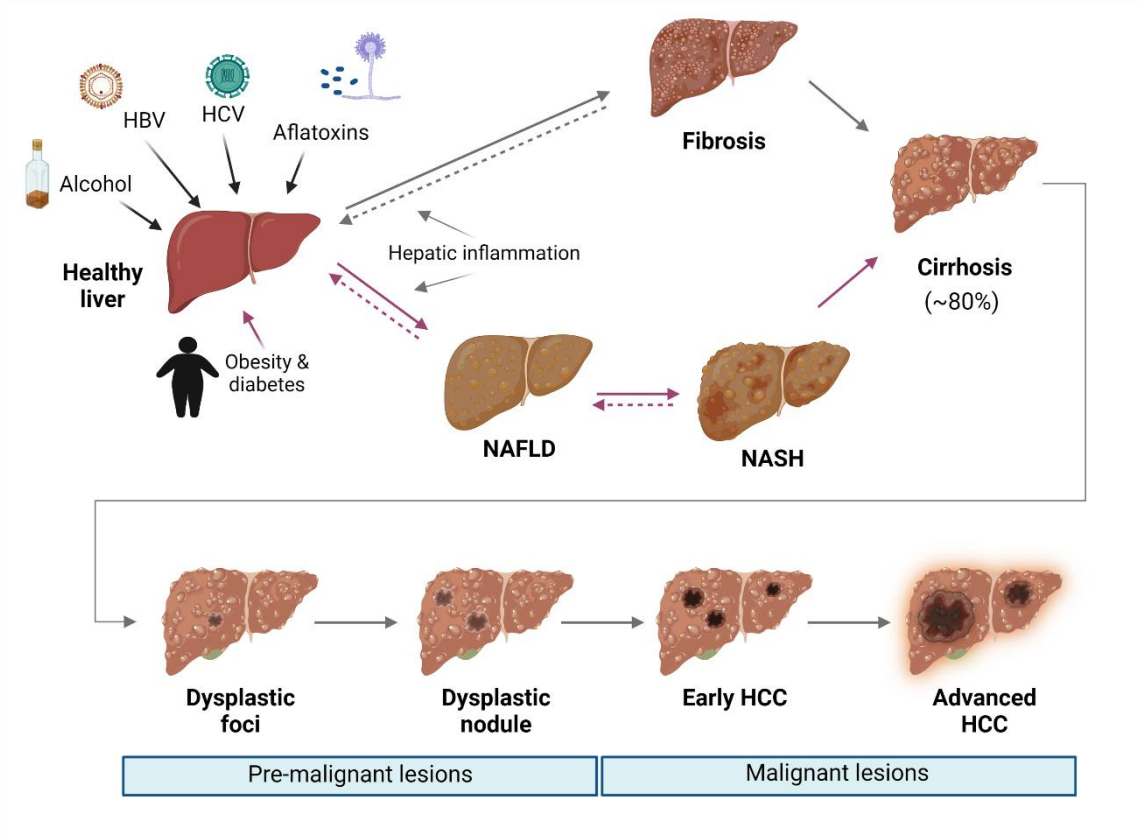

Figure 3. Successive stages of hepatocarcinogenesis in a cirrhotic liver. Several etiology agents are responsible for inducing a chronic liver damage characterized by a pro-inflammatory microenvironment. Hepatocytes experience cycles of necrosis-regeneration and accumulate genetic and epigenetic alterations. Different cell types, such as HSCs, macrophages or fibroblasts, are recruited and secrete cytokines and growth factors that promote fibrosis and, in turn, cirrhosis. Steatosis-associated injury in the liver triggers the development of NAFLD that could advance to NASH establishment. Regardless of etiology, 80% of cases progress to a cirrhotic state of the liver, in which pre-neoplastic lesions could emerge as a consequence of mutations accumulation in hepatocytes, to ultimately turn into HCC. Created with BioRender.com.

3.1.4 Patient surveillance and HCC diagnosis

Given that most HCC cases develop in the context of a chronic hepatitis, patients could benefice from clinical surveillance to detect HCC in an early stage[8,11]. Surveillance programs aim at reducing the disease-related mortality by including patients with cirrhosis or chronic hepatitis[11,16]. Criteria for the inclusion of patients in these surveillance programs is based on the potential risk for developing HCC as well as on cost-effective analysis[2,16]. Patients with chronic HCV infection and fibrosis are eligible, while those diagnosed with NAFLD without a cirrhotic background will not be enrolled[11]. A chronic hepatitis caused by HBV has different risk depending on several characteristics of the patient, such as age, liver fibrosis, genotype C, among others[2,11]. Even though numerous investigations demonstrated the survival benefits of HCC surveillance, current information is still limited to validate HCC risk and perform a proper enrollment[11,16]. The recommended techniques for screening during HCC surveillance are the ultrasonography with or without alpha fetoprotein (AFP), since AFP has lower effectiveness in early-stage HCC[8,16].

At initial stages, HCC is asymptomatic and, in consequence, diagnosis is hindered and frequently delayed to advanced stages when curative options are not available[16,17]. Nonetheless, management of HCC has improved in the last decade, in which novel diagnostic tools have emerged as potential methods, such as liquid biopsy[8,11]. Nowadays, there are different options available for HCC detection including from imaging techniques to analytical determinations[16].

The preferred test for HCC diagnosis is ultrasonography, because of the high accessibility and tolerability of patients[2]. Sensitivity of this method ranges from 60% to 80% with a specificity higher than 90%[2,11], although both parameters depend on the tumor size, with the highest detection for a diameter of 3-5 cm[17]. During HCC screening in patients, ultrasonography should be performed every six months to get beneficial results[16].

Together with ultrasonography, the serum marker AFP is commonly used for diagnosis; however, its sensitivity is approximately 60% with a lower effectiveness in small HCCs in early stages[11,16]. In the clinical practice, the use of ultrasonography detection is usually accompanied by determination of AFP serum levels, increasing sensitivity from 45% to 63%[2,8]. On the other hand, some HCC cases have shown to be

AFP negative, hindering the early detection of this liver tumor[18]. In this line, some molecules have proved an interesting potential as HCC biomarkers, such as protein induced by vitamin K deficiency or antagonist-II (PIVKA-II), AFP-L3 or some microRNAs (miRNAs); nevertheless, further efforts are necessary to establish them in the clinical setting[2,18].

Among imaging techniques, computed tomography (CT) and magnetic resonance imaging (MRI) are also employed for HCC detection for lesions higher than 1 cm, after identification by ultrasonography[8,16]. Diagnostic by CT and MRI is based on the different brightness of the tumor tissue compared to the surrounding tissue, due to the blood supply that the malignant lesions received from the hepatic artery, while benign nodules are supplied by the portal system[8,11]. In this case, CT and MRI have an 89% sensitivity and 96% specificity[8].

Recent efforts have been focused on the rise of sensitivity of these diagnostic techniques, for example by using extracellular agents instead of hepatobiliary contrast on the MRI, and on the search of novel serum and tumor biomarkers that could be used in combination with the conventional marker AFP[2,8]. Nonetheless, when imaging tools fail to display a clear result, a biopsy should be requested to perform a suitable analysis[2,16]. This technique provides useful molecular information and has a sensitivity of 70%[8]. Moreover, the use of liquid biopsy as a source of potential serum biomarkers have increased the interest by providing specific and individualized information from the patient[11]. In this field, great advances have been accomplished in the last years that improved the precision and quality of the diagnostic tools[16].

3.1.5 Staging and management of HCC

After establishing the diagnosis of HCC, patients should be classified into prognostic groups based on several clinical parameters that would help clinicians to provide the best treatment option[19]. In the last decade the management of HCC has improved substantially and, despite there are more than 11 different staging systems, the Barcelona Clinic Liver Cancer (BCLC) classification is the most applied algorithm[8,19]. The BCLC staging system links HCC prognosis with the most suitable treatment option based on relevant clinical parameters that provide a strong clinical evidence[16] (**Figure 4**). The classification by BCLC establishes five groups (0, A-D) to identify HCC patients based on the tumor burden, the performance status (PS) and the liver function[16,20].

Assessment of tumor burden includes determination of the tumor size and number, and the presence or absence of invasion or extrahepatic metastasis[11,20]. The PS analysis usually includes the tumor-associated symptoms, regardless of the previous baseline symptoms of the patient, and patient PS is classified according to the Eastern Cooperative Oncology Group (ECOG) scale[19,20]. Finally, the patient liver function is assessed by the Child-Pugh score, however, this classification has a limited predictive power[11,20].

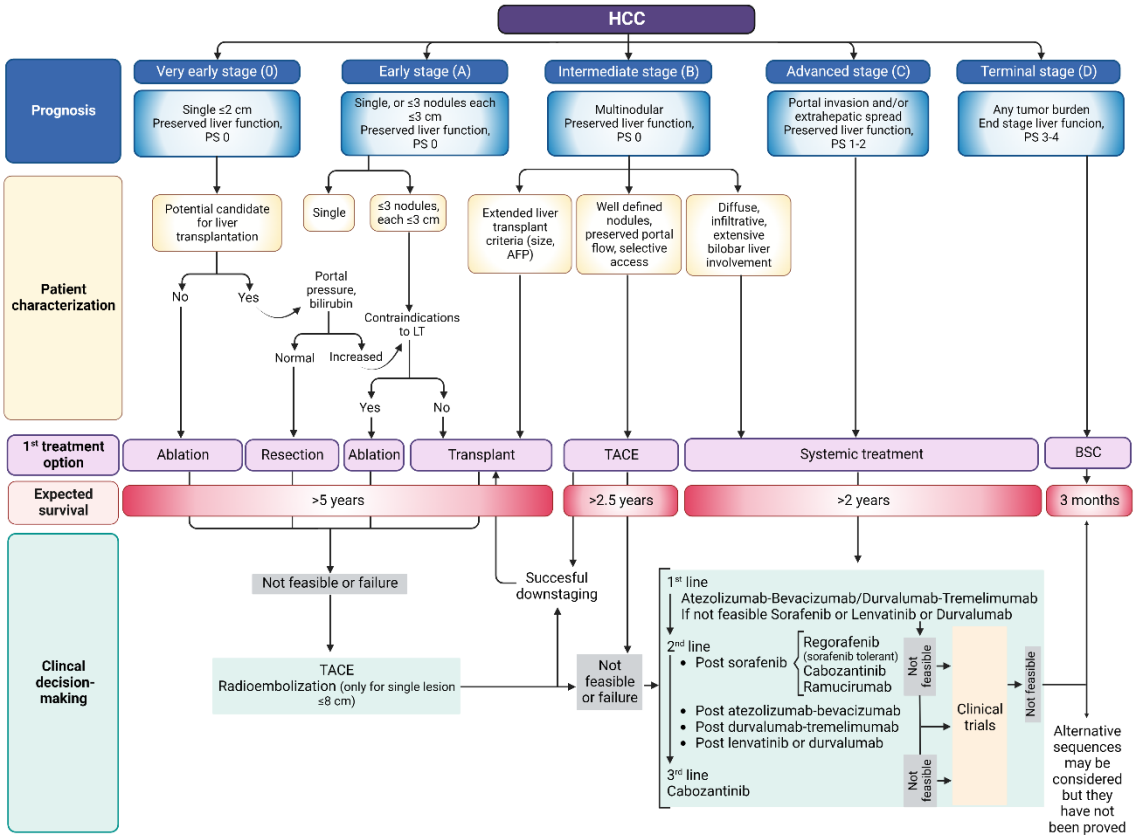

Figure 4. BCLC staging system and strategy in 2022. Classification of HCC patients based on tumor burden, PS and liver function to establish an association between cancer prognosis and clinical decision-making according to the BCLC system. The expected survival is expressed as median survival of each tumor stage and the liver function should be assessed with the Child-Pugh score. Figure adapted from [20]. BSC, best supportive care; TACE, transarterial chemoembolization. Created with BioRender.com.

As described in **Figure 4**, patients included in the very early stage (0) or early stage (A) are eligible for curative treatment options and have an overall survival (OS) rate of 50%-75% at 5 years[16]. In these groups, a single HCC nodule should be identified irrespective of the size, or either less than 3 nodules smaller than 3 cm[19,20]. Symptoms are not present in these stages, and liver function is preserved[19,20].

In the BCLC B group, intermediate stages, patients also lack symptoms and preserve liver function; nonetheless, multiple HCC nodules are identified without tumor spread or vascular invasion[16,19]. Most patients of this group require locoregional therapy, such as transarterial chemoembolization (TACE), which could provide up to four years of OS[16,20]. Some patients classified in an intermediate stage could reach the criteria for performing liver transplant (LT) if HCC nodules are well-defined, experiencing an improvement in the prognostic[20]. Nonetheless, a subgroup of patients could be also considered for systemic treatment when TACE therapy is not beneficial if HCC tumor is diffuse and infiltrative[20] (**Figure 4**).

For HCC tumors in which either vascular invasion or extrahepatic metastasis have occurred, patients are classified in an advanced stage (BCLC C), where curative treatment options are not further available[16,20]. Systemic therapy is the standard of care for this group, with a recent complex scheme lately discussed, that provides a median survival of approximately one year and up to two years[19,20] (**Figure 4**).

Patients with major tumor-related symptoms and impaired liver function are considered in the terminal stage (BCLC D), in which best supportive care (BSC) is selected to treat symptoms and there is a short survival expectancy[19,20] (**Figure 4**).

3.1.6 Treatment approaches

The objective of the treatment is to simultaneously increase patient survival and maintain a high quality of life[2]. The selection of the therapeutic strategy for each patient is based on the tumor stage according to the clinical parameters previously described by BCLC[8]. Among therapeutic approaches, surgical resection, liver transplantation and radiofrequency ablation (RFA), constitute the main curative treatment options; while TACE is selected for intermediate stages, and systemic treatment for advanced stages when no curative options are available[2,21].

Surgical therapy

Surgical treatment includes both hepatic resection and liver transplantation and yields the best patient outcomes, with a 5-year survival of 70%-80%[8]. Hepatic resection remains the treatment of choice in absence of cirrhosis to prevent life-threatening complications, whereas patients with cirrhosis are usually eligible for liver transplantation[2,21]. Nevertheless, the decision between both surgical options is more complex, since liver function, presence of portal hypertension, PS and other tumor characteristics should be considered[8,21]. Tumor recurrence is the main complication associated to hepatic resection, with a 70% of recurrence rate at 5 years, which can be differentiated between early (<2 years) or late (>2 years) recurrence[2,8].

Interventional radiologic and locoregional therapy

The characteristic arterial hypervascularity of HCC offers an interesting opportunity for the therapeutic landscape[22]. Firstly, methods such as ligation of the hepatic artery to interrupt tumor blood supply or hepatic artery infusion led to the development of the current transarterial embolization and TACE methods, which have demonstrated survival benefits in patients[2,22]. TACE has been established as the treatment of choice in intermediate-stage HCC, combining the blockade of the arterial blood supply with the injection of chemotherapy into the tumor[2,8]. However, potential efficacy of tumor radioembolization (TARE) has placed this procedure as an eligible option also for patients with intermediate-stage HCC[2]. TARE involves the delivery of glass or resin microspheres embedded with yttrium into the hepatic arteria and have shown a tumor response between 40% and 90% together with a survival increase[2,8].

Percutaneous ablation together with radiotherapy are the two major locoregional therapies employed for HCC[23]. In patients diagnosed with early HCC, image-guided tumor ablation is a broadly accepted treatment option, which aims at inducing tumor necrosis by temperature alteration or chemical administration and provides a better disease control[2,8]. Although percutaneous injection of ethanol is still recommended in some cases, RFA and microwave ablation (MWA) are the procedures established for HCC treatment by ablation[8,23]. Both RFA and MWA has demonstrated benefits in terms of treatment efficacy and patient response, being chosen mainly for early-stage HCC[8].

Molecular-targeted therapy

Patients with advanced HCC are eligible for systemic therapy[8]. The benchmark in the treatment landscape of advanced HCC was the Sorafenib Hepatocellular Carcinoma Assessment Randomized Protocol (SHARP) trial which triggered the approval in 2007 by the Food and Drug Administration (FDA) of sorafenib as the first drug available for advanced-stage HCC[8,11]. Sorafenib is an oral tyrosine kinase inhibitor (TKI) with multiple molecular targets that showed survival advantages[2,11]. TKIs are able to inhibit tumor progression through disruption of different signaling pathways associated to tyrosine kinase receptors (RTKs), such as vascular endothelial growth factor receptor (VEGFR), platelet-derived growth factor receptor (PDGFR), among others[3,11]. However, despite benefits observed with targeted therapy, for over a decade sorafenib remained as the only first-line drug approved for advanced HCC, until the approval of lenvatinib in 2017 by the FDA[3,24] (**Figure 5**). Since sorafenib approval, several advances have been accomplished in the systemic therapy, with regorafenib and cabozantinib as current available drugs for the treatment of HCC that developed resistance against sorafenib[8,11] (**Figure 5**). These systemic therapeutic options have achieved to increase patient survival for approximately 1-2 years[2].

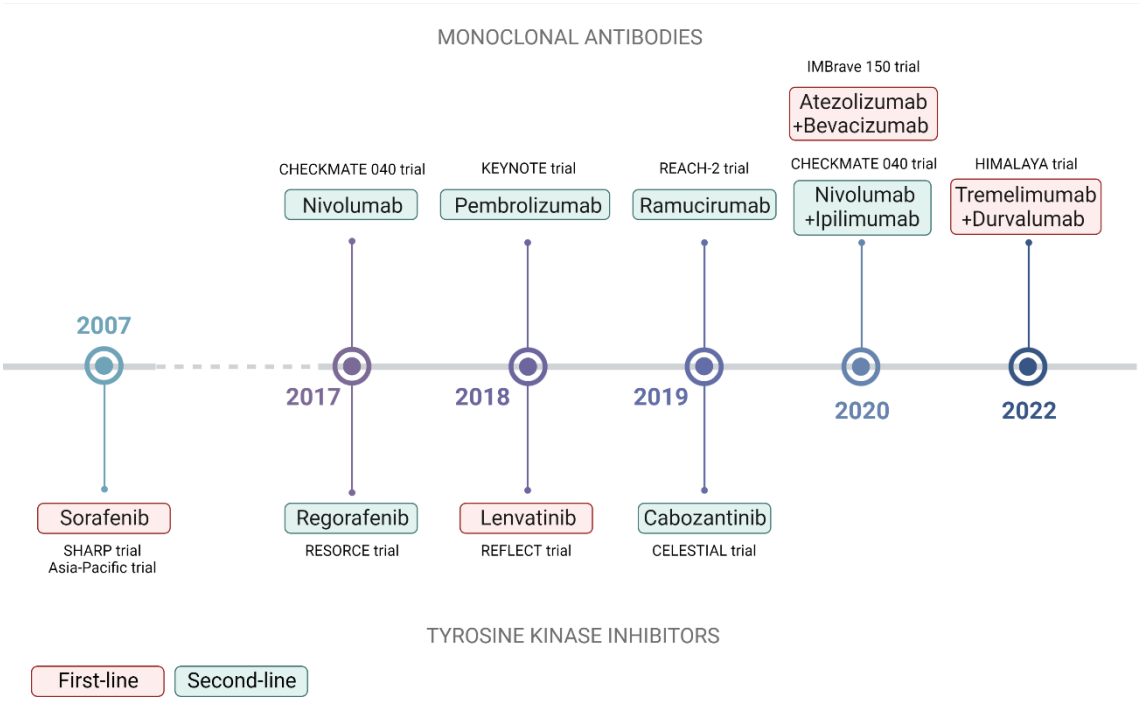

Figure 5. Timeline approval of the targeted drugs currently available for the treatment of advanced HCC. Graphical representation of the drugs and the trial that triggered their approval, as first-line treatment (red) or second-line treatment (green), for both monoclonal antibodies (top side) and TKIs (bottom side). Created with BioRender.com.

Immunotherapy

Immune-based treatments have been included in the therapeutic setting of HCC due to the effectiveness showed in several studies[10,25]. Immune checkpoint inhibitors are able to disrupt an immune-associated mechanism employed by cancer cells to avoid the immune response, thus promoting an effective patient response[3,10]. Trials with immune checkpoint inhibitors, between 2013 and 2017, showed positive results in advanced HCC which led to the approval of several monoclonal antibodies as first-line and second-line treatments since 2017[11,25] (**Figure 5**). In this regard, nivolumab was the first monoclonal antibody that demonstrated to increase patient survival as second-line option, followed by pembrolizumab, ramucirumab, and combined nivolumab and ipilimumab as second-line treatments, while in the first-line setting only the combination of atezolizumab with bevacizumab, and tremelimumab with durvalumab have been approved by the FDA[3,24] (**Figure 5**).

3.2 LENVATINIB

Lenvatinib is an oral multikinase drug classified as a TKI that has showed benefits in several tumor types, being approved against thyroid carcinoma, renal cell cancer, HCC and endometrial cancer[26,27].

3.2.1 Clinical landscape of lenvatinib in HCC

For over a decade, sorafenib has remained as the only available drug as the standard of care for HCC patients in advanced stages[28]. Despite the high number of clinical trials evaluating different pharmacological agents, positive results, either superiority or non-inferiority, were not obtained until the study conducted with lenvatinib[3,28]. The approval of lenvatinib (Lenvima®) in 2017 placed it as the unique alternative in the first-line setting against HCC, and was triggered after the efficacy showed by both the phase 2 and phase 3 studies[26,29,30].

Firstly, safety and pharmacokinetics of lenvatinib were assessed in 20 HCC patients to determine the maximum tolerable dose (MTD) and the preliminary clinical data for the following trial[31]. Plasma determinations and clinical evidence showed that 12 mg lenvatinib once daily is the recommended dose for performing the phase 2 clinical

study with manageable toxicity and efficacy[31]. The phase 2 study was conducted in patients diagnosed with HCC who were not eligible for surgical resection or locoregional therapies[30]. Lenvatinib was orally administered at 12 mg once daily for 28-day cycles, establishing time to progression (TTP) as the main outcome, and objective response rate (ORR), disease control rate (DCR) and OS as the secondary endpoints[30]. Results proved clinical activity of lenvatinib and an acceptable toxicity profile, regardless of the dosage modification in patients with lower body weight (<60 kg)[30].

After these clinical investigations, lenvatinib was included in a phase 3 trial (REFLECT trial) to compare OS of patients treated with lenvatinib in comparison to sorafenib and registered at ClinicalTrials.gov (NCT01761266)[26]. In this phase 3 study, HCC patients were enrolled and randomly assigned (1:1) to the lenvatinib or sorafenib group, with OS as primary endpoint and progression-free survival (PFS), TTP, ORR, quality-of-life measurements and plasma pharmacokinetics exposure parameters[26]. Main differences were initially observed in the dose and frequency of lenvatinib and sorafenib administration. Lenvatinib was orally administered at 12 mg/day (≥60 kg body weight) or 8 mg/day (<60 kg body weight) once daily, while sorafenib was orally administered at 400 mg twice daily[26]. Findings obtained from this clinical trial (**Table I**) displayed beneficial effects of lenvatinib in terms of the clinical parameters analyzed, with non-inferiority to sorafenib (13.6 months versus 12.3 months, respectively) in unresectable HCC[26]. In addition, a posterior study performed a covariate-adjusted analysis of this phase 3 REFLECT study in order to consider baseline variables observed before and after randomization[32]. Results from the REFLECT trial were found to underestimate the true effect of lenvatinib on OS compared to sorafenib, mainly due to an imbalance in AFP levels[32].

Table I. Clinical results from the parameters of primary and secondary endpoints from the phase 3 REFLECT trial.

Clinical parameter	Lenvatinib arm (n=478)	Sorafenib arm (n=476)
OS (months)	13.6 (12.1-14.9)	12.3 (10.4-13.9)
PFS (months)	7.4 (6.9-8.8)	3.7 (3.6-4.6)
TTP (months)	8.9 (7.4-9.2)	3.7 (3.6-5.4)
ORR (%, 95%CI)	115 (24.1%, 20.2%-27.9%)	44 (9.2%, 6.6%-11.8%)
DCR (%, 95% CI)	361 (75.5%, 71.7%-79.4%)	288 (60.5%, 56.1%-64.9%)

Data obtained from [26].

Although some adverse events observed with lenvatinib treatment were classified as grade 3, both lenvatinib and sorafenib displayed similar adverse events rates[26]. Hypertension, diarrhea and decreased appetite were the most common adverse events derived from lenvatinib administration, while palmar-plantar erythrodysesthesia, diarrhea and hypertension were mainly found in the sorafenib group[26]. Based on the positive results from the phase 3 REFLECT trial, the FDA approved lenvatinib in 2018 for the first-line treatment of advanced HCC[3].

3.2.2 Cellular and molecular targets of lenvatinib

Lenvatinib is a multi-targeted drug that selectively inhibit the tyrosine kinases VEGFR1-3, PDGFR-α, PDGFR-β, fibroblast growth factor receptors (FGFR) 1-4, mast/stem cell growth factor receptor (KIT) and proto-oncogene tyrosine-protein kinase receptor (RET)[28,29] (**Figure 6**). Interestingly, the targeting of FGFR4 is considered a crucial factor in the antitumor effects exerted by lenvatinib in HCC[28]. The half maximal inhibitory concentration (IC_{50}) values of this TKI were lower than those of sorafenib for the targets analyzed, highlighting a more potent inhibitory effect of lenvatinib on VEGFR, FGFR and KIT[28].

Through blockade of these tyrosine kinases, lenvatinib is able to disrupt key pathways associated to the development and progression of HCC[28]. Angiogenesis, defined as the generation of new blood vessels from pre-existent vessels, is the main process disrupted by lenvatinib in HCC, mainly through a VEGF-associated blockade[33,34]. This drug showed to restrain invasion and metastasis of human HCC cells by modulating the balance between matrix metalloproteinases (MMPs) and tissue inhibitors of MMPs (TIMPs)[35]. Similarly, through inhibition of VEGFR, lenvatinib decreased angiogenesis in both *in vitro* and *in vivo* models of HCC[33] and exerted an antiangiogenic effect in a VEGF-overexpressing HCC xenograft model[34]. Lenvatinib also demonstrated to diminish blood vessels and microvessel density when administered to different cell lines and a mouse model of HCC[36].

Antitumor effects of lenvatinib have been mainly associated to the inhibitory action on angiogenesis, invasion and metastasis[28]. However, this TKI is also able to directly restrain tumor progression by blocking cell proliferation and promoting cell death[33,36–39]. Tumor growth both *in vitro* and *in vivo* was disrupted after lenvatinib treatment, increasing necrosis of HCC cells[36]. Programmed cell death or apoptosis was

also induced by lenvatinib in diverse studies conducted with HCC models[37,38], being partially associated to the downregulation of FGF-signaling mediators[33,38]. Although lenvatinib has shown potential antitumor properties by modulating several cellular processes associated to different signaling pathways, further studies are needed to clarify the exact mechanisms modulated by this TKI[28].

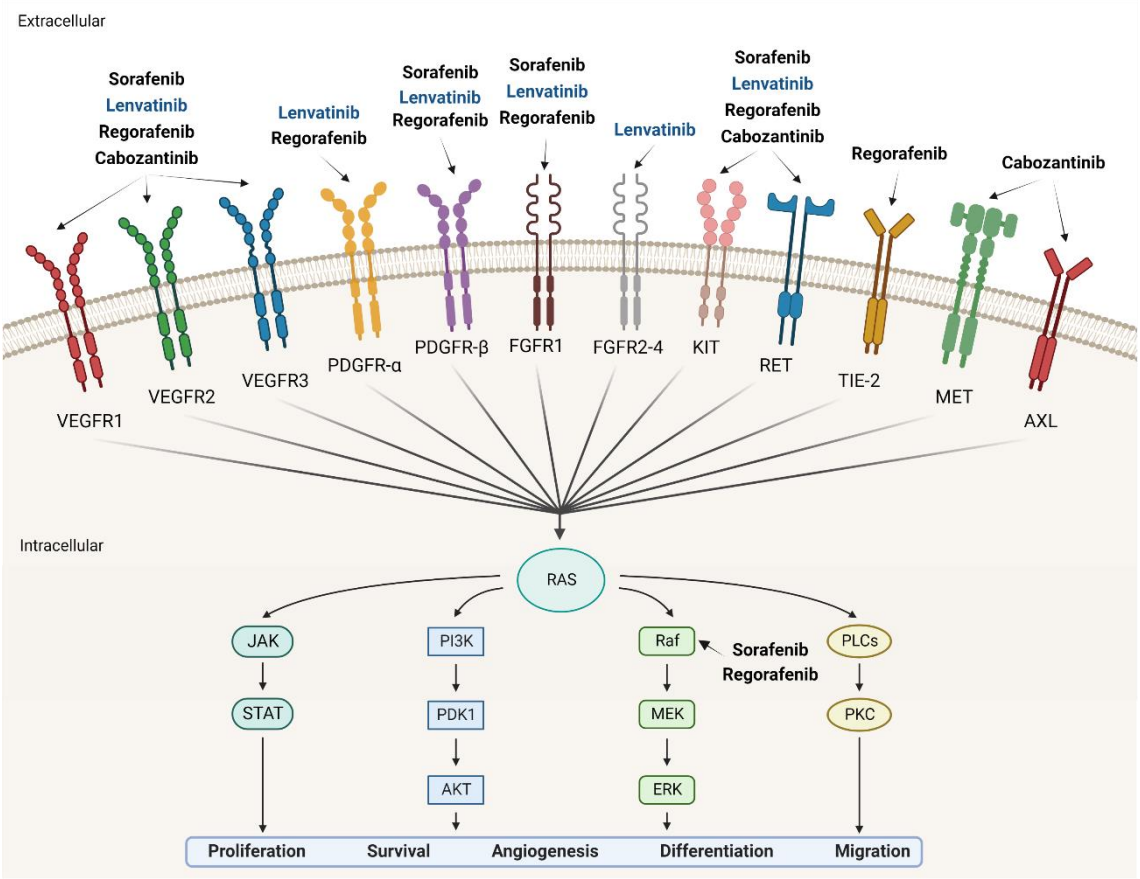

Figure 6. Main RTKs and downstream signaling pathways modulated by the current TKIs approved for the treatment of HCC. Specific lenvatinib effects are blue-marked for the different RTKs. AKT, RAC-alpha serine/threonine-protein kinase; MET, hepatocyte growth factor receptor; PI3K, phosphatidylinositol 3-kinase. Created with BioRender.com.

3.2.3 Loss of therapeutic sensitivity to lenvatinib

Even though TKIs have demonstrated to improve patient survival, prolonged administration could lead to loss of sensitivity and, therefore, to development of resistance[40,41]. Several mechanisms have been identified to be involved in the acquisition of chemoresistance in HCC, but most studies have focused on the alterations derived from sorafenib resistance[11,24], in which different processes have been described, such as apoptosis evasion, autophagy modulation or hypoxia-related response[42]. Since the lenvatinib approval against HCC, growing evidence has found that multiple signaling

pathways could promote the loss of sensitivity to lenvatinib, favoring cell survival and therapeutic failure[43–68]. Current findings on key molecular mediators of lenvatinib failure in different models of HCC are summarized in **Table II**.

Table II. Current findings on the potential mediators of the loss of lenvatinib sensitivity in HCC.

Mechanism involved in the loss of lenvatinib sensitivity		
Molecular alteration	**Cellular process**	**Ref.**
▼ KEAP1 (inactivation) ▲ Nrf2 downstream genes NQO1, GPX2 and TXNRD1	▲ Cell viability ▼ ROS production	43
▲ HGF/c-MET axis ▲ PI3K/AKT pathway activation ▲ MAPK/ERK pathway activation	▲ Cell proliferation ▲ Cell invasion ▼ Apoptosis ▲ EMT	44
▲ FGFR2	Maintenance of tumor vasculature	45
▲ MAPK/ERK pathway activation ▲ EMT markers ▲ VEGF, PDGF-AA and angiogenin	▲ Cell proliferation ▲ Cell invasion	46
▲ ADAMTSL5	▲ Cell proliferation	47
▲ IRF2	▲ Cell proliferation ▼ Apoptosis	48
YRDC → KRAS translation	▲ Cell proliferation ▲ Cell migration	49
▲ Hedgehog signaling	▲ Cell proliferation ▲ Cell migration ▼ Apoptosis	50
▲ EGFR activation	▲ Cell proliferation	51
▼ NF1 → ▲PI3K/AKT and MAPK/ERK signaling ▼ DUSP9 → ▲ MAPK/ERK signaling FOXO3 inactivation	▲ Cell proliferation ▲ Cell migration	52
▲ lncRNA MT1JP	▲ Cell proliferation ▼ Apoptosis	53
▲ FGFR1 ▲ AKT/mTOR and ERK signaling	▲ Cell proliferation ▼ Apoptosis	54
▲ ETS-1 → ▲ VEGFR2 ▲ RAS/MEK/ERK signaling	▲ Cell proliferation ▲ Cell migration	55
▲ ERK signaling	▲ Cell proliferation Cell cycle arrest	56

Mechanism involved in the loss of lenvatinib sensitivity		
Molecular alteration	**Cellular process**	**Ref.**
▲ EGFR activation ▲ IGF1R/INSR activation ▲ ROS levels	▲ Cell proliferation	57
▲ ITGB8 → ▲ HSP90-derived AKT stabilization	▲ Cell proliferation	58
▲ EGFR-STAT3-ABCB1 signaling axis	▲ Cell proliferation	59
▼ DUSP4 expression	▲ Cell proliferation ▲ Cell migration	60
▲ METTL1 → EGFR activation	▲ Cell proliferation ▼ Apoptosis	61
▲Caspase-3 → SREBP2 cleavage → cholesterol biosynthesis	▲ Cell proliferation	62
▲ LAPTM5	▲ Cell proliferation ▲ Autophagy	63
▲ MDR1 and BCRP ▲ EGFR/PI3K pathway	▲ Cell proliferation ▼ Apoptosis	64
LncRNA AC026401.3 interaction with OCT1 ▲ E2F2 signaling activation	▲ Cell proliferation	65
▲ FBXO9	▲ Cell proliferation ▲ Cell migration	66
▲ c-MET ▼ miR-128-3p	▲ Cell proliferation ▼ Apoptosis	67
▲ circMED27	▲ Cell proliferation	68

ABCB1, ATP binding cassette transporter B1; ADAMTSL5, a disintegrin-like and metalloprotease domain containing thrombospondin type 1 motif-like protein 5; AKT, RAC-alpha serine/threonine-protein kinase; BCRP, breast cancer resistance protein; circMED27, circular RNA mediator complex subunit 27; DUSP9, dual specificity phosphatase 9; E2F2, transcription factor E2F2; EGFR, epidermal growth factor receptor; ERK, extracellular signal-regulated kinase; ETS-1, protein C-ets-1; FBXO9, F-box only protein 9; FOXO3, forkhead box protein O3; GPX2, glutathione peroxidase 2; HGF, hepatocyte growth factor; HSP90, heat shock protein 90; IGF1R, insulin-like growth factor 1 receptor; INSR, insulin receptor; IRF2, interferon regulatory factor 2; ITGB8, integrin beta-8; LAPTM5, lysosomal-associated transmembrane protein 5; lncRNA, long non-coding RNA; MAPK, MAP kinase; MDR1, multidrug resistance protein 1; MEK, mitogen-activated protein kinase kinase; MET, hepatocyte growth factor receptor; METTL1, tRNA (guanine-N(7)-)-methyltransferase; mTOR, mammalian target of rapamycin; NF1, neurofibromin; NQO1, NAD(P)H dehydrogenase [quinone] 1; Nrf2, nuclear factor erythroid 2-related factor 2; OCT1, organic cation transporter 1; PI3K, phosphatidylinositol 3-kinase; Ref, reference; ROS, reactive oxygen species; SREBP2, sterol regulatory element-binding protein 2; TXNRD1, thioredoxin reductase 1; YRDC, threonylcarbamoyl-AMP synthase.

Nevertheless, despite the increasing number of articles published that evaluates potential mechanisms responsible for lenvatinib failure in HCC since 2019[43–68] (**Table II**), a clear understanding of the molecular and cellular processes implicated is still lacking[28,40].

3.3 NEUROPILIN-1

Neuropilins (NRPs) are type I transmembrane proteins of 120-140 kDa with pleiotropic functions in different physiological and pathological processes[69,70]. Initially, these NRPs were identified as key proteins in the axon guidance and neural development; however, their role on angiogenesis and other cellular processes involved in tumor development has been identified and become of great interest[70,71].

3.3.1 Types and structure of neuropilins

NRPs are multifunctional non-tyrosine kinase surface receptors that are expressed in all vertebrates and have a wide tissue distribution[70,71]. There are two conserved NRP family members, neuropilin-1 (NRP1) and neuropilin-2 (NRP2), that are encoded by two different genes on independent chromosomes (10p12 and 2q34, respectively)[70,72,73]. Despite NRP1 and NRP2 share only 44% homology in their amino acid sequences, the protein structure is very similar (**Figure 7**)[72,73]. In general, NRPs structure is based in an extracellular region, a transmembrane stretch and a short intracellular tail[72], which are constituted by domains with specific functions[74]. The extracellular region is constituted by five domains named as a1, a2, b1, b2 and c[71,74]. At the N-terminus NRP1 and NRP2 present two Cubilin homology (CUB) domains, two FV/VIII (FV/VIII) domains, and a meprin-like protease/A5 antigen/receptor tyrosine phosphatase μ and κ (MAM) domain[70,72] (**Figure 7**). Particularly, the CUB domains share homology with the complement binding factors C1r/C1s, Uegf, bone morphogenetic protein 1 (BMP1) and Tolloid proteins, while both FV/VIII have significant homology with the coagulation factor FV/VIII, the receptor-type tyrosine kinase DDR and discoidin-1[70,71]. Both NRP1 and NRP2 are single pass transmembrane proteins, with an intracellular PSF-95/Dlg/ZO-1 (PDZ) binding domain and a serine-glutamic acid-alanine (SEA) triplet of amino acids at the C-terminus[73,74] (**Figure 7**). Curiously, as consequence of alternative splicing, soluble forms of NRP1 (sNRP1) and NRP2 (sNRP2) could be generated, which lack the

transmembrane and cytoplasmic domains[73] (**Figure 7**). Moreover, membrane bound NRP2 also experiences alternative splicing which generates two NRP2 isoforms, NRP2A and NRP2B, mainly differentiated in the presence or absence of the SEA triplet[71,73].

The extracellular domains participate in the interaction with different ligands and receptors, being the a1, a2 and b1 involved in the binding to class 3 semaphorins (SEMA3); while the b1 and b2 domains are the responsible for interacting with VEGF and other growth factors[70,74] (**Figure 7**). Both MAM and transmembrane regions have shown to be essential for homo- and heterodimerization[72] and the PDZ domain that, although it lacks catalytic activity, acts as docking site for the interaction with partners to form signaling complexes[71,73,74].

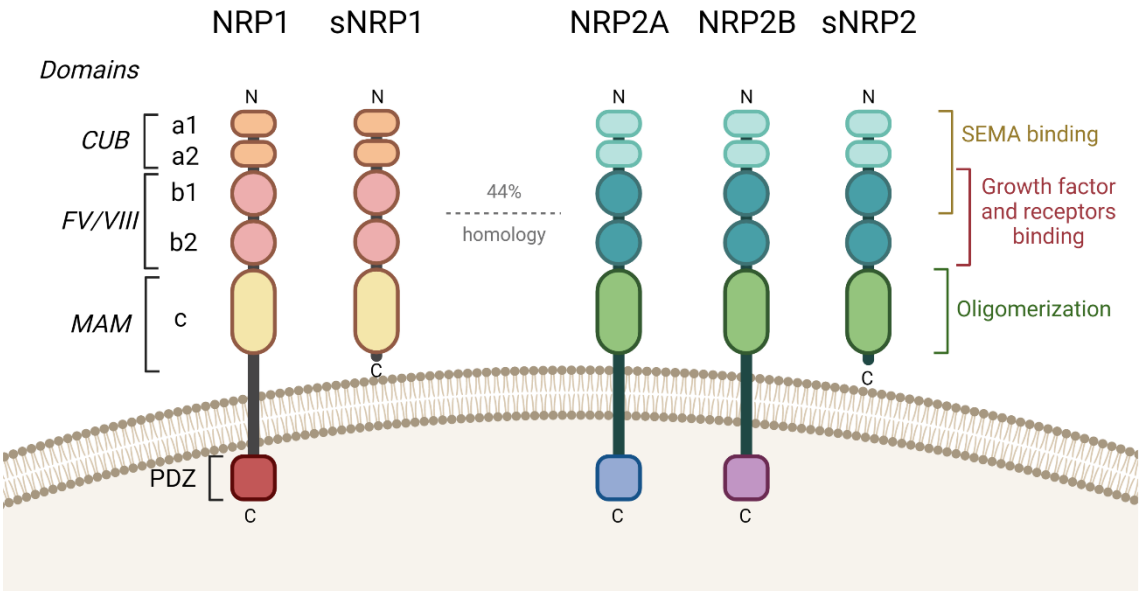

Figure 7. General structure of the main types of NRPs, NRP1 and NRP2, and splice variants. Both NRPs consists of domains with different cellular functions, and soluble isoforms (sNRP1 and sNRP2) also exist lacking the transmembrane and cytosolic domains. Two splice variants are derived from the gene of NRP2, NRP2A and NRP2B, distinguished in an 89% of homology in the C-terminus. Created with BioRender.com.

NRP1 was the first member of the NRP family described in 1987[72] and, although both NRP1 and NRP2 play key functions, NRP1 has been more studied and widely characterized[74]. These receptors differ in several properties that are, at least in part, responsible for the diverse cellular function exerted by each one[71]. Glycosylation patterns between NRP1 and NRP2 are not identical, since NRP1 is mainly N-glycosylated and NRP2 only could be polysialylated[70,71]. Moreover, NRPs have a specific tissue distribution, finding NRP1 expressed in arterial endothelial cells and in the tumor

vasculature, being overexpressed in heart and placenta, and moderately expressed in lung, liver, skeletal muscle, kidney and pancreas[70]. On the other hand, NRP2 is mainly found in venous or lymphatic endothelial cells, as well as in neural crest-derived cells such as hepatocytes and epithelial cells of proximal and distal renal tubules[70].

3.3.2 Cellular and molecular modulatory effects of neuropilin-1

The role of NRPs, and mainly NRP1, in the embryonic development is crucial for reaching a complete and adequate vascular phenotype[73,75]. Loss of NRP1 in a knockout mice model led to an embryonic lethality between 10 days and 12.5 days; while NRP1 overexpression also triggered an embryonic lethality in 12.5 days, approximately, demonstrating the essential role played by NRP1 in angiogenesis[73,75].

In adults, NRP1 has shown to modulate a variety of cellular processes and signaling routes due to its interaction with multiple receptors as heterodimers[70,73]. NRP1 acts as a coreceptor of growth factor receptors, mostly RTKs, and, therefore, increases the activation of key pathways, such as phosphatidylinositol 3-kinase (PI3K)/RAC-alpha serine/threonine-protein kinase (AKT) and MAP kinase (MAPK)[70]. The first binding partners described for NRP1 were proteins from the SEMA3 family, which participate in axon guidance and migration, cell apoptosis and tumor suppression[73]. Although NRP1 has the highest affinity to SEMA3A, it also interacts with other members of SEMA3 family[73,74] (**Figure 8**). Plexins are SEMA receptors that participate in the formation of SEMA3/NRP1/Plexin complexes that suppress angiogenesis and metastasis, thus, exerting an inhibitory role in tumor progression[70] (**Figure 8**).

Regardless these molecular partners, NRP1 stands out for its interaction with multiple growth factors and the corresponding receptors that exert key functions in cancer[70,73]. The most studied interaction of NRP1 is VEGF-A and the VEGFR family, highly involved in the vasculature development and angiogenesis[69,74]. In these complexes NRP1/VEGFR/VEGF, NRP1 plays a critical role, enhancing the signaling cascade and promoting angiogenesis[70,72] (**Figure 8**). Additionally, NRP1 has been found to couple with many other RTKs and ligands, which include PDGFR/PDGF, FGFR/FGF, transforming growth factor-β receptor (TGF-βR)/TGF-β and hepatocyte growth factor receptor (MET)/hepatocyte growth factor (HGF)[72,73] (**Figure 8**). Through these interactions, NRP1 has shown to activate the MAPK and PI3K/AKT pathways, among others, promoting cell survival, angiogenesis, epithelial-to-mesenchymal transition

(EMT) and migration, as well as to induce an immune tolerance response[69,70,73] (**Figure 8**). Interestingly, although most studies have described an essential VEGFR-dependent role of NRP1 in angiogenesis induction, in some tumors without VEGFR expression, NRP1 was able to interact with VEGF and induce cell migration and angiogenesis[73] (**Figure 8**). Increasing evidence have showed the relevant function of NRP1, not only as coreceptor, in cellular processes crucial for tumor development and progression[69,70,73].

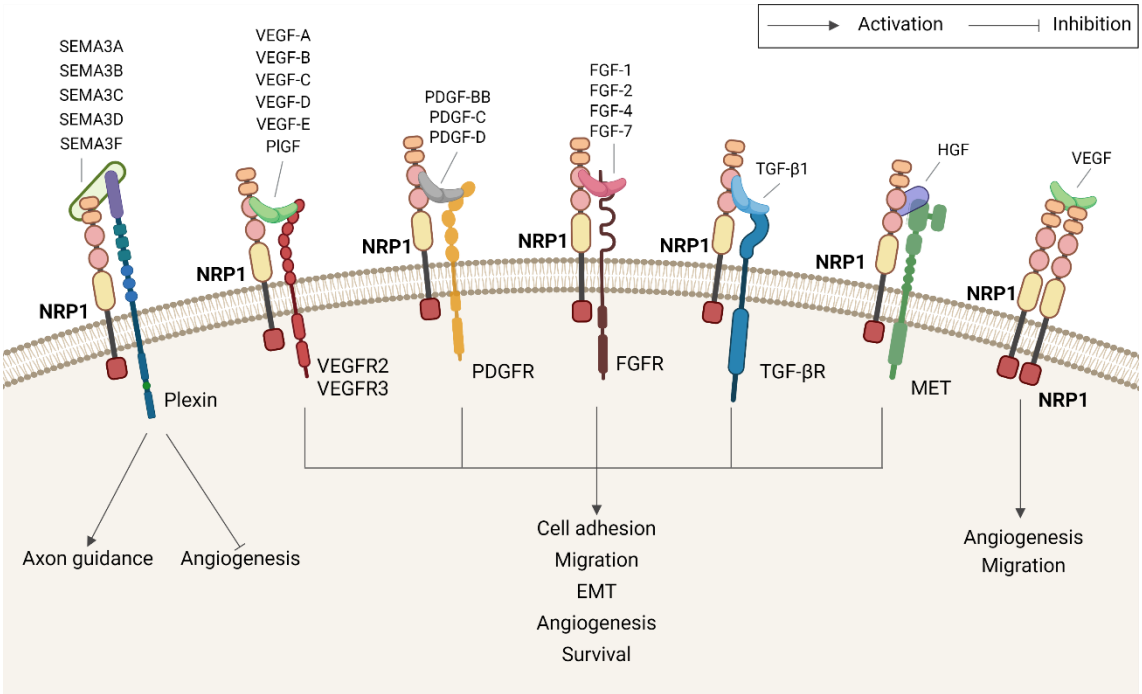

Figure 8. Molecular interactions and derived effects of membrane bound NRP1. NRP1 acts as a coreceptor of multiple ligands and their corresponding receptors, and modulates key cellular processes, such as axon guidance, angiogenesis, cell adhesion, migration, EMT and cell survival, by interacting with different growth factors and other proteins. PlGF, placenta growth factor. Created with BioRender.com.

3.3.3 Neuropilin-1 and HCC

The increasing interest aroused by NRP1 in cancer has also been translated to HCC[70], in which a broad number of studies have described potential functions of NRP1 in different biological aspects described below.

NRP1 as a biomarker

The identification of useful biomarkers is one of the main objectives to increase the rate of early diagnosis in the HCC landscape[8]. In this line, several investigations have found an overexpression of NRP1 in the tumor tissue of patients diagnosed with HCC compared to the healthy liver tissue[76–85]. Similar results were also described in preclinical studies, showing increased NRP1 levels in different HCC cell lines with respect to the normal liver L02 cell line[85,86]. Although fewer investigations have analyzed the potential use of NRP1 as serum biomarker, positive findings have been also published[79,87], highlighting the potential role of this NRP receptor in the diagnostic field of HCC[76–87].

Prognosis of HCC patients remain complex and novel advances are being conducted in the identification of suitable strategies and useful prognostic biomarkers[13]. Likewise, an increased expression of NRP1 has been strongly associated to worse prognosis of HCC patients, reporting shorter OS, PFS and recurrence-free survival (RFS)[78,84,88–91]. Furthermore, not only survival, but also other tumor-associated parameters have been closely related to NRP1[78,79,84,92]. Specifically, NRP1 was correlated with advanced stages of HCC and higher AFP levels,[78,79], finding a significant association with multi-nodularity and tumor size in one study[87], but without significant results in different investigations[78,84,92]. Altogether, NRP1 could be a useful biomarker for both diagnosis and prognosis, as well as for other tumor-associated parameters in HCC patients.

Role in tumor invasion and migration

The main effects derived from NRP1 in human pathologies, including cancer, have been widely associated with the modulation of signaling routes that drive angiogenesis and migration of tumor cells[70]. For this reason, most articles have assessed the interplay between NRP1 and invasion in HCC. Different preclinical studies have broadly established a direct modulation of cell invasion and migration abilities by NRP1[76,78,85,93–103]; data supported by clinical investigations in which NRP1 was markedly correlated with an increased probability of venous invasion and metastasis[84,87] (**Figure 9**). Although several mechanisms have been described to participate in this NRP1-associated angiogenesis, VEGF-dependent activation remains as the main mechanism responsible[102] (**Figure 9**).

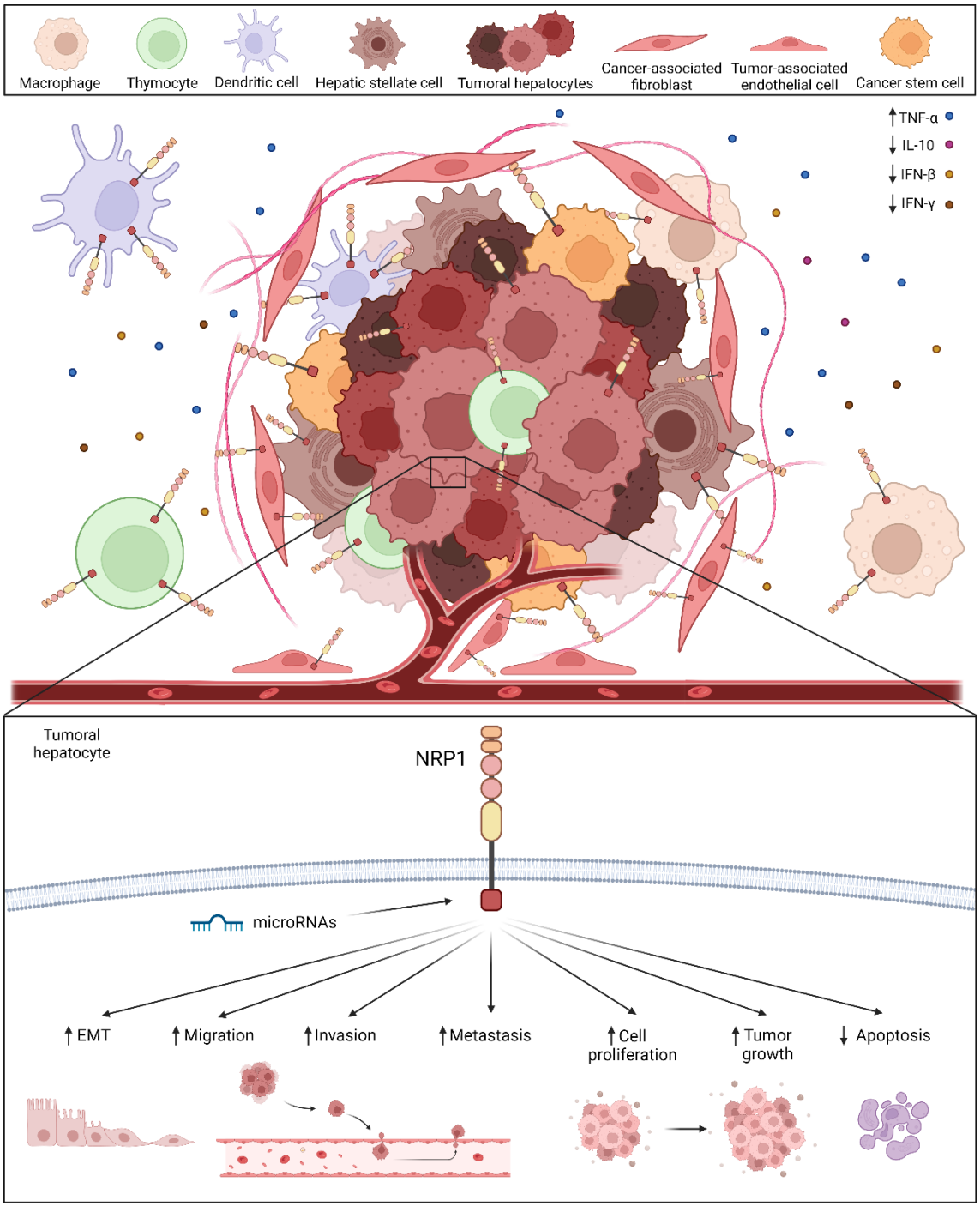

Figure 9. Main modulatory actions of NRP1 in tumor hepatocytes and NRP1 role in the tumor microenvironment in HCC. NRP1 is broadly expressed in cancer cells and other tumor-associated cell populations of the tumor microenvironment and the immune response. This receptor, NRP1, is expressed in a high number of cell types and participates in several cellular and molecular mechanisms involved in the development and progression of HCC, modulating crucial cellular processes. IFN-β, interferon beta, IFN-γ, interferon gamma. Created with BioRender.com.

Furthermore, NRP1 has also demonstrated to regulate clinical parameters associated to invasion and metastasis, reporting a decrease of tumor vascular remodeling in two different studies after NRP1 knockdown[76,94], together with an inhibition of the formation of capillary-like structures[76] and lower neovascularization[96] (**Figure 9**). Similar results were also found with *in vitro* HCC models analyzing the tube formation ability[95,97] (**Figure 9**). Overall, these findings suggest that angiogenesis, invasion and migration, key processes of tumor progression, are strongly modulated by NRP1.

NRP1 modulation of cancer-associated pathways

The role of NRP1 in tumor growth and progression has been widely studied in recent years, establishing a direct association between NRP1 expression and an enhanced tumor cell survival and progression in HCC[76,79,85,93–99,104–111] (**Figure 9**). These findings have been reported by cellular[76,79,85,96–99] and animal models[76,94–96,98,107,112], as well as in human clinical studies[106,110]. However, not only cancer cell proliferation, but also apoptosis and other tumor-related pathways have been identified as mechanisms potentially modulated by NRP1[76,104,105,108,109]. Among them, NRP1 proved to be correlated with the immune marker CD36[109] and insulin-like growth factor binding protein-3 (IGFBP3)[108] (**Figure 9**). In summary, although several investigations have described a broad variety of signaling mediators that are regulated by NRP1, there is still a lack of evidence that clarify the underlying mechanisms of the NRP1-related promotion of tumor survival[76,79,85,93–99,104–111].

NRP1 and the immune-related response

Interestingly, several findings published on tumor effects of NRP1 in HCC have been strongly associated to the ability of suppressing the immune response against cancer cells[91,94,95,113–118]. In this line, NRP1 overexpression has been observed in macrophages[113], thymocytes[114] and dendritic cells[91,115], being significantly correlated with different immune markers, such as IL-10[116], interferon (IFN)-γ[94], IFN-β and TNF-α[95] (**Figure 9**). Nonetheless, one study found no correlation between NRP1 and killer cell lectin-like receptor B1 (KLRB1) employing human samples data from public databases[117]. These investigations have reported interesting results showing the key function of NRP1 in the tumor-related immune response, placing this receptor as a potential biomarker of tumor progression and survival.

Modulation by microRNAs

MiRNAs are crucial modulators of gene expression and their dysregulation demonstrated to be a key indicator during oncogenesis[119]. In the context of HCC, miR-148-b and miR-340-5p/miR-452-5p have shown to target NRP1 in preclinical models[97,100,120]. On the other hand, overexpression of miR-124 or circular RNA (circRNA) circ-ABCB10 led to increased levels of NRP1[120,121], highlighting the ability of miRNAs and other non-coding RNAs to modulate NRP1 in HCC (**Figure 9**).

Furthermore, NRP1 targeting caused by miRNAs has also shown to trigger a tumor-associated response. MiR-148-b-derived NRP1 downregulation triggered the inhibition of tube formation and cell division in an HCC *in vivo* model[97], and of cell migration in the Huh-7 cell line[100]. Despite the promising findings observed, further studies should be performed to provide a complete understanding of the miRNA-NRP1 interplay and its role in HCC and another tumor types[97,100,120,121].

Interplay between NRP1 and the tumor microenvironment

The tumor microenvironment plays an essential role in the progression and adaptation of cancer cells, being constituted by a broad diversity of cell populations, mainly cancer stem cells (CSCs), cancer-associated fibroblasts (CAFs), tumor-associated endothelial cells (TECs) and HSCs[122]. Recent studies have focused on the role of NRP1 in the tumor microenvironment, reporting that NRP1 knockdown led to a reduction in the CSC population[85], and was found overexpressed in the CSC side population of HCC cells[97] (**Figure 9**). Similarly, a specific expression of NRP1 was also observed in both CAFs and TECs from HCC patients[90], suggesting a potential function of NRP1 in the tumor microenvironment of HCC (**Figure 9**).

Increasing evidence has revealed hypoxia, defined as low oxygen conditions, as one of the main processes involved in tumor progression and drug resistance development in HCC[123,124]. The hypoxia-associated response is able to modify the signaling cascades in tumor cells, promoting cell survival and proliferation even in presence of targeted drugs[123,124]. Among the altered mechanisms, initial studies have identified NRP1 to be involved in the hypoxia response. Specifically, hypoxia induction triggered NRP1 downregulation *in vitro* in two different studies[102,104] and was negatively correlated with the hypoxia-inducible factor 1α (HIF-1α) in a mouse model of HCC[104] (**Figure 9**).

Altogether, these results suggest that NRP1 may be involved in HCC progression through modulation of a broad variety of cellular and molecular processes, placing NRP1 as a potential target for future investigations in the HCC landscape.

3.4 AUTOPHAGY

Autophagy is an evolutionary cellular process highly conserved that mediates the degradation of cellular components through the fusion with lysosomes[125]. This process accounted for the name of the main mediators of autophagy, named autophagy-related genes (ATG)[126]. In physiological conditions, autophagy is responsible for the removal of damaged organelles and intracellular biomolecules, such as lipids or proteins, providing nutrients and new sources for biosynthesis for cell survival[125,127].

3.4.1 Types of autophagy

Autophagy is a dynamic and complex process with multiple steps that is classified depending on the cargo delivery to the lysosomes[125]. Although some researches have described numerous types of autophagy, such as aggrephagy, peroxisome autophagy, mitophagy, lipophagy, among others, this classification is based on the cargo type for selective autophagy[125,126]. The major types of autophagy are macroautophagy, chaperone-mediated autophagy (CMA) and microautophagy[125,128].

During the process of macroautophagy, misfolded proteins and dysfunctional organelles are engulfed by double-membrane vesicles, named autophagosomes, and delivered to lysosomes for degradation[128]. Microautophagy, or small autophagy, occurs in the absence of autophagosome formation, being the small cargos directly phagocyted by lysosomes[125,126]. Similarly, the CMA process is started by chaperones that bind to intracellular proteins and traffics them to a lysosome for an enzymatic digestion[125,126].

These processes represent the main types of autophagy described in the scientific literature, nevertheless, based on the nutritional status we can find non-selective autophagy, activated under starvation or stress conditions, and selective autophagy, under nutrient-rich conditions[126,128]. Within them, mitochondria autophagy or mitophagy, lipid autophagy or lipophagy, and ER-phagy are some of the most common types studied[125,129]. Despite the broad variety of autophagy types, the mechanism from the initial steps to the

final lysosomal degradation seems to be similar and share the main mediator molecules[126].

3.4.2 The dynamics of autophagy: process phases

The process of autophagy consists of five consecutive steps: initiation, nucleation, elongation, fusion and degradation, where ATG proteins are the main mediators[128].

Initiation

Initially, the mammalian target of rapamycin (mTOR), that act as the primary regulator of autophagy is inhibited by several signals and, therefore, the associated signaling[128]. In this condition, autophagy is induced, leading to the formation of the ATG1/unc-51-like autophagy activating kinase 1 (ULK1) complex[128,129] (**Figure 10**). The regulator AMP-activated protein kinase (AMPK) also participates in modulating ULK1 activation, and, under specific cellular signals AMPK induce ULK1 complex formation[126]. This complex recruits different autophagy-related factors, mainly ATG13, FAK family kinase-interacting protein of 200 kDa (FIP200) and ATG101, responsible for the autophagy initiation[126,129] (**Figure 10**).

Nucleation

Once the initial complex is generated and active, a small membrane named phagophore is formed[129]. Together with the ULK1 complex, the Class III PI3K complex, constituted by different proteins, participates in this step, contributing to the formation of the phagophore[128,129] (**Figure 10**). Recruitment of lipids and other components for the phagophore is primarily performed by the WD repeat domain phosphoinositide interacting protein (WIPI), activated by phosphatidylinositol-3-phosphate (PI3P), ATG2, key protein for lipid transport, and ATG9[126,129] (**Figure 10**).

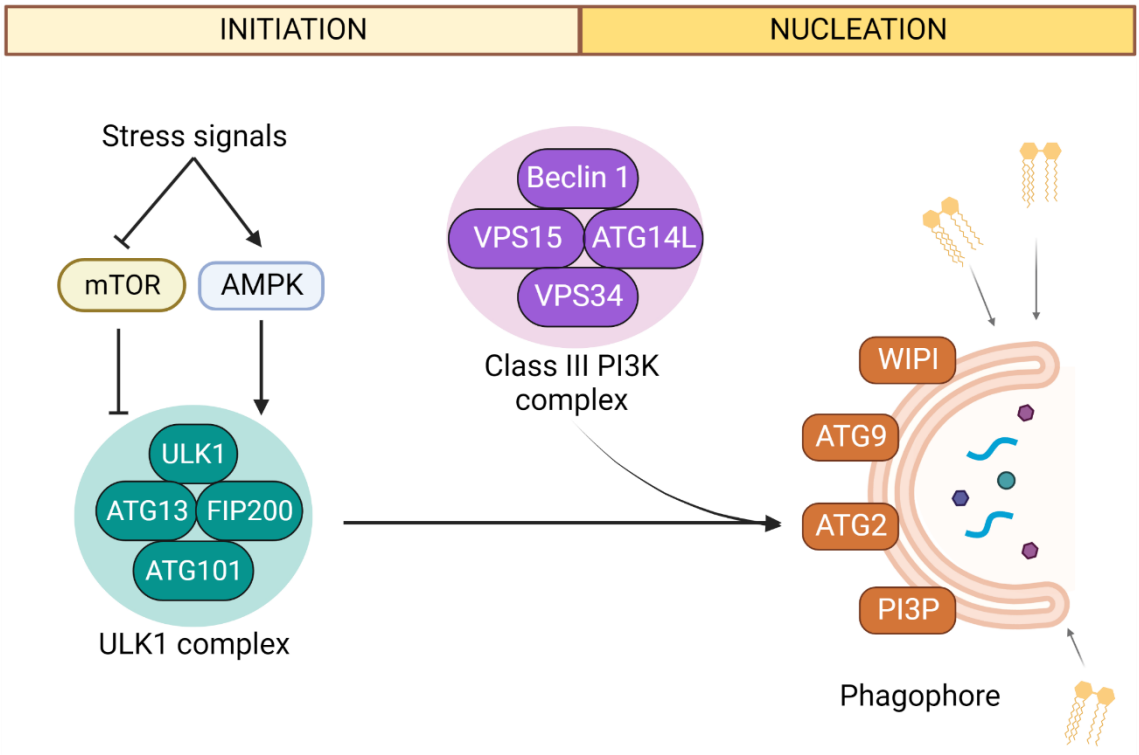

Figure 10. Initiation and nucleation steps of the autophagy process. Main molecular mediators and complexes involved in these steps, including from the initial molecular signals and pathways to the formation of the phagophore membrane. ATG14L, ATG14-like protein; VPS15, phosphoinositide 3-kinase regulatory subunit 4; VPS34, phosphatidylinositol 3-kinase catalytic subunit type 3. Created with BioRender.com.

Elongation

To accomplish the expansion and closure of the phagophore membrane, two ATG conjugation systems are necessary to attach ATG8 to phosphatidylethanolamine (PE) in the membrane[128,130]. Firstly, as represented in **Figure 11**, a complex activation and recruitment cascade occurs, involving several ATGs, which leads to conjugation and activation of the microtubule-associated protein light chain 3 (LC3) to LC3-II, PE-conjugated LC3[129,130]. The LC3/PE and the ATG12-ATG5 binding reaction systems constitute the two complexes responsible for the membrane elongation[129]. LC3-II binds to the phagophore and mediates the interaction between the autophagic cargo and the membrane, through sequestosome-1 (p62/SQSTM1), an adaptor protein that recognizes ubiquitin-marked proteins[128,130]. After this process, the phagophore matures into a lipid bilayer vesicle named autophagosome, which finally engulf cytosolic material[128,129] (**Figure 11**).

Fusion and degradation

Autophagosomes and lysosomes need to be close to allow the membrane fusion between them, being transported by the microtubules[127]. In this step, two different complexes interact and form conjugates with proteins from the lysosomal membrane, enabling fusion of the outer autophagosome membrane and the unique lysosomal membrane[127,129] (**Figure 11**). Once this initial fusion is accomplished, the lysosomal enzymes degraded the inner autophagosome membrane and the autophagic cargo is released into the lysosomal lumen[127,128] (**Figure 11**). Finally, lysosomal hydrolases degrade the autophagic content and the cellular and molecular components are recycled[128,129] (**Figure 11**).

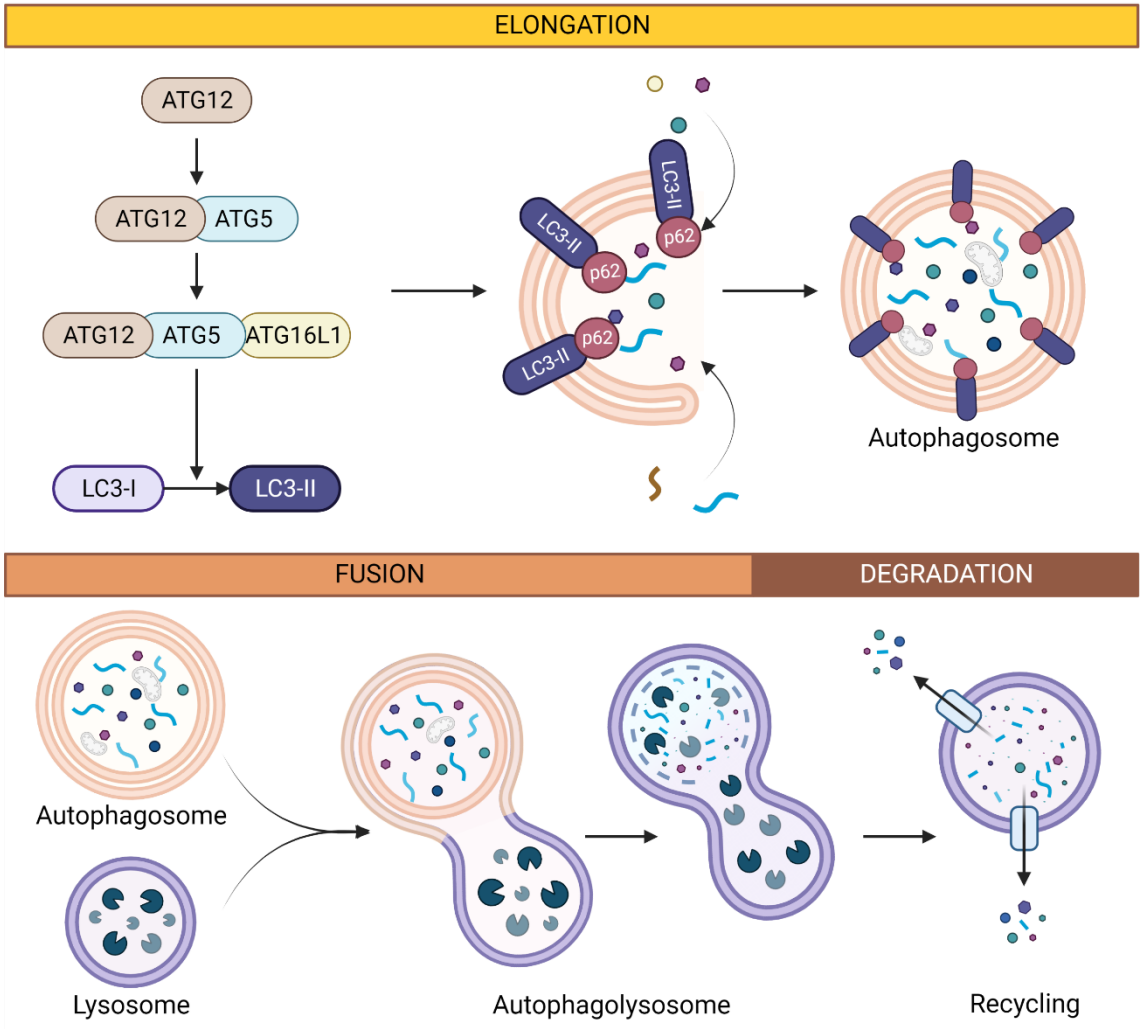

Figure 11. Elongation, fusion and degradation steps of autophagy. Key events that take part in the three stages, including the activation and recruitment of ATG proteins that end with PE-conjugation of LC3-I which becomes LC3-II and mediates cargo incorporation to the autophagosome. Final steps of interaction between autophagosomes and lysosomes, their fusion into autophagolysosomes, and lysosomal degradation and recycling of proteins and organelles are also represented. Created with BioRender.com.

3.4.3 Autophagy in HCC

Under physiological conditions, autophagy exerts an essential function through the maintenance of cellular and metabolic homeostasis in the liver[125] (**Figure 12**). However, the exact role played by autophagy during chronic liver injury and tumor carcinogenesis of HCC remains unclear[131,132].

At initial stages, autophagy promotes genomic stability and prevent the acquisition of a malignant phenotype by the hepatocytes[132] (**Figure 12**). In addition, autophagy is able to prevent and decrease the level of inflammation, while a disrupted autophagy leads to a persistent inflammation, contributing to the hepatocarcinogenesis[133] (**Figure 12**). Together with the anti-inflammatory effects, autophagy also inhibits protein accumulation of p62/SQSTM1 and other dysfunctional components, which restrains tumor initiation[128]. Curiously, several investigations have reported that the etiologic agents involved in HCC development can disrupt this process, identifying autophagy as a tumor suppressor mechanism in healthy liver[125,131].

Even though a general consensus seems to be established in the tumor suppressor role of autophagy in hepatocarcinogenesis, contradictory results have been observed in established tumors, suggesting a double-edged role depending on the HCC stage[128]. Once the hepatocytes become malignant cells, autophagy favors cell survival and adaptation to the stress conditions through regulation of different modulators, including ATG proteins, non-coding RNAs and other associated pathways[131,132] (**Figure 12**). Hypoxia, nutrient starvation and oxidative stress, among others, constitutes relevant conditions of the tumor microenvironment that are able to induce an autophagic response in the tumor hepatocytes, promoting tumorigenesis and HCC progression[132,133]. Liver tumor cells have an increased migration ability developing metastatic nodules, since HCC metastasis rate is higher than 90%[132]. Autophagy induction has shown to foster cellular migration by providing energy and altering cellular adhesions[128,133], and, mutually, metastasis also triggers an autophagic response to facilitate colonization and adaptation of HCC cells in the new microenvironment[128].

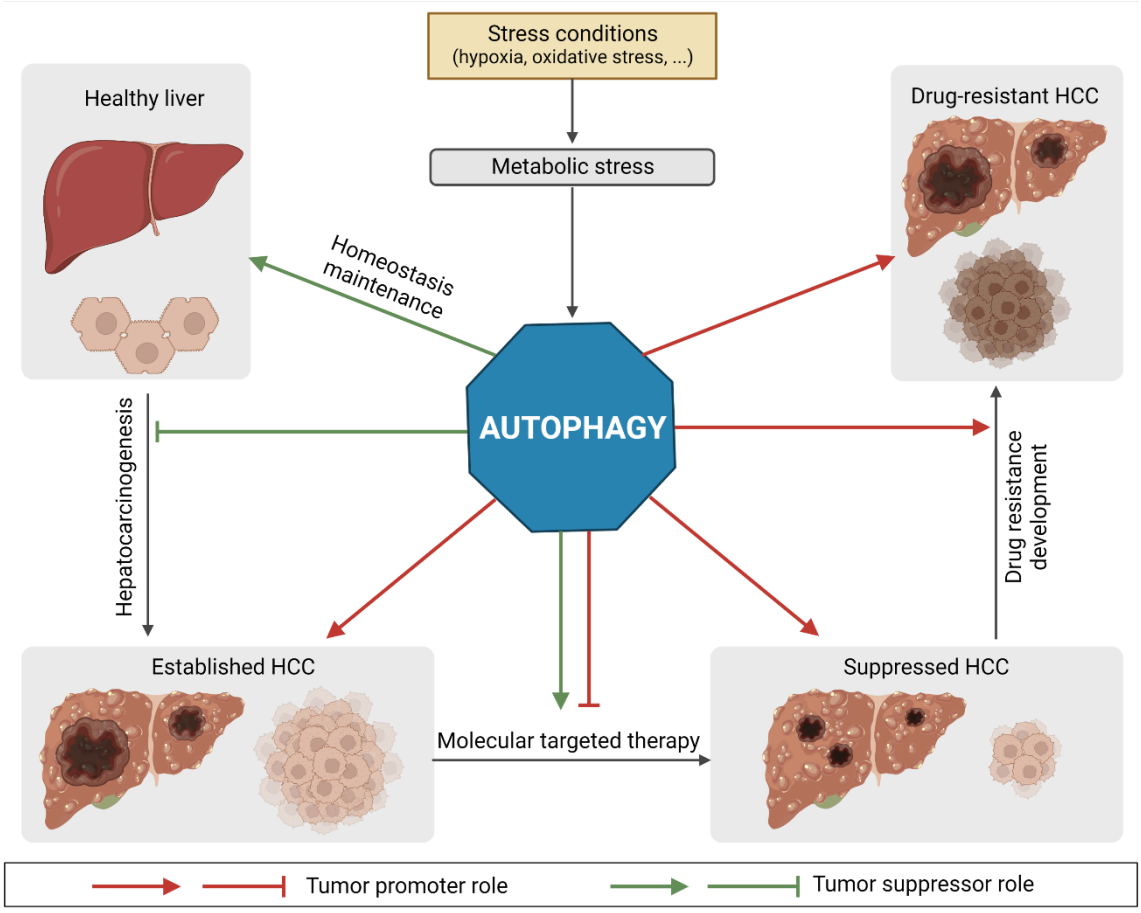

Figure 12. Role of autophagy in the different stages of HCC development, progression and drug resistance acquisition. Autophagy could act as either tumor suppressor (green) or tumor promoter (red), depending on the context, from the transformation of healthy hepatocytes into tumor liver cells to the development of drug resistance. Figure scheme based on [132]. Created with BioRender.com.

3.4.4 Autophagy and targeted drug response

The cellular response to the treatments used in HCC is crucial for the determination of patient's outcomes, where autophagy has a context-dependent function[128] (**Figure 12**). Despite autophagy has already a complex role during hepatocarcinogenesis and HCC progression, findings have evidenced an even more intricate mechanism in the autophagic process during tumor treatment with molecular targeted drugs[131,132].

Autophagy induction has been proved to inhibit tumor growth in different HCC models, being associated to some of the approved drugs against HCC, such as sorafenib, which seems to be an autophagy inducer[132,133]. In this line, the autophagic flux is initially increased after sorafenib treatment as part of the antitumor effects of this TKI in HCC cells; nonetheless, autophagy could turn into a cytoprotective mechanism in tumor cells, favoring the acquisition of drug resistance[128,132] (**Figure 12**).

On the other hand, controversial results have revealed that autophagy blockade could also act as a therapeutic strategy in HCC[133]. There are several autophagy inhibitors that have proved antitumor activities against this liver tumor, highlighting chloroquine (CQ), 3-methyladenine (3-MA) and bafilomycin A1 (Baf)[126,131,133]. These compounds exert their function at different stages of autophagy, while 3-MA inhibits molecular autophagic complexes at early stages, CQ blocks lysosomal degradation and Baf prevents autophagosome lysosome fusion[134]. Combination of some of these inhibitors with drugs has restrained HCC progression, increasing the effectiveness of several chemotherapeutic agents, such as cisplatin, doxorubicin or sorafenib[132,133]. Therefore, autophagy has a dual role in drug responsiveness by HCC cells which is also hindered by a context- and cellular-dependent modulation[128] (**Figure 12**).

Molecular targeted drugs have shown to be effective against HCC and confers longer survival to patients[128]. Nonetheless, tumor cells could develop molecular mechanisms that lead to the loss of drug sensitivity and therapeutic failure[132]. Drug resistance remains a challenge mainly due to the still unclear underlying mechanisms, in which autophagy has a crucial role[131,132]. Induction of autophagy by some chemotherapeutic agents is initially associated to their antitumor effects, but a persistent autophagy triggers drug resistance acquisition[128]. Although different signaling pathways have been identified as part of the autophagy-associated resistance, current findings do not provide a clear understanding[132,133]. Contrariwise, there are also studies that reveal a tumor suppressor role of autophagy during drug treatment, which supports the necessity of further studies to deep into the study of autophagy[128,131] (**Figure 12**).

3.5 HYPOXIA

Hypoxia is caused by a lower oxygen availability, ranging from 1% to 2% oxygen, and is a common feature of solid malignancies[135,136]. In cancer, the excessive proliferation of tumor cells leads to an increment in the oxygen demand, greater than the supply, and the inability of blood vessels to provide enough oxygen, triggering an intratumoral hypoxic microenvironment[135,136]. Depending on the duration, hypoxia can be classified as acute or chronic hypoxia[136]. The term acute hypoxia is used to define a temporary and initial restriction of blood supply and, therefore, of oxygen; while chronic hypoxia is irreversible and long-term[135,136]. Response of tumor cells to hypoxia relies on the duration

and adaptation ability to the tumor microenvironment; nonetheless, hypoxia often induces gene expression alterations that prompt changes in cellular and molecular signaling strongly associated to a higher tumor aggressiveness[136–138]. Consequently, cancer cells are able to adapt to the oxygen imbalance, obtaining a malignant phenotype, being hypoxic conditions markedly correlated with poor prognosis in cancer patients[137]. Nevertheless, the interaction and response of the cells to the hypoxia establishment in a solid tumor remains uncertain[138].

3.5.1 Hypoxia-inducible factors (HIFs)

At the transcriptional level, the cellular adaptation to the low oxygen conditions is regulated by the hypoxia-inducible factors (HIFs), which reprogram the cell transcription pattern to survive in the new microenvironment[139]. HIFs are transcription factors that mediate the adaptive cellular response by promoting the expression of genes involved in key processes, including metabolism, angiogenesis, invasion and cell proliferation[137,140].

These factors are heterodimers constituted by an oxygen-sensitive subunit, named as HIF-α, and a constitutive subunit, known as HIF-1β or aryl hydrocarbon receptor nuclear translocator (ARNT)[139]. There are three isoforms of the HIF-α subunit, HIF-1α, HIF-2α and HIF-3α, whose expression is regulated by the oxygen levels[140]. Under normoxia conditions, HIF-α subunits are hydroxylated by prolyl-4-hydroxilases (PHDs) enzymes, consequently ubiquitinated and degraded by the proteasome[137,140]. Moreover, the factor inhibiting HIF-α (FIH) is able to block the transactivation domain of HIF-α, and, therefore disrupting its interaction with the coactivators p300/cAMP response element-binding protein (CREB)-binding protein (CBP) and gene transcription[139,141]. Otherwise, in hypoxia, PHDs are inactive and HIF-α is stabilized and accumulated in the cytoplasm[141]. Afterwards, HIF-α subunits are translocated into the nucleus, dimerize with HIF-1β forming different heterodimers, HIF-1, HIF-2 and HIF-3, for each subunit HIF-1α, HIF-2α and HIF-3α, respectively, and bind to the hypoxia-responsive elements (HRE) placed in the promoter regions of their target genes, inducing their expression[137,139,140]. There is also an oxygen-independent regulation of the HIFs expression and activity, where different signaling cascades directly modulate HIFs expression, including PI3K/AKT and MAPK/ERK pathways[140].

Although the HIF-α subunits share the regulation mechanisms described and are responsible for transducing the hypoxia response, they show differences in terms of target genes and activation kinetics[137]. The effects derived from the HIF-3α isoform remain unknown, being described a likely role in cancer and a partial overlapping with transcription targets of HIF-1α and HIF-2α[141]. However, both HIF-1α and HIF-2α have been widely studied and their functions in several human pathologies, and mainly in cancer, have been the focus of multiple studies[123,141]. Although both factors are crucial mediators of the hypoxia response, HIF-1α is responsible for the cellular adaptation to an initial acute hypoxic microenvironment; while HIF-2α levels increase over time, guiding the cellular response to a chronic hypoxia[123,142]. Moreover, both HIF-α isoforms differ in the transcriptional targets activated by them and, in consequence, their modulatory activity on different cellular processes[123,137].

3.5.2 HIF-1α-mediated hypoxia response in HCC

Human HCC is characterized by a high vascularization and a rapid tumor growth that often leads to the generation of a hypoxic microenvironment[143]. In these conditions, HIF-1α and HIF-2α directly mediate an adaptive response by increasing the transcription of key proteins involved in angiogenesis, migration, invasion, metabolism, cell survival and drug response[141,143] (**Figure 13**). Even though both HIF-α isoforms participate in tumor progression in HCC, HIF-1α has proved to act as the main mediator of HCC cell response to hypoxia[123,141].

Cell metabolism constitutes one of the main processes altered by HIF-1α as part of the hypoxia response, switching from an oxidative to a glycolytic metabolism in the tumor hepatocytes[144] (**Figure 13**). Overexpression of HIF-1α is very frequent in HCC and is associated to an increased expression of several enzymes involved in key metabolic pathways, such as glucose transporter (GLUT)-1, GLUT-3, or hexokinase-2, among others[141,143]. As consequence, under hypoxia HCC cells are able to obtain energy from an oxygen-independent mechanism[143].

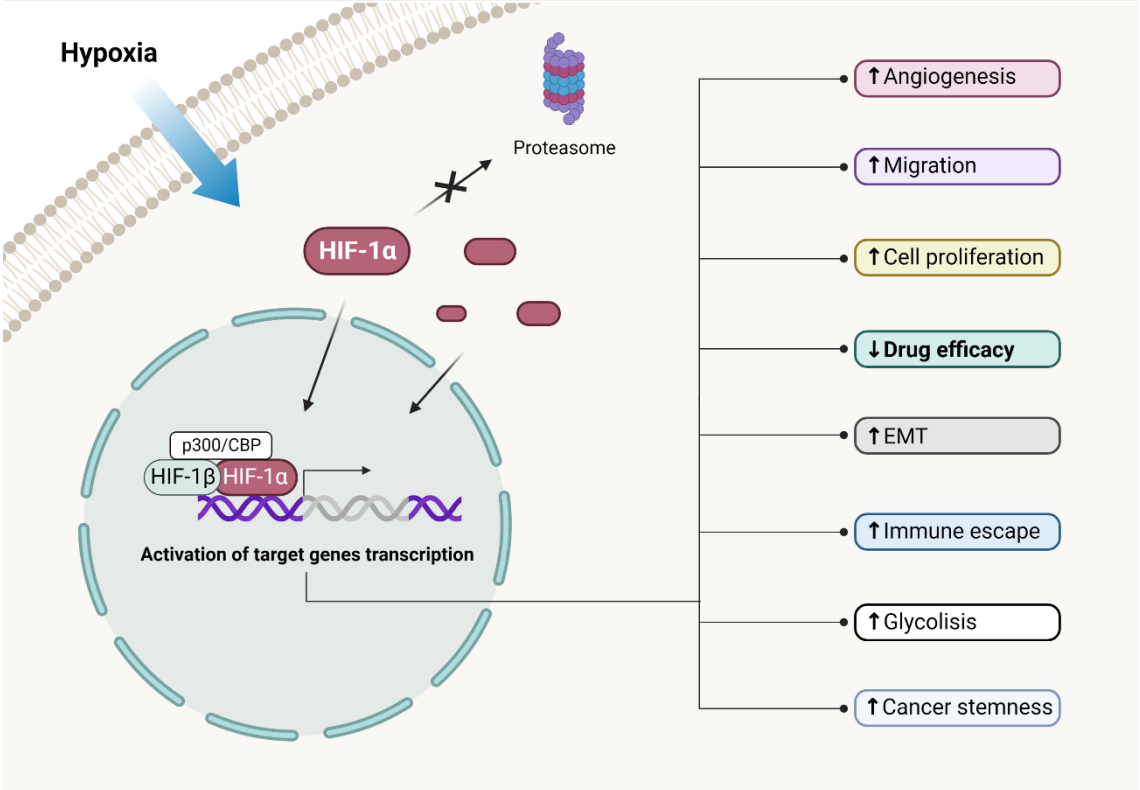

Figure 13. Main cellular processes modulated by the HIF-1α-derived hypoxia response. HIF-1α acts as transcription factor of multiple proteins with key functions in tumor development, progression and chemoresistance in HCC, inducing and blocking different cellular processes. Created with BioRender.com.

Under hypoxia, important changes occur in the processes of angiogenesis, invasion, migration and metastasis due to a HIF-1α-derived hypoxia response in cancer cells[139] (**Figure 13**). Specifically, HIF-1α is able to induce EMT and the expression of pro-angiogenic proteins, highlighting VEGF as a direct target gene of both HIF-1α and HIF-2α, that promotes the generation of new blood vessels for the transport of nutrients and oxygen[141,143]. Besides, along with VEGF, HIF-1α modulates different mechanisms that triggers EMT and metastasis of tumor hepatocytes, including the Snail homolog 1 (SNAI1) and SMAD-interacting protein 1 (SIP1), NF-κB, Wnt, and Notch signaling pathways[141]. In order to favor the migration of tumor hepatocytes, under hypoxic conditions, MMPs expression is also transcriptionally increased, being MMP2 and MMP9 described as HIF-1α targets, which leads to the remodeling of ECM, a key step for tumor metastasis[141,145] (**Figure 13**).

In addition, during the cellular adaptation to hypoxia, HIF-1α-derived effects have been correlated with a promotion of HCC stem cells, favoring the maintenance and induction of CSC and EMT phenotypes[141,145] (**Figure 13**). Although CSCs play an

essential role in HCC, the exact mechanism by which hypoxia is able to modulate stemness is still unclear, highlighting its association with the EMT induction derived from HIF-1α response[141,145]. Interestingly, a hypoxic microenvironment in HCC has been correlated with an increased number of immune cells that participate in the tumor escape from immune surveillance[145] (**Figure 13**). An increase in the cell population of myeloid-derived suppressor cells (MDSCs) and plasmacytoid dendritic cells (pDCs) has shown to be a direct effect derived from the HIF-1α-mediated hypoxia[145]. Moreover, this transcription factor also modulates tumor-associated macrophages (TAMs) and crucial cytokines as part of the immune escape mechanism in HCC prompted by hypoxia[141,145].

The key function exerted by hypoxia, mainly mediated by HIF-1α, during hepatocarcinogenesis has been broadly studied[143]. Several proteins that act as oncogenes, such as forkhead box protein M1 (FoxM1) and aurora kinase A (AURKA), have exhibited a direct transcriptional regulation by HIF-1α, which induces cell survival and proliferation in HCC[143] (**Figure 13**). Remarkably, hypoxic conditions have been also strongly linked to the loss of chemotherapeutic effectiveness, being broadly described as a resistance mechanism of several drugs, such as sorafenib[135,145] (**Figure 13**), which is further discussed in the following section.

3.5.3 HIFs response and drug resistance in HCC

Sustained treatment with sorafenib and other molecular targeted drugs with important antiangiogenic effects frequently drift in the establishment of a hypoxic microenvironment[123]. Activation of the hypoxia response can induce the acquisition of a resistant phenotype by tumor hepatocytes, which leads to the therapeutic failure[146]. Although studies assessing the potential association between hypoxia and resistance development have focused in the mechanisms of sorafenib resistance, several mechanisms have also been associated to sensitivity loss of other drugs, such as doxorubicin, etoposide and cisplatin[143,144].

Among the cellular and molecular processes involved in the acquisition of sorafenib resistance by HCC cells, hypoxia has been revealed as a key mechanism, mainly mediated by HIF-1α[123,146]. Different signaling routes have found altered in HCC cells with resistance to sorafenib and other chemotherapeutic agents, including PI3K/AKT, MAPK/ERK, Yes-associated protein (YAP) or TGF-α/EGFR pathways[143,146]. Moreover, angiogenesis, through a HIF-1α-derived VEGF expression, metastasis, cell proliferation

and mitophagy have been also described as underlying mechanisms on the sorafenib resistance acquisition in HCC[123,146]. Increased expression of multidrug resistance protein 1 (MDR1) has been also associated to the development of sorafenib resistance, being transcriptionally induced by HIF-1α and, in consequence, leading to a higher sorafenib expulsion from the cells[123]. HIF-1α has demonstrated in several studies to directly mediate an adaptive response of tumor hepatocytes to, not only stress conditions that often lead to cell death, but also to initially effective drugs triggering a resistant phenotype and worse patient's outcomes[123,143,146]. Therefore, despite most investigations have identified resistance mechanisms to sorafenib, the hypoxic microenvironment, and specifically HIF-1α, remains a promising target strategy for improving the efficacy of current therapeutic options[146].

4 Aims

According to the previous information, the aim of this PhD Thesis was to elucidate the potential role of NRP1 as a biomarker for prognosis, diagnosis and other tumor-associated parameters in HCC patients, as well as to elucidate the mechanisms underlying the antitumor effects and potential efficacy loss of lenvatinib in an *in vitro* model of human HCC.

Therefore, to accomplish this purpose, the following specific objectives were established:

1. To identify the potential correlation between increased levels of NRP1 and a worse prognosis by meta-analysis of available data from HCC patients.
2. To determine the likely association of NRP1 overexpression with the development of HCC through meta-analysis of data from HCC and paired non-tumor samples.
3. To evaluate the clinical correlation of NRP1 with different clinicopathological features in samples from HCC patients.
4. To characterize the expression of NRP1 in human HCC samples from public databases and in different HCC cell lines.
5. To assess the antitumor properties of lenvatinib *in vitro* and the likely implication of NRP1 in the inhibitory effects in cell proliferation and migration of lenvatinib.
6. To identify the cellular mechanism responsible for the NRP1 downregulation caused by lenvatinib in the HCC cell lines Hep3B and Huh-7.
7. To analyze the potential involvement of the autophagy-associated NRP1 degradation in the antitumor effects of lenvatinib in HCC cells.
8. To investigate the derived effects from hypoxia induction *in vitro* in the NRP1 expression and the likely role played by autophagy in the Hep3B and Huh-7 cell lines.
9. To determine the implication of a HIF-1α-driven hypoxia response in the therapeutic efficacy of lenvatinib mediated by the autophagy-dependent NRP1 modulation in the HCC cell lines Hep3B and Huh-7.

5 Material and methods

5.1 WORKSPACE

The present PhD Thesis has been performed at the Institute of Biomedicine (IBIOMED) of the University of León. Confocal and fluorescence microscopy experiments were carried out at the Microscopy Service of the University of León.

5.2 SYSTEMATIC REVIEW WITH META-ANALYSIS

Since results from individual studies are frequently not robust enough to provide confident information, a meta-analysis might be a useful tool for solving conflicts between studies[147]. A meta-analysis is a statistical method that combines the results from different investigations on the same topic which have been increasingly used in the medical research[147]. This statistical tool generates a precise estimate of the global effect size from a broad number of studies, reducing the bias among them[147]. In this PhD Thesis, the potential association of NRP1 with pathogenesis, prognosis and several clinicopathological characteristics in HCC patients was assessed by systematic review with meta-analysis.

5.2.1 Systematic review and meta-analysis objectives and protocol registration

This study aimed at evaluating the diagnostic and prognostic potential of NRP1 in patients with HCC, by analyzing the correlation between high NRP1 levels and different survival parameters and other clinical and pathological characteristics.

The study protocol of the present systematic review with meta-analysis was registered in the International Prospective Register for Systematic Reviews (PROSPERO) with the registration code CRD42022307062. Besides, the Preferred Reporting Items for Systematic Reviews and Meta-Analyses (PRISMA) guidelines were used for conducting the study (**Supplementary Tables SI and SII**)[148].

5.2.2 Search strategy

A complete and exhaustive search of the scientific literature was performed in five databases, PubMed, Scopus, Web of Science (WOS), Embase and the Cochrane Library, including articles published up to 31st May 2022. Potential studies to be included were identified by using the following search strategy: (“nrp1” OR “nrp-1” OR “nrp 1” OR “neuropilin 1” OR “neuropilin-1” OR “CD304” OR “VEGF165R”) AND

("hepatocellular carcinoma" OR "hepatocarcinoma" OR "HCC"), which was specifically established for each database (**Table III**).

Table III. Full search strategy used for each database.

Database	Search strategy
PubMed	("nrp1"[All Fields] OR "nrp-1"[All Fields] OR "nrp 1"[All Fields] OR "neuropilin 1"[All Fields] OR "neuropilin-1"[All Fields] OR "CD304"[All Fields] OR "VEGF165R"[All Fields]) AND ("hepatocellular carcinoma"[All Fields] OR "hepatocarcinoma"[All Fields] OR "HCC"[All Fields])
Scopus	TITLE-ABS-KEY (("nrp1" OR "nrp-1" OR "nrp 1" OR "neuropilin 1" OR "neuropilin-1" OR "CD304" OR "VEGF165R") AND ("hepatocellular carcinoma" OR "hepatocarcinoma" OR "HCC"))
WOS	TS=(("nrp1" OR "nrp-1" OR "nrp 1" OR "neuropilin 1" OR "neuropilin-1" OR "CD304" OR "VEGF165R") AND ("hepatocellular carcinoma" OR "hepatocarcinoma" OR "HCC")) *Indexes=SCI-EXPANDED, SSCI, A&HCI, CPCI-S, CPCI-SSH, BKCI-S, BKCI-SSH, ESCI, CCR-EXPANDED, IC* *Timespan=All years*
Embase	('nrp1' OR 'nrp-1' OR 'nrp 1' OR 'neuropilin 1'/exp OR 'neuropilin 1' OR 'neuropilin-1' OR 'neuropilin-1' OR 'cd304' OR 'vegf165r') AND ('hepatocellular carcinoma' OR 'hepatocellular carcinoma' OR 'hepatocarcinoma' OR 'hepatocarcinoma' OR 'hcc')
Cochrane Library	("nrp1" OR "nrp-1" OR "nrp 1" OR "neuropilin 1" OR "neuropilin-1" OR "CD304" OR "VEGF165R") AND ("hepatocellular carcinoma" OR "hepatocarcinoma" OR "HCC"):ti, ab, kw

5.2.3 Eligibility criteria

Articles that met the following criteria were included in this analysis: (1) patients diagnosed with HCC; (2) evaluation of NRP1 expression either in tumor tissue or tumor-derived samples; (3) association of NRP1 expression levels with survival parameters or other clinicopathological features with data reported or potentially extracted; (4) full text in English.

Otherwise, articles complying with the following criteria were excluded: (1) studies conducted exclusively with *in vitro* or *in vivo* models; (2) reviews, book chapters,

conference communications and similar; (3) articles without useful data or data that cannot be estimated; (4) full text in English not available.

5.2.4 Data extraction and quality assessment

Two researchers, including the author of the present PhD Thesis, performed independently the steps of study screening, data extraction and quality evaluation of the included studies, and discrepancies were solved through discussion and consensus.

Study quality was assessed with the Newcastle-Ottawa scale (NOS), assigning a score between 0 and 9[149], where high quality was defined by a NOS score of 5 or higher, and low quality when NOS score was lower than 5. Research articles with a low-quality score were excluded from the quantitative analysis.

Data extraction was conducted for all the included articles and compiled in a results table, summarizing specifications of the antibodies and staining protocols from the studies that analyzed NRP1 levels by immunohistochemistry (IHC) in **Supplementary Table SIII**.

5.2.5 Statistical analysis

Pooled analysis

For the statistical analysis the STATA 16 software (Stata Corporation, College Station, TX, USA) was used. The parameter OS was determined from the intervention time to the date of the last follow up. We pooled the OS by hazard ratio (HR) with 95% confidence interval (CI) to determine the association of NRP1 overexpression and HCC prognosis. When data was not directly provided, the Parmar method[150] was employed for a mathematical estimation of the HR. Global effects were assessed by combining HR and 95% CI of all studies. Otherwise, the potential correlation of NRP1 with tumor pathogenesis and other clinicopathological features was determined by odds ratio (OR) and 95% CI. For both HR and OR, a value higher than one manifested that NRP1 overexpression is correlated with an increased risk of shorter prognosis or increased incidence of the clinical parameters, respectively, being significant when $p<0.05$.

Heterogeneity analysis

Heterogeneity among studies was evaluated with two different methods, the chi-square-based Q test, with the Q test *p*-value as indicator, and the I^2 statistic, which ranges from 0% (no heterogeneity) to 100% (maximal heterogeneity). A significant heterogeneity was identified when $I^2 \geq 50\%$ and/or Q test *p*-value<0.10, using the Restricted Maximum Likelihood (REML) method for the random-effects model. Otherwise, the Inverse Variance (IV) procedure was employed for the fixed-effects model when heterogeneity was not significant among studies. The assessment of the likely sources of heterogeneity was conducted by meta-regression and analysis of subgroups, with sample size, NOS score and follow up time as moderators.

Publication bias assessment

Finally, the presence of publication bias between included studies was determined by identification of funnel plot asymmetry and Egger's test analysis. Significant publication bias was defined when Egger's test *p*-value<0.05 and when a strong asymmetry was observed. Those analysis that resulted in a significant bias were subjected to the trim-and-fill method to obtain an estimated overall effect size with a mathematical correction that consider the risk of bias.

5.3 EXPERIMENTAL STUDY

The role of NRP1 in the loss of lenvatinib sensitivity in HCC was evaluated employing the subsequent described methodology, which included the analysis of data from publicly available databases and the use of different cell lines as *in vitro* HCC model.

5.3.1 Public human databases

Gene expression analysis

Data from publicly available databases, broadly described in **Table IV**, was employed for analyzing gene expression levels of NRP1 in HCC patients. Data analysis and graphical representations were conducted with the tools from the databases, regardless of the data obtained from the Gene Expression Omnibus (GEO) database (**Table IV**), accession GSE14520[151]. For this, RNA-seq results from tumor and paired non-tumor tissues of HCC patients were used for representing the fold change of multiple genes, detecting the differential NRP1 expression. Globally, 1039 and 662 samples from HCC and healthy liver, respectively, were analyzed from four dataset sources: (1) The Cancer Genome Atlas (TCGA), (2) Genomic Data Commons (GDC)-TCGA, (3) Genotype-Tissue Expression (GTEx) and (4) GSE14520.

Table IV. Databases employed for the analysis of gene expression levels of NRP1 and correlation analysis with autophagy-related genes and HIF-1α. Public databases used for each analysis are identified, describing the analysis performed with data from each database, the link and the bibliographic source.

Database	Analysis	Link	Ref.
HPA	Gene expression levels	https://www.proteinatlas.org/	152
UALCAN	Gene expression levels Gene correlation with autophagy-related genes Gene correlation with HIF-1α	http://ualcan.path.uab.edu/analysis.html	153
GEPIA	Gene expression levels Gene correlation with HIF-1α	http://gepia.cancer-pku.cn/	154
UCSC Xena	Gene expression levels Gene correlation with HIF-1α	https://xenabrowser.net/heatmap/	155
GEO	HCC *vs* healthy liver tissues expression	https://www.ncbi.nlm.nih.gov/geo/	156

GEPIA, Gene Expression Profiling Interactive Analysis; HPA, Human Protein Atlas; Ref., reference; UCSC, University of California Santa Cruz.

Gene correlation analysis of NRP1 in HCC patient samples

The potential correlation between NRP1 gene expression and several autophagy-associated genes was performed with the UALCAN database (**Table IV**), based on the autophagy KEGG pathway (hsa04140) for the identification of key autophagy mediators. Positive or negative correlations with NRP1 were evaluated and identified, and Pearson-coefficient correlation (Pearson-CC) values were calculated for each significant association. Similarly, correlation analysis of NRP1 and HIF-1α gene expression was conducted with the UALCAN, University of California Santa Cruz (UCSC) Xena and Gene Expression Profiling Interactive Analysis (GEPIA) databases (**Table IV**), which included the TCGA and GDC-TCGA datasets. Pearson-CC and graphical representations were also obtained from the databases to determine the presence of gene correlation.

5.3.2 Cell culture and reagents

HCC cell lines

The three human HCC cell lines, Hep3B, HepG2 and Huh-7 were purchased from the American Type Culture Collection (Manassas, VA, USA). Cell lines were cultured under controlled conditions of 37ºC and an atmosphere with 5% CO_2, employing the DMEM-high glucose medium (D5796, Sigma-Aldrich, Sant Louis, MO, USA) supplemented with 10% fetal bovine serum (FBS, ref. 10270106) and penicillin/streptomycin (P/S, ref. 15140122) (100 U/ml) (Gibco™, Gaithersburg, MD, USA) for cell maintenance. Cell passages were performed when confluency reached 80% and cell culture was maintained for no longer than 25 passages. For cell passaging, cells were washed with phosphate buffered saline (PBS) (D8537, Sigma-Aldrich) and incubated with 0.05% trypsin-EDTA 1x (25300, Gibco™) for 3-5 min at 37ºC. Then, double amount of complete medium was added to stop the enzymatic activity of the trypsin, and cells were centrifuged at 1,100 rpm for 3 min. The pellet was resuspended in complete fresh medium and $2x10^6$ cells were seeded in 75 cm^2 flasks (353136, Corning® Inc, New York, NY, USA). For other culture plates the number of cells was proportionally adapted based on the surface area.

Culture reagents and treatments

Reagents employed for cell treatments of the different experiments conducted are identified in **Table V**, specifying the function (e.g. inhibitor, targeted drug), and the doses used for each experiment.

Table V. Reagents employed for cell treatments. Name, concentration and function of each compound, and the experiment in which is employed, is specified.

Reagent (Reference)	**Distributor**	**Function**	**Experiment**	**Concentration**
Lenvatinib (E7080, S1164)	Selleckchem (Houston, TX, USA)	TKI First-line drug approved against HCC	Viability assay	0.5 – 30 µM
			NRP1 Western blot	2.5 and 5 µM
			All the experiments with silencing	2.5 µM
EG00229 trifluoroacetate (6986)	Tocris Bioscience (Bristol, UK)	NRP1 antagonist	Viability assay	2.5 – 50 µM
			Rest of experiments	15 µM
CHX (0970)	Tocris Bioscience	Synthesis inhibitor	All the experiments	300 µM
MG132 (1748)	Tocris Bioscience	Inhibitor of the proteasome-mediated protein degradation	All the experiments	30 µM
Bafilomycin A1 (1334)	Tocris Bioscience	Inhibitor of the autophagosome-lysosome fusion	All the experiments	100 nM
$CoCl_2$ (131257.1208)	Panreac AppliChem (Barcelona, Spain)	PHD stabilization Induction of hypoxia response	All the experiments	100 µM

CHX, cycloheximide.

5.3.3 Transient gene silencing

Specific gene silencing was conducted by seeding $2x10^5$ cells per well in 6-well plates (353046, Corning®). After 24 h, the silencing protocol was started. Firstly, the corresponding siRNAs, ON-TARGETplus Non-targeting Control Pool (a negative control pool of 4 siRNA), ON-TARGETplus Human HIF1A siRNA SMARTPool (a mixture of 4 siRNA targeting HIF1A) or ON-TARGETplus Human NRP1 siRNA SMARTPool (a mixture of 4 siRNA targeting NRP1), were prepared at 5 µM in 1x siRNA Buffer (60 mM KCl, 6 mM pH 7.5 HEPES, 0.2 mM $MgCl_2$). 5 µM siRNA was mixed with the OPTI-MEM® reduced serum medium (31985062, Gibco™) to a final concentration of 0.25 µM; and, separately, the total same amount of DharmaFECT™ 4 Transfection Reagent (T-2004-03, Horizon Discovery, Waterbeach, UK) with serum-reduced OPTI-MEM® medium was prepared at 1:25. After 5 min incubation at room temperature (RT), both solutions of siRNA-OPTI-MEM® and DharmaFECT 4 Transfection Reagent-OPTI-MEM® were mixed 1:1, and incubated for 20 min at RT. During this incubation, cell medium was replaced by P/S-free medium (1.6 mL per well). Finally, 0.4 mL of silencing mix was added dropwise to each well.

After 8 h from gene transfection, medium was replaced by complete fresh medium and, when necessary, cells were re-seeded for the corresponding experiment conditions. 24 h post-transfection, cell treatments were added according to the established experiment, and kept for additional 24 h. Therefore, the assays were performed after 24 h of treatments and 48 h of gene silencing.

5.3.4 Analysis of cell viability and proliferation

Two assays were performed to analyze cell viability, the CellTiter-Glo® Luminescent Cell Viability Assay (G7572, Promega, Madison, WI, USA) and the 3-(4,5-dimethylthiazol-2-yl)-2,5-diphenyl-tetrazolium bromide (MTT) (M5655, Sigma-Aldrich) assay. For both methods, $5x10^3$ cells per well were seeded in 96-well plates (07-6096, Biologix, Camarillo, CA, USA) and, after 24 h, cells were silenced and/or treated for the corresponding experiments, considering that the final volume per well was 100 µL for CellTiter-Glo® assay, and 200 µL for MTT assay. Once the final time point was reached, the following procedure was performed for each technique.

CellTiter-Glo® assay

For CellTiter-Glo® assay, 100 µL of the commercial solution were added to each well, mixing for 10 min protected from light. Afterwards, 100 µL of each well were placed in a 96-well plate white polystyrene (3362, Corning®) to conduct the luminescence reading with the Synergy™ HT Multi-Mode Microplate Reader (BioTek Instruments, Winooski, VT, USA) and Gen5 1.11 software.

MTT assay

MTT assay was performed by preparing a 5 mg/mL solution of MTT in PBS which, immediately before the assay, was diluted 1:10 with FBS-free medium. Firstly, medium was removed from cells, washing with PBS and incubating with the MTT solution previously prepared, for 3 h at 37ºC and 5% CO_2. After incubation, medium was removed, and formazan crystals formed were dissolved by adding 200 µL dimethyl sulfoxide (DMSO, D5879, Honeywell, Charlotte, NC, USA) per well. For complete dissolution, the 96-well plate was agitated for 5 min under dark conditions and absorbance at 560 nm was measured with the Synergy™ HT Multi-Mode Microplate Reader and Gen5 1.11 software (BioTek Instruments).

5.3.5 Analysis of colony formation ability

To analyze the colony formation ability, $2x10^4$ cells per well were seeded in 6-well plates, letting cell attachment for 24 h. Cells were silenced and/or treated according to the experiment conditions, and maintained for 7 days at 37ºC and 5% CO_2. At final time point, medium was removed, and cells were washed twice with PBS and fixed with 4% formaldehyde (28908, Thermo Fisher Scientific, Waltham, MA, USA) for 15 min at RT. Then, cells were washed with Milli-Q water and incubated for 15 min with 0.1% crystal violet (69710, Sigma-Aldrich) in 10% ethanol for cell staining. Lastly, cells were washed again with Milli-Q water and air-dried, and colonies were photographed to subsequently count them with Fiji/ImageJ software (National Institute of Mental Health, Bethesda, MD, USA).

5.3.6 Analysis of mRNA expression

Gene expression was analyzed by quantitative real-time reverse transcription polymerase chain reaction (qRT-PCR). Cells were seeded in p60 plates (150288, Thermo Fisher Scientific) at $8x10^5$ cell density and, after 24 h, cells were silenced and/or treated for the corresponding times. Initially, total RNA was extracted employing TRIzol® Reagent (15596026, Invitrogen, Waltham, MA, USA) and quantified with the Nanodrop™ ND-1000 Spectrophotometer (Thermo Fisher Scientific). Elimination of residual DNA was conducted by treating with RQ1 RNase-free DNase kit (M6101, Promega) and 1 µg per sample was retrotranscribed into cDNA by using the High-Capacity cDNA Reverse Transcription Kit (4368813, Applied Biosystems, Waltham, MA, USA). Resulting cDNA was subsequently subjected to the PCR amplification employing the *Power* SYBR™ Green PCR Master Mix (4367659, Applied Biosystems) and the human primers for NRP1 forward 5'-CGGGACCCATTCAGGATCAC-3') and reverse (5'-CAGGTCTGCTGGTTTTGCAC-3'), and, as endogenous control, 18S rRNA forward (5'-CCGAAGATATGCTCATGTGG-3') and reverse (5'-TCTTGTACTGGCGTGGATTC-3') (Sigma-Aldrich), using the QuantStudio® 5 System qRT-PCR (Thermo Fisher Scientific). All the steps were performed in accordance to the manufacturer's instructions and relative gene expression changes were quantified by the $2^{-\Delta\Delta Ct}$ method[157].

5.3.7 Analysis of protein expression by western blot

Western blot assay represents a useful technique to determine the protein expression levels of a specific molecular target, based on the extraction, purification and quantification of total protein content from cells. By using polyacrylamide gels, proteins are separated through electrophoresis based on the size, which, after transference to a membrane, are incubated with primary antibodies against the target protein of interest, and, subsequently, with the corresponding secondary antibodies to visualize the protein expression levels[158].

Cell lysis and protein extraction

At first, cells were seeded onto p60 plates at $8x10^5$ cell density and, after 24 h, cells were silenced and/or treated for the corresponding time periods. Once finished the specific treatments and manipulations, cells were placed on ice to stop enzymatic activity

and washed once with ice-cold PBS. 100 µL of homogenization buffer were added per plate. This homogenization buffer is constituted by 0.25 mM sucrose, 1 mM EDTA pH 7.4, 10 mM Tris-HCl, complemented with protease inhibitor cocktail (04 906 845 001, Roche Diagnostics GmbH, Mannheim, Germany) and phosphatase inhibitor cocktail (11836170001, Roche Diagnostics GmbH) 1x. With the homogenization buffer in the plate placed on ice, cells were harvested with a cell scraper and collected into tubes. Afterwards, cell lysis was performed by sonication with the UP50H Compact Ultrasonic Processor (Hielscher Ultrasonics, Teltow, Germany). 2 pulses with 60% amplitude and 20 s duration were performed for each sample, and cells were then centrifuged at 14,000 rpm for 15 min and 4ºC. In this step, samples can be stored at -20ºC.

Total protein quantification

Total amount of protein in each sample was quantified by employing the Bradford colorimetric assay. The Bradford solution, Bio-Rad Protein Assay Dye Reagent Concentrate (5000006, Bio-Rad, Hercules, CA, USA) employed is based on the Bradford method and uses the Coomassie® Brilliant Blue G-250 dye, whose absorbance maximum shifts from 465 nm to 595 nm when binds to proteins. Initially, the Bradford reagent was dissolved 1:4 in Milli-Q water and a standard curve of bovine serum albumin (BSA) was prepared. Both samples and standard curve were loaded in a 96-well plate, and the 1:4 Bradford solution was finally added to each well following the manufacturer's instructions, mixing for 20 min in dark. After incubation, absorbance at 595 nm was measured with the Synergy™ HT Multi-Mode Microplate Reader using the Gen5 1.11 software (BioTek Instruments). Total protein levels were calculated based on the absorbance values and the standard curve values for absorbance and protein concentration.

Gel handcasting and gel electrophoresis

For an appropriate identification of differences in protein expression, the same amount of protein (20 µg) was loaded for every sample in the polyacrylamide gels. The protein samples were prepared by mixing in a 1:4 proportion with Laemmli Buffer 4x (1x final concentration), which contains 277.8 mM Tris-HCl pH 6.8, 44.4% glycerol, 4.4% sodium dodecyl sulfate (SDS), 0.02% bromophenol blue and was previously complemented 1:10 with 2-mercaptoethanol (576631, Panreac AppliChem). Once

prepared, samples were incubated at 100ºC for 3 min to accomplish protein denaturization, and, they were subsequently loaded into the polyacrylamide gels.

Polyacrylamide gels are constituted by the resolving and stacking gel solutions and were prepared in the laboratory by using: 30% Acrylamide/Bis Solution, 29:1 (1610156, Bio-Rad); 1.5 M Tris-HCl pH 8.8 for resolving and 0.5 M Tris-HCl pH 6.8 for stacking; ammonium persulfate (APS, 1610700, Bio-Rad); SDS; and tetramethylethylenediamine (TEMED, 161-0800, Bio-Rad). The corresponding amounts were established following the manufacturer's instructions (Bio-Rad) to prepare polyacrylamide gels of 8%, 10% and 12% for protein separation.

With the polyacrylamide gels prepared, samples were loaded along with the PageRuler™ Prestained Protein Ladder (26617, Thermo Fisher Scientific), and sodium dodecyl sulfate-polyacrylamide gel electrophoresis (SDS-PAGE) was performed. Gels were subjected to an electric field of 70 V until rising the resolving part, where 120 V were applied. When samples were appropriately separated, the running was stopped.

Rapid transference and membrane blocking

Gels carrying the separated proteins were transferred to polyvinylidene difluoride (PVDF) membranes (1620177, Bio-Rad), which were previously activated by embedding them in methanol for 15 s, washing with Milli-Q water and stabilizing in transfer buffer. For the transference, the Trans-Blot® Turbo™ Transfer System (Bio-Rad) was used according to the manufacturer's instructions. After completion, proteins from the gel were transferred to the PVDF membrane, letting an easier manipulation for the following steps. Membranes were then blocked for 1 h at RT in a solution of 5% milk powder dissolved in 0.05% PBS-Tween 20 (PBS-T) (170-6531, Bio-Rad) to prevent unspecific antibody binding.

Antibody incubation and protein detection

After blocking, membranes were incubated with the corresponding primary antibody for the detection of the protein of interest (**Table VI**) O/N at 4ºC. After primary incubation, membranes where washed three times with PBS-T and incubated with the secondary antibodies conjugated with horseradish peroxidase (HRP) (**Table VI**) for 1 h at RT. As loading control, a peroxidase-conjugated antibody of β-actin was used (**Table VI**).

To accomplish protein detection, membranes were washed three times after secondary antibody, and incubated with Pierce™ ECL Western blotting Substrate (32106, Thermo Fisher Scientific) for 1 min, which contains the HRP substrate. In the presence of the substrate, a chemiluminescent reaction occurs that can be detected by photographic revealing with the films Amersham™ Hyperfilm™ ECL (28906837, Cytiva, Uppsala, Sweden). Specifically, after substrate incubation, membranes were placed into X-ray film cassettes, and films were used for capturing the chemiluminescent signal. These films were immersed in the developer solution (933739, Fuji Hunt, Barcelona, Spain), washed with water, and fixed with the fixer solution (933747, Fuji Hunt, Barcelona, Spain). Finally, films were washed again with water, air-dried and scanned for protein quantification by densitometry reading of each protein band with Fiji/ImageJ software.

Table VI. Antibodies employed for Western blot and immunofluorescence experiments. The type of antibody, the protein that detects, the dilution employed and the reference and distributor for each antibody are specified.

Assay	Type of antibody	Protein	Molecular weight	Dilution	Ref.	Distributor
			Primary antibodies			
WB	Rabbit polyclonal IgG	HIF-1α	100 kDa	1:500	ab2185	Abcam
WB IF	Rabbit monoclonal IgG	NRP1	120 kDa	1:1,000 1:250	ab81321	Abcam
WB	Rabbit polyclonal	p62/ SQSTM1	62 kDa	1:1,000	#5114	Cell Signaling
WB	Rabbit monoclonal IgG	LC3	14/16 kDa	1:1,000	#12741	Cell Signaling
WB	Peroxidase conjugate mouse monoclonal	β-actin	42 kDa	1:50,000	A3854	Sigma-Aldrich
IF	Mouse monoclonal IgG_1	Ki67	395/345 kDa	1:200	sc-23900	Santa Cruz Biotechnology
			Secondary antibodies			
WB	Goat anti-rabbit polyclonal	Anti-rabbit	–	1:20,000	31460	Thermo Fisher Scientific
IF	Goat anti-rabbit IgG	Alexa Fluor® 647	–	1:1,000	ab150079	Abcam
IF	Goat anti-mouse IgG	Alexa Fluor® 488	–	1:1,000	ab150113	Abcam

IF, immunofluorescence; Ref., reference; WB, Western blot.

5.3.8 Analysis of protein expression by immunofluorescence and laser confocal microscopy

For protein analysis by immunofluorescence, $3x10^4$ cells per well were seeded in 24-well plates (353047, Becton Dickinson, Franklin Lakes, NJ, USA) containing a coverslip (13 mm, 83.1840.002, Sarstedt, Newton, NC, USA) coated with 0.2% gelatin (G9391, Sigma-Aldrich) dissolved in PBS. After 24 h, cells were silenced and/or treated according to the experiment settings. In the 24-well plate, cells were washed thrice with PBS and fixed with 4% formaldehyde for 15 min at RT. Between each step, cells were washed three times with PBS. After fixation, cells were incubated with 0.2% saponin (47036, Sigma-Aldrich), dissolved in PBS, for 20 min at RT to permeabilize the cell membrane, washed again and blocked by incubation with 1% BSA (A0281, Sigma-Aldrich), dissolved in PBS, for 30 min at RT. Cells were then washed and, using forceps, coverslips were placed in a humidified recipient with the solutions of the corresponding primary antibodies (**Table VI**), prepared in 1% BSA, and were incubated O/N at 4ºC.

The following day, cells were washed thrice with PBS and incubated with the corresponding secondary antibodies (**Table VI**) for 1 h at RT, protected from light hereinafter, and washed again. Afterwards, DAPI solution (9542, Sigma-Aldrich) was used for a 5 min incubation at RT as nucleic acid staining, and cells were finally washed three times with PBS. Coverslips were mounted on glass slides with the Fluoromount-G™ mounting medium (00-4958-02, Invitrogen) and samples were visualized in the Zeiss LSM 800 confocal laser scanning microscope with the Zeiss Zen software (Zeiss, Jena, Germany). Fluorescence was quantified with the Fiji/ImageJ software, using the corrected total cell fluorescence (CTCF) formula[159]:

CTCF = Integrated density – (area of selected cell X mean fluorescence of background readings)

After calculation of the CTCF value, each sample result was relativized to the cell number in the image to represent results.

5.3.9 Analysis of cell migration

Migration ability of cells was assessed by wound-healing assay, seeding cells in 6-well plates at 90% confluency. After 24 h, cells were silenced and/or treated, and medium was removed. A straight scratch in the cell monolayer was done by using a 200-µL pipette tip, and then, two washes with medium were performed to remove the non-adherent cells. Complete fresh medium was then added, and pictures were taken after 0, 4, 8, 12 and 24 h for the initial analysis of migration ability, and after 0 and 24 h for the other experiments, with the Eclipse TE2000 inverted microscope (Nikon Instruments Inc., Melville, NY, USA). For cell migration analysis, Fiji/ImageJ software was used for measuring the wound area, and cell migration ability was calculated based on the following formula[160]:

[(wound area at 0 h – wound area at time point) / (wound area at 0 h)]*100

5.3.10 Analysis of autophagosome-lysosome content

The analysis of the autophagy process is complex due to the dynamics that characterize it. Among the available techniques, the quantification of the autophagosome-lysosome content provides useful information on the basal autophagic flux when specific autophagy inhibitors are employed as positive controls. In this regard, the acridine orange staining is an acidotropic dye that stains acidified vesicular compartments conferring a red-orange fluorescence. This technique represents a suitable method for the determination of the levels of autophagolysosome structures and, therefore, for monitoring the autophagy process; even though, its combination with additional measurements, such as analysis of LC3 or p62/SQSTM1 levels, is recommended[134,159].

Initially, $2.5x10^4$ cells per well were seeded in 8-chamber culture slides (354108, Becton Dickinson) and, after 24 h, the silencing and/or treatments were performed. At the end point, medium was removed, and cells were washed with warmed PBS (at 37ºC) to prevent cell death. Then, an incubation with 1 µg/mL acridine orange (1333, Merck, Darmstadt, Germany) was conducted for 15 min at 37ºC under dark conditions. The dye excess was eliminated, and cells were washed with warmed PBS. Samples were briefly dried and mounted, being immediately visualized in the Nikon Eclipse E600 microscope (Nikon Instruments Inc.) with the NIS-Elements software (Nikon Instruments Inc.). Images were analyzed with Fiji/ImageJ software and the CTCF formula was also

employed for calculating the red and green fluorescence for each image. For results representation, the red/green CTCF ratio, relativized to cell number, was used.

5.3.11 Autophagic flux assay

For measuring autophagy flux, an index was calculated by using the protein expression levels of LC3-II in presence and absence of the autophagic inhibitor Baf. The autophagic flux index was calculated with the following formula, using the protein levels from the western blot determination of LC3-II, relativized to the loading control β-actin.

LC3-II protein levels after Baf treatment / LC3-II protein levels in the absence of Baf*

*With or without the corresponding treatments employed in each experiment.

5.3.12 Statistical analysis

The statistical analysis for the human datasets was performed as described in the 4.3.1 section, obtaining the *p*-values directly from the databases. Only for the GEO database, in which the GSE14520 dataset was analyzed, the *p*-value for the differential expression of NRP1 was determined with the GraphPad Prism 8 software (GraphPad Software, San Diego, CA, USA).

Experimental analysis from the *in vitro* results were also conducted with the GraphPad Prism 8 software, representing the results as mean values ± standard deviation (SD). For experiments comparing only one group with the control group, an unpaired t-test was performed. When three or more groups were compared in the presence of only one factor or variable (e.g. lenvatinib administration), we performed one-way ANOVA; whereas when the effect of two different factors was evaluated (e.g. lenvatinib administration and gene silencing), a two-way ANOVA was used. After both ANOVA tests, the Tukey, Dunnett or Sidak post-hoc tests were conducted to identify the groups with significant differences. Statistical significance was considered when p-value<0.05.

6 Results

6.1 SYSTEMATIC REVIEW WITH META-ANALYSIS: CLINICAL ASSOCIATION OF NRP1 WITH PROGNOSIS, DIAGNOSIS AND CLINICOPATHOLOGICAL FEATURES IN HCC

Even though recent findings have evidenced the potential function of NRP1 in cancer, including HCC, the role played by NRP1 in the development and progression of this liver tumor remains unclear[70,73]. For this reason, in this study we aimed at assessing the potential association of NRP1 with prognosis, tumor development, and different clinical and pathological characteristics of human patients diagnosed with HCC, describing the main results obtained in the following sections.

6.1.1 Selection and characteristics of included studies

After conducting an exhaustive search of the literature in five databases, a total of 191 articles were initially identified. Duplicates between databases were removed, where 112 studies were subjected to the following steps. At first, a screening based on title and abstract was performed, removing 48 records and performing a full-text screening of the 64 remaining articles. Based on the eligibility criteria previously established, 57 studies were excluded, and a total of seven articles were finally included in the quantitative analysis (**Figure 14**).

Main baseline characteristics of the included studies are compiled in **Table VII**. All studies achieved the quality threshold established with the NOS score (≥5). The seven articles meta-analyzed comprised a total of 1305 patients diagnosed with HCC, from which 785 patients (60.15%) were subjected to surgical therapy. Besides, from those providing data on follow up times, a wide variety was observed, ranging from 48 to 140 months of follow up. Among the seven studies, only two[78,85] provided clinicopathological data, highlighting the superiority of male gender (84.88% male patients) and the advanced age (53.78% patients older than 50 years) among patients from these investigations (**Table VII**).

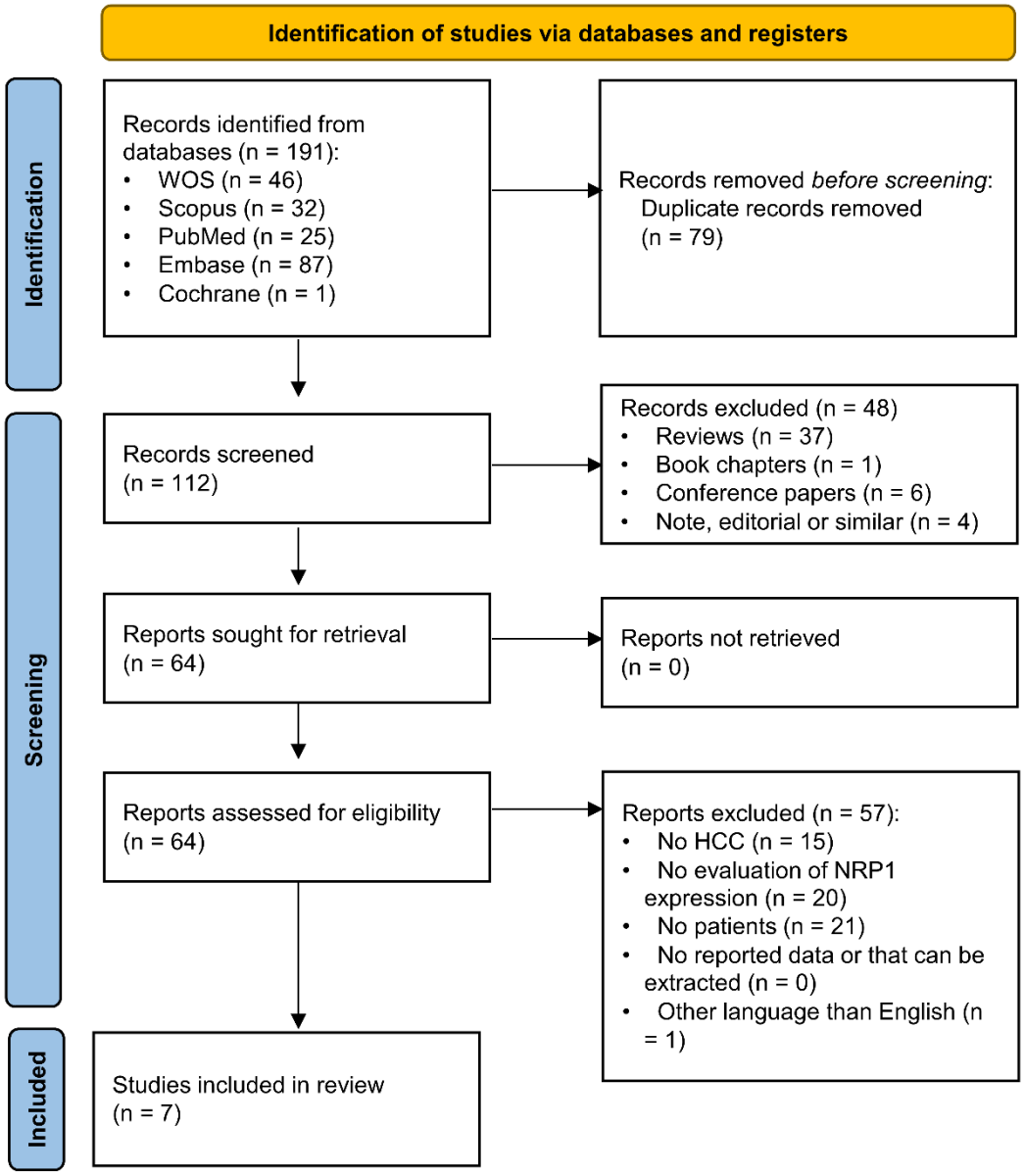

Figure 14. PRISMA flowchart for the selection process of the studies included in the meta-analysis.

Table VII. Baseline characteristics of the studies included in the quantitative analysis.

First author (Ref.)	Year	Tumor sample size (M/F)	Non-tumor sample size	Inter-vention	Pre- or post-surgery treatment	Study quality (NOS score)	Measurement of NRP1 expression	Cut-off value for "high" NRP1	% of tumor samples "high" NRP1 (% of non-tumor)	Parameter analyzed	HR
Deng[161]	2021	371 (NR)	NA	NR	NR	5/9	Tissue-RNA-seq	>median	25.20 (NA)	OS	RP
Li[85]	2021	239 (215/24)	16	Surgery	No	7/9	Tissue–IHC	>1[a]	57.74 (37.50)	OS, CF, Pathog.	ES
Giannelli[162]	2020	149 (127/22)	NA	No	Yes[b]	6/9	Serum	>median	NR (NA)	OS	RP
Lin[79]	2018	40 (28/12)	30	Surgery	No	6/9	Tissue–IHC	NR	72.50 (0.00)	Pathog.	NR
Zhang[78]	2016	105 (77/28)	105	Surgery	No	7/9	Tissue–IHC	>3[c]	53.33 (20.95)	OS, RFS, CF, Pathog.	ES
Yaqoob[163]	2012	93 (NR)	NA	Surgery	No	5/9	Tissue–PCR array	>75% expression	63.44 (NA)	OS	ES
Bergé[76]	2011	308 (NR)	31	Surgery	No	6/9	Tissue–IHC	≥1[d]	50.65 (0.00)	Pathog	NR

CF, clinicopathological features; ES, estimated; F, female; M, male; NA, not applicable; NR, not reported; PCR, polymerase chain reaction; Pathog, pathogenesis; Ref., reference, RP, reported.

[a] Semi-quantitative analysis of NRP1 expression was performed based on the density of cells staining as follows: 0) <5%; 1) 6-35%; 2) 36-70%; 3) >70%. Specimens with scores of 0 and 1 are regarded as NRP1 low expression (NRP1Low), while scores of 2 and 3 are classified as NRP1 high expression (NRP1High).

[b] Patients who had received sorafenib and had progressed or were ineligible for sorafenib were included. After surgery, patients were treated with galunisertib.

[c] Score obtained from multiplying staining intensity and percent of positive cells. Staining was scored as follows: absent staining (negative, 0), weak staining (1), moderate staining (2), and strong staining (3). The percent of positive cell was also scored following 4 categories, in which 1 was given for 0-10 %, 2 for 11-50 %, 3 for 51-80 %, and 4 for 81-100 %.

[d] Based in a four-tiered intensity scoring system as follows: 0, no staining; 1, weak staining; 2, moderate staining; 3, strong staining.

6.1.2 NRP1 association with HCC prognosis and pathogenesis

The potential correlation of higher levels of NRP1 with clinical parameters of survival in patients with HCC was only performed with the OS parameter, since only one study analyzed RFS in patients. This analysis was conducted including data from five studies[78,85,161–163], and results showed that NRP1 overexpression in HCC patients was significantly correlated with a shorter OS (HR 1.75, 95% CI 1.20-2.56, $p = 0.004$) (**Figure 15A**). Nonetheless, a significant heterogeneity was also found between studies (I^2 = 82.97%, Q-test $p<0.001$), therefore employing a random-effects model and REML method (**Figure 15A**).

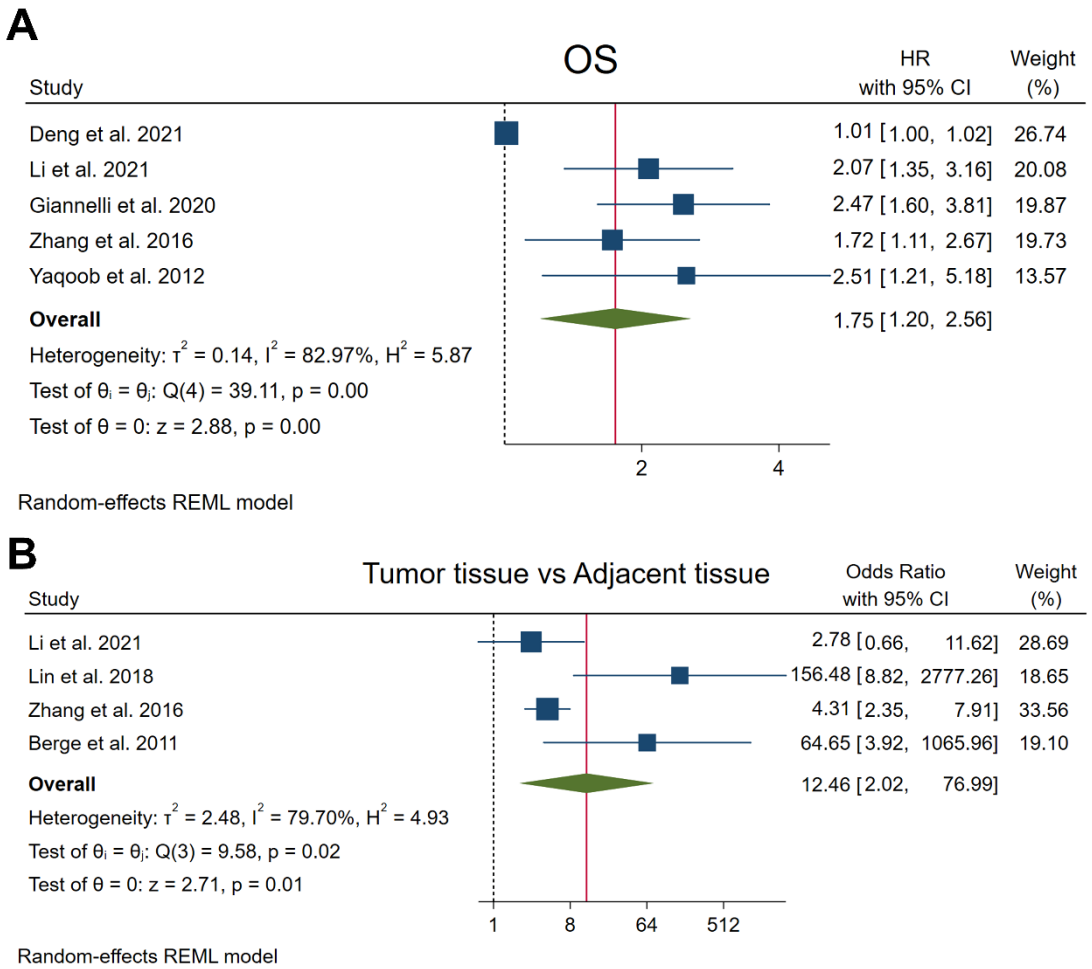

Figure 15. Meta-analysis of the potential correlation of NRP1 overexpression with (A) OS and (B) tumor pathogenesis in HCC patients. Forest plots representing the individual and pooled results from the meta-analysis evaluating the association of NRP1 overexpression with OS and tumor pathogenesis in the corresponding articles.

Furthermore, four articles analyzed the clinical association of high NRP1 expression with tumor development by assessing the number of patients with higher NRP1 levels in the HCC tissue compared to the expression levels in the adjacent non-tumor tissue[76,78,79,85]. After meta-analysis, pooled results demonstrated that NRP1 expression did correlate with tumor pathogenesis (OR 12.46, 95% CI 2.02-76.99, p = 0.01) (**Figure 15B**). Despite this significant correlation, studies included also showed a strong heterogeneity among them (I^2 = 79.70%, Q-test p = 0.02) (**Figure 15B**).

6.1.3 Correlation of NRP1 with clinicopathological features in HCC patients

To further investigate the role of NRP1 in the clinical setting of HCC patients, the relationship between higher levels of this protein and several clinicopathological characteristics was assessed. For this purpose and considering the clinicopathological data obtained from the included studies in which only two articles provided useful data[78,85], we extracted and meta-analyzed the correlation of NRP1 overexpression with gender, age, tumor size, and the risk of metastasis and invasion (**Figure 16**).

Overall effect size obtained after pooled results reported that increased expression of NRP1 significantly correlated with age, specifically with patients younger than 50 years old (OR 0.62, 95% CI 0.40-0.97, p = 0.04), as well as with a higher risk of venous invasion (OR 2.34, 95% CI 1.51-3.63, p<0.001) (**Figure 16**). However, a significant association was not found with the parameters gender (OR 1.60, 95% CI 0.59-4.29, p = 0.35), tumor size (OR 1.15, 95% CI 0.75-1.78, p = 0.52) and metastasis (OR 1.64, 95% CI 0.85-3.15, p = 0.14) (**Figure 16**).

Evaluation of the heterogeneity among studies also showed a marked heterogeneity only in the meta-analysis of NRP1 correlation with gender in HCC patients (I^2 = 60.75%, Q-test p = 0.11) (**Figure 16**). Nonetheless, the meta-regression and subgroup analysis, performed to elucidate the heterogeneity sources, could not be conducted, since subgroups with only one study cannot be meta-analyzed. Substantial heterogeneity was not observed in any of the others clinicopathological parameters: age (I^2 = 0.00%, Q-test p = 0.76), invasion (I^2 = 0.00%, Q-test p = 0.34), metastasis (I^2 = 0.00%, Q-test p = 0.66), tumor size (I^2 = 45.97%, Q-test p = 0.17), employing the fixed-effects model and the IV method (**Figure 16**).

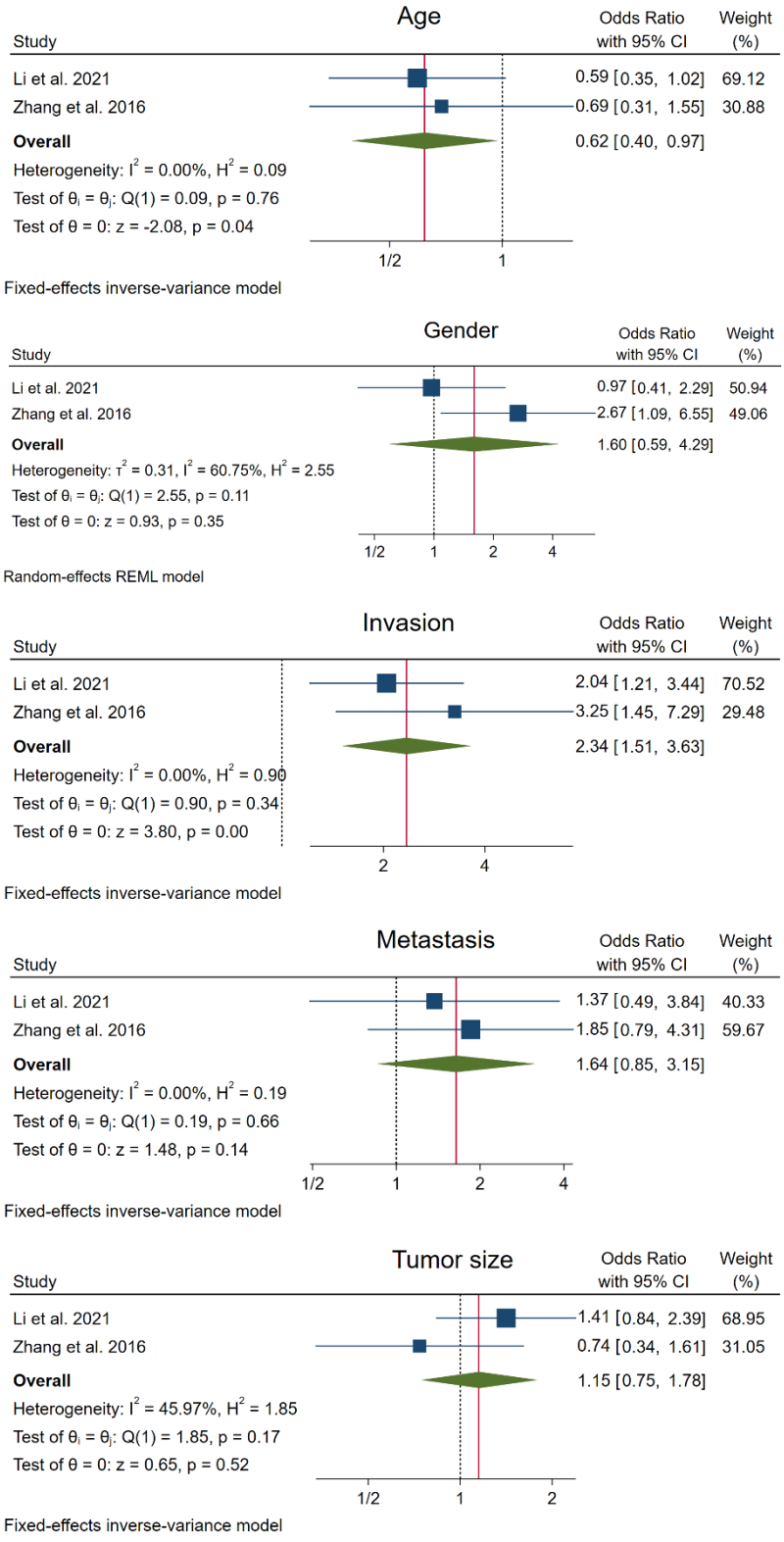

Figure 16. Meta-analysis of the potential correlation of increased NRP1 expression with different clinicopathological features. Forest plots of the pooled overall effect sizes analyzing the correlation of higher NRP1 levels with the clinicopathological parameters of age (≥ 50 years old), gender (male), venous invasion (presence), metastasis (presence) and tumor size (≥ 5 cm) in HCC patients.

6.1.4 Analysis of heterogeneity sources

In order to assess and identify the potential sources of heterogeneity, both meta-regression and subgroup analyses were conducted when a significant heterogeneity was observed between studies. Therefore, the parameters OS and tumor pathogenesis were subjected to these analyses, using sample size, follow up times and NOS score as moderators to explore the likely heterogeneity sources.

Meta-regression

Meta-regression aimed at identifying variables that could explain the heterogeneity in a defined outcome variable. In this line, we evaluated the total sample size included in each study, the last follow up date and the study quality as potential covariates that could modify the effect size among studies and, in consequence, be responsible for the heterogeneity observed.

Results obtained for NRP1 correlation with OS proved that only sample size could partially explain the heterogeneity observed between studies (**Table VIII, Figure 17A**). When the total sample size was used as moderator, heterogeneity substantially decreased (I^2 = 38.57%, Q-test p = 0.21), and was mostly solved (R^2 = 76.01%) (**Table VIII**). Moreover, a negative association was observed between the effect sizes and the sample size in the graphical representation of the meta-regression results (**Figure 17A**).

Table VIII. Assessment of the heterogeneity sources through meta-regression in OS and tumor pathogenesis.

Variable	beta coefficient	z	*p*-value	95% CI	Residual heterogeneity		
					I^2	Q test *p*-value	R^2
OS							
Sample size	0.997	-2.83	0.005*	0.995-0.999	38.57%†	0.21†	76.01%†
Follow up	0.995	-0.96	0.34	0.984-1.006	71.29%	0.02	16.88%
NOS	1.176	0.75	0.45	0.769-1.797	73.74%	0.006	0.97%
Tumor tissue *vs* Adjacent tissue							
Sample size	0.997	-0.24	0.81	0.975-1.020	83.17%	0.01	0.00%
NOS	0.04	-3.02	0.003*	0.005-0.326	0.00%†	0.78†	100.00%†

*Significant correlation, *p*-value<0.05
†High heterogeneity solved (I^2<50% and Q test *p*-value>0.10)

On the other hand, heterogeneity between studies in the correlation analysis with tumor pathogenesis was completely reduced when the NOS score was used as moderator (I^2 = 0.00%, Q-test *p* = 0.78), with R^2 = 100% (**Table VIII**). Likewise, studies were distributed along the bubble plot representation with NOS score as covariate, showing a direct relationship between the study quality and the effect size result (**Figure 17B**).

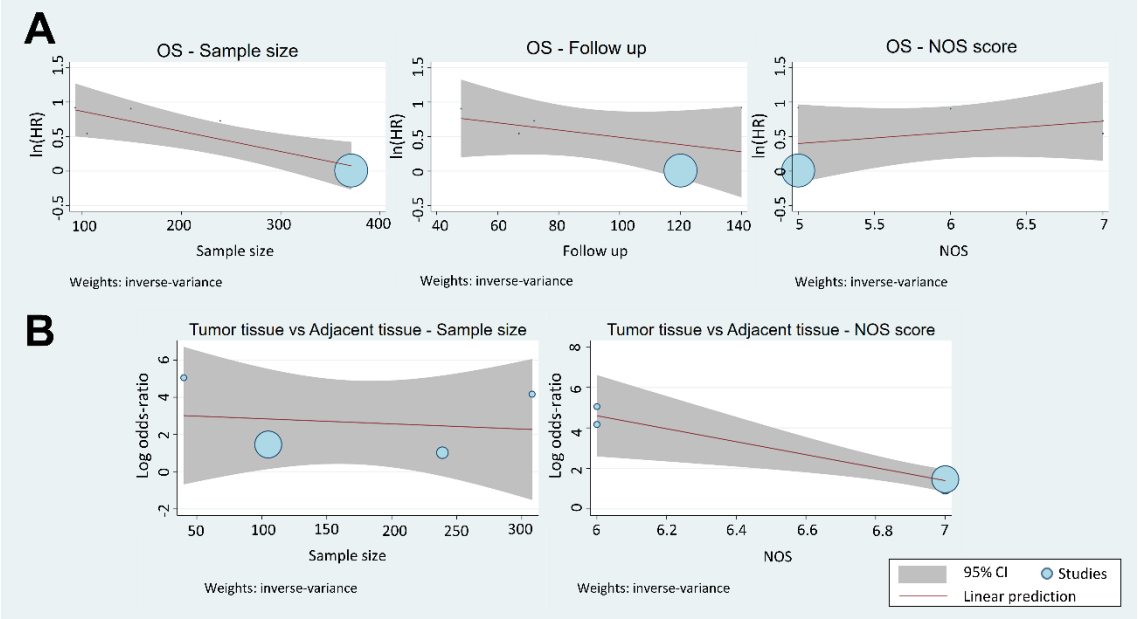

Figure 17. Meta-regression results represented with bubble plots for (A) OS and (B) tumor pathogenesis using the total sample size, follow up times and NOS score as moderators.

For both clinical parameters, OS and tumor pathogenesis, any other variable was not able to explain or reduce the initial heterogeneity between studies (**Table VIII, Figure 17**).

Subgroup analysis

Assessment of heterogeneity sources was also performed by subgroup analysis employing the same moderators as for meta-regression (**Table IX**). In this line, for OS the sample size of each investigation was able to reduce heterogeneity, revealing that for studies with sample size equal or lower than 300 patients, heterogeneity was solved (I^2 = 0.00%, Q-test *p* = 0.67) and NRP1 overexpression was also significantly correlated with a shorter OS (HR 2.11, 95% CI 1.67-2.67, *p* < 0.001) (**Table IXA**). In addition, the score obtained with the NOS scale strongly decreased the heterogeneity when NOS >5 (I^2 = 0.00%, Q-test *p* = 0.52), being NRP1 also correlated with OS (HR 2.07, 95% CI 1.61-

2.66, $p < 0.001$) (**Table IXA**). Contrariwise, subgroups based on follow up times did not decrease heterogeneity.

NRP1 association with tumor pathogenesis was subjected to subgroup analysis to further analyze the potential sources (**Table IXB**), demonstrating that sample size was also responsible for the heterogeneity found. When analyzed studies with sample size higher than 100 patients separately, heterogeneity was significantly reduced ($I^2 = 49.09\%$, Q-test $p = 0.14$), and higher levels of NRP1 also correlated with tumor development (OR 4.48, 95% CI 2.59-7.75, $p < 0.001$) (**Table IXB**). Separation of the total four studies analyzed for tumor pathogenesis based on the NOS score showed that heterogeneity was completely solved in both subgroups (NOS = 6, $I^2 = 0.00\%$, Q-test $p = 0.67$; NOS = 7, $I^2 = 0.00\%$, Q-test $p = 0.58$) (**Table IXB**).

Overall, for NRP1 correlation analysis with OS, the sample size of the included studies has been identified as a potential source of heterogeneity by both meta-regression and subgroup analysis, while NOS score, identified by subgroups, could also partially explain this heterogeneity. Otherwise, for tumor pathogenesis association with NRP1, the NOS score was detected as the main source by both methods, with a potential role of sample size observed by subgroup analysis. Therefore, sample size and NOS score of each article could be responsible, at least in part, for the high heterogeneity found between studies included in the meta-analysis of OS and tumor pathogenesis.

Table IX. Analysis of heterogeneity by subgroups for OS and tumor pathogenesis correlated with NRP1 overexpression.

A. OS

Subgroup	Studies (n)	Cases (n)	Pooled HR			Test for heterogeneity		Model used
			HR	95% CI	*p*-value	I^2	Q test *p*-value	
Sample size								
≤ 100	1	93	2.51	1.21-5.18	—	—	—	—
> 100	4	864	1.66	1.09-2.53	0.02*	86.09%	0.00	REM
≤ 200	3	347	2.13	1.60-2.83	0.00*	0.00%	0.46	FEM†
> 200	2	610	1.40	0.69-2.82	0.35	90.92%	0.00	REM
≤ 300	4	586	2.11	1.67-2.67	0.00*	0.00%	0.67	FEM†
> 300	1	371	1.01	1.00-1.02	—	—	—	—
NOS scale								
5	2	464	1.47	0.61-3.55	0.39	83.41%	0.01	REM
6	1	149	2.47	1.60-3.81	—	—	—	—
7	2	344	1.89	1.40-2.57	0.00*	0.00%	0.56	FEM†
NOS scale (threshold 5)								
≤ 5	2	464	1.47	0.61-3.55	0.39	83.41%	0.01	REM
> 5	3	493	2.07	1.61-2.66	0.00*	0.00%	0.52	FEM†
NOS scale (threshold 6)								
≤ 6	3	613	1.73	0.91-3.29	0.09	88.15%	0.00	REM
> 6	2	344	1.89	1.40-2.57	0.00*	0.00%	0.56	FEM†
Follow up (months)								
≤ 60	1	149	2.47	1.60-3.81	—	—	—	—
> 60	4	808	1.61	1.05-2.45	0.03*	81.77%	0.00	REM
≤ 120	4	864	1.66	1.09-2.53	0.02*	86.09%	0.00	REM
> 120	1	93	2.51	1.21-5.18	—	—	—	—

B. Tumor tissue *vs* Adjacent tissue

Subgroup	Studies (n)	Cases (n)	Cases with high NRP1 levels (%)	Pooled OR			Test for heterogeneity		Model used
				OR	95% CI	*p*-value	I^2	Q test *p*-value	
Sample size									
≤ 100	1	40	72.50	156.48	8.82-2777.26	—	—	—	—
> 100	3	652	38.34	4.48	2.59-7.75	0.00*	49.09%	0.14	FEM†
≤ 200	2	145	73.79	19.50	0.60-629.71	0.09	82.56%	0.02	REM
> 200	2	547	31.44	10.54	0.50-222.18	0.13	73.98%	0.05	REM
≤ 300	3	384	32.03	8.40	1.13-62.52	0.04*	82.75%	0.04	REM
> 300	1	308	50.65	64.65	3.92-1065.96	—	—	—	—
NOS scale									
6	2	348	53.16	99.43	13.36-740.11	0.00*	0.00%	0.67	FEM†
7	2	344	27.33	4.03	2.31-7.05	0.00*	0.00%	0.58	FEM†

FEM, fixed-effects model; REM, random-effects model
*Significant correlation, *p*-value<0.05
†High heterogeneity solved (I^2<50% and Q test *p*-value>0.10)

6.1.5 Analysis of publication bias

Presence of publication bias risk between studies was analyzed in order to identify potential bias due to unpublished articles with non-significant results. For this purpose, the Egger's test, together with detection of funnel plot asymmetry, were performed.

After analysis, substantial risk of bias was detected for the NRP1 association with OS and tumor pathogenesis, conducting for both parameters the trim-and-fill method (**Table X, Figure 18**). This method imputed in both cases one additional study to estimate an adjusted overall effect size for OS (**Table X, Figure 18A**) and tumor pathogenesis (**Table X, Figure 18B**).

Table X. Assessment of publication bias risk between studies for OS, tumor pathogenesis and different clinicopathological features.

Survival parameter	**Studies (n)**	**Egger's test (*p*-value)**	**Model used**	**Trim-and-fill analysis**		**Studies imputed (n)**
				HR	**95% CI**	
OS	5	0.00*	REM	1.65	1.17-2.33	1
Clinicopathological feature	**Studies (n)**	**Egger's test (*p*-value)**	**Model used**	**Trim-and-fill analysis**		**Studies imputed (n)**
				OR	**95% CI**	
Tumor tissue *vs* Adjacent tissue	4	0.04*	REM	6.40	0.72-57.35	1
Age	2	0.76	FEM	—	—	—
Gender	2	0.11	REM	—	—	—
Invasion	2	0.34	FEM	—	—	—
Metastasis	2	0.66	FEM	—	—	—
Tumor size	2	0.17	FEM	—	—	—

FEM, fixed-effects model; REM, random-effects model.
*Significant publication bias, *p*-value<0.05.

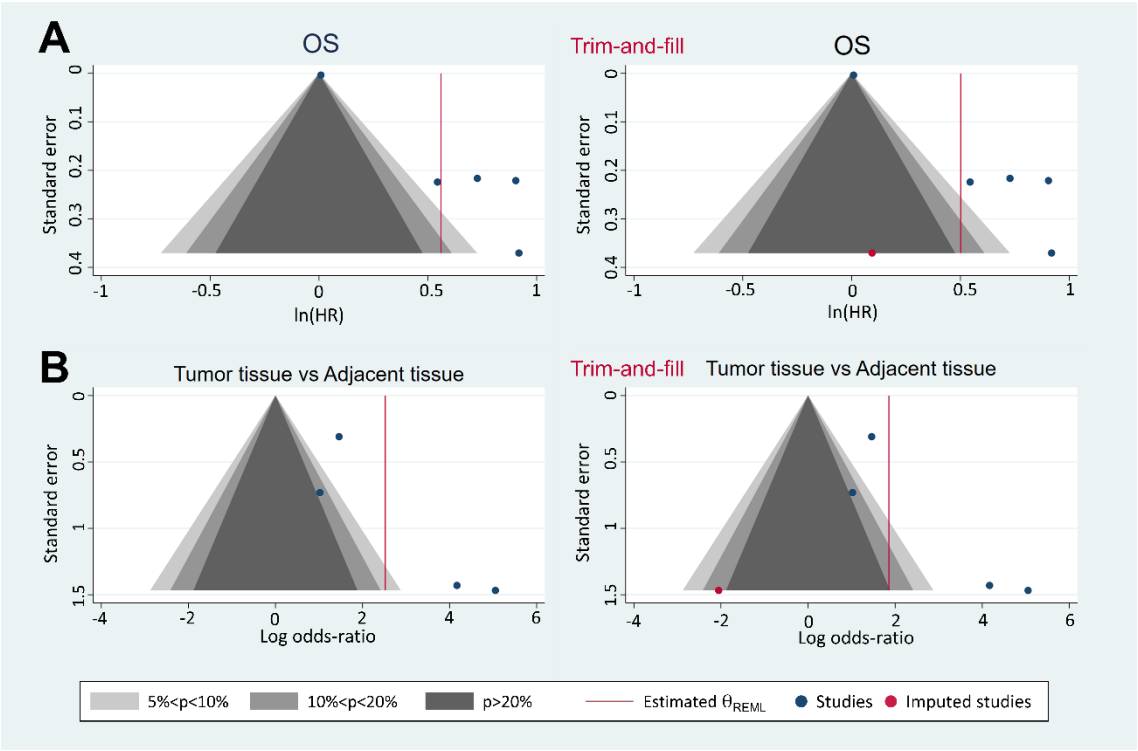

Figure 18. Evaluation of publication bias through detection of funnel plot asymmetry for NRP1 correlation analysis with (A) OS and (B) tumor pathogenesis. For both parameters, the funnel plots obtained after conducting trim-and-fill method were also represented, which include the missing studies that could be responsible for the publication bias.

Otherwise, evaluation of publication bias in the NRP1 association with the clinicopathological characteristics age, gender, invasion, metastasis and tumor size by both Egger's test and funnel plots did not report a significant bias among studies for any parameter (**Table X, Figure 19**).

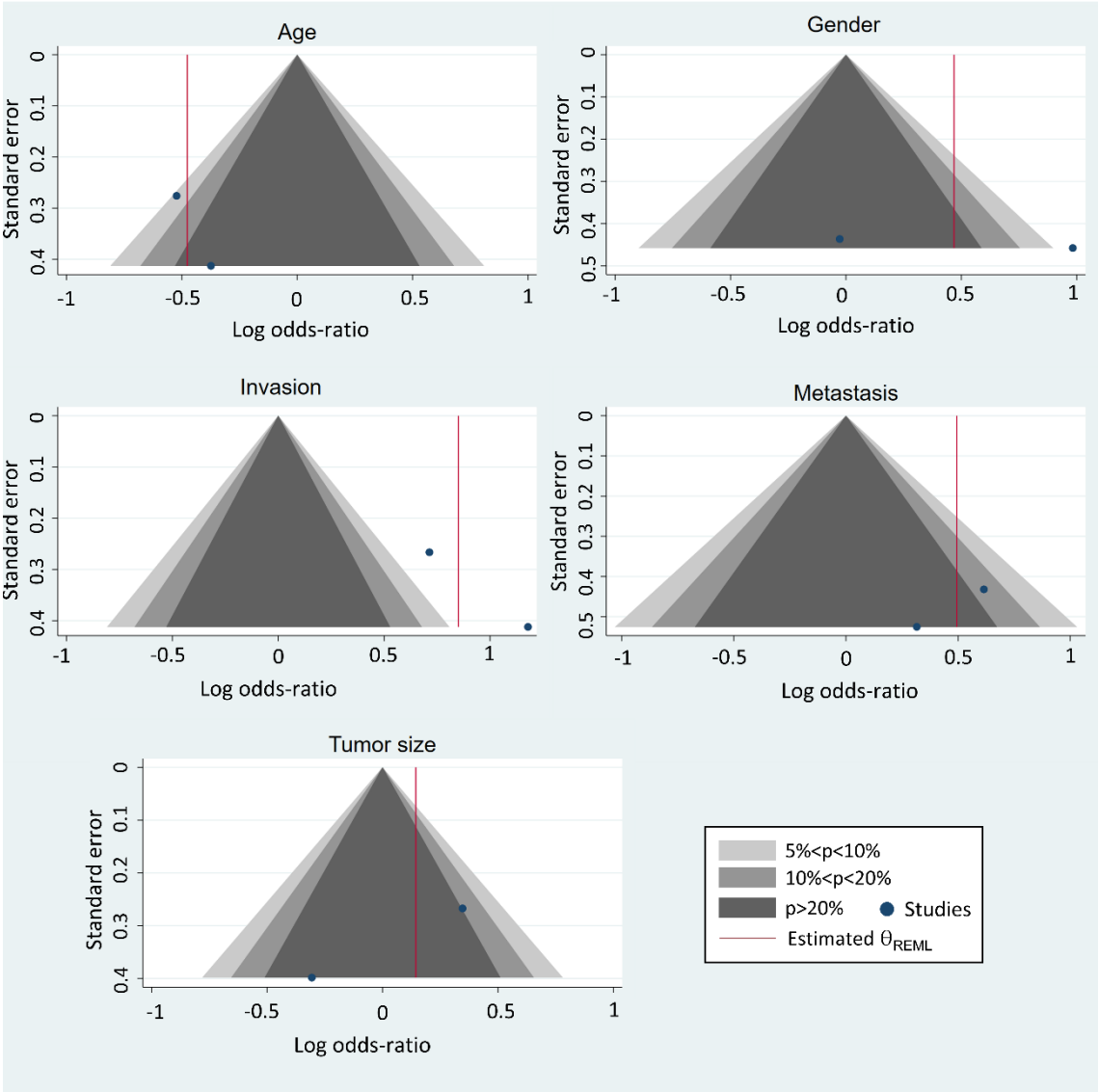

Figure 19. Evaluation of publication bias through detection of funnel plot asymmetry for NRP1 correlation analysis with age, gender, venous invasion, metastasis and tumor size.

6.2 NRP1 MODULATION THROUGH AN AUTOPHAGY AND HYPOXIA INTERPLAY IN THE LOSS OF LENVATINIB SENSITIVITY IN HCC: EXPERIMENTAL STUDY

NRP1 has aroused as an interesting protein with potential functions in cancer and with increasing evidence that highlights its role in human HCC[69,70]. Even though numerous studies have evaluated and described key processes involved in the progression and drug responsiveness of HCC, where NRP1 could exert a crucial function, the precise mechanisms underlying therapeutic failure are still unknown[144,164]. Autophagy has demonstrated to dually modulate cell response to stress conditions, either by promoting or restraining tumor development and drug efficacy[132]. Nevertheless, the contradictory and multiple roles played by autophagy in HCC places it as a crucial modulator of the molecular and cellular processes involved in cancer cell survival that should be studied more in depth[165,166]. Furthermore, hypoxia conditions are closely associated to the resistance development against TKIs, due to the mostly anti-angiogenic effects of these targeted drugs, including lenvatinib, which derive into the establishment of a hypoxic microenvironment[42,123]. The hypoxia response, primarily mediated by HIF-1α, has proved to drive the cellular response in cancer, favoring the acquisition of an aggressive phenotype by tumor hepatocytes and the loss of sensitivity to TKIs[124,167,168]. Therefore, further studies are necessary to unravel the complex mechanisms that underly the loss of drug sensitivity in HCC cells. For this reason, in this study we investigated the role of NRP1 in the loss of lenvatinib efficacy through an autophagy-mediated modulation, and the effects derived from the HIF-1α-related response to hypoxia.

6.2.1 Analysis of NRP1 expression levels in samples from HCC patients and its correlation with tumor stages

In order to assess the potential implication of NRP1 in the processes of HCC development and progression, we evaluated the gene expression levels of NRP1 in HCC samples from different datasets obtained from public databases (**Figure 20**). NRP1 expression in normal healthy liver and HCC samples was evaluated in the TCGA dataset, showing the NRP1 IHC detection with representative images from the Human Protein Atlas (HPA) database with two different antibodies (HPA030278 and CAB004511). For both antibodies, immunohistochemical NRP1 was strongly stained in HCC samples in

comparison to the normal liver tissue (**Figure 20A**). Moreover, NRP1 was found to be overexpressed in the tumor samples after the analysis with the UALCAN database (**Figure 20B**). These results were confirmed with the GSE14520 dataset by an independent evaluation of genes differentially expressed in HCC samples, in which a significant overexpression of NRP1 was also detected compared to paired non-tumor samples (**Figure 20C**).

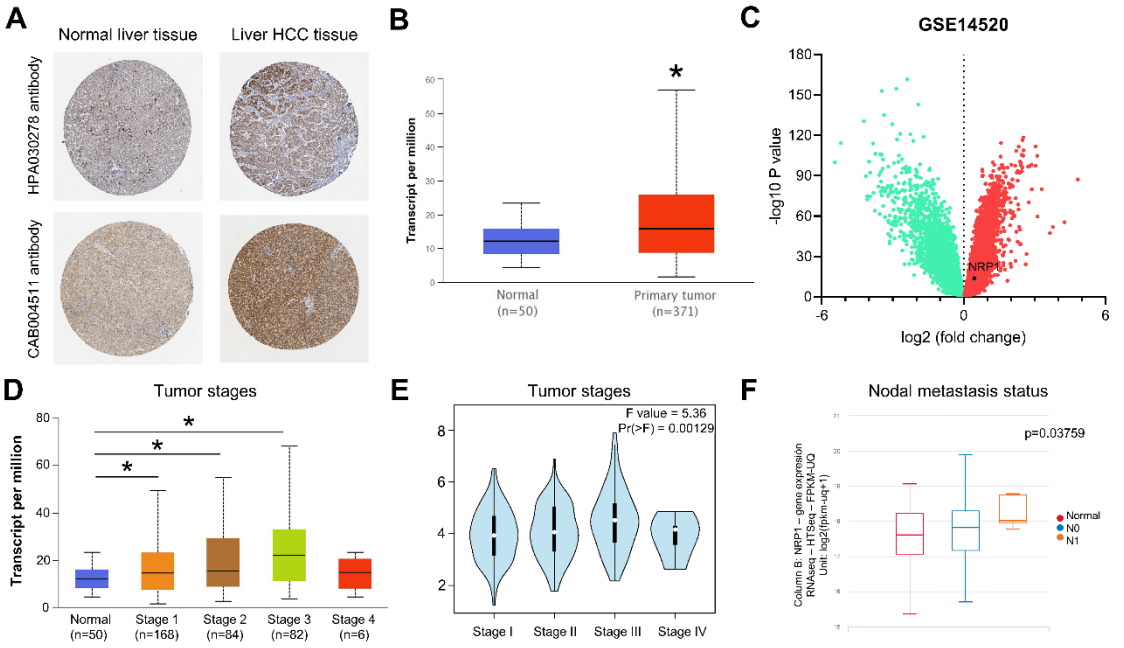

Figure 20. Determination of NRP1 expression levels and clinical association in samples of HCC patients obtained from public databases. (**A**) Immunohistochemical staining of NRP1 in normal liver and HCC tissues showing representative images from HPA database. (**B**) Expression levels of NRP1 in normal liver and HCC samples obtained from the UALCAN database. (**C**) Significantly upregulated (red) and downregulated (green) genes expressed in HCC samples from the GSE14520 dataset of GEO database, identificating the differential expression of NRP1. Clinical correlation of NRP1 with different tumor stages in HCC patients analyzed in the (**D**) UALCAN and (**E**) GEPIA databases; and (**F**) with diverse nodal metastasis status analyzed in the UCSC Xena database. Significant differences when **p*<0.05.

Interestingly, NRP1 showed a significant correlation with advanced tumor stages in HCC patients through assessment in two different databases, UALCAN (**Figure 20D**) and GEPIA (**Figure 20E**). When analysis of the association of NRP1 expression was conducted with different nodal metastasis status in the UCSC Xena database, results exhibited a significant correlation with advanced nodal stages in samples from HCC patients (**Figure 20F**).

6.2.2 Characterization of NRP1 expression and migration ability of HCC cells

Expression levels of NRP1 were analyzed at both transcriptional and translational levels in three HCC cell lines, HepG2, Huh-7 and Hep3B, to confirm previous results obtained from clinical data (**Figure 21**). After experimental determinations, NRP1 levels were found significantly increased in the Huh-7 and Hep3B cell lines in comparison to HepG2 cells at both mRNA (**Figure 21A**) and protein levels (**Figure 21B**).

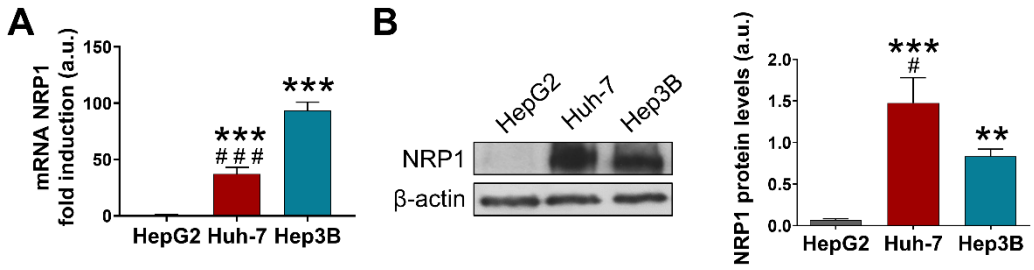

Figure 21. Analysis of NRP1 expression in different HCC cell lines at (A) mRNA and (B) protein levels. (**A**) mRNA and (**B**) protein NRP1 expression was measured by qRT-PCR and western blot, respectively. Representative immunoblots with the densitometric quantification levels of the corresponding triplicates are shown. Data are expressed as mean values of arbitrary units (a.u.) ± SD (n = 3). Significant differences **p*<0.05, ***p*<0.01, **p*<0.001 *vs* HepG2 cell line; $^{\#}p$<0.05, $^{\#\#}p$<0.01, $^{\#\#\#}p$<0.001 *vs* Hep3B cell line.

Furthermore, migration ability of the three HCC cell lines was thoroughly assessed by measuring wound closure ability at different time points, 4 h, 8 h, 12 h and 24 h (**Figure 22**). Firstly, individual comparison was done for each cell line, observing a significant decrease of the wound area from 8 h for Huh-7, from 12 h for Hep3B and only at 24 h for HepG2 (**Figure 22B**). When migration ability was compared between cell lines, a strong difference was found, exhibiting HepG2 cells the lowest wound closure, while both Huh-7 and Hep3B cells showed the highest migration ability, with more than 60% closure reached at 24 h (**Figure 22C**).

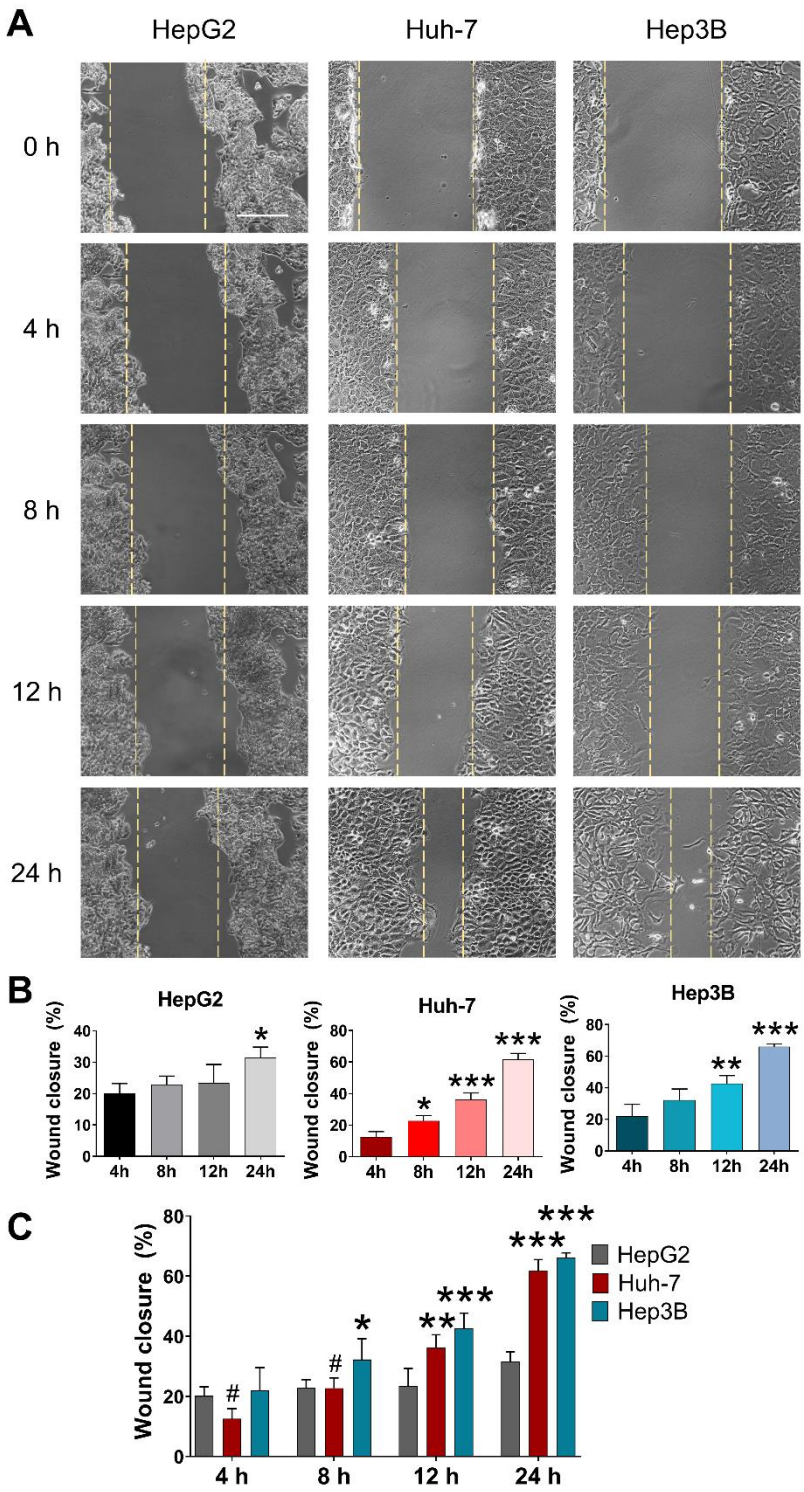

Figure 22. Analysis of cell migration ability of the HepG2, Huh-7 and Hep3B cell lines. Cell migration was evaluated by wound-healing assay, showing (**A**) a representative image from triplicates for the different time points. Magnification 10×, scale bar 50 µm. Percentage of wound closure was analyzed and represented for (**B**) each cell line and (**C**) globally comparing the three HCC lines, expressed as mean values ± SD (n = 3). (**B**) Significant differences *p<0.05, **p<0.01, ***p<0.001 *vs* 4 h. (**C**) Significant differences *p<0.05, **p<0.01, ***p<0.001 *vs* HepG2, and $^{\#}p$<0.05 *vs* Hep3B.

6.2.3 Determination of the *in vitro* efficacy of lenvatinib in HCC cell lines

Once analyzed the potential implication of NRP1 in the progression of the HCC lines HepG2, Hep3B and Huh-7, we decided to evaluate the antitumor effects of lenvatinib in these lines through diverse assays.

At first, a significant reduction of cell viability was observed from 1 µM lenvatinib in the HepG2 line, and from the lowest concentration (0.5 µM) of lenvatinib in Hep3B and Huh-7 (**Figure 23**). As observed in this **Figure 23**, HepG2 cells proved to be less sensitive to lenvatinib treatment compared to the Hep3B and Huh-7 cell lines, not reaching a 50% of cell viability inhibition with the highest dose used. On the other hand, a 50% viability inhibition was observed after 1 µM and 2.5 µM lenvatinib administration to Hep3B and Huh-7, respectively (**Figure 23**). For the following experiments, lenvatinib concentrations were selected in accordance to the IC_{50} values, choosing 2.5 µM and 5 µM for Hep3B and Huh-7 cells, while 20 µM and 40 µM were used for the HepG2 cell line.

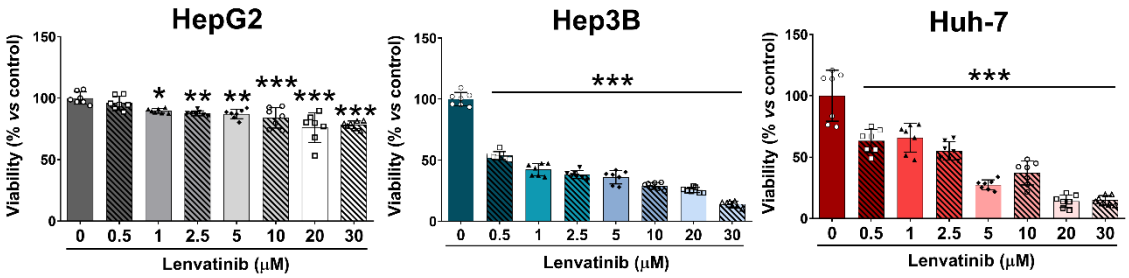

Figure 23. Lenvatinib effects in cell viability of the HepG2, Hep3B and Huh-7 HCC cell lines. Analysis of cell viability of the three HCC cell lines after administration of lenvatinib concentrations from 0.5 µM to 30 µM for 48 h by CellTiter-Glo® assay. Data are represented as percentage of cell viability relativized to untreated cells (control condition) ± SD (n = 7). Significant differences *p<0.05, **p<0.01, ***p<0.001 *vs* 0 µM (untreated cells).

Subsequently, colony formation ability and Ki67-based proliferation index were also assessed to corroborate the antitumor effects of lenvatinib (**Figure 24**). Results exhibited a significant reduction of both number of colonies (**Figure 24A**) and nuclear localization of Ki67 (**Figure 24B**) with 2.5 µM and 5 µM in the Hep3B and Huh-7 lines, showing also a higher susceptibility than HepG2. After lenvatinib administration, HepG2 cells experienced a slight but significant decrease in colony formation with 40 µM lenvatinib (**Figure 24A**), and in Ki67 proliferation index with both 20 µM and 40 µM (**Figure 24B**). Altogether, these findings revealed the HepG2 cell line as the less susceptible line to lenvatinib, as well as with the lowest expression of NRP1.

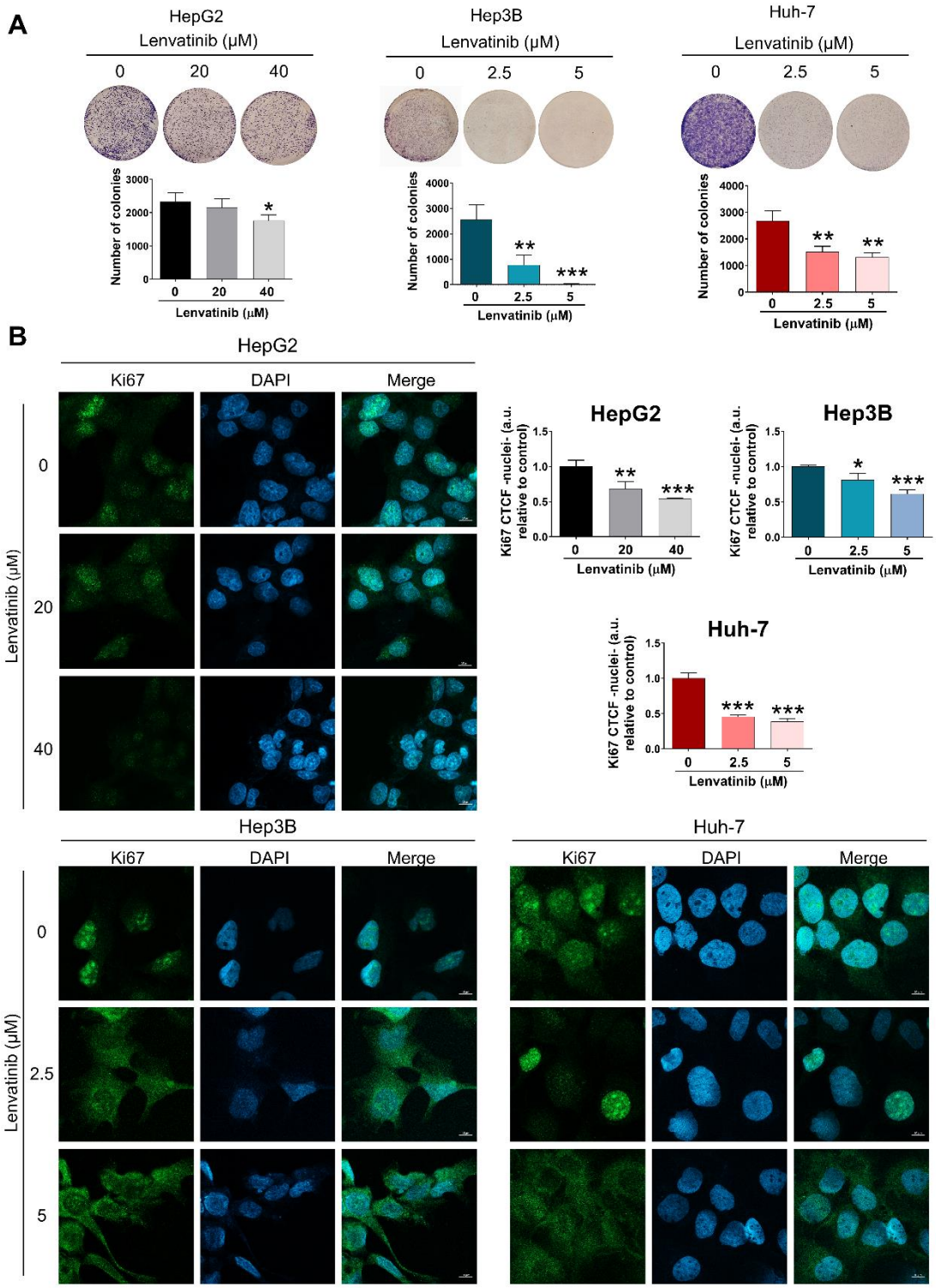

Figure 24. Antitumor effects of lenvatinib analyzed in the *in vitro* models of HCC. (**A**) Colony formation ability and (**B**) proliferation index based on nuclear Ki67 localization were measured after 48 h administration of 20 μM and 40 μM lenvatinib in HepG2 cells, and 2.5 μM and 5 μM lenvatinib in Hep3B and Huh-7 cell lines. (**A**) Data are represented as mean values ± SD (n = 3). (**B**) Representative images with magnification 63×, scale bar 10 μm, are shown and data are represented as the nuclear CTCF ratio of Ki67 expressed as arbitrary units (a.u.) ± SD (n = 3). Significant differences *p<0.05, **p<0.01, ***p<0.001 *vs* 0 μM (untreated cells).

In order to evaluate and clarify the potential role of NRP1 in the lenvatinib effectiveness, we decided to perform the following experiments with the Hep3B and Huh-7 cell lines, based on the analysis of NRP1 expression and lenvatinib sensitivity.

6.2.4 Evaluation of the potential role of NRP1 on lenvatinib-derived effects on cell proliferation and migration

To unravel the potential interplay between lenvatinib antitumor effects on HCC cells and NRP1 expression, we determined the NRP1 levels after 48 h of lenvatinib administration (**Figure 25**). At transcriptional level, lenvatinib did not show significant alterations in NRP1 mRNA (**Figure 25A**). However, protein expression measured by both western blot (**Figure 25B**) and immunofluorescence with confocal microscopy (**Figure 25C**) was strongly diminished in both cell lines, Hep3B and Huh-7, with both concentrations, 2.5 µM and 5 µM. Therefore, NRP1 protein levels were significantly decreased by lenvatinib treatment, while no changes were observed at mRNA levels (**Figure 25**).

These results suggested that NRP1 modulation by lenvatinib could be mediating its antitumor activity *in vitro*. For this reason, we employed the NRP1 antagonist EG00229 to compare the effects derived from the disruption of NRP1 activity with the effects derived from lenvatinib. Specifically, the compound EG00229 acts by blocking NRP1-VEGFA interaction and, in consequence, inhibiting NRP1 activity[169]. At first, we determined the concentration of EG00229 to perform the subsequent experiments through the analysis of cell viability in presence of this antagonist (**Figure 26**). For both cell lines, Hep3B and Huh-7, EG00229 was able to significantly reduce cell viability from the lowest dose (2.5 µM) at both 24 h and 48 h (**Figure 26**). Nonetheless, although Huh-7 showed a higher sensitivity to this compound, cell viability of both lines did not experience a dose-dependent inhibition at 24 h, while a slight decrease was observed at 48 h, not reaching a 50% cell viability decrease except with 50 µM at 48 h in Huh-7 (**Figure 26**). Considering these findings, and concentrations of EG00229 used by previous studies[170,171], we selected 15 µM to perform the following experiments.

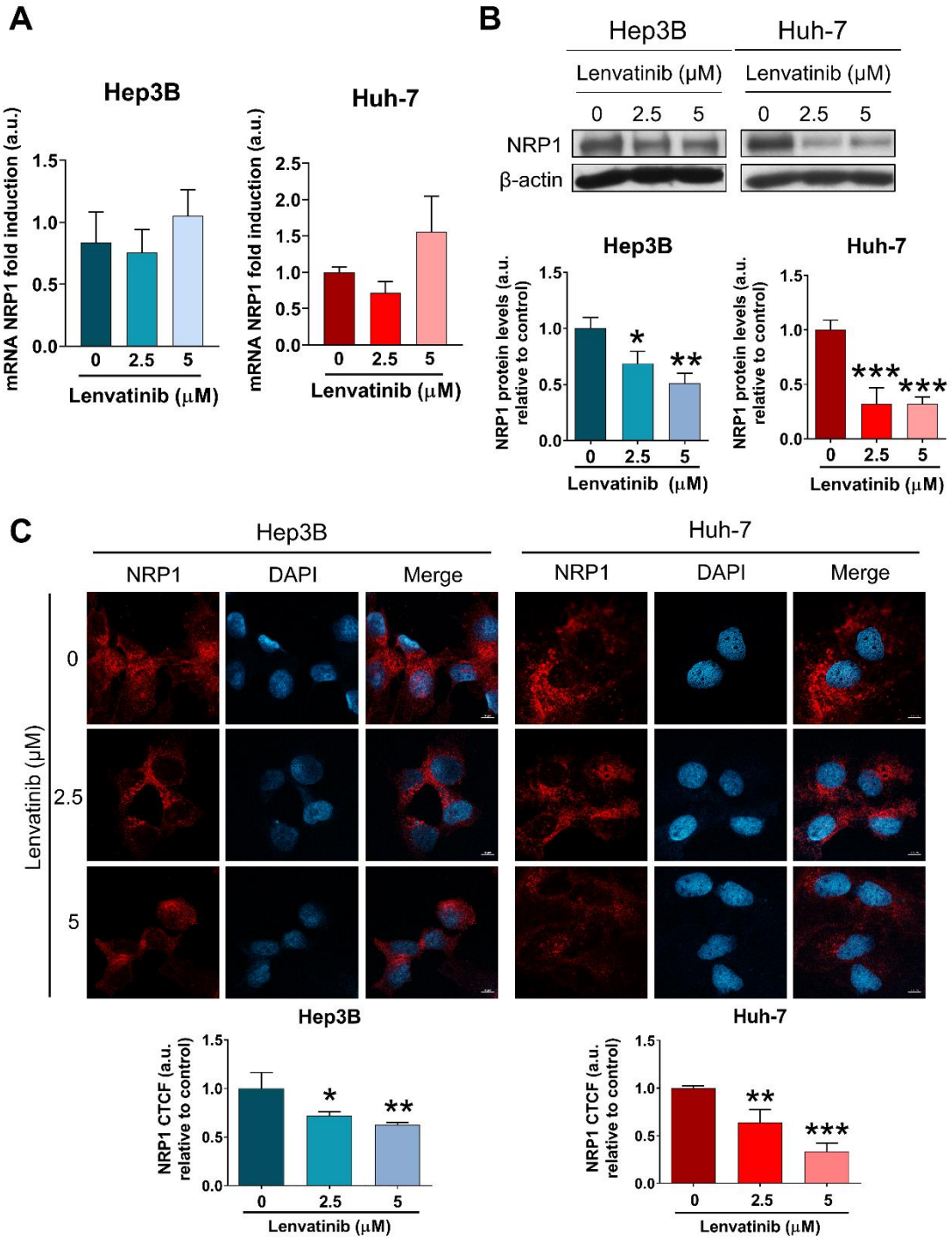

Figure 25. Modulation of NRP1 expression by lenvatinib treatment in HCC cells. After treatment with 2.5 μM and 5 μM lenvatinib for 48 h in Hep3B and Huh-7 cell lines, NRP1 expression was determined at (**A**) transcriptional level by qRT-PCR, and at protein level by (**B**) western blot and (**C**) immunofluorescence. Data are represented as mean values of arbitrary units (a.u.) ± SD (n = 3). (**B**) A representative immunoblot from triplicates is displayed. (**C**) Representative images with magnification 63×, scale bar 10 μm, are shown with quantification data showing NRP1 CTCF ratio. Significant differences *p<0.05, **p<0.01, ***p<0.001 *vs* 0 μM (untreated cells).

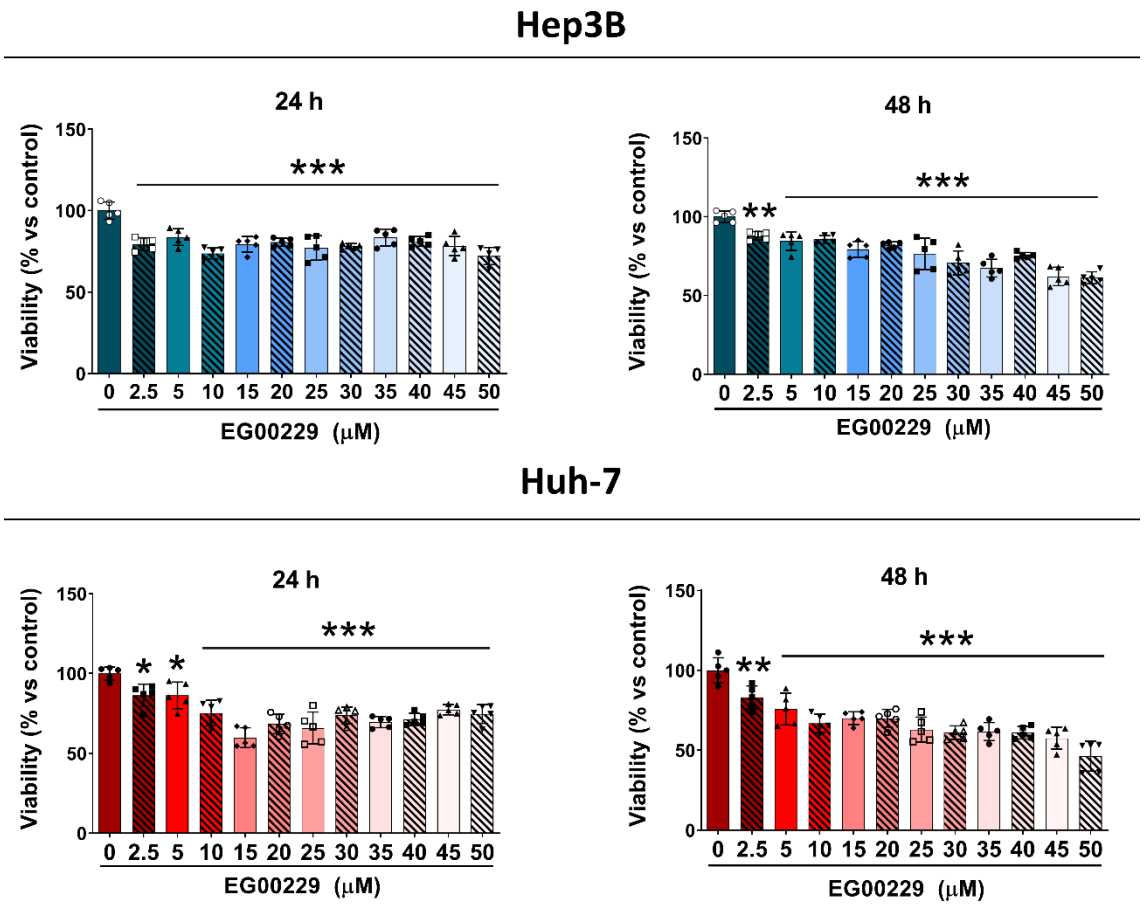

Figure 26. Analysis of cell viability after administration of the NRP1 antagonist EG00229. Cell viability of Hep3B and Huh-7 cell lines was analyzed by MTT assay after EG00229 treatment with different concentrations for 24 h and 48 h. Data are expressed as percentage of mean values ± SD (n = 5). Significant differences **p*<0.05, ***p*<0.01, ****p*<0.001 *vs* 0 μM (untreated cells).

Once treatment conditions were defined, we decided to perform the specific gene silencing of NRP1 in combination with lenvatinib and/or EG00229 to evaluate the role of lenvatinib in NRP1-derived effects in HCC cells (**Figures 27 and 28**). Initially, efficacy of NRP1 silencing was verified by determination of protein levels through western blot (**Figure 27**) and immunofluorescence (**Figure 28**), showing a strong decrease in NRP1 expression. Moreover, lenvatinib treatment also led to significant lower levels of NRP1 measured by western blot, while EG00229 did not alter NRP1 protein expression (**Figure 27**). Combination of lenvatinib and EG00229 exhibited similar results, diminishing NRP1 levels, but without significant differences to lenvatinib administration alone (**Figure 27**). When NRP1 silencing was conducted, significant changes were not observed between individual treatments and co-administrations (**Figure 27**).

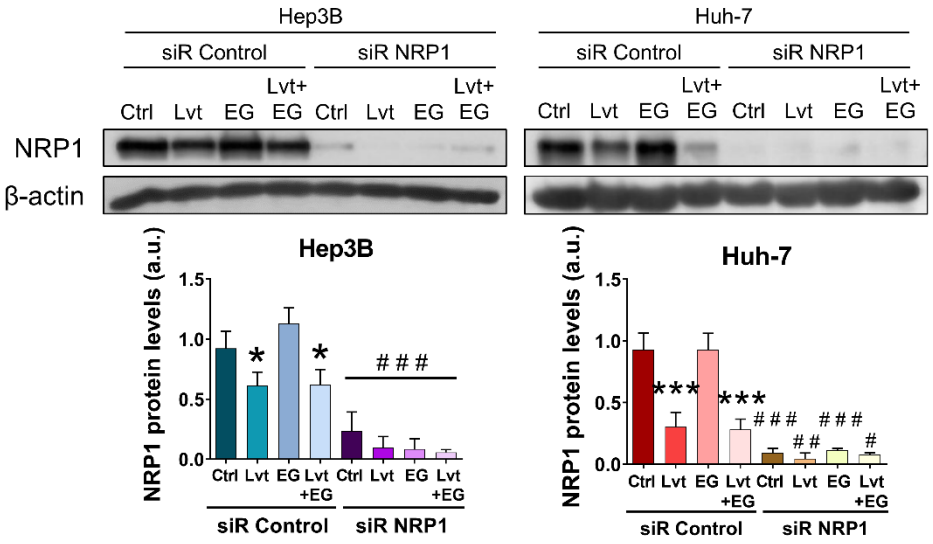

Figure 27. Determination of the NRP1 protein levels by western blot after NRP1 gene silencing in combination with lenvatinib and/or EG00229 treatment in HCC cells. Protein NRP1 expression was measured by western blot after 48 h of gene silencing and 24 h of compound administration. 2.5 µM lenvatinib (Lvt) and/or 15 µM EG00229 (EG) were administered for 24 h. A representative immunoblot for each protein is shown. Data are expressed as mean values of arbitray units (a.u.) ± SD (n = 3). Significant differences **p*<0.05, ***p*<0.01,****p*<0.001 *vs* control (Ctrl) (untreated cells); $^{\#}p$<0.05, $^{\#\#}p$<0.01, $^{\#\#\#}p$<0.001 *vs* siR Control for each treatment.

Protein assessment by laser confocal microscopy displayed similar results (**Figure 28**). Efficacy of NRP1 silencing was also identified and individual administration of EG00229 did not alter NRP1 protein levels (**Figure 28**). Likewise, both lenvatinib alone and combined with the antagonist showed similar downregulation effects on NRP1 expression, which were significantly enhanced after genetic silencing in both HCC cell lines (**Figure 28**). For Hep3B cells, NRP1 silencing increased the effects of lenvatinib and EG00229, alone and in combination; while for Huh-7 cells, NRP1 knockdown enhanced effects of lenvatinib and its combination with EG00229 (**Figure 28**).

After comparing the modulation exerted by lenvatinib and EG00229 on the protein expression of NRP1, we analyzed their involvement in cell proliferation of Hep3B and Huh-7 cell lines, by performing the same experiment layout.

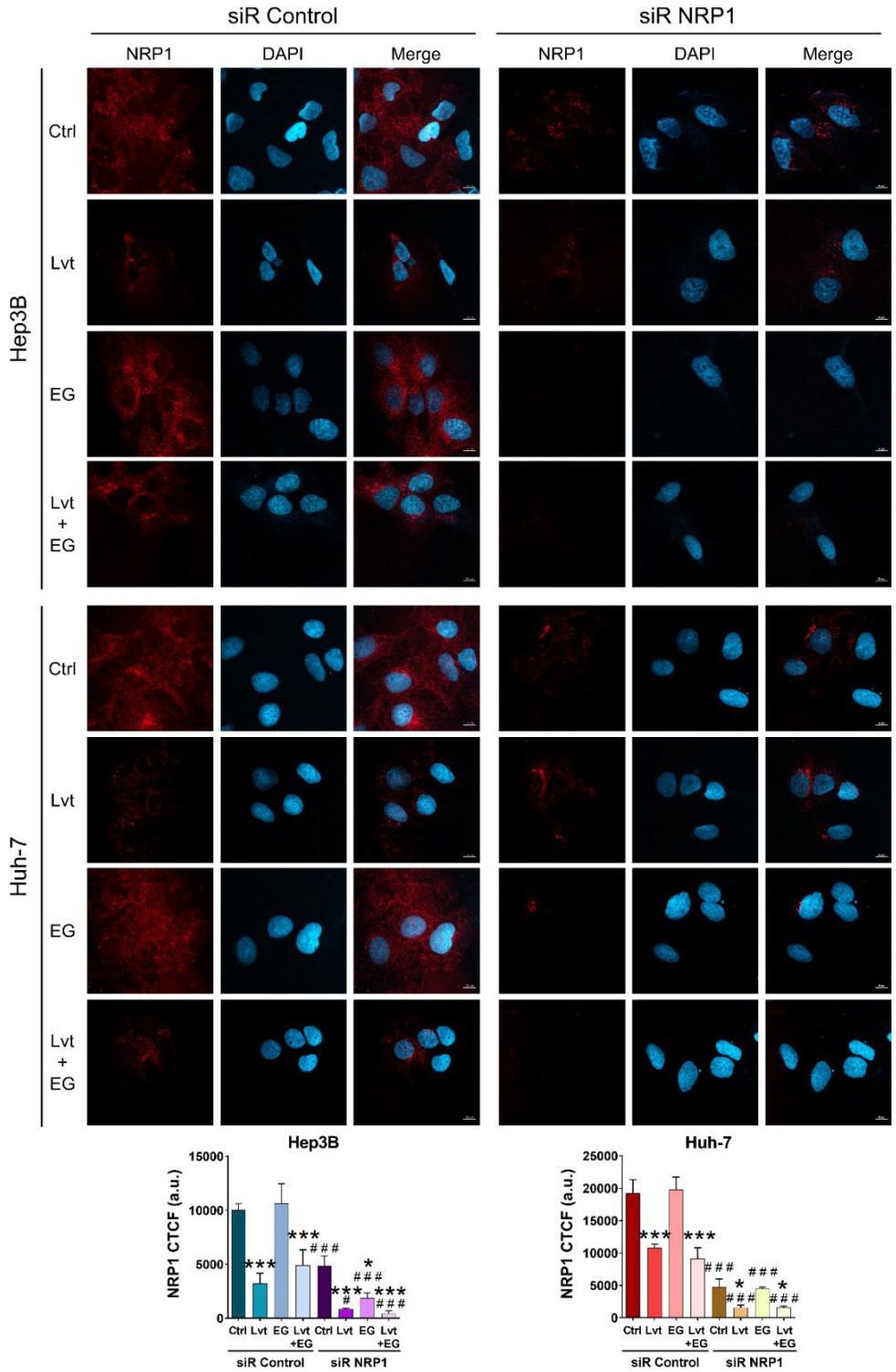

Figure 28. Determination of the NRP1 protein levels by immunofluorescence after NRP1 gene silencing in combination with lenvatinib and/or EG00229 treatment in HCC cells. Protein NRP1 expression was analyzed by immunofluorescence after 48 h of gene silencing and 24 h of compound administration with 2.5 µM lenvatinib (Lvt) and/or 15 µM EG00229 (EG). Representative images are shown with magnification 63×, scale bar 10 µm, representing the NRP1 CTCF ratio. Data are expressed as mean values of arbitray units (a.u.) ± SD (n = 3). Significant differences **p*<0.05, ***p*<0.01,****p*<0.001 *vs* control (Ctrl) (untreated cells); $^{\#}p$<0.05, $^{\#\#}p$<0.01, $^{\#\#\#}p$<0.001 *vs* siR Control for each treatment.

Evaluation of cell viability and proliferation also revealed interesting results (**Figures 29 and 30**). Not only lenvatinib, but also EG00229, led to significant reduction of cell viability (**Figure 29A**), number of colonies (**Figure 29B**) and nuclear localization of Ki67 (**Figure 30**), when administered alone and in combination. Nevertheless, combined drugs did not show synergy for any analysis, regardless of the colony formation ability in the Huh-7 cell line (**Figure 29B**). When NRP1 was genetically silenced, enhanced inhibitory effects were observed for these treatments in cell viability (**Figure 29A**) and colony formation (**Figure 29B**), even though NRP1 silencing only increased lenvatinib antitumor effects on Ki67-based proliferation index in both Hep3B and Huh-7 (**Figure 30**).

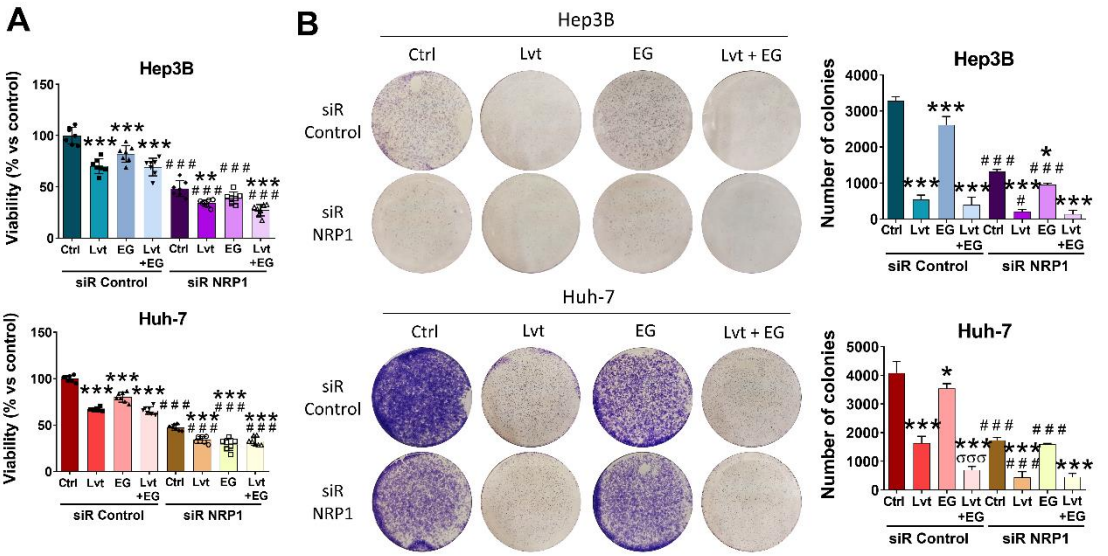

Figure 29. Analysis of cell viability and colony formation after NRP1 gene silencing in combination with lenvatinib and/or EG00229 treatment in HCC cells. Cell viability of Hep3B and Huh-7 cell lines was assessed by (**A**) CellTiter-Glo® assay and (**B**) colony formation ability after 48 h of gene silencing and 24 h of compound administration. 2.5 µM lenvatinib (Lvt) and/or 15 µM EG00229 (EG) were administered for 24 h. (**A**) Data are expressed as percentage of mean values ± SD (n = 7). (**B**) Data are expressed as mean values ± SD (n = 3), showing representative images from triplicates. Significant differences *p<0.05, **p<0.01,***p<0.001 *vs* control (Ctrl) (untreated cells); $^{\#}p$<0.05, $^{\#\#}p$<0.01, $^{\#\#\#}p$<0.001 *vs* siR Control for each treatment; $^{\sigma}p$<0.05, $^{\sigma\sigma}p$<0.01, $^{\sigma\sigma\sigma}p$<0.001 Lvt+EG *vs* Lvt treatment.

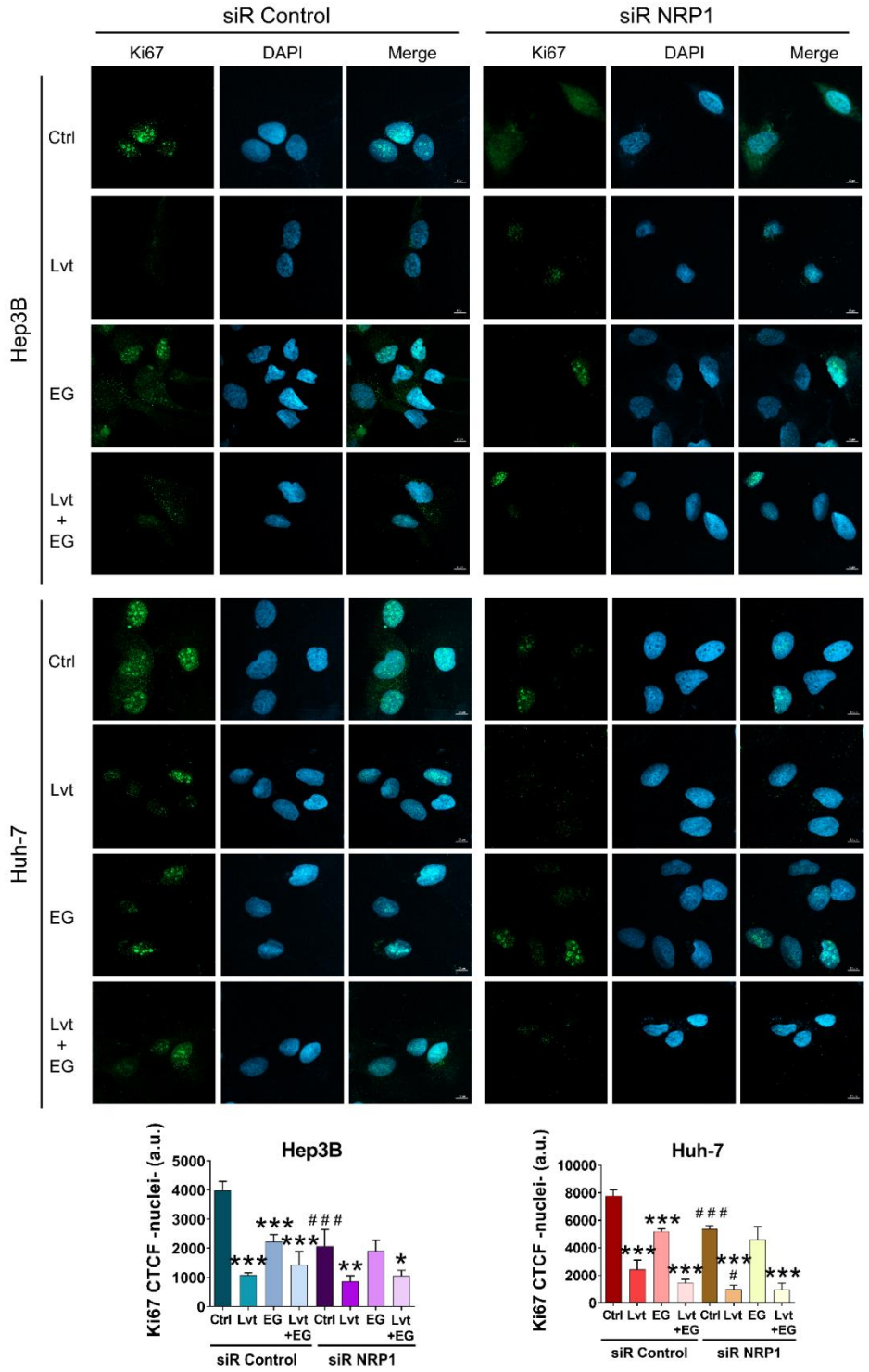

Figure 30. Analysis of cell proliferation based on Ki67 after NRP1 gene silencing in combination with lenvatinib and/or EG00229 treatment in HCC cells. Cell proliferation of Hep3B and Huh-7 cell lines was analyzed through nuclear localization of Ki67 by immunofluorescence after 48 h of gene silencing and 24 h of compound administration. 2.5 µM lenvatinib (Lvt) and/or 15 µM EG00229 (EG) were administered for 24 h. Data are expressed as mean values of arbitray units (a.u.) ± SD (n = 3), showing representative images with magnification 63×, scale bar 10 µm, and representing the NRP1 CTCF ratio. Significant differences **p*<0.05, ***p*<0.01, ****p*<0.001 *vs* control (Ctrl) (untreated cells); $^{\#}p$<0.05, $^{\#\#}p$<0.01, $^{\#\#\#}p$<0.001 *vs* siR Control for each treatment.

In consequence, the analysis of survival ability of the HCC cell lines reported interesting results in the role played by NRP1 on the cellular effects derived from lenvatinib. For this reason, we further assessed this potential link in the migratory abilities of the HCC cell lines.

In order to corroborate these results in the lenvatinib-associated effects previously observed in cell migration, wound closure ability was also assessed in our *in vitro* models of HCC. Similarly, individual administration of lenvatinib and EG00229 significantly inhibited wound closure ability of both Hep3B and Huh-7 cells, displaying a synergistic effect when combined in Huh-7 (**Figure 31**). Gene silencing of NRP1 accomplished to heighten lenvatinib effects in both lines, but only augmented EG00229-derived inhibition in Hep3B (**Figure 31**). NRP1 silencing in combination with both lenvatinib and EG00229 only enhanced inhibition in Hep3B cells, where this drug co-administration did not show a synergy in absence of silenced NRP1 (**Figure 31**). Simultaneously, Huh-7 did not exhibit raised effects of NRP1 silencing with lenvatinib and EG00229 co-treatment, but this combination did show higher effects compared to lenvatinib alone in absence of gene silencing (**Figure 31**). Hence, these findings reveal that NRP1 silencing is able to increase effects of lenvatinib only when its co-administration with EG00229 did not accomplish a higher inhibition of HCC cell migration compared to lenvatinib alone.

Altogether, NRP1 seems to have a key role in the proliferation and migration abilities of HCC cells, since either blocking NRP1 activity with EG00229 or promoting NRP1 downregulation with lenvatinib triggered a strong decrease on cell proliferation and migration of both Hep3B and Huh-7 cell lines.

NRP1 might be involved in the antitumor effects of lenvatinib observed in these HCC cell lines on cell proliferation and migration. Interestingly, although results obtained suggest that lenvatinib modulates NRP1 in a previous step of its activity, the precise mechanism of NRP1 modulation by lenvatinib remains unclear.

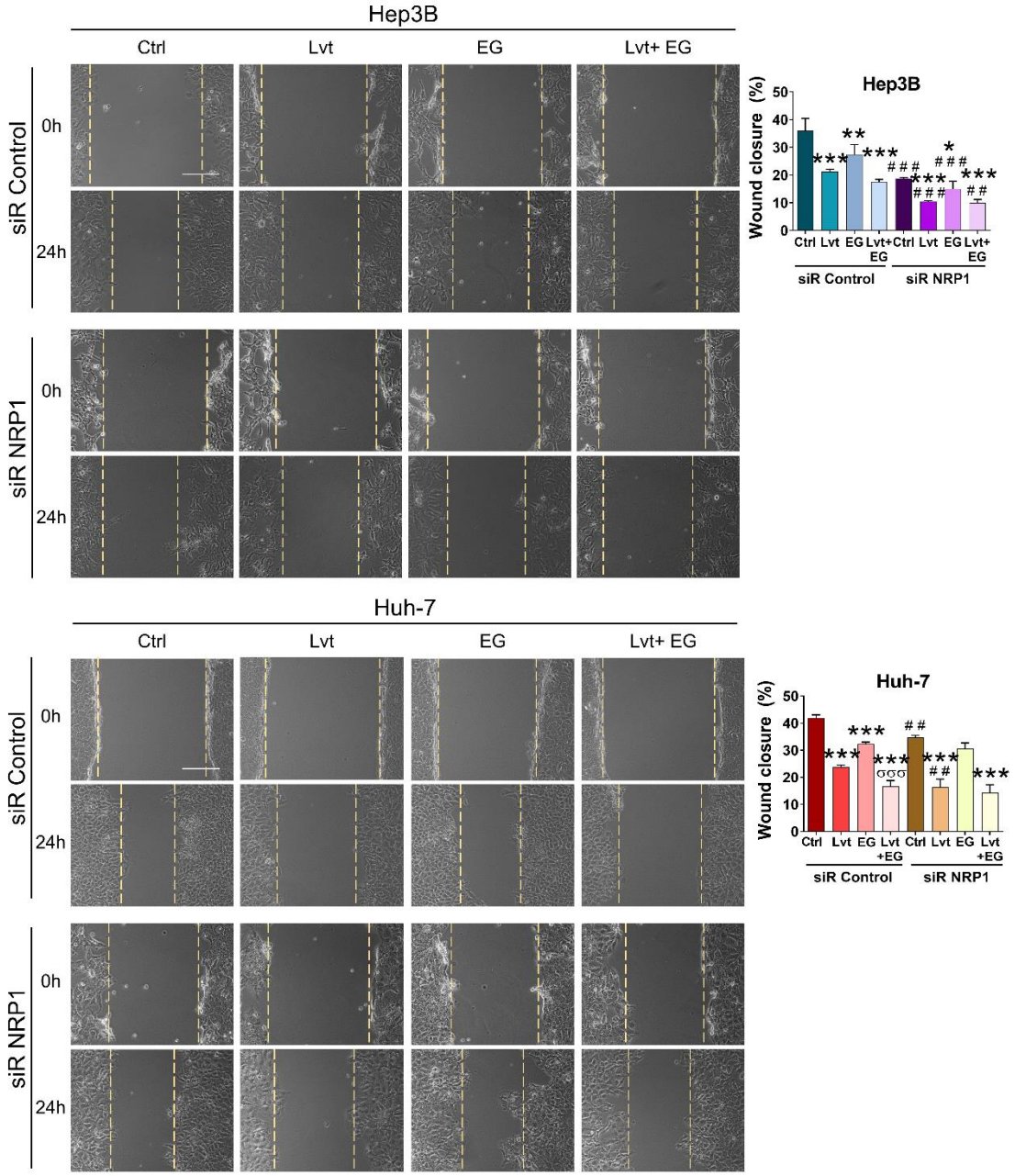

Figure 31. Determination of effects on cell migration after NRP1 gene silencing in combination with lenvatinib and/or EG00229 treatment in HCC cells. Cell migration ability was analyzed in Hep3B and Huh-7 cell lines by wound-healing assay after 48 h of gene silencing and 24 h of compound administration. 2.5 µM lenvatinib (Lvt) and/or 15 µM EG00229 (EG) were administered for 24 h. A representative image is shown with magnification 10×, scale bar 50 µm. Data are expressed as percentage of wound closure ± SD (n = 3). Significant differences *p<0.05, **p<0.01, ***p<0.001 *vs* control (Ctrl) (untreated cells); $^{\#}p$<0.05, $^{\#\#}p$<0.01, $^{\#\#\#}p$<0.001 *vs* siR Control for each treatment; $^{\sigma}p$<0.05, $^{\sigma\sigma}p$<0.01, $^{\sigma\sigma\sigma}p$<0.001 Lvt+EG *vs* Lvt treatment.

6.2.5 Identification of the underlying mechanisms responsible for the lenvatinib-derived downregulation of NRP1 in HCC cells

With the purpose of elucidating the process through which lenvatinib downregulates NRP1 in Hep3B and Huh-7 cells, and to determine the potential value of NRP1 as a molecular target to improve efficacy of current available drugs, we performed mechanistic analysis employing specific inhibitors of protein synthesis (CHX, 300 µM) and proteasome-mediated protein degradation (MG132, 30 µM), as well as with Baf (100 nM) as inhibitor of the autophagic flux (**Figure 32**).

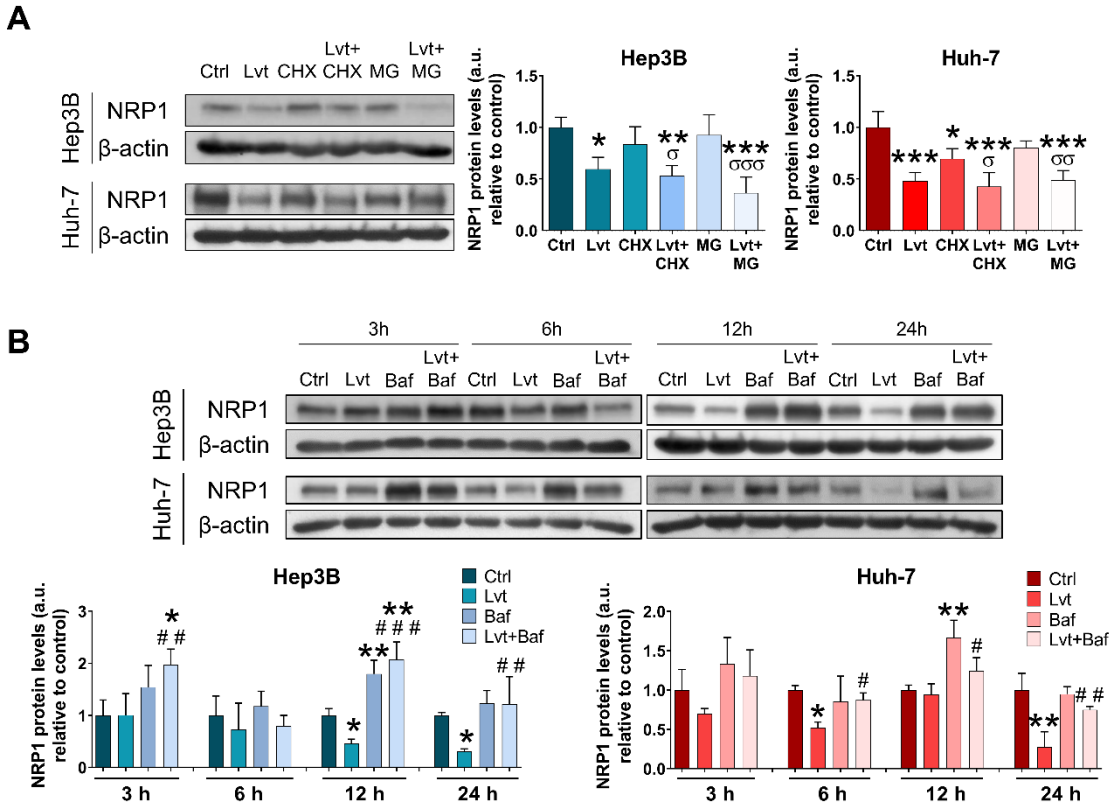

Figure 32. Identification of the mechanism responsible for the lenvatinib-derived NRP1 downregulation in HCC cells. Protein levels of NRP1 were determined by western blot employing (**A**) 2.5 µM lenvatinib (Lvt), 300 µM CHX, 30 µM MG132 (MG), alone or in combination for 24 h; (**B**) 2.5 µM lenvatinib (Lvt) and/or 100 nM Baf for 3, 6, 12 and 24 h. A representative immunoblot for each protein is shown, and data are expressed as mean values of arbitrary units (a.u.) ± SD (n = 3). Significant differences *p<0.05, **p<0.01, ***p<0.001 *vs* control (Ctrl) (untreated cells); $^{\#}p$<0.05, $^{\#\#}p$<0.01, $^{\#\#\#}p$<0.001 compound combination *vs* individual lenvatinib; $^{\sigma}p$<0.05, $^{\sigma\sigma}p$<0.01, $^{\sigma\sigma\sigma}p$<0.001 compound combination *vs* individual inhibitor.

Protein expression analysis showed that its inhibition with CHX slightly diminished NRP1 levels, but a stronger reduction was observed after lenvatinib treatment (**Figure 32A**). Protein NRP1 expression was not altered after protein degradation through MG132 administration, while lenvatinib significantly decreased NRP1 levels alone and in combination with MG132 (**Figure 32A**). These findings indicated that neither protein synthesis or degradation are the mechanisms responsible for the strong effects of lenvatinib on NRP1 expression. For this reason, we decided to evaluate the likely role played by autophagy using the inhibitor Baf alone and combined with lenvatinib for a time-course to study the dynamic process of autophagy (**Figure 32B**). As previously observed, lenvatinib diminished NRP1 protein levels mainly after 6 h or 12 h treatment; but, interestingly, Baf administration was able to increase NRP1 expression even in presence of lenvatinib, from 12 h and 6 h in Hep3B and Huh-7 cell lines, respectively, restoring NRP1 protein levels (**Figure 32B**).

To clearly determine the effectiveness of autophagy blockade, the autophagolysosome content was analyzed by acridine orange staining (**Figure 33**), together with the measurement of protein levels of the autophagic markers p62/SQSTM1 and LC3 (**Figure 34**).

Through fluorescence imaging with acridine orange, autophagy process was evaluated employing the inhibitor Baf (**Figure 33**). Results exhibited a lenvatinib-derived induction of autophagy from early time points (3 h), which were effectively decreased by Baf to levels close to basal (**Figure 33**). We also assessed p62/SQSTM1 and LC3 expression, which aimed at measuring a relative autophagic flux index (**Figure 34**). Likewise, lenvatinib treatment led to lower expression of p62/SQSTM1 from 12 h and LC3-II from 24 h, which was markedly prevented by Baf, triggering protein accumulation of both autophagic markers (**Figure 34**). Therefore, treatment with Baf achieved an effective blockade of autophagy even in presence of lenvatinib, settling the crucial role of lenvatinib-induced autophagy in the modulation of NRP1 protein expression. These findings suggest that the dynamic process of autophagy is responsible, at least in part, of the lenvatinib effects in NRP1 expression levels.

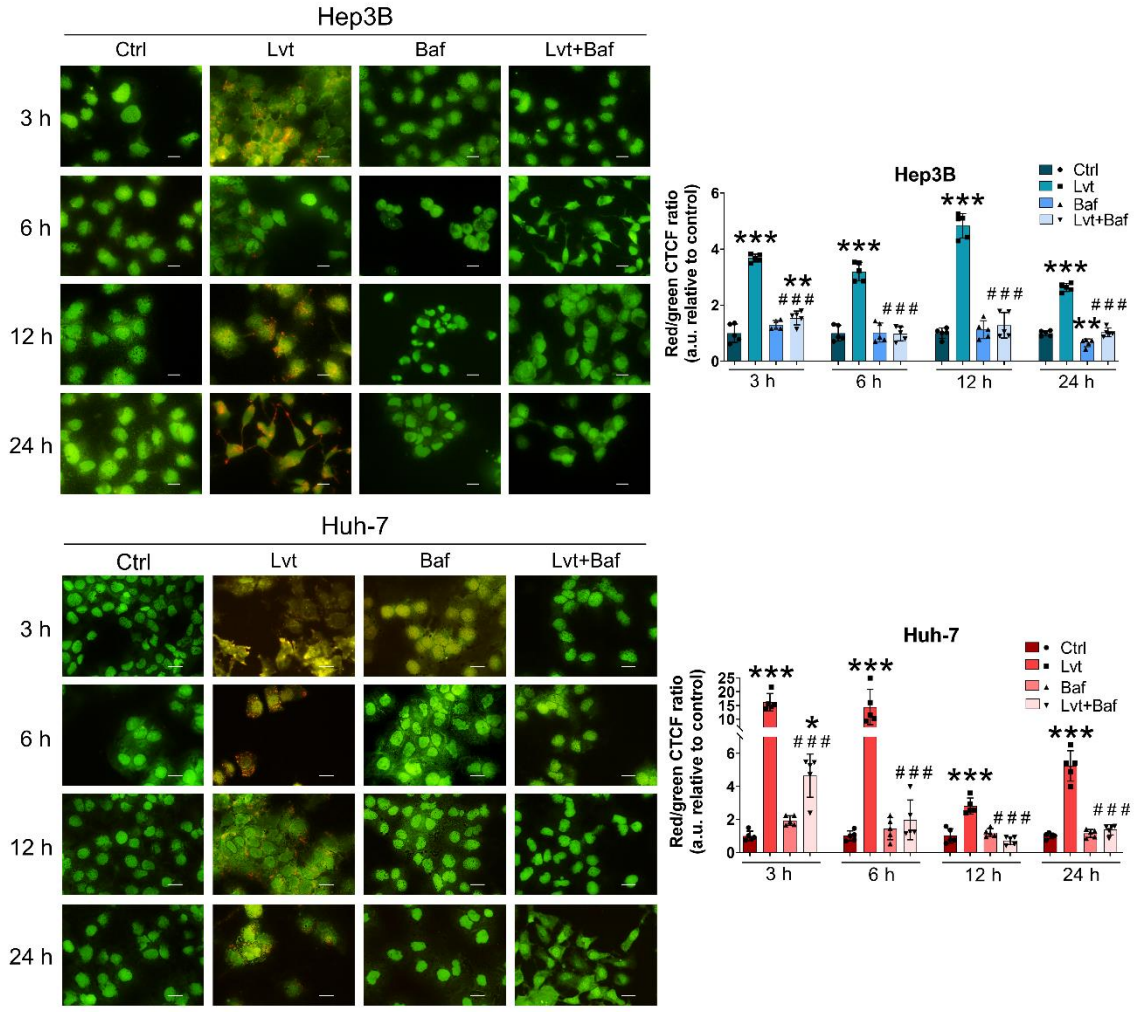

Figure 33. Evaluation of the lenvatinib and Baf effects on autophagy. Autophagolysosome content was analyzed by acridine orange staining in both Hep3B and Huh-7 cell lines employing 2.5 µM lenvatinib (Lvt) and 100 nM Baf, alone or combined, for 3, 6, 12 and 24 h of treatment. For each condition a representative image is shown, with magnification 40×, scale bar 25 µm. Bar graphs represent the CTCF ratio of the red/green fluorescence, expressed as mean values of arbitrary units (a.u.) ± SD (n = 5). Significant differences *p<0.05, **p<0.01, ***p<0.001 *vs* control (Ctrl) (untreated cells) for each time point; $^{\#}p$<0.05, $^{\#\#}p$<0.01, $^{\#\#\#}p$<0.001 compound combination *vs* individual lenvatinib.

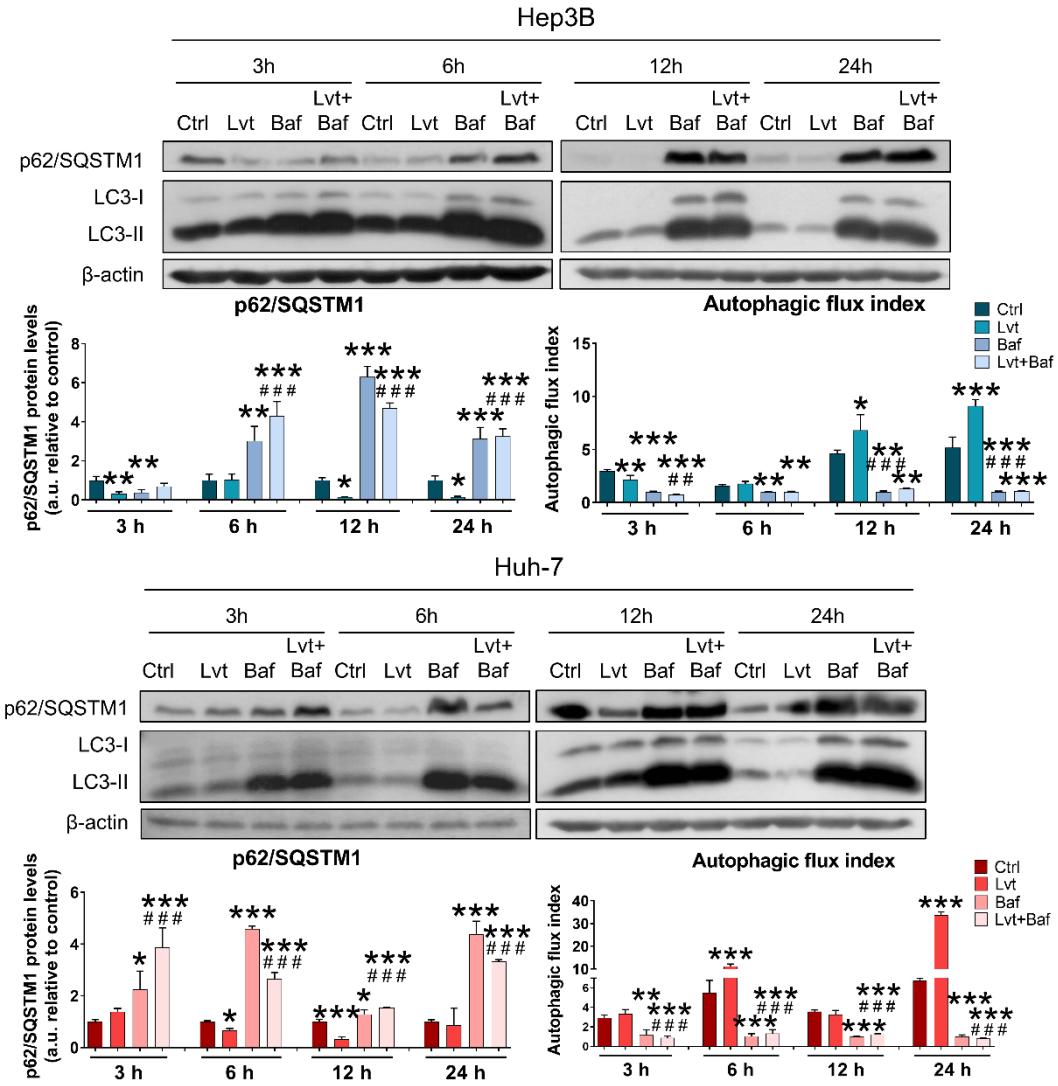

Figure 34. Assessment of autophagy through the autophagic markers p62/SQSTM1 and LC3. Protein expression of p62/SQSTM1 and LC3 (LC3-I and LC3-II) was measured by western blot after treatment with 2.5 µM lenvatinib (Lvt) and 100 nM Baf, alone or combined, for 3, 6, 12 and 24 h. For p62/SQSTM1, data are expressed as mean values of arbitrary units (a.u.) ± SD (n = 3), and for LC3, the autophagic flux index was determined by using the LC3 turnover assay, representing mean values ± SD (n = 3). A representative immunoblot of each protein is shown. Significant differences *p<0.05, **p<0.01, ***p<0.001 *vs* control (Ctrl) (untreated cells) for each time point; $^{\#}p$<0.05, $^{\#\#}p$<0.01, $^{\#\#\#}p$<0.001 compound combination *vs* individual lenvatinib.

6.2.6 Study of the potential role of autophagy-mediated NRP1 degradation in the antitumor effects of lenvatinib in HCC cells

As observed in previous results, autophagy seems to mediate the NRP1 downregulation promoted by lenvatinib. For this reason, we firstly analyzed the potential correlation between NRP1 and autophagy-associated genes in human samples from the UALCAN database (**Table XI**) to determine the likely association of NRP1 with this

process. Results displayed that NRP1 gene expression in HCC patients is positively correlated with 59 different genes involved in several steps of autophagy, with Pearson-CC ranging from +0.31 to +0.60 and a strong significance found (p<0.0001) (**Table XI**). In consequence, we further studied the interesting interplay between autophagy and NRP1, and their role in the lenvatinib effectiveness in our *in vitro* model.

Table XI. Autophagy-related genes showing significant correlation with NRP1 (p<0.0001) in human samples of HCC patients obtained from the UALCAN database.

Abbreviation	Full gene name	Pearson-CC
BCL2L1	BCL2 like 1	+0.60
MTMR3	Myotubularin-related protein 3	+0.60
RRAGB	Ras related GTP binding B	+0.60
CFLAR	CASP8 and FADD like apoptosis regulator	+0.58
AKT3	AKT serine/threonine kinase 3	+0.57
BCL2	BCL2 apoptosis regulator	+0.56
SH3GLB1	SH3 domain containing GRB2 like, endophilin B1	+0.55
MAPK3	Mitogen-activated protein kinase 3	+0.54
GABARAPL2	GABA type A receptor-associated protein like 2	+0.53
ATG16L1	Autophagy-related 16 like 1	+0.52
MAP2K1	Mitogen-activated protein kinase kinase 1	+0.51
RRAGA	Ras related GTP binding A	+0.51
TRAF6	TNF receptor associated factor 6	+0.51
WDR41	WD repeat domain 41	+0.51
ATG3	Autophagy-related 3	+0.50
IGBP1	Immunoglobulin binding protein 1	+0.50
MAP1LC3B	Microtubule associated protein 1 light chain 3 beta	+0.50
MAPK1	Mitogen-activated protein kinase 1	+0.50
PPP2CB	Protein phosphatase 2 catalytic subunit beta	+0.50
RAB7A	RAB7A, member RAS oncogene family	+0.49
SMCR8	SMCR8-C9orf72 complex subunit	+0.48
RAB1A	RAB1A, member RAS oncogene family	+0.47
RRAS	RAS related	+0.47
PIK3C3	Phosphatidylinositol 3-kinase catalytic subunit type 3	+0.46
TANK	TRAF family member associated NFκB activator	+0.46
UVRAG	UV radiation resistance associated	+0.45

Abbreviation	Full gene name	Pearson-CC
TSC1	TSC complex subunit 1	+0.44
DAPK1	Death associated protein kinase 1	+0.42
EIF2AK3	Eukaryotic translation initiation factor 2 alpha kinase 3	+0.42
RRAGC	Ras related GTP binding C	+0.42
MAP1LC3B2	Microtubule associated protein 1 light chain 3 beta 2	+0.41
BECN1	Beclin 1	+0.40
DAPK3	Death associated protein kinase 3	+0.40
EIF2S1	Eukaryotic translation initiation factor 2 subunit alpha	+0.40
PIK3R4	Phosphatidylinositol 3-kinase regulatory subunit 4	+0.40
PDPK1	3-phosphoinositide dependent protein kinase 1	+0.39
PPP2CA	Protein phosphatase 2 catalytic subunit Alpha	+0.39
TBK1	TANK binding kinase 1	+0.39
HMGB1	High mobility group box 1	+0.38
ATG4B	Autophagy-related 4B	+0.36
ATG4C	Autophagy-related 4C	+0.36
ATG7	Autophagy-related 7	+0.36
PRKACB	Protein kinase cAMP-activated catalytic subunit beta	+0.36
ATG9A	Autophagy-related 9A	+0.35
RRAS2	RAS related 2	+0.35
ITPR1	Inositol 1,4,5-trisphosphate receptor type 1	+0.34
RHEB	Ras homolog, mTORC1 binding	+0.34
NRAS	NRAS proto-oncogene, GTPase	+0.33
STX17	Syntaxin 17	+0.33
ATG2B	Autophagy-related 2B	+0.32
KRAS	KRAS proto-oncogene, GTPase	+0.32
MAP3K7	Mitogen-activated protein kinase kinase kinase 7	+0.32
PRKCD	Protein kinase C delta	+0.32
ULK2	Unc-51 like autophagy activating kinase 2	+0.32
AKT1	AKT serine/threonine kinase 1	+0.31
ATG5	Autophagy-related 5	+0.31
GABARAP	GABA type A receptor-associated protein	+0.31
GABARAPL1	GABA type A receptor-associated protein like 1	+0.31
ZFYVE1	Zinc finger FYVE-type containing 1	+0.31

To clarify the function exerted by autophagy in the antitumor effects of lenvatinib through modulation of NRP1 expression, we silenced NRP1 and, subsequently, administered lenvatinib and Baf alone or in combination, analyzing the effects on NRP1 levels by western blot (**Figure 35**) and immunofluorescence (**Figure 36**), on cell viability (**Figure 37**) and proliferation (**Figure 38**), and on cell migration (**Figure 39**).

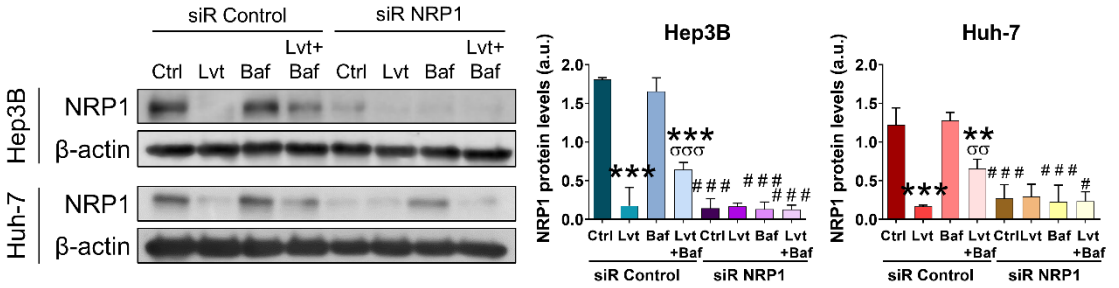

Figure 35. Analysis of the role of autophagy inhibition in NRP1 expression by western blot. Protein expression of NRP1 was analyzed by western blot after 48 h of gene silencing and 24 h of compound administration. 2.5 µM lenvatinib (Lvt) and/or 100 nM Baf were administered for 24 h. Data are represented as mean values of arbitrary units (a.u.) ± SD (n = 3), showing a representative immunoblot for each protein. Significant differences **p*<0.05, ***p*<0.01, ****p*<0.001 *vs* control (Ctrl) (untreated cells); $^{\#}p$<0.05, $^{\#\#}p$<0.01, $^{\#\#\#}p$<0.001 *vs* siR Control for each treatment; $^{\sigma}p$<0.05, $^{\sigma\sigma}p$<0.01, $^{\sigma\sigma\sigma}p$<0.001 Lvt+Baf *vs* Lvt treatment.

Analysis of NRP1 protein levels displayed an effective gene silencing, observed by both western blot (**Figure 35**) and immunofluorescence (**Figure 36**). By western blot, lenvatinib-derived downregulation of NRP1 was also observed in both HCC cell lines, not showing significant differences by individual Baf addition (**Figure 35**). Although autophagy blockade did not alter NRP1 expression, co-administration of Baf with lenvatinib increased NRP1 levels in comparison to individual administration of lenvatinib, partially restoring NRP1 expression (**Figure 35**). Curiously, NRP1 silencing not only decreased its expression, but also prevented this recovery of NRP1 levels caused by Baf in combination with lenvatinib (**Figure 35**). Through immunofluorescence and laser confocal microscopy, similar results were observed (**Figure 36**). Autophagy inhibition by Baf also exhibited an increment in NRP1 levels when combined with lenvatinib versus individual administration of this drug (**Figure 36**). In addition, effective gene silencing of NRP1 was accomplished and prevented the recovery of NRP1 protein expression when Baf was co-administered with lenvatinib (**Figure 36**).

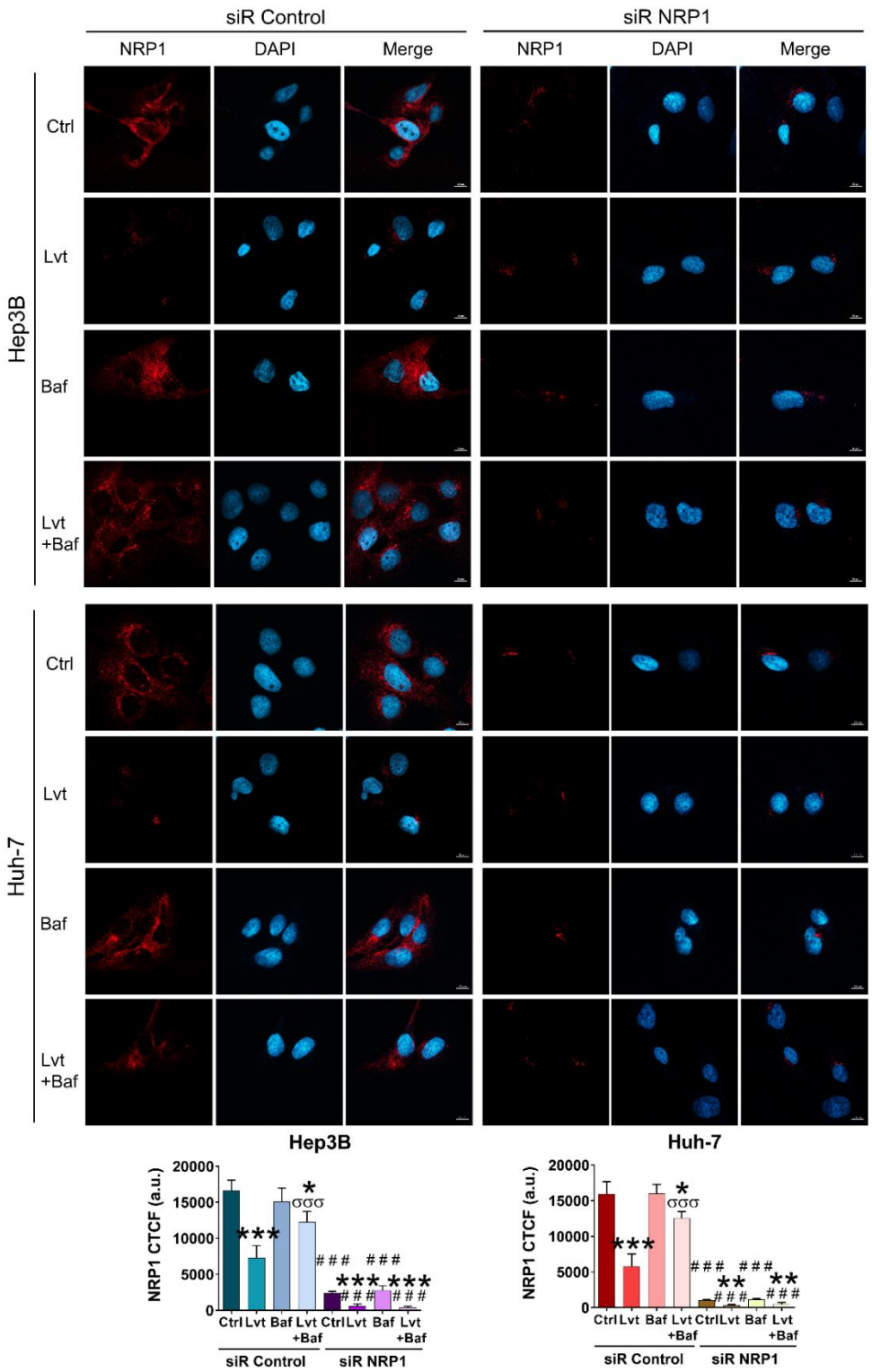

Figure 36. Analysis of the role of autophagy inhibition in NRP1 expression by immunofluorescence. Protein expression of NRP1 was analyzed through immunofluorescence after 48 h of gene silencing and 24 h of compound administration with 2.5 µM lenvatinib (Lvt) and/or 100 nM Baf. Data are represented as mean values of arbitrary units (a.u.) ± SD (n = 3). Representative confocal images are shown, with magnification 63×, scale bar 10 µm, and with bar graphs representing the NRP1 CTCF ratio. Significant differences *p<0.05, **p<0.01, ***p<0.001 *vs* control (Ctrl) (untreated cells); $^{\#}p$<0.05, $^{\#\#}p$<0.01, $^{\#\#\#}p$<0.001 *vs* siR Control for each treatment; $^{\sigma}p$<0.05, $^{\sigma\sigma}p$<0.01, $^{\sigma\sigma\sigma}p$<0.001 Lvt+Baf *vs* Lvt treatment.

Since NRP1 targeting seems to be an interesting strategy to enhance the lenvatinib effects associated to NRP1 downregulation, we evaluated the role of the autophagy-NRP1 interplay in the *in vitro* effectiveness of lenvatinib.

Both HCC cell lines, Hep3B and Huh-7, exhibited a significant inhibition of cell viability and colony formation by lenvatinib, not observing significant changes with Baf administration (**Figure 37**). Addition of Baf to lenvatinib treatment proved to prevent the initial inhibition derived from lenvatinib alone in cell viability for both cell lines (**Figure 37A**), and in the number of colonies for Huh-7 cells (**Figure 37B**). In all the analysis, genetic silencing of NRP1 significantly diminished cell viability and colony number, enhancing the effects of individual and combined treatments on both determinations (**Figure 37**). Interestingly, this NRP1 silencing was able to prevent the loss of lenvatinib-derived inhibition caused by autophagy blockade, showing same or decreased viability and colony formation ability compared to lenvatinib alone in both cell lines, Hep3B and Huh-7 (**Figure 37**).

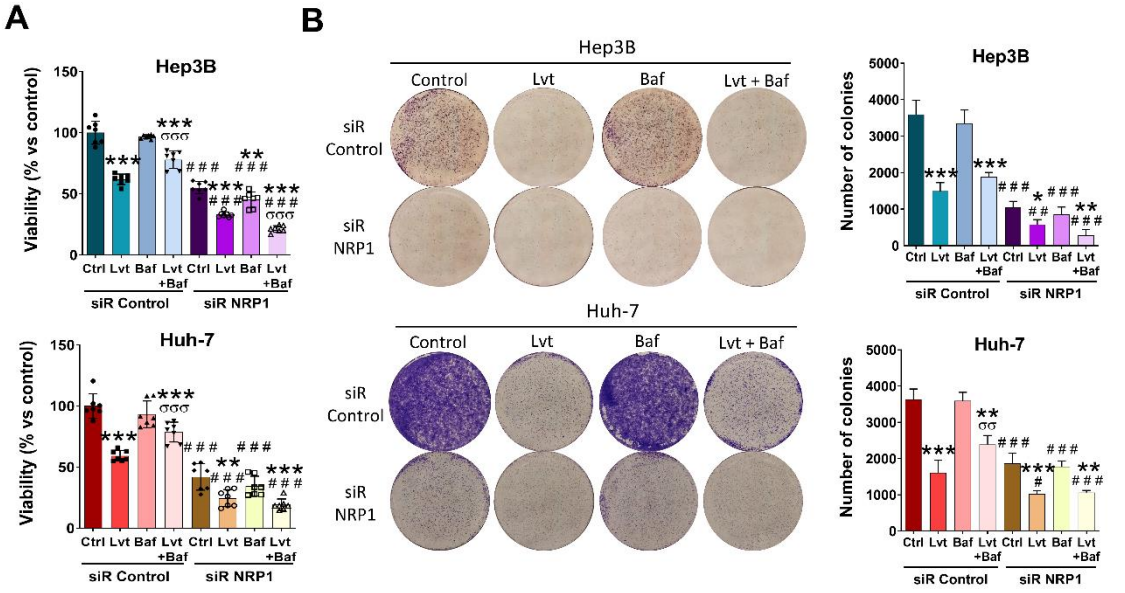

Figure 37. Evaluation of the role of autophagy-dependent degradation of NRP1 in cell viability and colony formation ability of HCC cell lines. (**A**) Cell viability and (**B**) colony formation ability were analyzed in Hep3B and Huh-7 cell lines after 48 h of gene silencing and 24 h of compound administration. 2.5 µM lenvatinib (Lvt) and/or 100 nM Baf were administered for 24 h. (**A**) Data are represented as percentage of mean values ± SD (n = 7). (**B**) Representative images are shown, and data are expressed as mean values ± SD (n = 3). Significant differences *p<0.05, **p<0.01, ***p<0.001 *vs* control (Ctrl) (untreated cells); $^{\#}p$<0.05, $^{\#\#}p$<0.01, $^{\#\#\#}p$<0.001 *vs* siR Control for each treatment; $^{\sigma}p$<0.05, $^{\sigma\sigma}p$<0.01, $^{\sigma\sigma\sigma}p$<0.001 Lvt+Baf *vs* Lvt treatment.

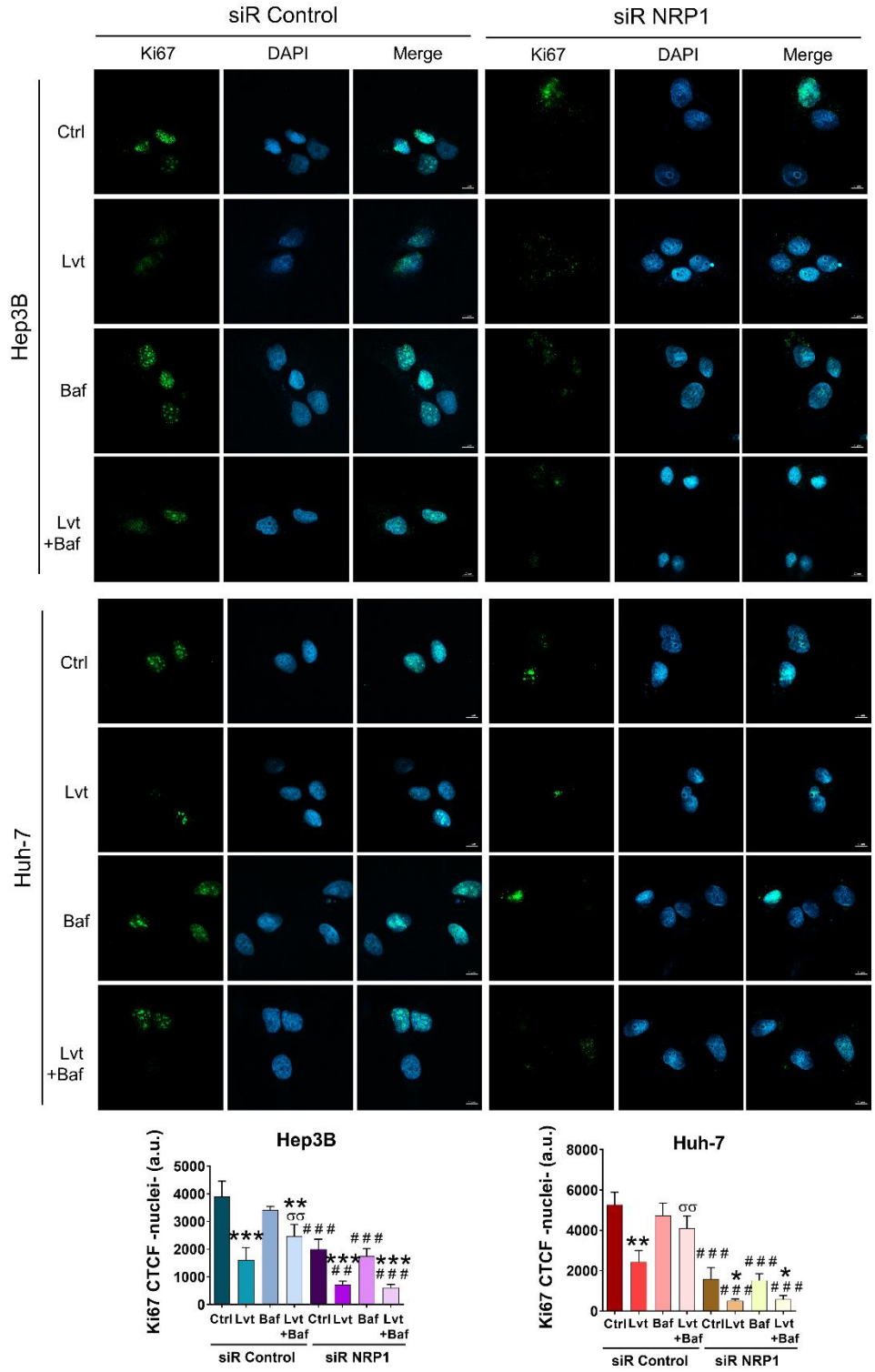

Figure 38. Evaluation of the role of autophagy-dependent degradation of NRP1 in Ki67-based proliferation of HCC cell lines. Nuclear localization of Ki67 was analyzed by immunofluorescence and laser confocal microscopy in Hep3B and Huh-7 cell lines after 48 h of gene silencing and 24 h of compound administration with 2.5 µM lenvatinib (Lvt) and/or 100 nM Baf. A representative image with magnification 63×, scale bar 10 µm, is shown, where bar graphs represent the nuclear CTCF ratio of Ki67 expressed as mean values of arbitrary units (a.u.) ± SD (n = 3). Significant differences **p*<0.05, ***p*<0.01, ****p*<0.001 *vs* control (Ctrl) (untreated cells); $^{\#}p$<0.05, $^{\#\#}p$<0.01, $^{\#\#\#}p$<0.001 *vs* siR Control for each treatment; $^{\sigma}p$<0.05, $^{\sigma\sigma}p$<0.01, $^{\sigma\sigma\sigma}p$<0.001 Lvt+Baf *vs* Lvt treatment.

As observed with viability and colony formation assays, assessment of Ki67-based proliferation index reported similar findings (**Figure 38**). Individual treatment with Baf did not modify Ki67 nuclear staining, but autophagy inhibition during lenvatinib treatment increased cell proliferation of both cell lines compared to lenvatinib administration alone (**Figure 38**). This partial loss of antitumor effects of lenvatinib on nuclear Ki67 localization accounted by Baf was not observed when NRP1 was silenced, appreciating enhanced effects for all the treatments after genetic NRP1 silencing (**Figure 38**).

In this line, we also analyzed migration ability of Hep3B and Huh-7 cells (**Figure 39**). Cell migration assessment disclosed similar results, where lenvatinib restrained wound closure ability of HCC cell lines, and Baf-dependent autophagy inhibition prevented this effect, slightly increasing cell migration (**Figure 39**). Likewise, gene silencing of NRP1 diminished migration of both Hep3B and Huh-7 cell lines and, despite NRP1 knockdown did not increment the inhibitory effects of lenvatinib, it prevented the recovery in the wound closure ability of HCC cells when lenvatinib and Baf were combined (**Figure 39**). Therefore, although Baf treatment could rise migratory abilities of HCC cells in presence of lenvatinib, decreasing the efficacy of this drug on cell migration, NRP1 silencing might be able to partially prevent this loss of efficacy in our *in vitro* model of HCC.

Collectively, autophagy seems to be the mechanism responsible for NRP1 degradation induced by lenvatinib, which could exert a crucial role in the loss of sensitivity to lenvatinib by the HCC cell lines Hep3B and Huh-7, increasing cell survival and migration abilities. Moreover, NRP1 might constitute an interesting therapeutic target to prevent the development of an autophagy-associated lenvatinib resistance in human HCC.

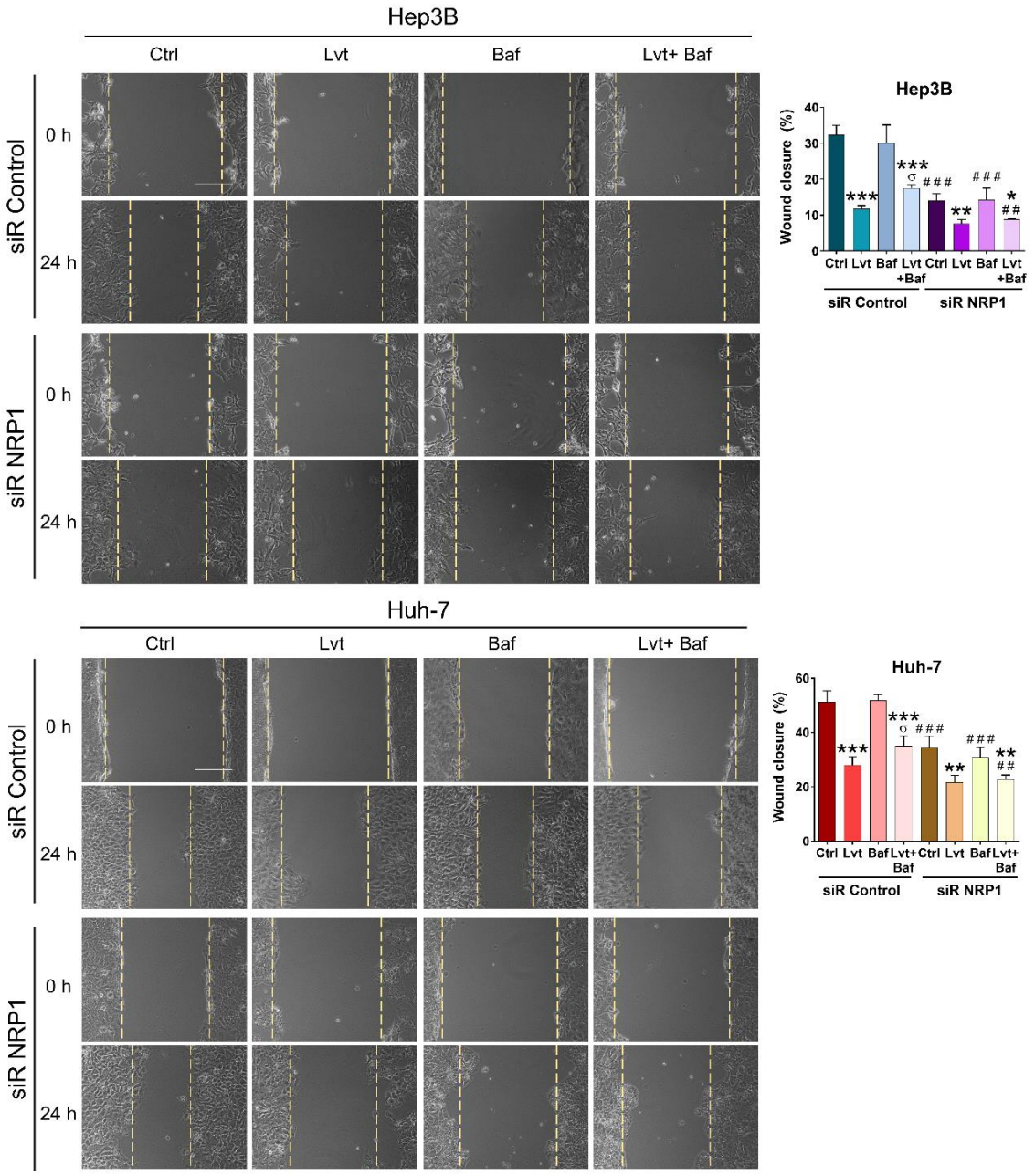

Figure 39. Determination of the role of the autophagy-dependent NRP1 degradation in cell migration ability of HCC cells. Cell migration was determined by wound-healing assay in the Hep3B and Huh-7 cell lines after 48 h of gene silencing and 24 h of compound administration. 2.5 µM lenvatinib (Lvt) and/or 100 nM Baf were administered for 24 h. A representative image with magnification 10×, scale bar 50 µm, is shown. Bar graphs represent the percentage of the wound closure area, expressed as mean values ± SD (n = 3). Significant differences **p*<0.05, ***p*<0.01, ****p*<0.001 *vs* control (Ctrl) (untreated cells); $^{\#}p$<0.05, $^{\#\#}p$<0.01, $^{\#\#\#}p$<0.001 *vs* siR Control for each treatment; $^{\sigma}p$<0.05, $^{\sigma\sigma}p$<0.01, $^{\sigma\sigma\sigma}p$<0.001 Lvt+Baf *vs* Lvt treatment.

6.2.7 Evaluation of the hypoxia-derived effects in the autophagy-dependent NRP1 degradation in HCC cells

Considering the key role that hypoxia has demonstrated to exert in the acquisition of drug resistance in several tumor types, including HCC[123,164], we decided to assess the potential implication of the hypoxia-derived response in the autophagy-related loss of lenvatinib sensitivity by modulating NRP1.

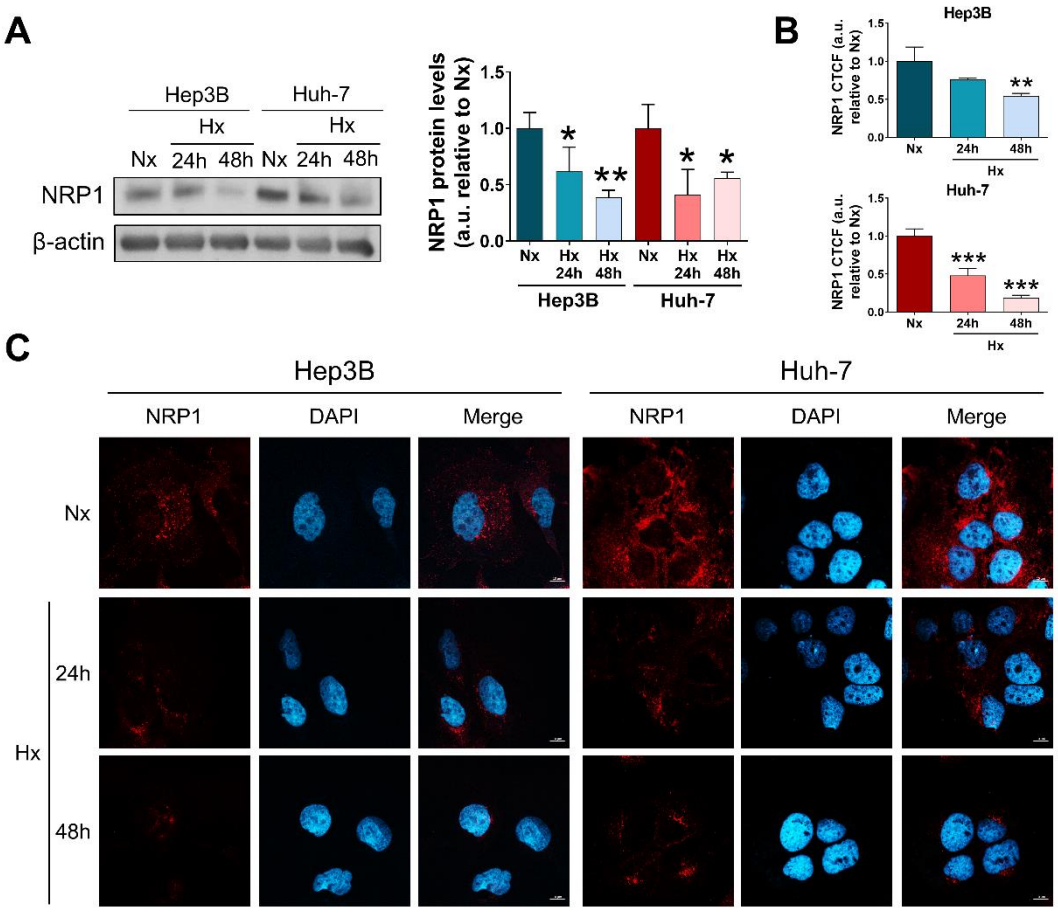

Figure 40. Study of the NRP1 modulation by inducing an *in vitro* hypoxia response. NRP1 expression was assessed at protein level by (**A**) western blot and (**B-C**) immunofluorescence with laser confocal microscopy. Hypoxia (Hx) was chemically induced by treating with 100 µM $CoCl_2$ for 24 h and 48 h, with normoxia (Nx) as control condition. (**A**) A representative immunoblot and (**C**) confocal image is shown, with magnification 63×, scale bar 10 µm. Bar graphs from (**B**) represent CTCF ratio of NRP1. Data are expressed as mean values of arbitrary units (a.u.) ± SD (n = 3). Significant differences *p<0.05, **p<0.01, ***p<0.001 *vs* normoxia (Nx).

In order to induce a hypoxic microenvironment, we employed the hypoximimetic $CoCl_2$, that promotes the stabilization of HIFs and, in consequence, drives a hypoxia response *in vitro*. The hypoxia-derived effects on protein expression of NRP1 were analyzed by western blot (**Figure 40A**) and immunofluorescence (**Figure 40B-C**). Hypoxia was induced for 24 h and 48 h, displaying lower levels of NRP1 under hypoxic conditions compared to normoxia by both techniques (**Figure 40**). As previously identified with lenvatinib, NRP1 downregulation under hypoxia could be associated to an autophagy induction in HCC cells, thus promoting NRP1 degradation.

The potential interplay between the hypoxic microenvironment and the autophagy process was further assessed with the purpose of determining if the same autophagy-related modulation was being conducted under hypoxia (**Figure 41**). As formerly observed, hypoxia prompted NRP1 downregulation, which was found significant from 12 h (**Figure 41A**). Autophagy blockade through Baf addition triggered an increase in the protein levels of NRP1 from 12 h and 6 h in Hep3B and Huh-7, respectively, recovering the NRP1 expression to normoxia levels (**Figure 41A**). Interestingly, this analysis was also conducted with the HepG2 cells, observing that even for this cell line, Baf treatment achieved to restore NRP1 expression (**Supplementary Figure S1**). Furthermore, the autophagy process was monitored by both acridine orange staining (**Figure 41B**) and protein expression of p62/SQSTM1 and LC3 (**Figure 41C**). Results demonstrated that the use of Baf effectively diminished autophagolysosome content from the first time point (3 h) in both cell lines, Hep3B and Huh-7 (**Figure 41B**). Likewise, p62/SQSTM1 levels were significantly higher after Baf administration, showing a protein accumulation from 12 h and 3 h in the Hep3B and Huh-7 cells, respectively, which is directly associated to autophagy inhibition (**Figure 41C**). Determination of the autophagic flux index, based on the LC3 turnover assay, also proved the usefulness of Baf as specific autophagic inhibitor, since a significant decrease was observed with Baf treatment under hypoxia (**Figure 41C**). Hence, NRP1 expression seems to be also modulated under hypoxia by an autophagy-mediated degradation, which could be involved in the loss of lenvatinib efficacy through an adaptive cellular response driven by hypoxia.

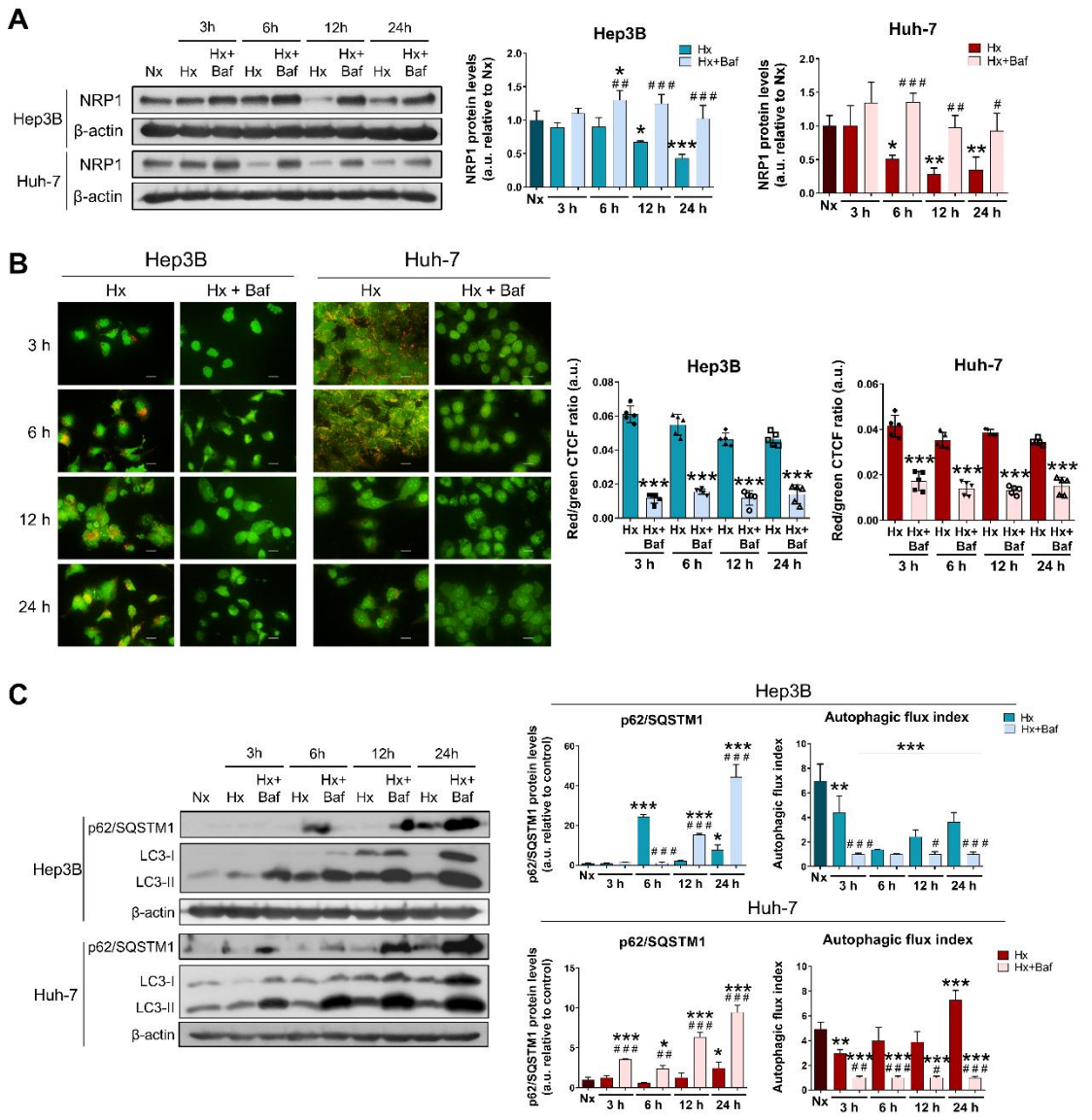

Figure 41. Analysis of the autophagy-associated effects on the modulation by hypoxia on NRP1 expression. Hypoxia (Hx) response was induced by 100 µM $CoCl_2$ with or without 100 nM Baf treatment. (**A**) Protein levels of NRP1 were determined by western blot. Autophagy was monitored by (**B**) acridine orange staining for quantification of autophagolysosome content and (**C**) protein expression of p62/SQSTM1 and LC3 through western blot. (**A**) and (**C**) A representative immunoblot is shown for each protein, and data are expressed as mean values of arbitrary units (a.u.) ± SD (n = 3). For LC3, the autophagic flux index was determined by using the LC3 turnover assay. (**B**) A representative confocal image with magnification 40×, scale bar 25 µm, is shown, and bar graphs represent CTCF of red/green ratio, expressed as mean values of arbitrary units (a.u.) ± SD (n = 5). (**A**) and (**C**) Significant differences *p<0.05, **p<0.01, ***p<0.001 *vs* normoxia (Nx); and $^{\#}p$<0.05, $^{\#\#}p$<0.01, $^{\#\#\#}p$<0.001 *vs* Hx for each time point. (**B**) Significant differences *p<0.05, **p<0.01, ***p<0.001 *vs* Hx for each time point.

6.2.8 Determination of the role of HIF-1α in the lenvatinib effectiveness through NRP1 modulation mediated by a hypoxia-induced autophagy

Under hypoxia conditions, HIFs are the main drivers of the cellular response, where HIF-1α has demonstrated a crucial role in the resistance development against TKIs treatment in HCC[42,123].

Initially, we investigated the potential correlation between NRP1 and HIF-1α in samples from HCC patients obtained from different databases (**Figure 42A-C**). Results displayed a significant positive correlation for the three databases, with Pearson-CC +0.51 (**Figure 42A**), +0.39 (**Figure 42B**), +0.52 (**Figure 42C**), and with $p<0.0001$ for all cases. To validate and complete these findings *in vitro*, NRP1 protein expression was analyzed after gene silencing of HIF-1α in Hep3B and Huh-7 cell lines (**Figure 42D**). Similarly, after HIF-1α silencing, protein levels of NRP1 were found markedly reduced in both cell lines (**Figure 42D**), suggesting a direct association between HIF-1α and NRP1 under hypoxia.

The potential role played by HIF-1α in the previously observed hypoxia-autophagy interplay was determined by combining Baf treatment with hypoxia induction and HIF-1α silencing (**Figure 42E-F**). HIF-1α was successfully silenced in both cell lines, showing a slight decrease in Hep3B cells after Baf addition (**Figure 42E**). Regarding NRP1, protein levels were strongly decreased under hypoxia and partially restored by autophagy blockade (**Figure 42E**). However, this expression recovery of NRP1 expression was not observed when HIF-1α was silenced (**Figure 42E**), highlighting the potential role of this transcription factor in the modulation of NRP1 expression and, in consequence, in the associated effects on lenvatinib sensitivity. This was further assessed by determining cell viability in the same conditions (**Figure 42F**). Results showed lower cell viability of both Hep3B and Huh-7 after hypoxia induction, which was potentiated when HIF-1α was silenced (**Figure 42F**). Even though autophagy disruption through Baf treatment displayed a higher cell viability compared to hypoxia, this was counteracted by HIF-1α knockdown, exhibiting the highest inhibitory effects on cell viability of HCC cell lines even in presence of Baf (**Figure 42F**).

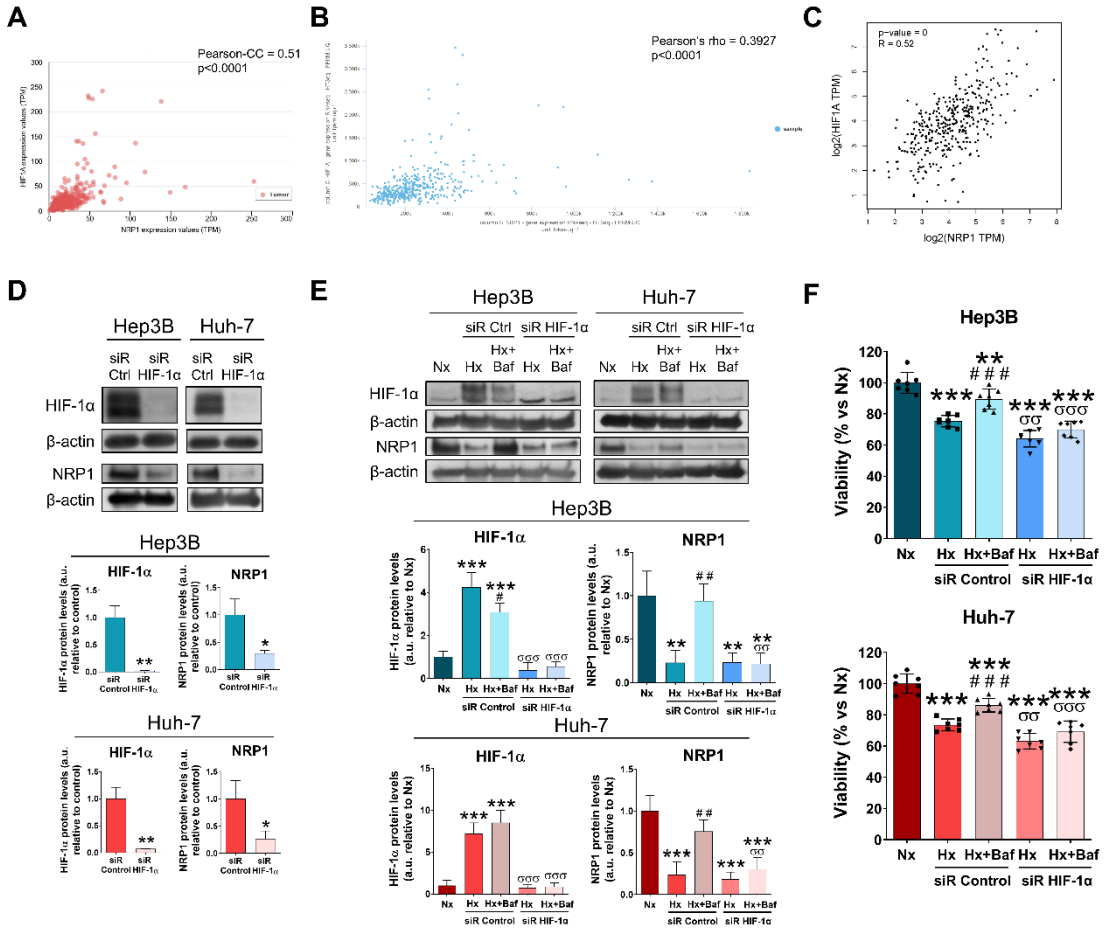

Figure 42. Assessment of the potential role of HIF-1α under hypoxia in the autophagy-associated modulation of NRP1. Correlation graphs between HIF-1α and NRP1 were obtained from (**A**) UALCAN, (**B**) UCSC Xena and (**C**) GEPIA databases, showing the corresponding *p* values and Pearson-CC. *In vitro* experiments were performed after 48 h of gene silencing and 24 h of drug treatments, using 100 µM $CoCl_2$ for hypoxia (Hx) induction, 2.5 µM lenvatinib (Lvt) and 100 nM Baf. (**D**) and (**E**) Protein expression of HIF-1α and NRP1 was analyzed by western blot, showing a representative immunoblot for each protein. Data are expressed as mean values of arbitrary units (a.u.) ± SD (n = 3). (**F**) Cell viability was measured by MTT assay and data are expressed as percentage of mean values relative to normoxia (Nx) ± SD (n = 7). (**D**) Significant differences **p*<0.05, ***p*<0.01, ****p*<0.001 *vs* siR Control. (**E**) and (**F**) Significant differences**p*<0.05, ***p*<0.01, ****p*<0.001 *vs* normoxia (Nx); $^{\#}p$<0.05, $^{\#\#}p$<0.01, $^{\#\#\#}p$<0.001 *vs* Hx for each siR group; and $^{\sigma}p$<0.05, $^{\sigma\sigma}p$<0.01, $^{\sigma\sigma\sigma}p$<0.001 siR HIF-1α *vs* siR Control.

Considering the interesting role played under hypoxia by HIF-1α in the modulation of NRP1 levels through autophagy, we further evaluated the effects of this interplay on lenvatinib sensitivity. For this purpose, we analyzed HIF-1α and NRP1 expression and cell viability after lenvatinib treatment, autophagy blockade with Baf and/or under hypoxia conditions and HIF-1α silencing (**Figure 43**).

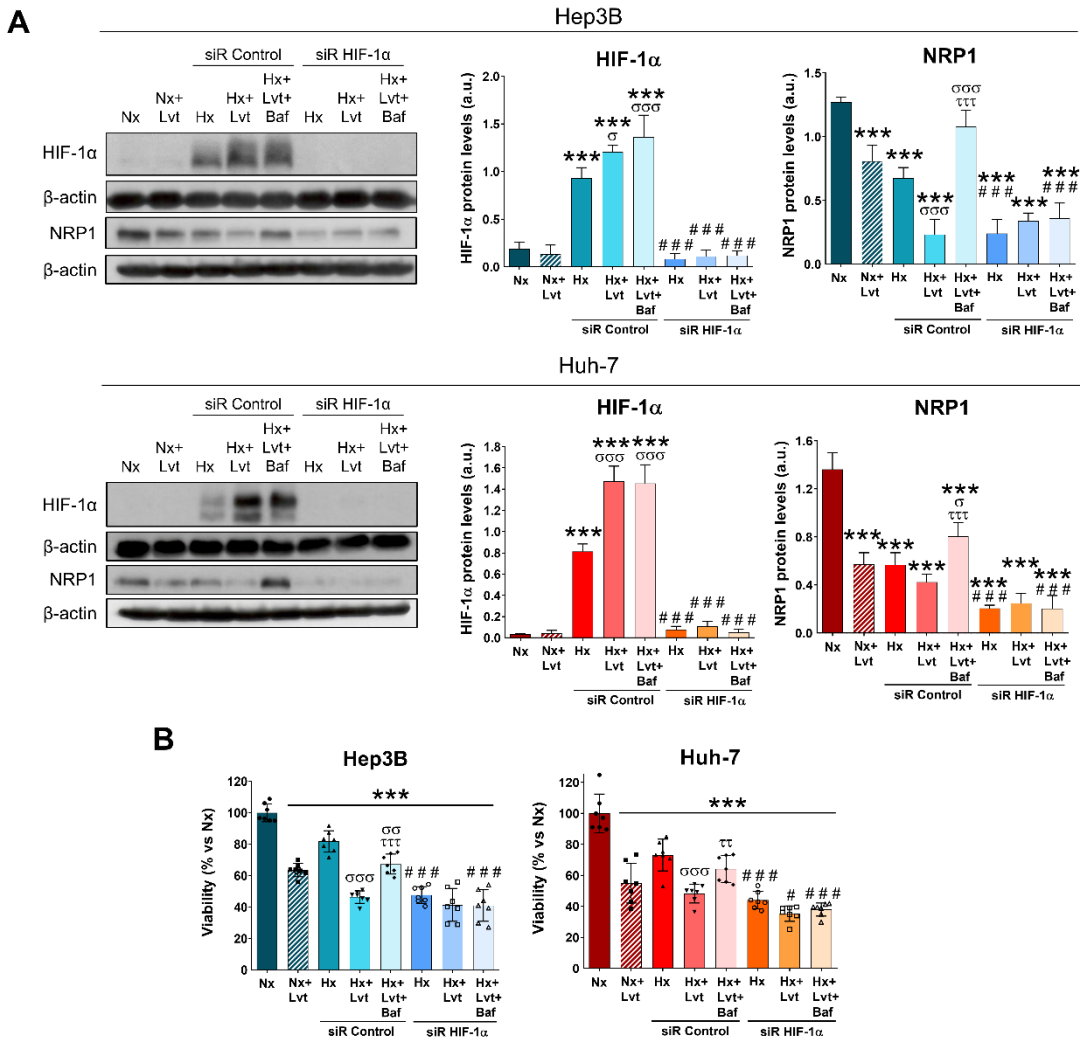

Figure 43. Analysis of the interplay between HIF-1α-mediated hypoxia response and autophagy in the cellular response to lenvatinib through NRP1 modulation. Experiments were conducted after 48 h of gene silencing and 24 h of cell treatments. 100 µM $CoCl_2$ was used for hypoxia (Hx) induction, 2.5 µM lenvatinib (Lvt) for cell treatment and 100 nM Baf for autophagy blockade. (**A**) Protein expression of HIF-1α and NRP1 was analyzed by western blot, showing a representative immunoblot for each protein, and (**B**) cell viability was measured by MTT assay. (**A**) Data are expressed as mean values of arbitrary units (a.u.) ± SD (n = 3). (**B**) Data are expressed as percentage of mean values relative to normoxia (Nx) ± SD (n = 7). Significant differences *p<0.05, **p<0.01, ***p<0.001 *vs* normoxia (Nx); $^{\#}p$<0.05, $^{\#\#}p$<0.01, $^{\#\#\#}p$<0.001 *vs* siR Control for each treatment; $^{\sigma}p$<0.05, $^{\sigma\sigma}p$<0.01, $^{\sigma\sigma\sigma}p$<0.001 *vs* Hx for each siR group; $^{\tau}p$<0.05, $^{\tau\tau}p$<0.01, $^{\tau\tau\tau}p$<0.001 *vs* Hx+Lvt for each siR group.

Analysis revealed that lenvatinib led to higher HIF-1α levels under hypoxia and intensified NRP1 downregulation (**Figure 43A**). Autophagy inhibition through Baf treatment prevented this decrease, restoring protein levels of NRP1 even under hypoxia and lenvatinib administration, whereas HIF-1α was not altered (**Figure 43A**). Remarkably, specific silencing of HIF-1α achieved to prevent these effects, not observing

a recovery of the protein NRP1 expression when Baf was co-administered with lenvatinib in hypoxia (**Figure 43A**). In terms of cell viability, induction of a hypoxic microenvironment diminished viability of both Hep3B and Huh-7, exhibiting a synergy with lenvatinib (**Figure 43B**). However, Baf-derived autophagy disruption triggered a lower susceptibility to lenvatinib, observing an increase of cell viability and, therefore, countering the inhibitory effects of lenvatinib (**Figure 43B**). Similar to that observed with NRP1 expression, HIF-1α silencing was able to not only significantly reduced cell viability, but also to avoid the loss of sensitivity to lenvatinib by the Hep3B and Huh-7 cells when autophagy was blocked (**Figure 43B**). These findings suggest the potential of both NRP1 and HIF-1α as therapeutic targets with an interesting role in the loss of lenvatinib efficacy associated to autophagy.

Overall, under hypoxia NRP1 seems to be directly regulated by HIF-1α, where autophagy exerts a key role by modulating NRP1 levels and, the complex interplay between these mechanisms could be involved in the loss of lenvatinib sensitivity by HCC cells.

7 Discussion

7.1 CLINICAL SIGNIFICANCE OF NRP1 AS BIOMARKER FOR PROGNOSIS, PATHOGENESIS AND VENOUS INVASION IN HCC PATIENTS

Solid tumors remain a global threat, where the primary liver tumor HCC represents the sixth and the third cancer in terms of incidence and mortality, respectively[1]. Notwithstanding the recent progress accomplished in the clinical landscape of this type of liver cancer, early diagnosis together with increased therapeutic efficacy and prevention of tumor recurrence are still a challenge for improving HCC patient's outcomes[8,172]. In this line, diverse studies have focused on the investigation of novel tumor biomarkers that provide useful tools for clinics[8]. Nevertheless, validation of these potential markers for diagnosis, prognosis and tumor response is still an important objective in the cancer research field[8].

For this reason, and due to the interesting role played by NRP1 in different cancers, previous studies have tried to elucidate the involvement of NRP1 in the tumor development and progression[70,73]. This transmembrane glycoprotein regulates key cellular processes, including cell proliferation, invasion, angiogenesis and cell migration, through binding and interaction with several growth factors and their corresponding receptors, mainly VEGF/VEGFR, HGF/cMET, placenta growth factor (PlGF)/VEGR, and TGF-β1/TGF-βR[70,72,73]. NRP1 is primarily located in the plasma membrane of cells modulating signaling pathways that promote angiogenesis and cell migration[70,73]. However, there is also a soluble isoform, known as sNRP1, that has demonstrated an interesting modulatory role in tumor cell angiogenesis and proliferation[72]. This receptor is widely expressed in multiple tissues and organs, whereas NRP1 overexpression has been found in several tumor types, revealing a key function as oncogene[70]. Therefore, a systematic review with meta-analysis was firstly conducted in order to assess the potential use of NRP1 as a tumor biomarker for patient's prognosis, early diagnosis and other clinical-associated parameters, which could benefice the prognostic and therapeutic landscape of HCC patients.

7.1.1 Significant association of NRP1 with worse prognosis and tumor pathogenesis in HCC patients

The total of the seven studies included in the meta-analysis provided data from 1305 patients diagnosed with HCC, from which five reports analyzed tumor prognosis,

including a total of 957 patients[78,85,161–163]. After performing statistical analysis, overall effect sizes displayed a strong and significant correlation of higher levels of NRP1 and shorter OS in HCC patients, confirming the individual results reported by each study. Furthermore, even though only one investigation analyzed the likely association between NRP1 and RFS, being not possible to meta-analyze this parameter, results obtained in this study showed the same correlation as for OS with $p = 0.0048$[78], which highlights the necessity of further studies to clarify these findings. Meta-analysis has aroused as a valuable resource for integrating data from individual investigations and obtaining a global interpretation of a more representative sample size, and has been previously performed to accomplish reliable studies in HCC recently published[173,174]. Despite there are no meta-analysis assessing the potential role of NRP1 as a biomarker for prognosis in patients with HCC or other tumor type, diverse investigations have observed a significant correlation of NRP1 overexpression with shorter survival in cervical cancer[175], gastric cancer[176,177], breast cancer[178], pancreatic ductal adenocarcinoma[179], nasopharyngeal carcinoma[180], and non-small cell lung cancer (NSCLC)[181], among others. Besides, a negative correlation of NRP1 was also found with disease-free survival (DFS) in osteosarcoma[182], and with PFS in NSCLC[181], gastric cancer[176] and nasopharyngeal carcinoma[180], supporting the consistent utility of NRP1 as a prognostic biomarker in cancer. Curiously, peritumoral levels of NRP1 were determined in HCC patients subjected to hepatic resection and results exhibited a negative correlation of NRP1 overexpression in the peritumoral tissue with OS and time to recurrence (TTR) in patients[104]. Additionally, responsiveness to therapeutic options has also shown to be modulated by NRP1[72], where raised expression levels of this protein have accounted for lower sensitivity to chemotherapy[182] and bevacizumab[183] in osteosarcoma and gastric cancer patients, respectively[182,183]. Collectively, NRP1 claims as a potential biomarker for prognosis, as well as for different parameters related to patient's survival and drug efficacy in patients diagnosed with HCC, which emphasizes the role of NRP1 as a biomarker and therapeutic target.

Interestingly, among the seven included articles, only one study determined NRP1 levels in serum samples from 149 HCC patients, displaying one of the strongest correlations between NRP1 overexpression and OS[162]. Nonetheless, although these results highlight the interest of this protein in the field of serum biomarkers, further

studies are required to validate the use of NRP1 in serum samples from HCC patients for diagnosis.

The potential association of NRP1 overexpression with tumor pathogenesis was also assessed in four articles[76,78,79,85]. Results obtained revealed that higher levels of NRP1 significantly correlated with HCC development by analyzing NRP1 expression in the tumor tissue in comparison to healthy liver tissue. Likewise, NRP1 overexpression in the tumor tissue was also reported in different cancer types, including cervical cancer[175], bladder cancer[184], NSCLC[181], osteosarcoma[182] and gastric cancer[177]; and plasma NRP1 was also described as an interesting serum biomarker in patients with breast cancer[178]. Overall, even though further studies are needed to clarify these findings, NRP1 could improve the clinical setting of HCC patients, displaying a potential use of NRP1 as a diagnostic and prognostic biomarker in HCC.

7.1.2 NRP1 overexpression correlated with age and higher risk of venous invasion in HCC patients

Initially, the potential association of NRP1 with diverse clinicopathological characteristics was assessed. However, no significant correlation was found with gender, tumor size or metastasis. Increased levels of NRP1 only correlated with age and venous invasion in patients with HCC, exhibiting a strong association after meta-analysis. In this line, a previous meta-analysis was conducted including gastric cancer patients, in which clinical relevance of NRP1 was analyzed associated to diverse clinicopathological parameters[185]. Results showed that NRP1 was not correlated with a higher tumor size, similar to that obtained in the present study; while a significant association was observed with advanced stages of tumor-node-metastasis (TNM) staging method, lymph node metastasis and poor differentiation[185]. Similarly, analysis of NRP1 overexpression in NSCLC also reported a marked association with advanced TNM, histological grade and presence of metastasis in lymph nodes, whereas significance results were not found with age, gender and the type of pathology[181]. Although NRP1 was found to correlate with patient's age, specifically with younger than 50 years, only two studies were meta-analyzed and few studies performed in HCC or other tumor types have obtained similar results. For this reason, further investigations are needed to clarify this interesting association.

In terms of invasive-related parameters, several investigations have described a direct association of higher NRP1 expression with invasion depth, lymph node metastasis, and distant metastasis in different types of cancer[177,180,182]. Even though NRP1 was not directly associated to metastasis in this meta-analysis, a higher risk of venous invasion was found markedly significant, being supported by results from these investigations conducted in other tumors[177,180,182]. Together with clinical reports, the role of NRP1 in tumor spread has been evaluated in preclinical models[175,177,186]. Results proved that NRP1 downregulation triggered lower migration, invasion, angiogenesis and EMT in NSCLC[186], cervical cancer[175] and gastric cancer[177], but increased cell proliferation in cervical cancer[175]. Nevertheless, the potential use of NRP1 as a biomarker in HCC should be clearly defined with additional studies. These findings support the key modulatory role of NRP1 in the invasive abilities of tumor cells, highlighting its likely use as a therapeutic target to prevent these malignant-associated features in HCC patients.

These results drive to diverse interpretations of the NRP1 use as either prognostic biomarker or therapeutic target in the clinical onset of HCC patients, since this protein showed to be strongly associated to tumor development, but also to worse prognosis and higher risk of venous invasion. Along with this, NRP1 has exhibited to directly modulate the cellular response to targeted drugs and chemotherapy, which prompts the crucial role of NRP1 as a therapeutic target in cancer[73,187]. Contrariwise, fewer studies have been performed to determine the involvement of this receptor in the process of tumor pathogenesis. The main NRP1-derived effect associated to angiogenesis induction was to promote an increased nutrient supply to tumor cells, hence, favoring cell proliferation and survival[188]. This tumor promoter activity of NRP1 was also described by another publication in which NRP1 knockdown in human hepatoma cell lines diminished tumor volume, reinforcing its potential function in tumor pathogenesis[180]. Nevertheless, there are still few studies published that clearly elucidate the suitability of NRP1 for its use as either tumor biomarker or therapeutic target in HCC.

At a molecular level, NRP1 has demonstrated to regulate key cancer processes, such as angiogenesis, invasion and cell proliferation, by interacting with several growth factor receptors and their corresponding ligands[73]. VEGFA has been described as one of the main ligands whose interaction with NRP1 is responsible for most of its modulatory actions through the induction of tumor angiogenesis and invasion, mainly by binding to the VEGFR2 receptor of tumor cells[70]. Aside from the correlation of NRP1 with invasion,

its interaction with VEGFA was evaluated by one of the included studies[76]. VEGFA binding to NRP1 showed to be crucial for the invasive abilities of HCC cells, since blockade of the interaction hindered vascular remodeling and HCC growth, supporting the interest of targeting NRP1 as a therapeutic strategy in HCC[76]. Another study performed with HCC patients decided to analyze NRP1 levels in the peritumoral tissue, observing that not only NRP1 but also VEGFR2 overexpression in this peritumoral tissue compared to tumor tissue correlated with lesser recurrence probability and increased OS[104]. Similar results were also described by another investigation, where augmented expression of NRP1 together with VEGF and VEGFR1/3 was significantly correlated with worse prognosis in CRC patients[189]. In this tumor type, the employment of a selective inhibitor of VEGFR1-3 known as tivozanib displayed antitumor effects similar to those observed with bevacizumab when combined with mFOLFOX6 in CRC patients[190]. Furthermore, classification of patients based on the NRP1 levels led to higher OS in the group classified as low NRP1 expression, reinforcing the key role of NRP1 and the growth factors VEGF-VEGFR in the prognosis of cancer patients as potential targets[190]. A strong correlation of NRP1 with VEGFR2 was also found in samples obtained from NSCLC patients, where overexpression of both receptors was identified[181]. These interesting findings, observed initially in clinical studies, have been also described in preclinical models[187,191]. By disrupting the interaction of NRP1 and VEGFR2, a significant reduction of tumor growth and angiogenesis was accomplished in an *in vivo* CRC model[191]. Likewise, blockade of NRP1 activity through treatment with a NRP1 antagonist restrained the increased migration of CRC cells that had lost sensitivity to sunitinib, a targeted drug against VEGFR[187]. Altogether, NRP1 seems to exert an important function in the regulation of the invasive abilities of HCC cells, closely related to the VEGF-VEGFR2-derived signaling, which emphasizes the potential use of NRP1 as a therapeutic target in human HCC.

7.1.3 Main limitations of the systematic review with meta-analysis

The systematic review with meta-analysis performed and included in the present PhD Thesis has been recently published[84], placing it as the first meta-analysis that evaluates the likely role of NRP1 in the prognosis, pathogenesis and associated clinical parameters in HCC patients. Despite the presence of heterogeneity and publication bias has been analyzed through several and different statistical tools, including subgroup analysis, meta-regression, Egger's test and funnel plot asymmetry, there were some major

limitations observed during the study performance. The exclusion of articles not written in English accounted for removal of two studies with full-text in Chinese language, which could partially explain the publication bias found in some analysis. In addition, etiology of HCC stands as a key factor in the molecular pathogenesis and tumor progression, which makes an important limitation the absence of complete information about the etiology of HCC patients provided by the included records. This limitation might condition the suitability of the interpretation of the results obtained in the present meta-analysis. In this line, some studies did not clarify the source of sample data used to analyze NRP1 expression. Moreover, NRP1 levels were differentially determined in the included studies, with articles measuring mRNA or protein levels of NRP1, which arouses the heterogeneity found among articles. The analysis in different tumor samples also supposes a critical limitation, since one investigation determined the serum expression of NRP1, whereas the other six articles analyzed NRP1 levels directly in the tumor tissue. In line with this, the criteria used for generating the "low" and "high" NRP1 groups were also different between the included records, increasing the uncertainty of the results obtained. Remarkably, even though a high number of patients was meta-analyzed, the limited number of studies included reduced the adequacy of the meta-regression analysis, since a higher number of articles, ten or more, should be considered to assess the heterogeneity sources. Although most data used for meta-analysis was directly reported, estimation of some of the data could increase the deviation of the pooled results from the overall effect size due to the error associated to these additional estimations. Finally, the most suitable analysis would have been conducted with all the included studies providing data for all the parameters analyzed, since only five were included for OS, four for tumor pathogenesis, and two for each clinicopathological feature.

7.1.4 Summary of main findings of the systematic review with meta-analysis

Overall, results from this meta-analysis revealed interesting results on the correlation of NRP1 overexpression with shorter prognosis, tumor development and a higher risk of venous invasion in HCC patients (**Figure 44**). In conclusion, NRP1 could be considered a potential biomarker as well as therapeutic target for preventing tumor progression and the associated malignant phenotype in HCC.

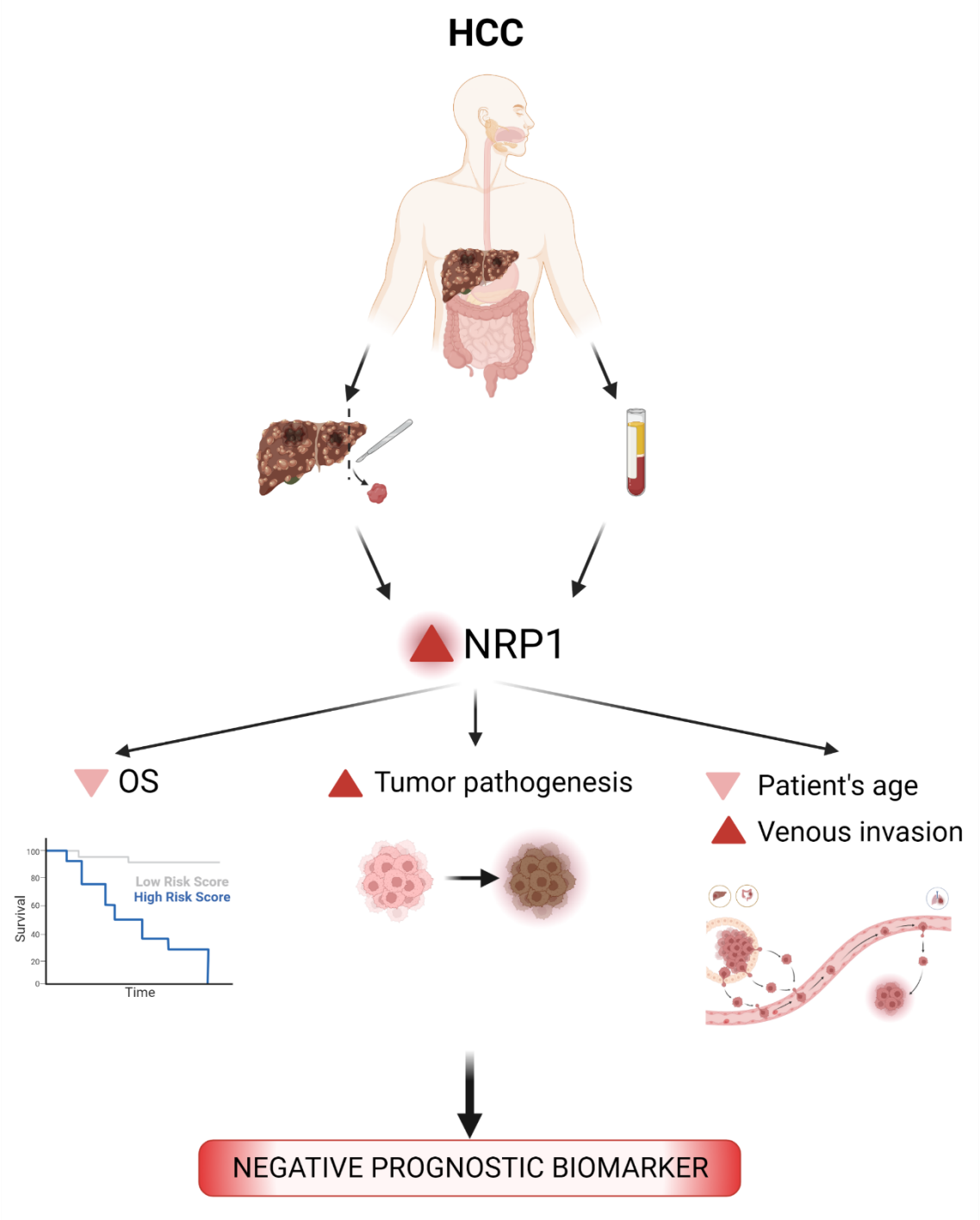

Figure 44. Graphical abstract of the findings from the meta-analysis. Summary of the main findings of the NRP1 role analyzed in the meta-analysis. Results obtained displayed a significant and strong association of increased levels of NRP1 with shorter OS, tumor pathogenesis, lower patient's age and higher risk of venous invasion in patients diagnosed with HCC, in which NRP1 expression was analyzed in either tumor tissue or serum samples.

7.2 AUTOPHAGY-DEPENDENT NRP1 DEGRADATION AND HYPOXIA RESPONSE ARE KEY MECHANISMS IN THE LOSS OF SENSITIVITY TO LENVATINIB IN HCC

The high incidence and mortality rates of HCC accounted for this primary liver tumor to become one of the main focus of interest in the cancer research field[8]. Despite recent progress achieved in the clinical onset of effective treatment options increasing patient's outcomes, the rates of recurrence and drug failure remain elevated and suppose an important challenge that needs to be addressed[11,164]. Most of these difficulties are derived from the complex and heterogeneous molecular pathogenesis of HCC, in which a broad number of signaling pathways and cellular processes are altered and, most important, are involved in the loss of drug efficacy and, hence, in the development of drug resistance[11,144,164]. In this way, autophagy has appealed for a crucial role associated to the double-edged function that exerts in cancer[42,164]. Although this process has proved to directly drive cellular response during carcinogenesis and drug treatment, the precise mechanisms underlying the derived effects on restraining or promoting tumor progression and therapeutic failure remain unclear[42,164]. As part of the tumor microenvironment, hypoxia conditions influence the ability of tumor cells to adapt to stress conditions with a modulatory role in HCC[123,164]. The transcription factor HIF-1α has been revealed as a crucial mediator of the cell response driven under hypoxia that mediates the acquisition of drug resistance by HCC cells, mainly to TKIs such as sorafenib and lenvatinib[42,123].

Considering this complex signaling and the novel interest arisen by NRP1 derived from the ability of this receptor to interact with multiple proteins with key roles in HCC progression and drug responsiveness[72,73], we decided to analyze *in vitro* the role of NRP1 in the susceptibility to lenvatinib by HCC cells and the underlying mechanisms involved.

7.2.1 Lenvatinib-derived NRP1 downregulation contributes to the antitumor effects of this targeted drug

NRP1 was initially found to be expressed in the cells of the central nervous system, with the function of axon guidance[70]. Nonetheless, posterior investigations observed that NRP1 was broadly expressed in multiple tissues and exerts diverse functions[70,73]. Remarkably, several studies have described an overexpression of NRP1 in the tumor tissues of different cancer types, such as HCC[70,78,79]. Similar findings were

obtained in the present study, in which increased levels of NRP1 were found in samples from HCC patients, as well as in two of the three HCC cell lines used for the experimental study. Moreover, a significant NRP1 overexpression was also observed in advanced stages and nodal metastasis status of HCC patients. Regarding lenvatinib activity, its antitumor properties have been described in preclinical models of HCC[36,39]; however, the role played by NRP1 in these antitumor actions have not been assessed by previous investigations.

For this reason, above indicated, we conducted an study in order to elucidate the involvement of this receptor in the lenvatinib effects on different HCC cell lines. Results showed that low doses of lenvatinib significantly decreased NRP1 protein expression and that the antitumor effects derived from lenvatinib are partially mediated by this NRP1 downregulation, which alters the inhibitory function of lenvatinib on cell proliferation and migration in our *in vitro* model. Even though the molecular implication of NRP1 has not been evaluated before, different studies have also identified proteins with a key role in the loss of lenvatinib effectiveness in HCC as potential molecular targets[47,54,192]. Specifically, A disintegrin-like and metalloprotease domain containing thrombospondin type 1 motif-like protein 5 (ADAMTSL5) promoted tumorigenesis *in vitro* and *in vivo*, and targeting this glycoprotein reduced the expression of several RTKs and, hence, increased susceptibility to lenvatinib, sorafenib and regorafenib[47]. Likewise, the use of oxysophocarpine was able to re-sensitize HCC cells with lenvatinib resistance to this TKI, inhibiting tumor growth by targeting FGFR1 and the derived AKT/mTOR signaling pathway[54]. The receptor FGFR1 was identified as the main responsible for the development of lenvatinib resistance in the Hep3B and HepG2 HCC cell lines, which could be overcome by oxysophocarpine co-administration with lenvatinib[54]. A recent study described an interesting role played by the mitochondria membrane protein stomatin-like protein 2, mitochondrial (STOML2) in the modulation of lenvatinib sensitivity[192]. Interestingly, results revealed that mitophagy induction derived from STOML2 led to a strong decrease in the cellular response to lenvatinib, together with higher tumor growth and cell migration[192], as observed in the present study with NRP1. Collectively, antitumor effects of lenvatinib observed in our *in vitro* HCC model seem to be directly associated to the downregulation of NRP1 protein levels.

7.2.2 Autophagy-dependent NRP1 degradation is involved in the modulation of the antitumor effects of lenvatinib in HCC cells

The double-edged process of autophagy has been the focus of interest in the cancer research field due to the crucial role autophagy seems to exert in the development, progression and resistance acquisition of cancer[166].

From results obtained in our study, autophagy proved to be the main mechanism involved in the NRP1 downregulation caused by lenvatinib. Moreover, autophagy modulation led to partial loss of lenvatinib sensitivity by HCC cells associated to the recovery of NRP1 levels after autophagy blockade. In this regard, contradictory findings have been reported in terms of autophagy with context-dependent effects on the cellular response to drug administration. In HCC, autophagy mediated the apoptosis of tumor hepatocytes and increased efficacy of lenvatinib[193]; whereas, excessive autophagy activation was associated to sorafenib resistance acquisition in a preclinical model of HCC[194]. Along with results obtained in this study, autophagy seems to be dually modulated by tumor hepatocytes, triggering an adaptive cellular response to the microenvironment and the treatment with molecular targeted drugs either promoting or inhibiting cell survival. Lenvatinib strongly decreased NRP1 expression through autophagy induction, and recovery of NRP1 protein levels by autophagy blockade decreased lenvatinib efficacy, which was prevented by gene targeting of NRP1. Similar to these results, administration of lenvatinib to Hep3B and Huh-7 cells was able to induce autophagy and drove cell death[39]. Gene silencing of the autophagy mediators ATG5 or Beclin 1 in liver cancer cells reduced the autophagy flux as well as the therapeutic effectiveness shown by the co-administration of lenvatinib and entinostat[39]. Likewise, a reduced autophagy was directly related to the development of sorafenib resistance derived from SREBP cleavage-activating protein (SCAP) in an *in vitro* HCC model[195]. Sensitivity to sorafenib of Huh-7 cells with acquired resistance to this drug was augmented after inducing autophagy with the inhibitors BEZ235[196] and AZD4547[197], showing even an increased migration of HCC cells without autophagy induction[196]. Contrariwise, a promoter role of autophagy on drug responsiveness has been also described in other HCC models, where osteopontin led to higher autophagy and, in consequence, to resistance acquisition against the chemotherapeutic agents epirubicin and cisplatin[198]. Similarly, DC661-derived targeting of autophagy, a palmitoyl-protein thioesterase 1 (PPT1) inhibitor, enhanced the sorafenib antitumor effects in Hep3B and Hep 1-6 cell lines[199].

Altogether, autophagy might act as a key mechanism potentially modulated by tumor hepatocytes to overcome the antitumor properties of molecular targeted drugs. In the present study, autophagy inhibition could be involved in the loss of lenvatinib efficacy by HCC cells, which seems to be mediated by NRP1.

Considering the potential development of a resistance mechanism to lenvatinib associated to the modulation of autophagy by HCC cells, we decided to evaluate the implication of NRP1 through combination of NRP1 targeting and autophagy blockade. Findings obtained exhibited a key role of NRP1, whose silencing prevented the loss of lenvatinib sensitivity caused by autophagy disruption. These antitumor effects associated to NRP1 knockdown were also obtained in two different models of HCC, where tumor hepatocytes exhibited lower proliferation and migration abilities after NRP1 targeting[85,96]. Furthermore, tumor volume and vasculature were significantly diminished with lower levels of NRP1 in a mouse model of HCC[96]. Studies conducted in other tumor types also described a NRP1-dependent mechanism of drug failure. Two *in vitro* investigations that employed CRC cell lines with and without sunitinib adaptation, displayed a switch from VEGFR to NRP1/cMET-derived signaling for accounting the treatment failure and migration induction[191,200]. The use of NRP1 as a molecular target led to reduced cell migration and the disruption of the sunitinib evasion mechanism[191,200]. Despite the interesting effects associated to NRP1 in HCC and the key role played by autophagy in resistance development[42,70], there are no studies in which the role of the autophagy-NRP1 interplay in the modulation of lenvatinib efficacy, or other targeted drugs, has been assessed. Only one study reported autophagy as the mechanism responsible for NRP1 degradation under starvation conditions[201].

Collectively, NRP1 could be a key mediator of the increased cell survival and migration of HCC cells used in this study, revealing the autophagy-derived NRP1 degradation as a key mechanism in the promotion of lenvatinib failure in our *in vitro* model of HCC.

7.2.3 HIF-1α-associated response to hypoxia could contribute to the loss of lenvatinib efficacy by modulating the autophagy-NRP1 interplay in HCC cells

Among the broad number of mechanisms involved in the resistance acquisition to molecular targeted drugs such as lenvatinib, the hypoxic microenvironment has shown to exert a crucial modulation[42,123,138]. The derived effects from inducing a cellular hypoxic

response in the previous described mechanism were evaluated in our *in vitro* model of HCC by using $CoCl_2$ as a chemical hypoximimetic. Interestingly, under hypoxia the protein levels of NRP1 experienced a significant decrease, which was also mediated by an autophagy induction and, therefore, NRP1 degradation. Although this direct association of hypoxia conditions with NRP1 levels have not been assessed in other HCC models, a significant correlation between the presence of peritumoral hypoxia and peritumoral NRP1 expression was observed in HCC patients[104]. In opposite, autophagy-dependent modulation of NRP1 was differentially influenced by hypoxia induction in other tumors[201–204]. In parallel to results obtained in our study, NRP1 expression was found diminished under hypoxia conditions through autophagy in tumor cells from breast and prostate carcinomas[201]. However, higher levels of NRP1 were observed after hypoxia induction in lung adenocarcinoma[203], oral squamous cell carcinoma[204] and cervical cancer[202].

Moreover, the hypoxia-derived response proved to have a relevant function in the development of drug resistance, mainly to sorafenib[42,123], but studies evaluating the alterations in the lenvatinib efficacy derived from hypoxia are scarce. In a recently published study from our group, hypoxia induction through a HIF-1α-driven response was closely linked to the sorafenib resistance phenotype of HCC cells[124]. Results obtained from another investigation showed that in both *in vitro* and *in vivo* models of HCC, hypoxia induction contributed to the loss of lenvatinib sensitivity associated to STOML2 overexpression[192]. A lower susceptibility to lenvatinib was also identified in the HCC cell line PLC/PRF/5 under hypoxic conditions[205]. This liver tumor line displayed a higher IC_{50} and a resistance phenotype to lenvatinib when induced hypoxia, mainly linked to alterations in the ECM[205]. A recent research published this year also found that a hypoxic microenvironment increased the expression of ubiquitin specific peptidase 2 antisense RNA 1 (USP2-AS1) and this led to lenvatinib failure mediated by HIF-1α[206]. Along with this, the obtained results evidence the potential role played by hypoxia as part of the tumor microenvironment in the cellular sensitivity to lenvatinib, mainly through the likely promotion of resistance acquisition.

As previously mentioned, HIF-1α is one of the main drivers of the hypoxia response and has been closely linked to the resistance development by cells of mainly solid tumors[124,144,167]. Considering this and previous evidence, we decided to analyze the likely modulation exerted by HIF-1α under hypoxia on NRP1 and the autophagy-

associated mechanism of lenvatinib failure. Findings showed a strong and significant positive correlation between NRP1 and HIF-1α in human HCC samples and a direct modulation of NRP1 levels by this transcription factor. Even though studies evaluating the underlying mechanisms of the NRP1-HIF-1α interplay have not been conducted in HCC, a research performed with human samples of lung adenocarcinoma also observed a significant gene correlation between them[203]. Additionally, NRP1 showed to be a target gene of HIF-1α in lung adenocarcinoma cells, through which HIF-1α endorsed vasculogenic mimicry and tumor cell metastasis[203]. In low Gleason grade cancers, HIF-1α also modulated NRP1, specifically the VEGFA/NRP1 axis, inducing EMT of tumor cells[207], reinforcing the potential association of NRP1 with HIF-1α.

Autophagy together with hypoxia have demonstrated to highly contribute to drug failure and resistance development in cancer and mainly in HCC[165,208]. For this reason, we decided to determine the interplay between autophagy and the HIF-1α-related hypoxia response and the modulation exerted in the loss of lenvatinib efficacy associated to NRP1. Curiously, transient knockdown of HIF-1α prompted lower NRP1 levels and decreased cell viability, being able to keep these inhibitory effects even during autophagy disruption and with or without hypoxia induction and/or lenvatinib treatment. Therefore, HIF-1α silencing achieved to prevent the recovery of cell viability observed after autophagy blockade in presence of lenvatinib and hypoxia conditions, increasing the cell susceptibility to lenvatinib and preventing a hypoxia-associated mechanism of adaptation to this targeted drug. A previous investigation employing a diethylnitrosamine (DEN)-induced HCC model reported a key role of beta-2-adrenergic receptor (ADRB2) in autophagy disruption, leading to hepatocarcinogenesis and resistance acquisition to sorafenib through a mechanism of HIF-1α stabilization[209]. Similar findings supporting the close relationship between autophagy and HIF-1α were described in HCC patients, where higher HIF-1α levels correlated with reduced expression of Beclin 1 and with tumor progression of HCC[168]. In the present study, results suggested that HCC cells could modulate the autophagy process in order to promote lenvatinib failure through a NRP1-mediated mechanism. In this line, a recent study described a shift in the autophagy process caused by prolonged administration of sorafenib in HCC cells[210]. Moreover, under hypoxia conditions, autophagy was responsible for the cellular adaptation to this low oxygen microenvironment, allowing cell survival and tumor progression of HCC[211]. As part of the hypoxia response, N6-methyladenosine (METTL3) was diminished and HCC

cells developed a sorafenib resistance phenotype, associated to autophagy induction with *in vitro* and *in vivo* models of HCC[212]. Overall, these findings denote the interesting potential of both NRP1 and HIF-1α as molecular targets in order to prevent the autophagy modulation associated to a hypoxic response for improving lenvatinib effectiveness in HCC.

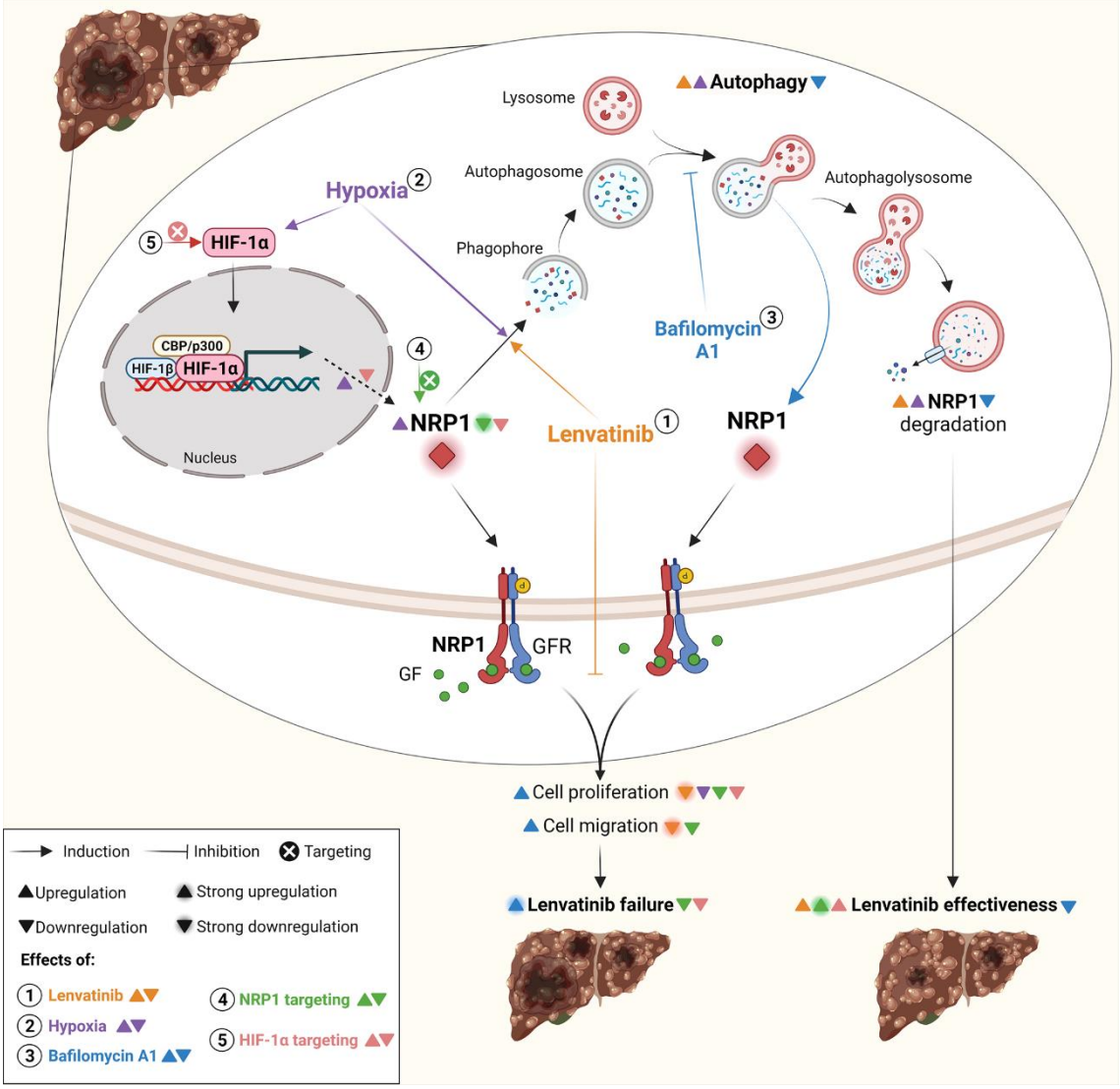

Figure 45. Graphical representation of the main findings that underlies the molecular mechanisms involved in the lenvatinib *in vitro* effects in HCC. Schematic summary of the experimental findings, where: (1) **lenvatinib** administration triggered an autophagy-dependent degradation of NRP1 along with lower cell migration and proliferation abilities. (2) Induction of an *in vitro* **hypoxia** response also induced autophagy and increased NRP1 degradation, while HIF-1α promotes NRP1 expression, with inhibitory effects on cell proliferation and migration. (3) In all cases, **autophagy disruption** by Baf led to slightly increase cell survival and reduce lenvatinib sensitivity in HCC cells. By both (4) **NRP1** and (5) **HIF-1α** targeting, the derived effects from inhibiting autophagy and increasing NRP1 protein levels were prevented, improving the antitumor activity of lenvatinib regardless of the autophagy flux. Created with BioRender.com.

In summary, results obtained from our study allow to obtain a clearer understanding of the molecular mechanisms associated to the cellular response that drives the loss of lenvatinib efficacy in HCC cells summarized in **Figure 45**. NRP1 seems to have a crucial role in the antitumor effects of lenvatinib, with autophagy as the main mechanism modulating NRP1 expression and, therefore, the cellular response to lenvatinib. The hypoxia response driven by HIF-1α also showed to dually regulate NRP1 expression and favor lenvatinib failure in the treatment of HCC cells, thus, being involved in the cellular response mediated by autophagy. Altogether, molecular targeting of NRP1 could improve lenvatinib effectiveness by preventing the development of an autophagy-mediated resistance to lenvatinib, standing as a potential therapeutic target in advanced HCC.

8 Conclusions

Considering the main findings obtained and discussed in this study, we can detail the following conclusions that correspond to the specific objectives previously stated:

1. Increased expression of NRP1 is significantly associated to a shorter OS in patients with HCC.
2. NRP1 overexpression correlates with tumor development in HCC patients, reinforcing the interesting role of NRP1 as a tumor biomarker in HCC.
3. Higher NRP1 levels are strongly associated to lower patient's age and to increased risk of venous invasion in patients diagnosed with HCC, placing NRP1 as a potential molecular target to prevent these tumor-associated characteristics.
4. NRP1 is overexpressed in both tissue HCC samples and the Hep3B and Huh-7 cell lines, with a strong correlation with advanced tumor stages and nodal metastasis status, displaying an interesting role played by NRP1 in HCC.
5. Lenvatinib exerts strong antitumor effects in the three HCC cell lines HepG2, Hep3B and Huh-7, with Hep3B and Huh-7 as the most susceptible lines, and NRP1 is involved in the antitumor effects of lenvatinib.
6. Autophagy induction by lenvatinib seems to be the main mechanism responsible for the downregulation of NRP1 levels derived from this targeted drug.
7. Antitumor effects of lenvatinib in cell proliferation and migration are partially disrupted after autophagy blockade and restoration of NRP1 levels in Hep3B and Huh-7 cells, which could be prevented by NRP1 targeting.
8. Induction of a hypoxia response in the Hep3B and Huh-7 cell lines triggers NRP1 downregulation through an autophagy-mediated degradation process.
9. HIF-1α directly modulates NRP1 expression under hypoxia, where autophagy inhibition increases cell survival after hypoxia induction and lenvatinib administration; whereas HIF-1α targeting prevents the recovery of NRP1 protein levels and the loss of cell sensitivity to lenvatinib in the Hep3B and Huh-7 HCC cell lines.

General conclusion

Overall, NRP1 potentially represents a novel biomarker with potential use for diagnosis and prognosis in HCC patients, as well as with a relevant role in the likely therapeutic failure of lenvatinib in HCC. NRP1 overexpression showed a reliable utility as a diagnostic and prognostic biomarker, which could benefit the clinical onset of HCC patients. Moreover, through an autophagy-associated mechanism, NRP1 might play a key role in the lenvatinib antitumor actions *in vitro*, where autophagy modulation by tumor hepatocytes could trigger NRP1 expression recovery and lenvatinib failure. A HIF-1α-related hypoxia response also showed to directly drive the autophagy-dependent NRP1 degradation and, in consequence, modulate the cellular sensitivity to lenvatinib. In conclusion, not only NRP1 but also HIF-1α could represent valuable molecular targets for improving therapeutic efficacy of lenvatinib in the treatment landscape of advanced HCC, through the prevention of an autophagy-associated mechanism of drug resistance potentially driven by a hypoxia response.

Tesis Doctoral

Estudio del papel de la neuropilina-1 en el desarrollo, pronóstico y la respuesta celular a lenvatinib en el carcinoma hepatocelular humano

Paula Fernández Palanca

Programa de Doctorado en Biomedicina y Ciencias de la Salud

Tutor: Dr. José Luis Mauriz Gutiérrez
Directores: Dr. Javier González Gallego y Dr. José Luis Mauriz Gutiérrez

Departamento de Ciencias Biomédicas
Instituto de Biomedicina (IBIOMED), Universidad de León

León, 2023

9 Resumen en español

La presente Tesis Doctoral se ha llevado a cabo en el Instituto de Biomedicina (IBIOMED) de la Universidad de León. A continuación, se describe de manera resumida el desarrollo de esta Tesis Doctoral en español.

Introducción

Según el último estudio global realizado en el 2020, el cáncer de hígado representa el sexto tipo de tumor más frecuente y la tercera causa de muerte por cáncer a nivel mundial. Se han descrito diferentes tipos de tumores hepáticos, siendo el principal el **carcinoma hepatocelular (HCC)** al representar el 75%-85% de los casos de cáncer de hígado. El HCC destaca por una compleja heterogeneidad molecular que está estrechamente asociada a la elevada variedad de agentes etiológicos que pueden desencadenar el proceso de hepatocarcinogénesis. Asimismo, este tipo de tumor hepático es principalmente diagnosticado en estadios avanzados debido a la dificultad de una detección temprana por la ausencia de síntomas en etapas iniciales y por la difícil distinción entre un estado cirrótico y uno tumoral. En estadios tempranos se pueden llevar a cabo terapias curativas, entre las que se incluyen desde una resección parcial del hígado hasta el trasplante hepático. Sin embargo, la mayoría de los pacientes son diagnosticados en etapas avanzadas, donde sólo están disponibles tratamientos paliativos, principalmente fármacos dirigidos. En la actualidad, la terapia sistémica se mantiene como la única opción terapéutica frente al HCC avanzado, permitiendo un incremento en la supervivencia entre 1 y 2 años, y está constituida por dos grupos de fármacos: inhibidores tirosín quinasa (TKIs) y anticuerpos monoclonales. Aunque se ha producido un avance en el desarrollo de fármacos cada vez más eficaces, siguen siendo necesarias más investigaciones que permitan mejorar el pronóstico y supervivencia de los pacientes con HCC avanzado.

Los fármacos TKI constituyen una pieza clave en la terapia sistémica frente a este tumor hepático, donde el sorafenib se ha mantenido como el único agente disponible para el tratamiento del HCC avanzado durante una década, hasta la aprobación del **lenvatinib** en el 2018. Este TKI, lenvatinib, estableció las bases para una nueva estrategia de tratamiento al convertirse en la única alternativa en el tratamiento de primera línea frente al HCC avanzado. No obstante, como se observó con el sorafenib, las células tumorales hepáticas son capaces de desarrollar mecanismos de adaptación al tratamiento con estos fármacos, dando lugar a la aparición de resistencias. Aunque desde la aprobación del

sorafenib en el 2008 se han llevado a cabo múltiples estudios donde se analizan los mecanismos implicados en el desarrollo de resistencia, aún se desconocen por completo qué procesos o vías de señalización celular participan en ella.

Como consecuencia de los distintos estudios realizados en este ámbito, se ha identificado la **neuropilina-1 (NRP1)** como una molécula importante en diversos tumores. NRP1 es una glicoproteína transmembrana perteneciente a la familia de las neuropilinas (NRPs) que se encuentra principalmente localizada en las membranas plasmáticas de numerosos tipos celulares, incluyendo los hepatocitos. Actúa como correceptor de numerosas proteínas con un papel fundamental en la supervivencia de las células tumorales e interacciona con factores de crecimiento y sus correspondientes receptores, destacando su afinidad por el factor de crecimiento del endotelio vascular (VEGF) y su receptor VEGFR. Por esta razón, investigaciones recientes se han centrado en el estudio de NRP1 y su función en distintas etapas, comprendiendo desde la hepatocarcinogénesis hasta la modulación de la respuesta a fármacos. Principalmente se ha descrito que actúa promoviendo la angiogénesis y la migración de las células tumorales hepáticas, sin embargo, un número creciente de estudios ha observado una implicación interesante de NRP1 en distintos procesos celulares, destacando su potencial interés en el estudio del HCC.

Múltiples procesos celulares interaccionan y participan en el desarrollo y progresión tumoral del HCC. Dentro de los mismos, la **autofagia** ha destacado por su papel dual al ser capaz de promover e inhibir la supervivencia de las células, actuando como inductor o supresor tumoral, dependiendo del contexto y el estadio del tumor. La autofagia se define como un proceso de autodegradación que, en condiciones fisiológicas, se encarga de mantener la homeostasis celular eliminando proteínas y orgánulos dañados. No obstante, su papel bajo condiciones patológicas es modulado de manera diferente, participando de las distintas respuestas celulares al estrés, bien favoreciendo o bien impidiendo la progresión tumoral del HCC. Asimismo, la autofagia es capaz de regular la respuesta celular a fármacos, donde se ha descrito un papel importante como uno de los mecanismos responsables de la pérdida de eficacia farmacológica por los hepatocitos tumorales. Sin embargo, a pesar de los diferentes estudios y funciones asociadas a este proceso, aún no se ha elucidado con exactitud el papel que juega la autofagia en el HCC humano.

Por otro lado, el microambiente tumoral destaca por ser uno de los componentes claves en la progresión del tumor, principalmente en los tumores sólidos como el HCC. Este tipo de tumores están caracterizados por presentar un núcleo hipóxico donde la disponibilidad de oxígeno y nutrientes es limitada, debido a la excesiva proliferación celular y una demanda de oxígeno muy superior al suministro. Bajo esta **hipoxia intratumoral**, los factores inducibles por hipoxia (HIFs) se encargan de dirigir la respuesta de adaptación celular, siendo **HIF-1α** el principal factor de transcripción implicado en la respuesta a hipoxia. La inducción de una respuesta a hipoxia mediada por HIF-1α ha sido estrechamente relacionada con una mayor capacidad de supervivencia, proliferación, angiogénesis, migración e invasión por parte de las células de HCC, promoviendo una mayor agresividad tumoral. Igualmente, este factor de transcripción también ha mostrado un papel importante en la respuesta adaptativa de las células al tratamiento prolongado con fármacos dirigidos, principalmente al sorafenib, desencadenando el desarrollo de resistencia y, por lo tanto, el fracaso terapéutico.

En resumen, el HCC humano se mantiene como un problema y un reto global, donde múltiples procesos y señalizaciones participan en el desarrollo y progresión tumoral, así como en la aparición de resistencia a fármacos. A pesar de los recientes avances alcanzados, son necesarios más estudios que permitan esclarecer los mecanismos exactos subyacentes a la complejidad del HCC, con el fin de identificar biomarcadores útiles y potenciales dianas terapéuticas para mejorar el pronóstico y supervivencia de los pacientes con HCC avanzado.

Objetivos

Por todo ello, el **objetivo** de la presente Tesis Doctoral fue esclarecer el potencial papel de NRP1 como biomarcador para el pronóstico, diagnóstico y otros parámetros asociados al tumor en pacientes con HCC, así como determinar los mecanismos subyacentes a los efectos antitumorales y la potencial pérdida de eficacia del lenvatinib en un modelo *in vitro* de HCC humano.

Para llevar a cabo este objetivo, se plantearon los siguientes **objetivos específicos**:

1. Identificar la potencial correlación entre niveles elevados de NRP1 y un peor pronóstico mediante el metaanálisis de datos disponibles de pacientes con HCC.
2. Determinar la posible asociación de la sobreexpresión de NRP1 con el desarrollo de HCC a través del metaanálisis de los datos procedentes de muestras de HCC y su correspondiente tejido no tumoral adyacente.
3. Evaluar la correlación clínica de NRP1 con diferentes características clinicopatológicas en muestras de pacientes con HCC.
4. Caracterizar la expresión de NRP1 en muestras de HCC humano obtenidas de bases de datos públicas y en diferentes líneas celulares de HCC humano.
5. Evaluar las propiedades antitumorales del lenvatinib *in vitro* y la posible implicación de NRP1 en los efectos inhibitorios del lenvatinib sobre la proliferación y migración celular.
6. Identificar los mecanismos celulares responsables de la disminución en la expresión de NRP1 causada por el lenvatinib en las líneas de HCC humano Hep3B y Huh-7.
7. Analizar la potencial participación de la degradación de NRP1 mediada por autofagia en los efectos antitumorales del lenvatinib en las células de HCC.
8. Investigar los efectos derivados de la inducción de hipoxia *in vitro* en la expresión de NRP1 y el posible papel de la autofagia en las líneas celulares de HCC humano Hep3B y Huh-7.
9. Determinar la implicación de la respuesta a hipoxia dirigida por HIF-1α en la eficacia terapéutica del lenvatinib mediada por la modulación de NRP1 dependiente de autofagia en las líneas Hep3B y Huh-7 de HCC humano.

Materiales y métodos

Inicialmente se llevó a cabo una **revisión sistemática con metaanálisis** con el fin de evaluar el potencial valor pronóstico y diagnóstico de NRP1, así como su correlación con distintos parámetros clinicopatológicos en pacientes con HCC. Para ello, se realizó una búsqueda exhaustiva de la literatura en cinco bases de datos: PubMed, Scopus, Web Of Science (WOS), Embase y Cochrane Library, incluyendo los estudios publicados hasta el 31 de mayo de 2022. El protocolo completo se encuentra registrado en PROSPERO (CRD42022307062), y se realizó siguiendo las normas PRISMA.

La selección de los artículos se realizó utilizando los siguientes criterios de inclusión: (1) estudios que utilicen pacientes diagnosticados con HCC; (2) estudios donde se evalúe la expresión de NRP1 en el tejido tumoral o muestras derivadas del tumor; (3) estudios donde se proporcionen o se puedan extraer datos sobre la asociación de los niveles de NRP1 con parámetros de supervivencia y/u otros parámetros clinicopatológicos; (4) estudios que estén escritos en inglés. Por otro lado, como criterios de exclusión se emplearon: (1) estudios realizados sólo en modelos preclínicos; (2) revisiones de la literatura, capítulos de libro, comunicaciones a congresos o similares; (3) artículos donde no se proporcionen datos o no se puedan extraer; (4) artículos no disponibles en inglés.

Todos los datos posibles se extrajeron y se analizó la calidad de los estudios mediante la escala *Newcastle-Ottawa* (NOS), que permite dar una puntuación de 0 a 9. Aquellos artículos con una calidad baja o puntuación NOS inferior a 5, fueron excluidos del metaanálisis, incluyendo sólo aquellos con una puntuación de 5 o superior. Asimismo, toda la información y los datos proporcionados por los artículos se extrajo y organizó en tablas.

El análisis estadístico se llevó a cabo con el software STATA 16. Se determinó la correlación entre la sobreexpresión de NRP1 y la supervivencia global (OS) como cociente de riesgo o *Hazard ratio* (HR), con un intervalo de confianza (CI) del 95%. Se empleó el método Parmar para estimar los HR no proporcionados directamente en el artículo. Además, la posible asociación de NRP1 con el desarrollo de HCC y otros parámetros clínicos asociados al tumor se determinó como relación de probabilidades u *odds ratio* (OR) con el 95% CI. Se consideraron diferencias significativas cuando $p<0,05$. Igualmente, se evaluó la presencia de heterogeneidad mediante la prueba Q basada en

chi-cuadrado y mediante el estadístico I^2. En presencia de una heterogeneidad significativa ($p(Q)<0,10$ y/o $I^2 \geq 50\%$) se evaluaron las posibles causas mediante meta-regresión y análisis de subgrupos.

Por último, se analizó la presencia de sesgo de publicación mediante la prueba de Egger, así como el estudio de la asimetría en los diagramas de embudo o *funnel plots*. Cuando se identificó un sesgo significativo ($p<0,05$) se llevó a cabo el método *trim-and-fill*, que permite estimar un efecto global corregido en base a los potenciales estudios omitidos en el metaanálisis.

Por otro lado, se llevó a cabo un **estudio experimental** para analizar el potencial papel de NRP1 en la respuesta celular y pérdida de eficacia del lenvatinib en HCC avanzado. Para ello se emplearon, por un lado, datos procedentes de muestras de pacientes con HCC obtenidos de distintas bases de datos públicas, y, por otro lado, tres líneas de HCC humano, HepG2, Hep3B y Huh-7, para analizar *in vitro* el papel de NRP1.

Las células fueron sometidas a distintos tratamientos, utilizando el fármaco lenvatinib; el antagonista de NRP1 EG00229; tres inhibidores específicos de la síntesis proteica, de la degradación por el proteasoma y de la autofagia: cicloheximida (CHX), MG132 y bafilomicina A1 (Baf), respectivamente; y el $CoCl_2$ como inductor químico de una hipoxia celular.

Como parte del estudio experimental, se llevó a cabo el silenciamiento génico específico de NRP1 y, posteriormente, del factor HIF-1α. El silenciamiento se mantuvo durante 48 h, sometiendo las células a los respectivos tratamientos las últimas 24 h, y realizando los ensayos tras las 48 h totales.

La viabilidad celular se analizó utilizando dos ensayos que permiten obtener una medición de la cantidad de células viables en un tiempo determinado. Se emplearon el ensayo comercial de luminiscencia CellTiter-Glo®, así como el ensayo de viabilidad basado en el bromuro de 3-(4,5-dimetiltiazol-2-il)-2,5-difenil-tetrazolio (MTT). Asimismo, se evaluó la capacidad de formación de colonias de las distintas líneas celulares de HCC mediante la medición del número de colonias que son capaces de formar en distintas condiciones experimentales tras siete días.

El análisis de expresión de distintas dianas moleculares se llevó a cabo tanto a nivel de ARN mensajero (mRNA), como a nivel de proteína. Por un lado, se realizó la

reacción en cadena de la polimerasa con transcripción reversa en tiempo real (qRT-PCR) para determinar los niveles de mRNA de los distintos genes analizados. Mientras que, la expresión proteica se analizó mediante la técnica de western blot y mediante inmunofluorescencia con microscopía de láser confocal.

La migración celular se evaluó mediante el ensayo de cierre de herida o *wound-healing*. Para ello, se monitorizó la capacidad de migración de las distintas líneas celulares mediante la realización de una grieta o "herida" en la monocapa de células adheridas a la superficie de cultivo y la consecuente monitorización de la migración de las células sobre el área de dicha "herida".

De otra manera, se analizó el proceso de autofagia a través de la medición del contenido en autofagolisosomas mediante la tinción con naranja de acridina. Este compuesto permite marcar las células y proporcionar un viraje en la tinción en aquellos compartimentos ácidos, como los autofagolisosomas, permitiendo obtener una medida proporcional al contenido en estas vesículas autofágicas en las células.

Finalmente, se llevó a cabo el análisis estadístico de los datos obtenidos en los correspondientes ensayos. Para aquellos datos obtenidos de las bases de datos públicas, se obtuvieron los valores *p* directamente de dichas plataformas, excepto en el análisis de la expresión diferencial de NRP1 con el conjunto de datos GSE14520, donde se empleó el software GraphPad Prism 8. Los datos obtenidos del estudio experimental fueron sometidos a distintos análisis estadísticos, incluyendo la prueba T no pareada y el análisis ANOVA de una vía y de dos vías. Tras las pruebas ANOVA se llevaron a cabo pruebas post-hoc de Tukey, Dunnett o Sidak para identificar aquellos grupos significativos. En todos los casos se consideraron diferencias significativas cuando $p<0,05$.

Resultados y discusión

Inicialmente, se incluyó información de 1305 pacientes obtenida de los siete artículos incluidos en la **revisión sistemática con metaanálisis**. Todos los estudios cumplieron los criterios de calidad previamente establecidos. Del total, el 53,81% de los pacientes mostraron una sobreexpresión de NRP1, y de los siete artículos incluidos, cinco mostraron datos de supervivencia u OS, cuatro proporcionaron datos sobre el diagnóstico y sólo dos presentaron información sobre distintos parámetros clinicopatológicos.

Tras el metaanálisis, los resultados obtenidos mostraron una correlación significativa entre la sobreexpresión de NRP1 y una menor OS en pacientes diagnosticados con HCC. Además, unos niveles incrementados de esta proteína también se encontraron significativamente asociados con el desarrollo tumoral del HCC, al mostrar una mayor correlación con muestras de tejido tumoral en comparación con sus correspondientes muestras de tejido sano adyacente. En relación a los distintos parámetros clinicopatológicos analizados, NRP1 exhibió una estrecha asociación con una edad inferior a 50 años en pacientes con HCC, así como con un mayor riesgo de sufrir invasión venosa por las células tumorales. No se encontraron resultados significativos con el resto de los parámetros evaluados, siendo estos el género, el tamaño del tumor, y la presencia de metástasis.

Con el fin de evaluar las posibles fuentes de heterogeneidad entre artículos en los distintos análisis estadísticos realizados, se llevó a cabo una meta-regresión y un análisis de subgrupos para aquellos con heterogeneidad significativa. Por lo tanto, se sometieron a dichos análisis la asociación de mayores niveles de NRP1 con OS y el desarrollo tumoral, no observando una heterogeneidad significativa para el resto de los parámetros. Los resultados obtenidos por ambos métodos mostraron que tanto el tamaño de la muestra utilizada por cada artículo, como la calidad establecida por la puntuación NOS podrían explicar la elevada heterogeneidad observada en los resultados del metaanálisis.

Por último, el análisis de la presencia de sesgo de publicación denotó un marcado sesgo en la asociación de sobreexpresión de NRP1 con OS y el desarrollo del tumor, al igual que lo observado en la evaluación de la heterogeneidad. En ambos parámetros, el método *trim-and-fill* estimó la presencia de un estudio que, al ser imputado, disminuyó el efecto global obtenido tras el metaanálisis para así disminuir el sesgo entre publicaciones.

Estudios llevados a cabo en modelos tanto de HCC como de otros tipos de tumores sólidos también mostraron resultados similares, aunque no se ha analizado previamente el papel de NRP1 mediante metaanálisis de datos. Los resultados aquí presentados sugieren que NRP1 parece tener una potencial utilidad como biomarcador pronóstico y diagnóstico, y presenta hallazgos interesantes en el empleo de NRP1 como posible diana terapéutica en el HCC. Sin embargo, aún son necesarios más estudios que corroboren estos resultados y permitan avanzar en el estudio de NRP1 en el HCC.

Para continuar con el estudio del papel de NRP1 en el HCC humano, llevamos a cabo un **estudio experimental** donde analizamos su expresión en muestras de pacientes directamente obtenidas y analizadas en bases de datos públicas. Estos análisis mostraron una asociación estadísticamente significativa entre NRP1 y estadios tumorales y de metástasis nodular avanzados. Asimismo, NRP1 se encontró sobreexpresada, no sólo en muestras de tejido tumoral de pacientes con HCC, sino también en las dos líneas de HCC humano Hep3B y Huh-7. Estas dos líneas celulares mostraron a su vez la mayor sensibilidad al fármaco lenvatinib *in vitro*. Por este motivo, se continuó el estudio utilizando estas dos líneas de HCC, descartando el empleo de la línea HepG2.

Los resultados observados tras el análisis de la proliferación y migración celular en las distintas líneas tratadas con lenvatinib y el antagonista de NRP1 EG00229 sugirieron que esta proteína, NRP1, parece estar implicada en los efectos antitumorales del lenvatinib. Tras el estudio del posible papel de la modulación de la síntesis proteica, o la degradación por proteasoma o por autofagia, se obtuvo que la autofagia parece ser la principal responsable de la disminución de la expresión de NRP1 tras el tratamiento con lenvatinib en las células Hep3B y Huh-7. Curiosamente, el bloqueo selectivo de la autofagia mediante el uso de Baf, y el consecuente incremento en los niveles de NRP1, redujo los efectos inhibitorios derivados del lenvatinib sobre la proliferación y migración celular. Sin embargo, esta pérdida en la sensibilidad del lenvatinib fue obstaculizada tras el silenciamiento génico de NRP1.

Por otro lado, se evaluó el potencial papel desempeñado por una respuesta celular a hipoxia a través del factor de transcripción HIF-1α en el mecanismo asociado a NRP1 anteriormente descrito. En primer lugar, tras la inducción de una respuesta a hipoxia con $CoCl_2$ se observó que los niveles de NRP1 disminuían significativamente. Al igual que lo descrito tras el tratamiento con lenvatinib, la menor expresión de NRP1 fue asociada a

un incremento en la autofagia basal de las células Hep3B y Huh-7. Sin embargo, bajo condiciones de hipoxia, se observó una modulación dual de NRP1, ya que su expresión disminuyó significativamente tras el silenciamiento del factor HIF-1α. En este caso, aunque el bloqueo de la autofagia también redujo la eficacia del lenvatinib incluso en hipoxia, el silenciamiento de HIF-1α consiguió impedir tanto la recuperación de los niveles de NRP1 como la pérdida de sensibilidad a lenvatinib por las líneas de HCC humano Hep3B y Huh-7.

A pesar de la ausencia de estudios que evalúen el interesante papel de NRP1 en los mecanismos asociados a la eficacia antitumoral del lenvatinib en HCC, otras investigaciones han descrito la potencial función de esta proteína como promotor tumoral en distintos tipos de cáncer. Asimismo, un número cada vez mayor de trabajos señalan tanto la autofagia como la respuesta a hipoxia como procesos clave en la supervivencia y adaptación de las células tumorales al tratamiento con distintos fármacos. En conjunto, estos resultados proporcionan un mayor conocimiento sobre los mecanismos implicados en la respuesta celular al lenvatinib y la pérdida de eficacia de éste, destacando el papel de NRP1 como potencial diana terapéutica frente al HCC avanzado, con el fin de evitar el desarrollo de resistencia a lenvatinib mediada por la autofagia y una respuesta a hipoxia.

Conclusiones

Teniendo en cuenta los resultados expuestos y discutidos en la presente Tesis Doctoral, podemos exponer las siguientes **conclusiones** correspondientes a los objetivos específicos previamente establecidos:

1. La expresión elevada de NRP1 está significativamente asociada con una menor OS en pacientes con HCC.
2. La sobreexpresión de NRP1 correlaciona con el desarrollo tumoral en pacientes con HCC, reforzando el interesante papel de NRP1 como biomarcador tumoral en el HCC.
3. Niveles incrementados de NRP1 están estrechamente asociados con una menor edad y un mayor riesgo de invasión en pacientes diagnosticados con HCC, posicionando a NRP1 como una potencial diana molecular para evitar estas características asociadas al tumor.
4. NRP1 está sobreexpresada tanto en muestras de tejido de HCC como en las líneas Hep3B y Huh-7, con una fuerte correlación con estadios tumorales y de metástasis a nódulos avanzados, mostrando un papel interesante de NRP1 en el HCC.
5. El lenvatinib ejerce fuertes efectos antitumorales en las tres líneas de HCC HepG2, Hep3B y Huh-7, siendo las líneas Hep3B y Huh-7 las más susceptibles, y NRP1 está implicada en los efectos antitumorales del lenvatinib.
6. La inducción de la autofagia por el lenvatinib parece ser el mecanismo responsable de la disminución de los niveles de NRP1 derivados de dicho fármaco.
7. Los efectos antitumorales del lenvatinib sobre la proliferación y migración celular son parcialmente bloqueados tras la inhibición de la autofagia y la recuperación de los niveles de NRP1 en las líneas celulares Hep3B y Huh-7, lo que puede ser evitado mediante el silenciamiento génico de NRP1.
8. La inducción de una respuesta a hipoxia en las líneas Hep3B y Huh-7 promueve el descenso de la expresión de NRP1 a través de un proceso de degradación mediado por autofagia.
9. HIF-1α modula directamente la expresión de NRP1 bajo hipoxia, donde la inhibición de la autofagia aumenta la supervivencia celular tras la administración de lenvatinib y la inducción de hipoxia; mientras que, el silenciamiento de HIF-1α evita la recuperación de los niveles de NRP1 y la pérdida de sensibilidad a lenvatinib en las líneas celulares Hep3B y Huh-7 derivadas de HCC.

En conjunto, NRP1 potencialmente representa un biomarcador novedoso con potencial utilidad para el diagnóstico y pronóstico de pacientes con HCC, jugando un papel clave en el posible fallo terapéutico del lenvatinib en el HCC. La sobreexpresión de NRP1 parece ser útil como biomarcador diagnóstico y pronóstico que podría beneficiar el entorno clínico de los pacientes con HCC. Asimismo, a través de un mecanismo asociado a la autofagia, NRP1 parece jugar un papel clave en la actividad antitumoral del lenvatinib *in vitro*, donde la modulación de la autofagia por los hepatocitos tumorales podría promover una recuperación de los niveles de NRP1 y el fallo del lenvatinib. Una respuesta a hipoxia mediada por HIF-1α también demostró promover una degradación de NRP1 mediante autofagia y, en consecuencia, regular la sensibilidad celular al lenvatinib. En conclusión, no sólo NRP1, pero también HIF-1α, parecen representar valiosas dianas moleculares que permitan mejorar la eficacia terapéutica del lenvatinib en el tratamiento del HCC avanzado, a través de la prevención de un mecanismo de resistencia a fármacos asociado a la autofagia y potencialmente modulado por la respuesta a hipoxia.

10 Supplementary information

Supplementary Figures

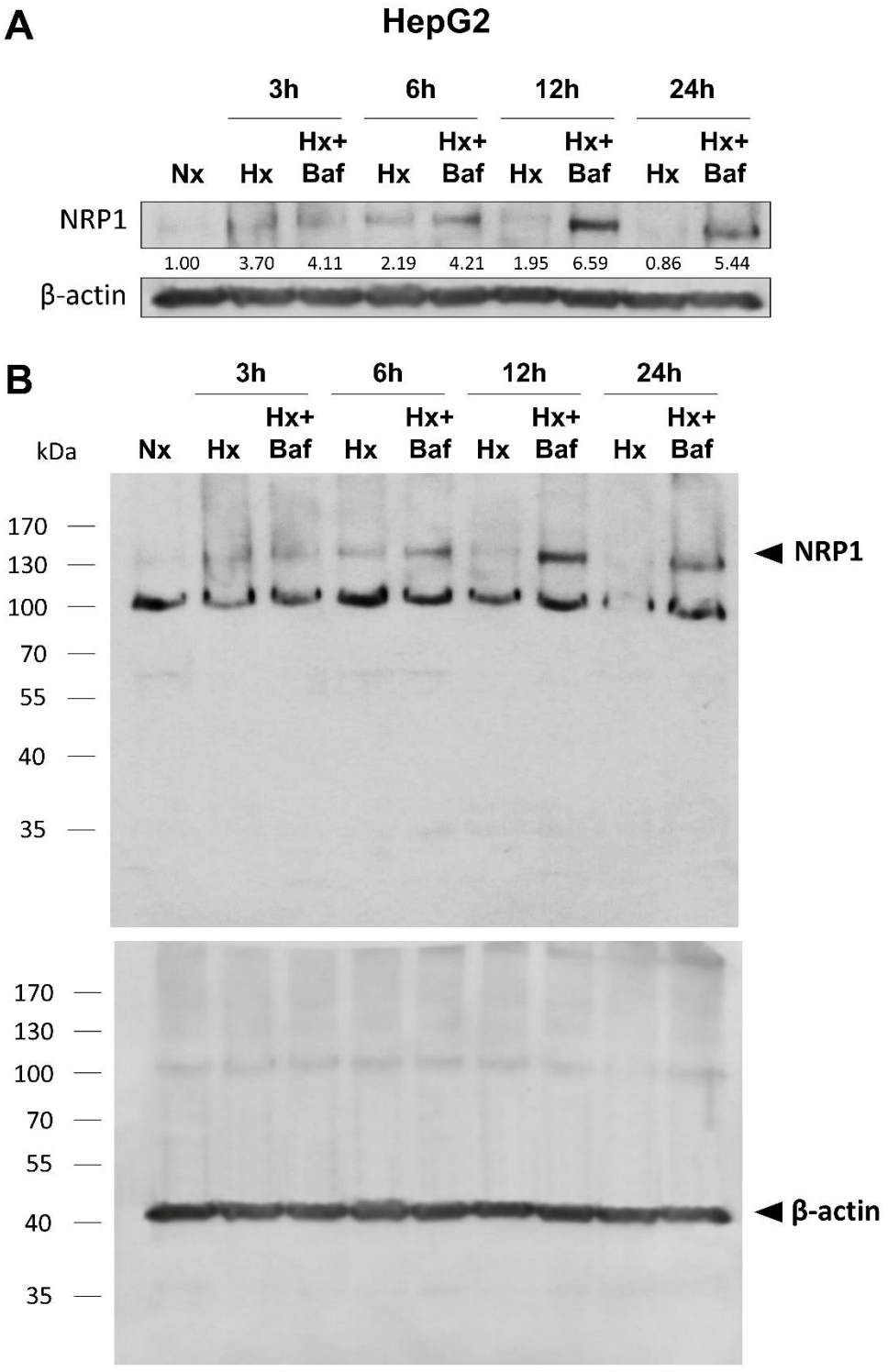

Supplementary Figure S1. Determination of the regulation of NRP1 levels by hypoxia induction and autophagy blockade in the HepG2 cell line. Protein expression of NRP1 was measured by western blot in normoxia (Nx) and hypoxia (Hx), with or without 100 nM bafilomycin A1 (Baf) treatment as autophagy inhibitor. (**A**) Crop immunoblots and (**B**) complete immunoblots, together with the densitometry reading of each band relativized to normoxia (Nx), are shown.

Supplementary Tables

Supplementary Table SI. Complete checklist corresponding to the PRISMA 2020 guidelines.*

Section and Topic	Item #	Checklist item	Location where item is reported
TITLE			
Title	1	Identify the report as a systematic review.	Page 1
ABSTRACT			
Abstract	2	See the PRISMA 2020 for Abstracts checklist.	Page 1 and Table S2
INTRODUCTION			
Rationale	3	Describe the rationale for the review in the context of existing knowledge.	Page 2
Objectives	4	Provide an explicit statement of the objective(s) or question(s) the review addresses.	Page 2
METHODS			
Eligibility criteria	5	Specify the inclusion and exclusion criteria for the review and how studies were grouped for the syntheses.	Page 3
Information sources	6	Specify all databases, registers, websites, organisations, reference lists and other sources searched or consulted to identify studies. Specify the date when each source was last searched or consulted.	Page 3
Search strategy	7	Present the full search strategies for all databases, registers and websites, including any filters and limits used.	Page 3 and Table S3
Selection process	8	Specify the methods used to decide whether a study met the inclusion criteria of the review, including how many reviewers screened each record and each report retrieved, whether they worked independently, and if applicable, details of automation tools used in the process.	Page 3
Data collection process	9	Specify the methods used to collect data from reports, including how many reviewers collected data from each report, whether they worked independently, any processes for obtaining or confirming data from study investigators, and if applicable, details of automation tools used in the process.	Page 3
Data items	10a	List and define all outcomes for which data were sought. Specify whether all results that were compatible with each outcome domain in each study were sought (e.g. for all measures, time points, analyses), and if not, the methods used to decide which results to collect.	Pages 3-4
	10b	List and define all other variables for which data were sought (e.g. participant and intervention characteristics, funding sources). Describe any assumptions made about any missing or unclear information.	Pages 3-4 and Table S4
Study risk of bias	11	Specify the methods used to assess risk of bias in the included studies, including details of the tool(s) used,	Page 3

Section and Topic	Item #	Checklist item	Location where item is reported
assessment		how many reviewers assessed each study and whether they worked independently, and if applicable, details of automation tools used in the process.	
Effect measures	12	Specify for each outcome the effect measure(s) (e.g. risk ratio, mean difference) used in the synthesis or presentation of results.	Page 3
Synthesis methods	13a	Describe the processes used to decide which studies were eligible for each synthesis (e.g. tabulating the study intervention characteristics and comparing against the planned groups for each synthesis (item #5)).	Pages 3-4
	13b	Describe any methods required to prepare the data for presentation or synthesis, such as handling of missing summary statistics, or data conversions.	Pages 3-4
	13c	Describe any methods used to tabulate or visually display results of individual studies and syntheses.	Pages 3-4
	13d	Describe any methods used to synthesize results and provide a rationale for the choice(s). If meta-analysis was performed, describe the model(s), method(s) to identify the presence and extent of statistical heterogeneity, and software package(s) used.	Pages 3-4
	13e	Describe any methods used to explore possible causes of heterogeneity among study results (e.g. subgroup analysis, meta-regression).	Pages 3-4
	13f	Describe any sensitivity analyses conducted to assess robustness of the synthesized results.	Pages 3-4
Reporting bias assessment	14	Describe any methods used to assess risk of bias due to missing results in a synthesis (arising from reporting biases).	Page 4
Certainty assessment	15	Describe any methods used to assess certainty (or confidence) in the body of evidence for an outcome.	-
RESULTS			
Study selection	16a	Describe the results of the search and selection process, from the number of records identified in the search to the number of studies included in the review, ideally using a flow diagram.	Page 4 and Figure 1
	16b	Cite studies that might appear to meet the inclusion criteria, but which were excluded, and explain why they were excluded.	Page 4 and Figure 1
Study characteristics	17	Cite each included study and present its characteristics.	Page 4, and Table 1
Risk of bias in studies	18	Present assessments of risk of bias for each included study.	Page 4 and Table 1
Results of individual studies	19	For all outcomes, present, for each study: (a) summary statistics for each group (where appropriate) and (b) an effect estimate and its precision (e.g. confidence/credible interval), ideally using structured tables or plots.	Figures 2, 3 and 4
Results of	20a	For each synthesis, briefly summarise the characteristics	Table 3 and

Section and Topic	Item #	Checklist item	Location where item is reported
syntheses		and risk of bias among contributing studies.	Figures 2, 3 and 4
	20b	Present results of all statistical syntheses conducted. If meta-analysis was done, present for each the summary estimate and its precision (e.g. confidence/credible interval) and measures of statistical heterogeneity. If comparing groups, describe the direction of the effect.	Pages 8-16, Tables 2 and 3, and Figures 2, 3 and 4
	20c	Present results of all investigations of possible causes of heterogeneity among study results.	Pages 10-16, Tables 2 and 3, and Figure S1
	20d	Present results of all sensitivity analyses conducted to assess the robustness of the synthesized results.	Page 17 and Table 4
Reporting biases	21	Present assessments of risk of bias due to missing results (arising from reporting biases) for each synthesis assessed.	Page 17, Table 4 and Figure 5
Certainty of evidence	22	Present assessments of certainty (or confidence) in the body of evidence for each outcome assessed.	-
DISCUSSION			
Discussion	23a	Provide a general interpretation of the results in the context of other evidence.	Pages 19-21
	23b	Discuss any limitations of the evidence included in the review.	Page 21
	23c	Discuss any limitations of the review processes used.	Page 21
	23d	Discuss implications of the results for practice, policy, and future research.	Pages 19-21
OTHER INFORMATION			
Registration and protocol	24a	Provide registration information for the review, including register name and registration number, or state that the review was not registered.	Pages 1-3
	24b	Indicate where the review protocol can be accessed, or state that a protocol was not prepared.	Pages 1-3
	24c	Describe and explain any amendments to information provided at registration or in the protocol.	-
Support	25	Describe sources of financial or non-financial support for the review, and the role of the funders or sponsors in the review.	Page 22
Competing interests	26	Declare any competing interests of review authors.	Page 22
Availability of data, code and other materials	27	Report which of the following are publicly available and where they can be found: template data collection forms; data extracted from included studies; data used for all analyses; analytic code; any other materials used.	-

*Pagination of this PRISMA 2020 checklist corresponds to the original meta-analysis published by our group (https://doi.org/10.3390/cancers14143455), that contains the data included in the meta-analysis section of the present PhD Thesis.

Supplementary Table SII. Complete checklist for the PRISMA 2020 guidelines corresponding to the Abstract.*

Section and Topic	Item #	Checklist item	Reported (Yes/No)
TITLE			
Title	1	Identify the report as a systematic review.	-
BACKGROUND			
Objectives	2	Provide an explicit statement of the main objective(s) or question(s) the review addresses.	Yes
METHODS			
Eligibility criteria	3	Specify the inclusion and exclusion criteria for the review.	No
Information sources	4	Specify the information sources (e.g. databases, registers) used to identify studies and the date when each was last searched.	Yes
Risk of bias	5	Specify the methods used to assess risk of bias in the included studies.	No
Synthesis of results	6	Specify the methods used to present and synthesise results.	Yes
RESULTS			
Included studies	7	Give the total number of included studies and participants and summarise relevant characteristics of studies.	No
Synthesis of results	8	Present results for main outcomes, preferably indicating the number of included studies and participants for each. If meta-analysis was done, report the summary estimate and confidence/credible interval. If comparing groups, indicate the direction of the effect (i.e. which group is favoured).	Yes
DISCUSSION			
Limitations of evidence	9	Provide a brief summary of the limitations of the evidence included in the review (e.g. study risk of bias, inconsistency and imprecision).	No
Interpretation	10	Provide a general interpretation of the results and important implications.	Yes
OTHER			
Funding	11	Specify the primary source of funding for the review.	No
Registration	12	Provide the register name and registration number.	Yes

*Pagination of this PRISMA 2020 checklist corresponds to the original meta-analysis published by our group (https://doi.org/10.3390/cancers14143455), that contains the data included in the meta-analysis section of the present PhD Thesis.

Supplementary Table SIII. Antibodies and staining procedures used by the included studies that performed IHC of NRP1.

Study	Publication year	Antibody	Dilution	Source	Ref.
Li et al.[85]	2021	Rabbit monoclonal	1:100	Abcam	NR
Lin et al.[79]	2018	Rabbit monoclonal	NR	Abcam	ab81321
Zhang et al.[78]	2016	Rabbit monoclonal (A6)	1:100	Self-produced	NR
Bergé et al.[76]	2011	Rabbit polyclonal	1:50	Invitrogen (Zymed laboratories)	34-7300

NR, not reported; Ref., reference.

11 References

1. Sung H, Ferlay J, Siegel RL, Laversanne M, Soerjomataram I, Jemal A, et al. Global cancer statistics 2020: GLOBOCAN estimates of incidence and mortality worldwide for 36 cancers in 185 countries. CA A Cancer J Clin. 2021;71(3):209–49.

2. Forner A, Reig M, Bruix J. Hepatocellular carcinoma. Lancet. 2018;391(10127):1301–14.

3. Alqahtani A, Khan Z, Alloghbi A, S. Said Ahmed T, Ashraf M, M. Hammouda D. Hepatocellular carcinoma: Molecular mechanisms and targeted therapies. Medicina. 2019;55(9):526.

4. Chidambaranathan-Reghupaty S, Fisher PB, Sarkar D. Hepatocellular carcinoma (HCC): Epidemiology, etiology and molecular classification. Adv Cancer Res. 2021;149(2021):1–61.

5. Singal AG, Lampertico P, Nahon P. Epidemiology and surveillance for hepatocellular carcinoma: New trends. J Hepatol. 2020;72(2):250–61.

6. Ferlay J, Ervik M, Lam F, Colombet M, Mery L, Piñeros M, et al. Global Cancer Observatory: Cancer Today. Lyon, France: International Agency for Research on Cancer [Internet]. 2020 [Accessed on 2022 Nov 23]. Available from: https://gco.iarc.fr/today

7. Yang JD, Hainaut P, Gores GJ, Amadou A, Plymoth A, Roberts LR. A global view of hepatocellular carcinoma: trends, risk, prevention and management. Nat Rev Gastroenterol Hepatol. 2019;16(10):589–604.

8. Llovet JM, Kelley RK, Villanueva A, Singal AG, Pikarsky E, Roayaie S, et al. Hepatocellular carcinoma. Nat Rev Dis Primers. 2021;7(1):6.

9. Eslam M, Newsome PN, Sarin SK, Anstee QM, Targher G, Romero-Gomez M, et al. A new definition for metabolic dysfunction-associated fatty liver disease: An international expert consensus statement. J Hepatol. 2020;73(1):202–9.

10. Llovet JM, Zucman-Rossi J, Pikarsky E, Sangro B, Schwartz M, Sherman M, et al. Hepatocellular carcinoma. Nat Rev Dis Primers. 2016;2(1):16018.

11. Cucarull B, Tutusaus A, Rider P, Hernáez-Alsina T, Cuño C, García de Frutos P, et al. Hepatocellular carcinoma: Molecular pathogenesis and therapeutic advances. Cancers. 2022;14(3):621.

12. Dhanasekaran R, Bandoh S, Roberts LR. Molecular pathogenesis of hepatocellular carcinoma and impact of therapeutic advances. F1000Res. 2016;5(F1000 Faculty Rev):879.

13. Craig AJ, von Felden J, Garcia-Lezana T, Sarcognato S, Villanueva A. Tumour evolution in hepatocellular carcinoma. Nat Rev Gastroenterol Hepatol. 2020;17(3):139–52.

14. Younossi ZM, Henry L. Epidemiology of non-alcoholic fatty liver disease and hepatocellular carcinoma. JHEP Rep. 2021;3(4):100305.

15. Kanda T, Goto T, Hirotsu Y, Masuzaki R, Moriyama M, Omata M. Molecular mechanisms: connections between nonalcoholic fatty liver disease, steatohepatitis and hepatocellular carcinoma. Int J Mol Sci. 2020;21(4):1525.

16. Ayuso C, Rimola J, Vilana R, Burrel M, Darnell A, García-Criado Á, et al. Diagnosis and staging of hepatocellular carcinoma (HCC): Current guidelines. Eur J Radiol. 2018;101(101):72–81.

17. Janevska D, Chaloska-Ivanova V, Janevski V. Hepatocellular carcinoma: Risk factors, diagnosis and treatment. Open Access Maced J Med Sci. 2015;3(4):732–6.

18. Luo P, Wu S, Yu Y, Ming X, Li S, Zuo X, et al. Current status and perspective biomarkers in AFP negative HCC: towards screening for and diagnosing hepatocellular carcinoma at an earlier stage. Pathol Oncol Res. 2020;26(2):599–603.

19. Zhuo Y, Chen Q, Chhatwal J. Changing epidemiology of hepatocellular carcinoma and role of surveillance. In: Hoshida Y, editor. Hepatocellular carcinoma: Translational precision medicine approaches. Cham: Springer International Publishing; 2019. p. 53–69.

20. Reig M, Forner A, Rimola J, Ferrer-Fàbrega J, Burrel M, Garcia-Criado Á, et al. BCLC strategy for prognosis prediction and treatment recommendation: The 2022 update. J Hepatol. 2022;76(3):681–93.

21. Hester CA, Yopp AC. Surgical therapies in hepatocellular carcinoma. In: Hoshida Y, editor. Hepatocellular carcinoma: Translational precision medicine approaches. Cham: Springer International Publishing; 2019. p. 145–67.

22. Sutphin PD, Lamus D, Kalva SP, Li J, Corbin IR. Interventional radiologic therapies for hepatocellular carcinoma: From where we began to where we are going. In: Hoshida Y, editor. Hepatocellular carcinoma: Translational precision medicine approaches. Cham: Springer International Publishing; 2019. p. 169–94.

23. Tateishi R, Fujiwara N. Precision locoregional therapies for hepatocellular carcinoma: Percutaneous ablation and radiotherapy. In: Hoshida Y, editor. Hepatocellular carcinoma: Translational precision medicine approaches. Cham: Springer International Publishing; 2019. p. 195–224.

24. Feng MY, Chan LL, Chan SL. Drug Treatment for advanced hepatocellular carcinoma: First-line and beyond. Curr Oncol. 2022;29(8):5489–507.

25. Brown ZJ, Greten TF. Immune therapies. In: Hoshida Y, editor. Hepatocellular carcinoma: Translational precision medicine approaches. Cham: Springer International Publishing; 2019. p. 239–53.

26. Kudo M, Finn RS, Qin S, Han KH, Ikeda K, Piscaglia F, et al. Lenvatinib versus sorafenib in first-line treatment of patients with unresectable hepatocellular carcinoma: a randomised phase 3 non-inferiority trial. Lancet. 2018;391(10126):1163–73.

27. Mo DC, Luo PH, Huang SX, Wang HL, Huang JF. Safety and efficacy of pembrolizumab plus lenvatinib versus pembrolizumab and lenvatinib monotherapies in cancers: A systematic review. Int Immunopharmacol. 2021;91(91):107281.

28. Al-Salama ZT, Syed YY, Scott LJ. Lenvatinib: A review in hepatocellular carcinoma. Drugs. 2019;79(6):665–74.

29. Hatanaka T, Naganuma A, Kakizaki S. Lenvatinib for hepatocellular carcinoma: A literature review. Pharmaceuticals. 2021;14(1):36.

30. Ikeda K, Kudo M, Kawazoe S, Osaki Y, Ikeda M, Okusaka T, et al. Phase 2 study of lenvatinib in patients with advanced hepatocellular carcinoma. J Gastroenterol. 2017;52(4):512–9.

31. Ikeda M, Okusaka T, Mitsunaga S, Ueno H, Tamai T, Suzuki T, et al. Safety and pharmacokinetics of lenvatinib in patients with advanced hepatocellular carcinoma. Clin Cancer Res. 2016;22(6):1385–94.

32. Briggs A, Daniele B, Dick K, Evans TRJ, Galle PR, Hubner RA, et al. Covariate-adjusted analysis of the Phase 3 REFLECT study of lenvatinib versus sorafenib in the treatment of unresectable hepatocellular carcinoma. Br J Cancer. 2020;122(12):1754–9.

33. Matsuki M, Hoshi T, Yamamoto Y, Ikemori-Kawada M, Minoshima Y, Funahashi Y, et al. Lenvatinib inhibits angiogenesis and tumor fibroblast growth factor signaling pathways in human hepatocellular carcinoma models. Cancer Med. 2018;7(6):2641–53.

34. Adachi Y, Matsuki M, Watanabe H, Takase K, Kodama K, Matsui J, et al. Antitumor and antiangiogenic activities of lenvatinib in mouse xenograft models of vascular endothelial growth factor-induced hypervascular human hepatocellular carcinoma. Cancer Invest. 2019;37(4–5):185–98.

35. He X xiao, Shi L liang, Qiu M jun, Li Q ting, Wang M meng, Xiong Z fan, et al. Molecularly targeted anti-cancer drugs inhibit the invasion and metastasis of hepatocellular carcinoma by regulating the expression of MMP and TIMP gene families. Biochem Biophys Res Commun. 2018;504(4):878–84.

36. Ogasawara S, Mihara Y, Kondo R, Kusano H, Akiba J, Yano H. Antiproliferative effect of lenvatinib on human liver cancer cell lines *in vitro* and *in vivo*. Anticancer Res. 2019;39(11):5973–82.

37. Hou FJ, Guo LX, Zheng KY, Song JN, Wang Q, Zheng YG. Chelidonine enhances the antitumor effect of lenvatinib on hepatocellular carcinoma cells. Onco Targets Ther. 2019;12:6685–97.

38. Hoshi T, Watanabe Miyano S, Watanabe H, Sonobe RMK, Seki Y, Ohta E, et al. Lenvatinib induces death of human hepatocellular carcinoma cells harboring an activated FGF signaling pathway through inhibition of FGFR–MAPK cascades. Biochem Biophys Res Commun. 2019;513(1):1–7.

39. Roberts JL, Poklepovic A, Booth L, Dent P. The multi-kinase inhibitor lenvatinib interacts with the HDAC inhibitor entinostat to kill liver cancer cells. Cell Signal. 2020;70(70):109573.

40. Niu M, Yi M, Li N, Wu K, Wu K. Advances of targeted therapy for hepatocellular carcinoma. Front Oncol. 2021;11:719896.

41. da Fonseca LG, Reig M, Bruix J. Tyrosine kinase inhibitors and hepatocellular carcinoma. Clin Liver Dis. 2020;24(4):719–37.

42. Tang W, Chen Z, Zhang W, Cheng Y, Zhang B, Wu F, et al. The mechanisms of sorafenib resistance in hepatocellular carcinoma: theoretical basis and therapeutic aspects. Sig Transduct Target Ther. 2020;5(1):87.

43. Zheng A, Chevalier N, Calderoni M, Dubuis G, Dormond O, Ziros PG, et al. CRISPR/Cas9 genome-wide screening identifies KEAP1 as a sorafenib, lenvatinib, and regorafenib sensitivity gene in hepatocellular carcinoma. Oncotarget. 2019;10(66):7058–70.

44. Fu R, Jiang S, Li J, Chen H, Zhang X. Activation of the HGF/c-MET axis promotes lenvatinib resistance in hepatocellular carcinoma cells with high c-MET expression. Med Oncol. 2020;37(4):24.

45. Ichikawa K, Watanabe Miyano S, Minoshima Y, Matsui J, Funahashi Y. Activated FGF2 signaling pathway in tumor vasculature is essential for acquired resistance to anti-VEGF therapy. Sci Rep. 2020;10(1):2939.

46. Ao J, Chiba T, Shibata S, Kurosugi A, Qiang N, Ma Y, et al. Acquisition of mesenchymal-like phenotypes and overproduction of angiogenic factors in lenvatinib-resistant hepatocellular carcinoma cells. Biochem Biophys Res Commun. 2021;549(549):171–8.

47. Arechederra M, Bazai SK, Abdouni A, Sequera C, Mead TJ, Richelme S, et al. ADAMTSL5 is an epigenetically activated gene underlying tumorigenesis and drug resistance in hepatocellular carcinoma. J Hepatol. 2021;74(4):893–906.

48. Guo Y, Xu J, Du Q, Yan Y, Geller DA. IRF2 regulates cellular survival and lenvatinib-sensitivity of hepatocellular carcinoma (HCC) through regulating β-catenin. Transl Oncol. 2021;14(6):101059.

49. Guo J, Zhu P, Ye Z, Wang M, Yang H, Huang S, et al. YRDC mediates the resistance of lenvatinib in hepatocarcinoma cells via modulating the translation of KRAS. Front Pharmacol. 2021;12:744578.

50. Hu Q, Hu X, Zhang L, Zhao Y, Li L. Targeting hedgehog signalling in CD133-positive hepatocellular carcinoma: improving lenvatinib therapeutic efficiency. Med Oncol. 2021;38(4):41.

51. Jin H, Shi Y, Lv Y, Yuan S, Ramirez CFA, Lieftink C, et al. EGFR activation limits the response of liver cancer to lenvatinib. Nature. 2021;595(7869):730–4.

52. Lu Y, Shen H, Huang W, He S, Chen J, Zhang D, et al. Genome-scale CRISPR-Cas9 knockout screening in hepatocellular carcinoma with lenvatinib resistance. Cell Death Discov. 2021;7(1):359.

53. Yu T, Yu J, Lu L, Zhang Y, Zhou Y, Zhou Y, et al. MT1JP-mediated miR-24-3p/BCL2L2 axis promotes Lenvatinib resistance in hepatocellular carcinoma cells by inhibiting apoptosis. Cell Oncol. 2021;44(4):821–34.

54. Zhao Z, Song J, Zhang D, Wu F, Tu J, Ji J. Oxysophocarpine suppresses FGFR1-overexpressed hepatocellular carcinoma growth and sensitizes the therapeutic effect of lenvatinib. Life Sci. 2021;264(264):118642.

55. Zhao Z, Zhang D, Wu F, Tu J, Song J, Xu M, et al. Sophoridine suppresses lenvatinib-resistant hepatocellular carcinoma growth by inhibiting RAS/MEK/ERK axis via decreasing VEGFR2 expression. J Cell Mol Med. 2021;25(1):549–60.

56. Hamaya S, Fujihara S, Iwama H, Fujita K, Shi T, Nakabayashi R, et al. Characterization of cisplatin effects in lenvatinib-resistant hepatocellular carcinoma cells. Anticancer Res. 2022;42(3):1263–75.

57. He X, Hikiba Y, Suzuki Y, Nakamori Y, Kanemaru Y, Sugimori M, et al. EGFR inhibition reverses resistance to lenvatinib in hepatocellular carcinoma cells. Sci Rep. 2022;12(1):8007.

58. Hou W, Bridgeman B, Malnassy G, Ding X, Cotler SJ, Dhanarajan A, et al. Integrin subunit beta 8 contributes to lenvatinib resistance in HCC. Hepatol Commun. 2022;6(7):1786–802.

59. Hu B, Zou T, Qin W, Shen X, Su Y, Li J, et al. Inhibition of EGFR overcomes acquired lenvatinib resistance driven by STAT3–ABCB1 signaling in hepatocellular carcinoma. Cancer Res. 2022;82(20):3845–57.

60. Huang S, Ma Z, Zhou Q, Wang A, Gong Y, Li Z, et al. Genome-wide CRISPR/Cas9 library screening identified that DUSP4 deficiency Induces lenvatinib resistance in hepatocellular carcinoma. Int J Biol Sci. 2022;18(11):4357–71.

61. Huang M, Long J, Yao Z, Zhao Y, Zhao Y, Liao J, et al. METTL1-mediated m7G tRNA modification promotes lenvatinib resistance in hepatocellular carcinoma. Cancer Res. 2022; Online ahead of print. doi:10.1158/0008-5472.CAN-22-0963.

62. Mok EHK, Leung CON, Zhou L, Lei MML, Leung HW, Tong M, et al. Caspase-3-induced activation of SREBP2 drives drug resistance via promotion of cholesterol biosynthesis in hepatocellular carcinoma. Cancer Res. 2022;82(17):3102–15.

63. Pan J, Zhang M, Dong L, Ji S, Zhang J, Zhang S, et al. Genome-Scale CRISPR screen identifies LAPTM5 driving lenvatinib resistance in hepatocellular carcinoma. Autophagy. 2022; Online ahead of print. doi:10.1080/15548627.2022.2117893.

64. Sun D, Liu J, Wang Y, Dong J. Co-administration of MDR1 and BCRP or EGFR/PI3K inhibitors overcomes lenvatinib resistance in hepatocellular carcinoma. Front Oncol. 2022;12:944537.

65. Wang Y, Tan K, Hu W, Hou Y, Yang G. LncRNA AC026401.3 interacts with OCT1 to intensify sorafenib and lenvatinib resistance by activating E2F2 signaling in hepatocellular carcinoma. Exp Cell Res. 2022;420(1):113335.

66. Wang Z, Chen X, Zhou L, Zhao X, Ge C, Zhao F, et al. FBXO9 mediates the cancer-promoting effects of ZNF143 by degrading FBXW7 and facilitates drug resistance in hepatocellular carcinoma. Front Oncol. 2022;12:930220.

67. Xu X, Jiang W, Han P, Zhang J, Tong L, Sun X. MicroRNA-128-3p mediates lenvatinib resistance of hepatocellular carcinoma cells by downregulating c-Met. J Hepatocell Carcinoma. 2022;9:113–26.

68. Zhang P, Sun H, Wen P, Wang Y, Cui Y, Wu J. circRNA circMED27 acts as a prognostic factor and mediator to promote lenvatinib resistance of hepatocellular carcinoma. Mol Ther-Nucl Acids. 2022;27(27):293–303.

69. Chaudhary B, Khaled YS, Ammori BJ, Elkord E. Neuropilin 1: function and therapeutic potential in cancer. Cancer Immunol Immunother. 2014;63(2):81–99.

70. Niland S, Eble JA. Neuropilins in the context of tumor vasculature. Int J Mol Sci. 2019;20(3):639.

71. Roy S, Bag AK, Singh RK, Talmadge JE, Batra SK, Datta K. Multifaceted role of neuropilins in the immune system: Potential targets for immunotherapy. Front Immunol. 2017;8:1228.

72. Napolitano V, Tamagnone L. Neuropilins controlling cancer therapy responsiveness. Int J Mol Sci. 2019;20(8):2049.

73. Dumond A, Pagès G. Neuropilins, as relevant oncology target: Their role in the tumoral microenvironment. Front Cell Dev Biol. 2020;8:662.

74. Broz M, Kolarič A, Jukič M, Bren U. Neuropilin (NRPs) Related Pathological Conditions and Their Modulators. Int J Mol Sci. 2022;23(15):8402.

75. Guo HF, Vander Kooi CW. Neuropilin functions as an essential cell surface receptor. J Biol Chem. 2015;290(49):29120–6.

76. Bergé M, Allanic D, Bonnin P, de Montrion C, Richard J, Suc M, et al. Neuropilin-1 is upregulated in hepatocellular carcinoma and contributes to tumour growth and vascular remodelling. J Hepatol. 2011;55(4):866–75.

77. Chishti MA, Kaya N, BinBakheet AB, Al-Mohanna F, Goyns MH, Colak D. Induction of cell proliferation in old rat liver can reset certain gene expression levels characteristic of old liver to those associated with young liver. AGE. 2013;35(3):719–32.

78. Zhang Y, Liu P, Jiang Y, Dou X, Yan J, Ma C, et al. High expression of neuropilin-1 associates with unfavorable clinicopathological features in hepatocellular carcinoma. Pathol Oncol Res. 2016;22(2):367–75.

79. Lin J, Zhang Y, Wu J, Li L, Chen N, Ni P, et al. Neuropilin 1 (NRP1) is a novel tumor marker in hepatocellular carcinoma. Clin Chim Acta. 2018;485(485):158–65.

80. Morin E, Sjöberg E, Tjomsland V, Testini C, Lindskog C, Franklin O, et al. VEGF receptor-2/neuropilin 1 *trans* -complex formation between endothelial and tumor cells is an independent predictor of pancreatic cancer survival: VEGFR2/NRP1 *trans* -complex in cancer. J Pathol. 2018;246(3):311–22.

81. Lyu Z, Jin H, Yan Z, Hu K, Jiang H, Peng H, et al. Effects of NRP1 on angiogenesis and vascular maturity in endothelial cells are dependent on the expression of SEMA4D. Int J Mol Med. 46(4):1321–1334.

82. Savier E, Simon-Gracia L, Charlotte F, Tuffery P, Teesalu T, Scatton O, et al. Bi-functional peptides as a new therapeutic tool for hepatocellular carcinoma. Pharmaceutics. 2021;13(10):1631.

83. Li X yu, Ma WN, Su L xin, Shen Y, Zhang L, Shao Y, et al. Association of angiogenesis gene expression with cancer prognosis and immunotherapy efficacy. Front Cell Dev Biol. 2022;10:805507.

84. Fernández-Palanca P, Payo-Serafín T, Fondevila F, Méndez-Blanco C, San-Miguel B, Romero MR, et al. Neuropilin-1 as a potential biomarker of prognosis and invasive-related parameters in liver and colorectal cancer: A systematic review and meta-analysis of human studies. Cancers. 2022;14(14):3455.

85. Li X, Zhou Y, Hu J, Bai Z, Meng W, Zhang L, et al. Loss of neuropilin1 inhibits liver cancer stem cells population and blocks metastasis in hepatocellular carcinoma via epithelial-mesenchymal transition. Neoplasma. 2021;68(02):325–33.

86. Sharma B, Srinivasan R, Chawla Y, Chakraborti A. Vascular endothelial growth factor: Evidence for autocrine signaling in hepatocellular carcinoma cell lines affecting invasion. Indian J Cancer. 2016;53(4):542.

87. Abdel Ghafar MT, Elkhouly RA, Elnaggar MH, Mabrouk MM, Darwish SA, Younis RL, et al. Utility of serum neuropilin-1 and angiopoietin-2 as markers of hepatocellular carcinoma. J Investig Med. 2021;69(6):1222–9.

88. Ono A, Aikata H, Yamauchi M, Kodama K, Ohishi W, Kishi T, et al. Circulating cytokines and angiogenic factors based signature associated with the relative dose intensity during treatment in patients with advanced hepatocellular carcinoma receiving lenvatinib. Ther Adv Med Oncol. 2020;12:175883592092205.

89. Huang ZL, Xu B, Li TT, Xu YH, Huang XY, Huang XY. Integrative analysis identifies cell-type-specific genes within tumor microenvironment as prognostic indicators in hepatocellular carcinoma. Front Oncol. 2022;12:878923.

90. Li JH, Tao YF, Shen CH, Li RD, Wang Z, Xing H, et al. Integrated multi-omics analysis identifies ENY2 as a predictor of recurrence and a regulator of telomere maintenance in hepatocellular carcinoma. Front Oncol. 2022;12:939948.

91. Xu H, Xiong C, Chen Y, Zhang C, Bai D. Identification of Rad51 as a prognostic biomarker correlated with immune infiltration in hepatocellular carcinoma. Bioengineered. 2021;12(1):2664–75.

92. Dong X, Guo W, Zhang S, Wu T, Sun Z, Yan S, et al. Elevated expression of neuropilin-2 associated with unfavorable prognosis in hepatocellular carcinoma. Onco Targets Ther. 2017;10:3827–33.

93. Wittmann P, Grubinger M, Gröger C, Huber H, Sieghart W, Peck-Radosavljevic M, et al. Neuropilin-2 induced by transforming growth factor-β augments migration of hepatocellular carcinoma cells. BMC Cancer. 2015;15(1):909.

94. Bergé M, Bonnin P, Sulpice E, Vilar J, Allanic D, Silvestre JS, et al. Small interfering RNAs induce target-independent inhibition of tumor growth and vasculature remodeling in a mouse model of hepatocellular carcinoma. Am J Pathol. 2010;177(6):3192–201.

95. Raskopf E, Vogt A, Standop J, Sauerbruch T, Schmitz V. Inhibition of neuropilin-1 by RNA-interference and its angiostatic potential in the treatment of hepatocellular carcinoma. Z Gastroenterol. 2010;48(01):21–7.

96. Xu J, Xia J. NRP-1 silencing suppresses hepatocellular carcinoma cell growth in vitro and in vivo. Exp Ther Med. 2013;5(1):150–4.

97. Liu Q, Xu Y, Wei S, Gao W, Chen L, Zhou T, et al. miRNA-148b suppresses hepatic cancer stem cell by targeting neuropilin-1. Biosci Rep. 2015;35(4):e00229.

98. Xu Z, Shen H, Chen C, Ma L, Li W, Wang L, et al. Neuropilin-1 promotes primary liver cancer progression by potentiating the activity of hepatic stellate cells. Oncol Lett. 2017;15(2):2245-51.

99. Lv Y, Hou X, Zhang Q, Li R, Xu L, Chen Y, et al. Untargeted metabolomics study of the in vitro anti-hepatoma effect of saikosaponin d in combination with NRP-1 knockdown. Molecules. 2019;24(7):1423.

100. Cheng C, Zhang Z, Wang S, Chen L, Liu Q. Reduction sensitive CC9-PEG-SSBPEI/miR-148b nanoparticles: Synthesis, characterization, targeting delivery and application for anti-metastasis. Colloid Surf B-Biointerfaces. 2019;183(183):110412.

101. Liao YL, Sun YM, Chau GY, Chau YP, Lai TC, Wang JL, et al. Identification of SOX4 target genes using phylogenetic footprinting-based prediction from expression microarrays suggests that overexpression of SOX4 potentiates metastasis in hepatocellular carcinoma. Oncogene. 2008;27(42):5578–89.

102. Raskopf E, Vogt A, Decker G, Hirt S, Daskalow K, Cramer T, et al. Combination of hypoxia and RNA-interference targeting VEGF induces apoptosis in hepatoma cells via autocrine mechanisms. Curr Pharm Biotechnol. 2012;13(11):2290–8.

103. Devbhandari RP, Shi GM, Ke AW, Wu FZ, Huang XY, Wang XY, et al. Profiling of the tetraspanin CD151 web and conspiracy of CD151/integrin β1 complex in the progression of hepatocellular carcinoma. Luk J, editor. PLoS ONE. 2011;6(9):e24901.

104. Zhuang PY, Wang JD, Tang ZH, Zhou XP, Yang Y, Quan ZW, et al. Peritumoral Neuropilin-1 and VEGF receptor-2 expression increases time to recurrence in hepatocellular carcinoma patients undergoing curative hepatectomy. Oncotarget. 2014;5(22):11121–32.

105. Lee J, Lee J, Yu H, Choi K, Choi C. Differential dependency of human cancer cells on vascular endothelial growth factor-mediated autocrine growth and survival. Cancer Lett. 2011;309(2):145–50.

106. Villa E, Critelli R, Lei B, Marzocchi G, Cammà C, Giannelli G, et al. Neoangiogenesis-related genes are hallmarks of fast-growing hepatocellular carcinomas and worst survival. Results from a prospective study. Gut. 2016;65(5):861–9.

107. Xu P, Zou M, Wang S, Wang L, Wang L, Luo F, et al. Preparation of truncated tissue factor antineuropilin-1 monoclonal antibody conjugate and identification of its selective thrombosis in tumor blood vessels. Anti-Cancer Drugs. 2019;30(5):441–50.

108. Arab JP, Cabrera D, Sehrawat TS, Jalan-Sakrikar N, Verma VK, Simonetto D, et al. Hepatic stellate cell activation promotes alcohol-induced steatohepatitis through Igfbp3 and SerpinA12. J Hepatol. 2020;73(1):149–60.

109. Chen YJ, Liao WX, Huang SZ, Yu YF, Wen JY, Chen J, et al. Prognostic and immunological role of CD36: A pan-cancer analysis. J Cancer. 2021;12(16):4762–73.

110. Liu Z, Zhang S, Ouyang J, Wu D, Chen L, Zhou W, et al. Single-cell RNA-seq analysis reveals dysregulated cell-cell interactions in a tumor microenvironment related to HCC development. Dis Markers. 2022;2022:4971621.

111. Lee J, Lee E, Kwon D, Lim Y, Oh S, Oh M, et al. Up-regulation of cancer-related genes in HepG2 cells by TCDD requires PRMT I and IV. Mol Cell Toxicol. 2010;6(2):111–8.

112. Li Z, Bao H. Deciphering key regulators of *Inonotus hispidus* petroleum ether extract involved in anti-tumor through whole transcriptome and proteome analysis in H22 tumor-bearing mice model. J Ethnopharmacol. 2022;296(296):115468.

113. Horwitz E, Stein I, Andreozzi M, Nemeth J, Shoham A, Pappo O, et al. Human and mouse *VEGFA* -amplified hepatocellular carcinomas are highly sensitive to sorafenib treatment. Cancer Discov. 2014;4(6):730–43.

114. Kisseleva EP, Krylov AV, Lyamina IV, Kudryavtsev IV, Lioudyno VI. Role of vascular endothelial growth factor (VEGF) in thymus of mice under normal conditions and with tumor growth. Biochemistry (Mosc). 2016;81(5):491–501.

115. Liu J, Kong X, Sun P, Wang R, Li W, Chen Q. An integrated pan-cancer analysis of TFAP4 aberrations and the potential clinical implications for cancer immunity. J Cell Mol Med. 2021;25(4):2082–97.

116. Beckebaum S, Zhang X, Chen X, Yu Z, Frilling A, Dworacki G, et al. Increased levels of interleukin-10 in serum from patients with hepatocellular carcinoma correlate with profound numerical deficiencies and immature phenotype of circulating dendritic cell subsets. Clin Cancer Res. 2004;10(21):7260–9.

117. Cheng X, Cao Y, Wang X, Cheng L, Liu Y, Lei J, et al. Systematic pan-cancer analysis of KLRB1 with prognostic value and immunological activity across human tumors. J Immunol Res. 2022;2022:5254911.

118. Chuckran CA, Liu C, Bruno TC, Workman CJ, Vignali DA. Neuropilin-1: a checkpoint target with unique implications for cancer immunology and immunotherapy. J Immunother Cancer. 2020;8(2):e000967.

119. Oura K, Morishita A, Masaki T. Molecular and functional roles of microRNAs in the progression of hepatocellular carcinoma—A review. Int J Mol Sci. 2020;21(21):8362.

120. Yang W. Circular RNA-ABCB10 suppresses hepatocellular carcinoma progression through upregulating NRP1/ABL2 via sponging miR-340-5p/miR-452-5p. Eur Rev Med Pharmacol Sci. 2020;24(5):2347–57.

121. Wang G, Liu H, Wei Z, Jia H, Liu Y, Liu J. Systematic analysis of the molecular mechanism of microRNA-124 in hepatoblastoma cells. Oncol Lett. 2017;14(6):7161–70.

122. Novikova MV, Khromova NV, Kopnin PB. Components of the hepatocellular carcinoma microenvironment and their role in tumor progression. Biochemistry Moscow. 2017;82(8):861–73.

123. Méndez-Blanco C, Fondevila F, García-Palomo A, González-Gallego J, Mauriz JL. Sorafenib resistance in hepatocarcinoma: role of hypoxia-inducible factors. Exp Mol Med. 2018;50(10):1–9.

124. Méndez-Blanco C, Fondevila F, Fernández-Palanca P, García-Palomo A, van Pelt J, Verslype C, et al. Stabilization of hypoxia-Inducible factors and BNIP3 promoter methylation contribute to acquired sorafenib resistance in human hepatocarcinoma cells. Cancers. 2019;11(12):1984.

125. Qian H, Chao X, Williams J, Fulte S, Li T, Yang L, et al. Autophagy in liver diseases: A review. Mol Asp Med. 2021;82(82):100973.

126. Cao W, Li J, Yang K, Cao D. An overview of autophagy: Mechanism, regulation and research progress. Bull Cancer. 2021;108(3):304–22.

127. Yu L, Chen Y, Tooze SA. Autophagy pathway: Cellular and molecular mechanisms. Autophagy. 2018;14(2):207–15.

128. Karampa AD, Goussia AC, Glantzounis GK, Mastoridou EM, Anastasopoulos NAT, Charchanti AV. The role of macroautophagy and chaperone-mediated autophagy in the pathogenesis and management of hepatocellular carcinoma. Cancers. 2022;14(3):760.

129. Ichimiya T, Yamakawa T, Hirano T, Yokoyama Y, Hayashi Y, Hirayama D, et al. Autophagy and autophagy-related diseases: A review. Int J Mol Sci. 2020;21(23):8974.

130. Lamark T, Johansen T. Mechanisms of selective autophagy. Annu Rev Cell Dev Biol. 2021;37:143–69.

131. Yang S, Yang L, Li X, Li B, Li Y, Zhang X, et al. New insights into autophagy in hepatocellular carcinoma: mechanisms and therapeutic strategies. Am J Cancer Res. 2019;9(7):1329–53.

132. Huang F, Wang BR, Wang YG. Role of autophagy in tumorigenesis, metastasis, targeted therapy and drug resistance of hepatocellular carcinoma. World J Gastroenterol. 2018;24(41):4643–51.

133. Yazdani H, Huang H, Tsung A. Autophagy: Dual response in the development of hepatocellular carcinoma. Cells. 2019;8(2):91.

134. Klionsky DJ, Abdel-Aziz AK, Abdelfatah S, Abdellatif M, Abdoli A, Abel S, et al. Guidelines for the use and interpretation of assays for monitoring autophagy (4th edition)[1]. Autophagy. 2021;17(1):1–382.

135. Shi R, Liao C, Zhang Q. Hypoxia-driven effects in cancer: characterization, mechanisms, and therapeutic implications. Cells. 2021;10(3):678.

136. Li Y, Zhao L, Li XF. Hypoxia and the tumor microenvironment. Technol Cancer Res Treat. 2021;20:153303382110363.

137. Yang G, Shi R, Zhang Q. Hypoxia and oxygen-sensing signaling in gene regulation and cancer progression. Int J Mol Sci. 2020;21(21):8162.

138. Xiong Q, Liu B, Ding M, Zhou J, Yang C, Chen Y. Hypoxia and cancer related pathology. Cancer Lett. 2020;486(486):1–7.

139. Wicks EE, Semenza GL. Hypoxia-inducible factors: cancer progression and clinical translation. J Clin Invest. 2022;132(11):e159839.

140. Corrado C, Fontana S. Hypoxia and HIF signaling: One axis with divergent effects. Int J Mol Sci. 2020;21(16):5611.

141. Guo Y, Xiao Z, Yang L, Gao Y, Zhu Q, Hu L, et al. Hypoxia-inducible factors in hepatocellular carcinoma (Review). Oncol Rep. 2020;43(1):3–15.

142. Wilson GK, Tennant DA, McKeating JA. Hypoxia inducible factors in liver disease and hepatocellular carcinoma: Current understanding and future directions. J Hepatol. 2014;61(6):1397–406.

143. Chen C, Lou T. Hypoxia inducible factors in hepatocellular carcinoma. Oncotarget. 2017;8(28):46691–703.

144. Bao MHR, Wong CCL. Hypoxia, metabolic reprogramming, and drug resistance in liver cancer. Cells. 2021;10(7):1715.

145. Chen H, Chen J, Yuan H, Li X, Li W. Hypoxia-inducible factor-1α: A critical target for inhibiting the metastasis of hepatocellular carcinoma (Review). Oncol Lett. 2022;24(2):284.

146. Zeng Z, Lu Q, Liu Y, Zhao J, Zhang Q, Hu L, et al. Effect of the hypoxia inducible factor on sorafenib resistance of hepatocellular carcinoma. Front Oncol. 2021;11:641522.

147. Lee YH. An overview of meta-analysis for clinicians. Korean J Intern Med. 2018;33(2):277–83.

148. Page MJ, McKenzie JE, Bossuyt PM, Boutron I, Hoffmann TC, Mulrow CD, et al. The PRISMA 2020 statement: an updated guideline for reporting systematic reviews. Syst Rev. 2021;10(1):89.

149. Wells G, Shea B, O'Connell D, Peterson J, Welch V, Losos M, et al. The Newcastle-Ottawa Scale (NOS) for assessing the quality of nonradomised studies in meta-analyses. The Ottawa Hospital Research Institute. 2021 [Accessed on 2022 Nov 21]. Available from: https://www.ohri.ca/programs/clinical_epidemiology/oxford.asp

150. Parmar MKB, Torri V, Stewart L. Extracting summary statistics to perform meta-analyses of the published literature for survival endpoints. Statist Med. 1998;17(24):2815–34.

151. Roessler S, Long EL, Budhu A, Chen Y, Zhao X, Ji J, et al. Integrative genomic identification of genes on 8p associated with hepatocellular carcinoma progression and patient survival. Gastroenterology. 2012;142(4):957-966.e12.

152. Uhlen M, Zhang C, Lee S, Sjöstedt E, Fagerberg L, Bidkhori G, et al. A pathology atlas of the human cancer transcriptome. Science. 2017;357(6352):eaan2507.

153. Chandrashekar DS, Bashel B, Balasubramanya SAH, Creighton CJ, Ponce-Rodriguez I, Chakravarthi BVSK, et al. UALCAN: A portal for facilitating tumor subgroup gene expression and survival analyses. Neoplasia. 2017;19(8):649–58.

154. Tang Z, Li C, Kang B, Gao G, Li C, Zhang Z. GEPIA: a web server for cancer and normal gene expression profiling and interactive analyses. Nucleic Acids Res. 2017;45(W1):W98–102.

155. Goldman MJ, Craft B, Hastie M, Repečka K, McDade F, Kamath A, et al. Visualizing and interpreting cancer genomics data via the Xena platform. Nat Biotechnol. 2020;38(6):675–8.

156. Barrett T, Wilhite SE, Ledoux P, Evangelista C, Kim IF, Tomashevsky M, et al. NCBI GEO: archive for functional genomics data sets—update. Nucleic Acids Res. 2012;41(D1):D991–5.

157. Livak KJ, Schmittgen TD. Analysis of relative gene expression data using real-time quantitative PCR and the $2^{-\Delta\Delta CT}$ method. Methods. 2001;25(4):402–8.

158. Meftahi GH, Bahari Z, Zarei Mahmoudabadi A, Iman M, Jangravi Z. Applications of western blot technique: From bench to bedside. Biochem Mol Biol Educ. 2021;49(4):509–17.

159. Thomé MP, Filippi-Chiela EC, Villodre ES, Migliavaca CB, Onzi GR, Felipe KB, et al. Ratiometric analysis of acridine orange staining in the study of acidic organelles and autophagy. J Cell Sci. 2016;129(24):4622–32.

160. Martinotti S, Ranzato E. Scratch wound healing assay. Methods Mol Biol. 2020;2109:225–9.

161. Deng C, Guo H, Yan D, Liang T, Ye X, Li Z. Pancancer analysis of neurovascular-related NRP family genes as potential prognostic biomarkers of bladder urothelial carcinoma. Biomed Res Int. 2021;2021:5546612.

162. Giannelli G, Santoro A, Kelley RK, Gane E, Paradis V, Cleverly A, et al. Biomarkers and overall survival in patients with advanced hepatocellular carcinoma treated with TGF-βRI inhibitor galunisertib. Kim DY, editor. PLoS ONE. 2020;15(3):e0222259.

163. Yaqoob U, Cao S, Shergill U, Jagavelu K, Geng Z, Yin M, et al. *Neuropilin-1* stimulates tumor growth by increasing fibronectin fibril assembly in the tumor microenvironment. Cancer Res. 2012;72(16):4047–59.

164. Fornari F, Giovannini C, Piscaglia F, Gramantieri L. Elucidating the molecular basis of sorafenib resistance in HCC: Current findings and future directions. J Hepatocell Carcinoma. 2021;8:741–57.

165. Yun CW, Jeon J, Go G, Lee JH, Lee SH. The dual role of autophagy in cancer development and a therapeutic strategy for cancer by targeting autophagy. Int J Mol Sci. 2021;22(1):179.

166. Ho CJ, Gorski SM. Molecular mechanisms underlying autophagy-mediated treatment resistance in cancer. Cancers. 2019;11(11):1775.

167. Chen Z, Yuan T, Yan F, Ye S, Xie Q, Zhang B, et al. CT-707 overcomes hypoxia-mediated sorafenib resistance in Hepatocellular carcinoma by inhibiting YAP signaling. BMC Cancer. 2022;22(1):425.

168. Osman NAA, Abd El-Rehim DM, Kamal IM. Defective Beclin-1 and elevated hypoxia-inducible factor (HIF)-1α expression are closely linked to tumorigenesis, differentiation, and progression of hepatocellular carcinoma. Tumor Biol. 2015;36(6):4293–9.

169. Jarvis A, Allerston CK, Jia H, Herzog B, Garza-Garcia A, Winfield N, et al. Small molecule inhibitors of the neuropilin-1 vascular endothelial growth factor A (VEGF-A) interaction. J Med Chem. 2010;53(5):2215–26.

170. Cong L, Yi J, Qiu S, Wang R, Jin S, Jiang R, et al. Effect of EG00229 on radiation resistance of lung adenocarcinoma cells. J Cancer. 2021;12(20):6105–17.

171. Dumond A, Brachet E, Durivault J, Vial V, Puszko AK, Lepelletier Y, et al. Neuropilin 1 and Neuropilin 2 gene invalidation or pharmacological inhibition reveals their relevance for the treatment of metastatic renal cell carcinoma. J Exp Clin Cancer Res. 2021;40(1):33.

172. Liu CY, Chen KF, Chen PJ. Treatment of liver cancer. Cold Spring Harb Perspect Med. 2015;5(9):a021535.

173. Méndez-Blanco C, Fernández-Palanca P, Fondevila F, González-Gallego J, Mauriz JL. Prognostic and clinicopathological significance of hypoxia-inducible factors 1α and 2α in hepatocellular carcinoma: a systematic review with meta-analysis. Ther Adv Med Oncol. 2021;13:175883592098707.

174. Fondevila F, Fernández-Palanca P, Méndez-Blanco C, Payo-Serafín T, Lozano E, Marin JJG, et al. Association of FOXO3 expression with tumor pathogenesis, prognosis and clinicopathological features in hepatocellular carcinoma: A systematic review with meta-Analysis. Cancers. 2021;13(21):5349.

175. Yang L, Liu L, Zhu Y, Wang B bing, Chen Y nan, Zhang F, et al. Neuropilin-1 is associated with the prognosis of cervical cancer in Henan Chinese population. Onco Targets Ther. 2019;12:2911–20.

176. Zhuo Y, Shi Y, Wu T. NRP-1 and KDR polymorphisms are associated with survival time in patients with advanced gastric cancer. Oncol Lett. 2019;18(5):4629–38.

177. Jin Q, Ren Q, Chang X, Yu H, Jin X, Lu X, et al. Neuropilin-1 predicts poor prognosis and promotes tumor metastasis through epithelial-mesenchymal transition in gastric cancer. J Cancer. 2021;12(12):3648–59.

178. Al-Zeheimi N, Naik A, Bakheit CS, Al Riyami M, Al Ajarrah A, Al Badi S, et al. Neoadjuvant chemotherapy alters neuropilin-1, PlGF, and SNAI1 expression levels and predicts breast cancer patients response. Front Oncol. 2019;9:323.

179. Ben Q, Zheng J, Fei J, An W, Li P, Li Z, et al. High neuropilin 1 expression was associated with angiogenesis and poor overall survival in resected pancreatic ductal adenocarcinoma. Pancreas. 2014;43(5):744–9.

180. Xu Y, Li P, Zhang X, Wang J, Gu D, Wang Y. Prognostic implication of neuropilin-1 upregulation in human nasopharyngeal carcinoma. Diagn Pathol. 2013;8(1):155.

181. Ding M, Liu L, Hu C, Liu Y, Qiao Y, Jiang X. Expression of VEGFR2 and NRP-1 in non-small cell lung cancer and their clinical significance. Chin J Cancer Res. 2014;26(6):669–77.

182. Zhu H, Cai H, Tang M, Tang J. Neuropilin-1 is overexpressed in osteosarcoma and contributes to tumor progression and poor prognosis. Clin Transl Oncol. 2014;16(8):732–8.

183. Van Cutsem E, de Haas S, Kang YK, Ohtsu A, Tebbutt NC, Ming Xu J, et al. Bevacizumab in combination with chemotherapy as first-line therapy in advanced gastric cancer: A biomarker evaluation from the AVAGAST randomized phase III trial. J Clin Oncol. 2012;30(17):2119–27.

184. Cheng W, Fu D, Wei ZF, Xu F, Xu XF, Liu YH, et al. NRP-1 expression in bladder cancer and its implications for tumor progression. Tumor Biol. 2014;35(6):6089–94.

185. Cao H, Li Y, Huang L, Bai B, Xu Z. Clinicopathological significance of neuropilin 1 expression in gastric cancer: A meta-analysis. Disease Markers. 2020;2020:4763492.

186. Hong TM, Chen YL, Wu YY, Yuan A, Chao YC, Chung YC, et al. Targeting neuropilin 1 as an antitumor strategy in lung xancer. Clin Cancer Res. 2007;13(16):4759–68.

187. Huang SW, Lien JC, Kuo SC, Huang TF. DDA suppresses angiogenesis and tumor growth of colorectal cancer *in vivo* through decreasing VEGFR2 signaling. Oncotarget. 2016;7(39):63124–37.

188. Hu C, Jiang X. Role of NRP-1 in VEGF-VEGFR2-independent tumorigenesis. Targ Oncol. 2016;11(4):501–5.

189. Spencer SKM, Pommier AJC, Morgan SR, Barry ST, Robertson JD, Hoff PM, et al. Prognostic/predictive value of 207 serum factors in colorectal cancer treated with cediranib and/or chemotherapy. Br J Cancer. 2013;109(11):2765–73.

190. Benson AB, Kiss I, Bridgewater J, Eskens FALM, Sasse C, Vossen S, et al. BATON-CRC: A phase II randomized trial comparing tivozanib plus mFOLFOX6 with bevacizumab plus mFOLFOX6 in stage IV metastatic colorectal cancer. Clin Cancer Res. 2016;22(20):5058–67.

191. Tomida C, Yamagishi N, Nagano H, Uchida T, Ohno A, Hirasaka K, et al. Antiangiogenic agent sunitinib induces epithelial to mesenchymal transition and accelerates motility of colorectal cancer cells. J Med Invest. 2017;64(3.4):250–4.

192. Zheng Y, Huang C, Lu L, Yu K, Zhao J, Chen M, et al. STOML2 potentiates metastasis of hepatocellular carcinoma by promoting PINK1-mediated mitophagy and regulates sensitivity to lenvatinib. J Hematol Oncol. 2021;14(1):16.

193. Ma X, Qiu Y, Sun Y, Zhu L, Zhao Y, Li T, et al. NOD2 inhibits tumorigenesis and increases chemosensitivity of hepatocellular carcinoma by targeting AMPK pathway. Cell Death Dis. 2020;11(3):174.

194. Fondevila F, Méndez-Blanco C, Fernández-Palanca P, Payo-Serafín T, van Pelt J, Verslype C, et al. Autophagy-related chemoprotection against sorafenib in human hepatocarcinoma: Role of FOXO3 upregulation and modulation by regorafenib. Int J Mol Sci. 2021;22(21):11770.

195. Li D, Yao Y, Rao Y, Huang X, Wei L, You Z, et al. Cholesterol sensor SCAP contributes to sorafenib resistance by regulating autophagy in hepatocellular carcinoma. J Exp Clin Cancer Res. 2022;41(1):116.

196. Cao W, Liu X, Zhang Y, Li A, Xie Y, Zhou S, et al. BEZ235 increases the sensitivity of hepatocellular carcinoma to sorafenib by inhibiting PI3K/AKT/mTOR and inducing autophagy. BioMed Research International. 2021;2021:5556306.

197. Feng Y, Zhang D, He G, Liu Y, Zhao Y, Ren X, et al. AZD4547 and the alleviation of hepatoma cell sorafenib resistance via the promotion of autophagy. Anti-Cancer Agents in Med Chem. 2022;22(18):3107–13.

198. Liu G, Fan X, Tang M, Chen R, Wang H, Jia R, et al. Osteopontin induces autophagy to promote chemo-resistance in human hepatocellular carcinoma cells. Cancer Lett. 2016;383(2):171–82.

199. Xu J, Su Z, Cheng X, Hu S, Wang W, Zou T, et al. High PPT1 expression predicts poor clinical outcome and PPT1 inhibitor DC661 enhances sorafenib sensitivity in hepatocellular carcinoma. Cancer Cell Int. 2022;22(1):115.

200. Tomida C, Yamagishi N, Nagano H, Uchida T, Ohno A, Hirasaka K, et al. VEGF pathway-targeting drugs induce evasive adaptation by activation of neuropilin-1/cMet in colon cancer cells. Int J Oncol. 2018;52(4):1350–62.

201. Bae D, Lu S, Taglienti CA, Mercurio AM. Metabolic stress induces the lysosomal degradation of neuropilin-1 but not neuropilin-2. J Biol Chem. 2008;283(42):28074–80.

202. Chen XJ, Wu S, Yan RM, Fan LS, Yu L, Zhang YM, et al. The role of the hypoxia-Nrp-1 axis in the activation of M2-like tumor-associated macrophages in the tumor microenvironment of cervical cancer. Mol Carcinog. 2019;58(3):388–97.

203. Fu R, Du W, Ding Z, Wang Y, Li Y, Zhu J, et al. HIF-1α promoted vasculogenic mimicry formation in lung adenocarcinoma through NRP1 upregulation in the hypoxic tumor microenvironment. Cell Death Dis. 2021;12(4):394.

204. Wu YY, Chen YL, Jao YC, Hsieh IS, Chang KC, Hong TM. miR-320 regulates tumor angiogenesis driven by vascular endothelial cells in oral cancer by silencing neuropilin 1. Angiogenesis. 2014;17(1):247–60.

205. Takahashi M, Okada K, Ouch R, Konno T, Usui K, Suzuki H, et al. Fibronectin plays a major role in hypoxia-induced lenvatinib resistance in hepatocellular carcinoma PLC/PRF/5 cells. Pharmazie. 2021;76(12):594–601.

206. Chen SP, Zhu GQ, Xing XX, Wan JL, Cai JL, Du JX, et al. LncRNA USP2-AS1 promotes hepatocellular carcinoma growth by enhancing YBX1-mediated HIF1α protein translation under hypoxia. Front Oncol. 2022;12:882372.

207. Mak P, Leav I, Pursell B, Bae D, Yang X, Taglienti CA, et al. ERβ impedes prostate cancer EMT by destabilizing HIF-1α and inhibiting VEGF-mediated Snail nuclear localization: Implications for Gleason grading. Cancer Cell. 2010;17(4):319–32.

208. Wu Y, Zhang J, Li Q. Autophagy, an accomplice or antagonist of drug resistance in HCC? Cell Death Dis. 2021;12(3):266.

209. Wu FQ, Fang T, Yu LX, Lv GS, Lv HW, Liang D, et al. ADRB2 signaling promotes HCC progression and sorafenib resistance by inhibiting autophagic degradation of HIF1α. J Hepatol. 2016;65(2):314–24.

210. Rodríguez-Hernández MA, González R, Rosa ÁJ, Gallego P, Ordóñez R, Navarro-Villarán E, et al. Molecular characterization of autophagic and apoptotic signaling induced by sorafenib in liver cancer cells. J Cell Physiol. 2018;234(1):692–708.

211. Owada S, Endo H, Shida Y, Okada C, Ito K, Nezu T, et al. Autophagy-mediated adaptation of hepatocellular carcinoma cells to hypoxia-mimicking conditions constitutes an attractive therapeutic target. Oncol Rep. 2018;39(4):1805–12.

212. Lin Z, Niu Y, Wan A, Chen D, Liang H, Chen X, et al. RNA m^6 A methylation regulates sorafenib resistance in liver cancer through FOXO 3-mediated autophagy. EMBO J. 2020;39(12):e103181.